CLT-Steel Composite Floors for Sustainable Multi-Storey Construction

By:

Kwesi Adade Okutu

A thesis submitted in partial fulfilment of the requirements for the degree of
Doctor of Philosophy

The University of Sheffield
Faculty of Engineering
Department of Civil & Structural Engineering

July 2019

Declaration Statement

Kwesi Adade Okutu certifies that all the material contained within this document is his own work except where it is clearly referenced to others

_____

Dedication & Acknowledgements

For Mum, who taught me perseverance,

For Dad, who taught me aspiration,

For Chloe, who taught me appreciation.

With the greatest of thanks to Buick Davison and Jon Carr, to whom I will forever be grateful for their guidance and understanding, and to my former colleagues in Sheffield for their advice and friendship, and to my colleagues in Liverpool for their advice, friendship and above, all their patience.

Executive Summary

This thesis encompasses the investigation of a novel proposed construction system that pairs Cross-Laminated Timber (CLT) floor panels with steel-frame multi-storey construction.

As a substitute for concrete floors, the promise of CLT lies in its reduced embodied carbon, and its lightness, which gives the promise of reduced material usage and a reduction in the environmental impact of a multi-storey building overall.

In addition to clarifying the environmental benefit such a system provides, this thesis seeks to determine whether forming composite sections from the CLT panels and the steel beam, can lead to meaningful enhancements to the section stiffness in bending. Finite element analysis is applied for this task, necessitating first a methodology for modelling CLT to capture its relevant complexities as a material, and subsequently incorporation of the behaviour of the joints between structural elements in the proposed system, with the key characteristics of the materials and joint models validated against physical test data.

Focussing predominantly on a slimfloor arrangement of panels and beams, the study provides the first evaluation of the effective width of CLT floor panels when acting compositely with steel beams, provides a prediction for composite action CLT panels and Asymmetric Steel Beams (ASBs) with a series of connectors, and identifies areas of development within the system that could bring about increased composite benefits.

The outcomes of the study are that in a slimfloor arrangement with contemporary panels, beams and connectors, the composite enhancement is small but measurable, and that with changes and development to the system components, much larger composite enhancement effects could be generated.

Contents

List of Figures

List of Tables

Chapter 1. Introduction

1.1 Scene Setting & Context

A new method of constructing multi-storey buildings has been investigated. It involves using Cross-Laminated Timber (CLT) panels acting as floor slabs with a steel framed support structure.

In 2011, the overall floor area constructed in all multi storey buildings in the UK amounted to 10,850,000m^2, 67.7% of which was steel frame construction[1]. Conventionally, concrete slabs are used for floor systems, either as precast units or cast in-situ on profiled metal formwork. Timber panels weigh approximately 1/3 of the equivalent concrete slabs, and hence the superstructure mass would be significantly reduced comparatively. Following through the implications of reduced floor mass, the superstructure itself requires smaller sections as the dead load is reduced, so less steel is needed overall, and also the foundations can be smaller and simpler. Research by Asiz & Smith has shown that CLT panels can be secured to steel with simple screw fasteners[2], so construction can be a quick, simple and a dry process. All these factors combine to make the proposed system potentially a much more efficient construction method, in terms of time, cost and environmental impact.

Using simple fasteners such as screws as the connection between floor panels, and provided the steel frame is bolted together rather than welded (as is typically the case in the UK), a CLT-steel hybrid frame offers great potential for designing for large scale material reuse. This will require connections to be designed in a thoughtful way and, combined with the use of CLT slabs, will facilitate the easy deconstruction and reuse of structural members. The concrete slabs in existing composite construction systems are very difficult to separate from the steel members, so reuse rates are low. Embracing deconstruction and reuse mitigates any increased initial material costs and pushes the environmental benefits even further.

1.2 System Overview

The use of asymmetric steel beams (ASBs) would allow the panels to rest on the bottom flange and mostly within the depth of the beam in a slim-floor arrangement (see Figure 1.1). This configuration gives practical benefits, as the slab can provide a safe working surface immediately after fixing. The system also enjoys the benefits of established slim-floor methods, such as reduced loads and costs associated with vertical elements e.g cladding, stairs, lifts vertical services and interior walls. This is because by having the slab within the depth of the beam, the floor-to-floor dimension is reduced for every storey and hence reduces the overall building height. The flat soffit of slim-floor systems (devoid of downstand beams) gives easier service integration allowing a flexibility in how the space is used[3].

In order to achieve the most efficient use of the materials involved, a degree of composite action between the steel and timber is sought. The research presented examines the potential of steel and timber working compositely and the most suitable methods of achieving this.
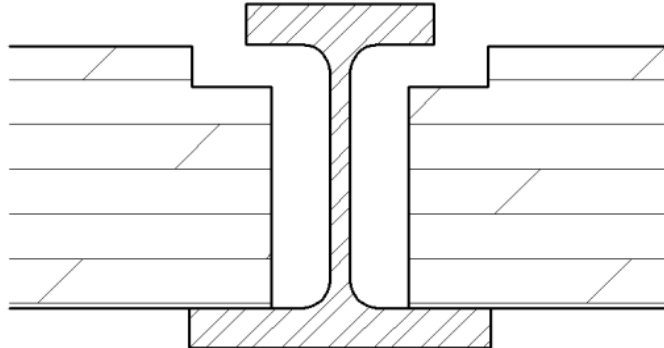
Figure 1.1: The slim-floor arrangement

1.3   Research Questions

Essentially, the research question this PhD seeks to answer is:

> Is there a benefit in designing/constructing multi-storey steel-framed buildings using CLT floors instead of traditional concrete floors/slabs?

In the course of answering this overarching question, the following sub-queries will be investigated:

> 1)   *Can the substitution of CLT floors in place of concrete slabs be justified by a reduction in environmental impact?*
>
> 2)   *Can the mechanical behaviour of CLT be modelled accurately by numerical means?*
>
> 3)   *Is it possible practically to generate composite behaviour between steel and timber, and can the degree of benefit be quantified?*

1.4 Composite Construction – Contributory Factors

1.4.1 Concept

Composite action occurs where two structural elements or materials are connected together in such a manner that they respond to loading as one, and with increased stiffness or strength compared to each of the elements on their own. Reinforced concrete, for example is a composite on several levels – within the concrete, the aggregate is bonded together by the cement in order to make the concrete matrix act as one entity, and similarly, the concrete and the steel reinforcing bars act compositely to enhance the poor tensile strength of the unreinforced concrete. When composite construction is referred to in structural engineering, this is most commonly understood as the use of steel framing (beams and columns), with concrete flooring. The concrete floor can consist of cast-in-situ concrete more commonly, cast-in-situ concrete on profiled metal decking (composite floor).

This research is centred on the composite action that can be generated by connecting timber flooring, in the form of CLT panels to steel beams.

1.4.2 Modular Ratio

Composite action enhances the stiffness of elements subjected to bending. Bending due to a given load is a function of geometrical properties (the 2nd Moment of Area, I) and the material stiffness (Young's Modulus, E) – together they are referred to as the "flexural stiffness" (EI). For convenience when performing design calculations, it is useful to consider an equivalent composite section to account for the enhanced stiffness when calculating deflections. When the two elements that form the composite section are of different materials, with different Young's moduli, the geometry of the section can be transformed using the Modular Ratio. The scaling is performed to the width of the section as this has a linear scaling effect on the 2nd Moment of Area.

Having performed the transformation, the composite flexural stiffness can be used in calculations that rely on this property, using only one Young's Modulus value and the composite 2nd Moment of Area.

1.4.3 Shear Flow and Shear Connector requirements

Composite behaviour is dependent on limiting the ability of the two component parts from bending independently of one another. Taking as a hypothetical arrangement, a purely simply supported beam consisting of two components as shown in Figure 1.2. When the two component pieces are completely independent, the interface has differing directions of strain on either side, leading to dimensional discrepancy on the two sides, known as slip. The tendency of the two components to move relative to one another creates a longitudinal shear at the interface which must be resisted to create composite action. If a perfect bond is created between the two components, there will be no discontinuity in strain at the interface and the two components will be acting as one element. In reality, it is very difficult to create a perfect interfacial bond – the connection will limit the slip to a point but will deform to some extent. The reduction in the interface slip determines how successfully composite action can be achieved with a particular connection method.

The slip arises as a result of the shearing force between the two sides of the interface, and this longitudinal shear force must be resisted by the shear connection. Restraint methods have evolved over the course of history, but the established method for concrete-steel composite beams is now the shear stud. Before shear studs were developed, metal loops or channel sections were embedded in the in-situ concrete to create the shear connection. Shear studs must transfer the load through the interface of the concrete and the steel through mechanical action, but must also prevent the concrete from lifting away from the beam – shear studs are flared at the top or headed for this purpose[4]. Their distribution along the beam will vary according to where shear forces and slip are greatest.
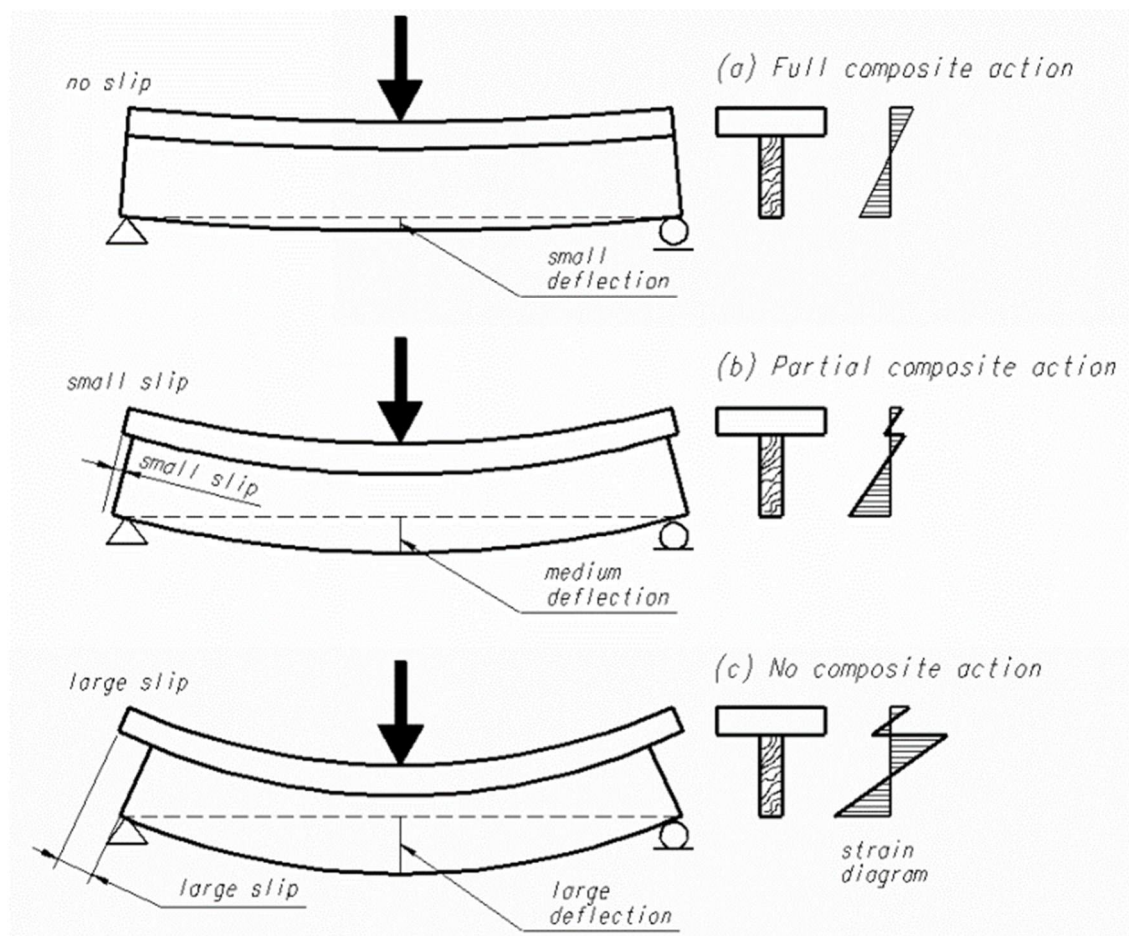
Figure 1.2 - Deflection and slip in composite section with (a) a rigid connection; (b) a partial connection; and (c) no connection or composite action[198]

1.4.4 Shear Lag and Effective Width

Shear lag is a phenomenon that manifests in load-bearing plates which are stiffened. Such plates include the top and bottom walls of box girders, and floor plates supported by beams. Because of in-plane flexibility of the plate, the normal stress distribution across a stiffening element such as a supporting beam is non-linear (see Figure 1.3), and the phenomenon is known as shear lag[5]. It is helpful in design to make the assumption that the slab is subject to a constant rather than non-linear in-plane stress distribution, and that the effective width is taken such that, if the assumed constant in-plane stress were

equal to the *actual* peak stress, the summation of stress across the slab width would be equal in both cases[6].

The shear lag effect determines how much of the floor slab can be assumed to act with the steel beam (termed "effective width"), and hence affects the overall strength and stiffness of a composite beam.
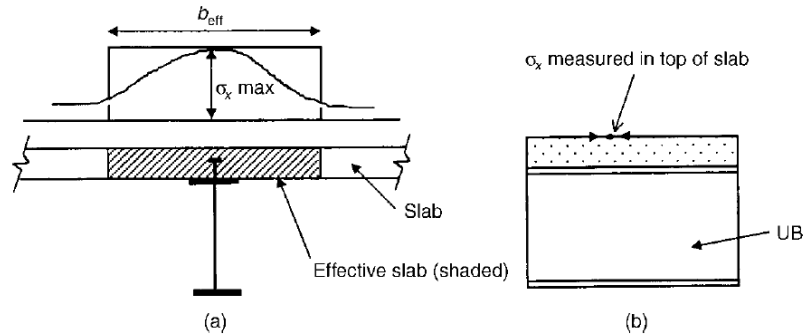
Figure 1.3: Effective Width of the slab in a composite beam[6]

1.4.5 Effective section properties

The effective section properties of the composite beam are needed to appropriately design structures using the proposed system. These properties will be influenced by the factors described above – effective width, degree of composite interaction, and modular ratio.

The underlying aim of this work is to explore how each of these factors affect this system, in order to determine the effective section properties and hence the suitability of using composite action within the system. Studying each of these factors will form the basis of recommendations for a procedure for structural designers to use for specifying the composite ASB-CLT system.

1.5   Structural System Components

1.5.1 Slim-floor Construction

SlimFlor®'s development arose from the ambition to reduce the depth taken up by the structural support system, and allow building services to be integrated more easily. Slim floor beams are almost entirely contained within the floor slab depth, and when combined compositely with concrete, this gives a high degree of resistance in the case of fire. According to Lawson et al, "the key features of slim-floor construction are the steel beams, which are located within the slab depth, and the floor plate of either precast concrete hollowcore units or a composite slab using deep steel decking, which spans between the beams"[7].

The outer cladding building represents one of the largest costs of a multi-storey structure. Hence, reducing a structure's overall height can give significant savings. This also reduces the height of other vertical elements and services, further lowering cost. In addition, in some areas such as central London,

new buildings are subject to height restrictions to protect sight-lines of landmarks - if floor-to-floor heights are as small as possible, an extra storey of rentable space can be created whilst the overall building remains within acceptable limits.

1.5.2 Cross Laminated Timber

Characteristics

CLT is an example of an engineered wood product. (Lam presents a good overview of the various other types available[8]). These are seen as a good way of extending the use of timber and capitalising on the associated environmental benefits (discussed in Chapter 3). Compared to traditional timber, engineered wood products have less variation in performance and have more predictable behaviour e.g. dimensional stability at different humidity levels.

Cross-laminated timber is formed by gluing together boards of softwood in layers of alternating orientation. They are usually made from spruce, though the middle layers or even whole panels may be formed from other wood species[9–11], and consist of between 3 and 8 layers of varying thickness that are symmetric about the middle layer[12](see Figure 1.4). Depths range from around 60mm to more than 300mm[9,10] and can span over 10m[13]. Panels can be used as roof, floor and/or wall elements, as their internal structure combined with the manufacture process bestows the panels with very good dimensional stability and strength about each axis[14].

Figure 1.4: CLT panel

During manufacture, the panels are kiln dried to a moisture content that reduces the risk of fungal or insect attack[11] and reduce movement in the panels in service. The layers of the panel are bonded together using adhesives (either melamine formaldehyde or polyurethane[9,10,12]) which are allowed to cure under pressure[15]. CLT is manufactured in large sheets, then cut into smaller panels of dimensions up to 20m x 4.8m but may need to be smaller for transportation practicalities[12]. They can be specified to a variety of timber grades, visual quality levels, and dimensional tolerances using laser assisted measurement and cutting technology[9,10,12].

CLT in Construction

The potential use of CLT within multi-storey buildings is a prescient topic. The idea has been the subject of TED talks[16] and articles e.g. in the New Civil Engineer magazine, CLT was claimed to be "central to meeting [the construction industry's] ambitions of driving a low carbon future while also creating an environment in which people feel comfortable living"[17]. An article in The New York Times summarised the potential for timber skyscrapers employing CLT in North America[18], highlighting a report by the respected multi-disciplinary firm, Skidmore Owings & Merrill, who have recently produced their own investigation into the possibility of timber skyscrapers (as shown in Figure 1.5) using CLT panels as floor plates[19], adding to the existing proposals by mgb Architecture + Design[20] but getting even more media exposure.
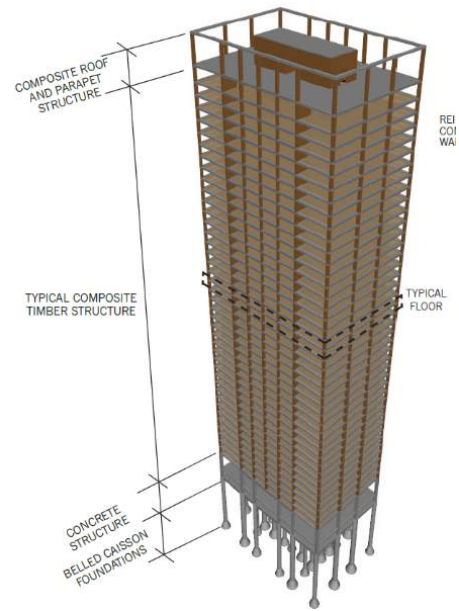
Figure 1.5: Timber Tower, by Skidmore, Owings & Merrill

Multi-storey buildings have been constructed from CLT already – StadtHaus (also known as Graphite Apartments) was constructed in Hackney London in 2009[21] and consists of 8 CLT storeys above a single-storey concrete podium. The Forté Tower in Melbourne was completed in 2012 and is now the tallest CLT building in the world, standing at 10 storeys (9 of CLT)[22]. Both Forté and StadtHaus are for residential use.

Residential buildings of between eight and twelve storeys constructed from CLT are being suggested in Seattle, U.S., with developers emphasising the material's environmental credentials and cost benefits compared to post-tension concrete (the dominant construction method in that market) when including the construction phase in analyses[23].

The currently completed and envisioned tall CLT buildings are for residential use – the cellular construction lends itself to housing as room dimensions are smaller and more intricate, so walls are utilised as loadbearing elements. The construction system proposed in this research does not require these walls, opening up the office market to CLT structures and providing more opportunities for flexibility in building use over time.

1.6   Thesis Outline

This thesis is arranged to demonstrate the scope of the field at the onset of the project (A), set out the justifications for researching the topic area (B), outline the development process performed (C), and finally contextualise the outcomes of the developmental and investigative processes (D).

Ch. 2 (A)   presents a literature review of the system components and composite action, both as a concept and in practice.

Ch. 3 (A/B)   details a study into the environmental impact of the proposed system, and the implications of specifying it.

Ch. 4 (A/C)   comprises of a literature review of numerical modelling pertaining to the research topic and reports the development and validation of a finite element (FE) modelling approach for CLT.

Ch. 5 (A/C)   concerns the FE modelling of the system connections, including literature review of existing approaches and validation via experimental data.

Ch. 6 (D)   reports the results and analysis of parametric investigation into the generation of composite action in the ASB-CLT composite system

Ch. 7 (D)   discusses the further issues to be addressed to create a successful construction system.

Ch. 8   Concludes the project and the thesis

The subject area of this project is potentially very large, and it was not possible to explore all the relevant areas. Instead the most pertinent areas to answering the research questions were explored in the literature review. Reporting this back in a single, defined chapter would have led to an incoherent chapter and difficulty finding the relevant background information when reading the later chapters. Consequently, the findings of the literature review have been distributed through the thesis; Chapter two presents the higher-level literature review findings relating to the overall system, and the main components, and is termed the "System Literature Review". In addition to this, three "Technical Literature Reviews" are compiled in the chapters where their findings and consequences are utilised in the development and analysis of the proposed system – these can be found in Chapter 3 (A: Environmental Performance), Chapter 4 (B: Modelling of Timber and CLT), and Chapter 5 (C: Behaviour and FE Modelling of Connections in Timber and CLT).

Chapter 2. System Literature Review

2.1   Introduction

As a note to the reader, whilst this chapter is titled "System Literature Review", it is not the only section of literature review within the thesis. For clarity and proximity to the relevant research within the structure of the document, there are further literature reviews focussed on FE modelling in Chapter 4, and on timber connections within Chapter 5. Chapter 3 also contains elements of literature review relating to environmental performance that was packaged with the environmental study for ease of reading. As such, this chapter provides insights into the relevant available literature on a more general background of composite action and the use of timber and CLT in structural engineering.

2.2   Composite Action

2.2.1 History and Development of Timber Engineering

As Cook[24] summarises, composite construction has been around for millennia, starting with the Assyrians' straw-reinforced mud bricks, through the veneered walls of the Greeks and Romans, and up to the 19th Century, which saw patents issued for composite trusses of timber and iron. The origins of modern composite construction lie in the ambition to create a fire-proof building. In many ways this project represents the completion of a full cycle in construction - timber was the original material of choice for floor systems. However, towards the end of the 18th Century, after prolonged industrial expansion, warehouse and mill fires were becoming more and more frequent. In addressing this issue, the direction taken was to substitute the timber floors and, in the absence of formalised building codes, a variety of floor systems were experimented with.

Composite beam construction as we now understand it (usually a reinforced concrete slab resting on top of a steel beam) has been in place since the 1950s and the first design code for composite structures, CP117, appeared in 1965[25]. Research continued apace throughout the 1960s and 70s, with the first substantial composite structure being of nine storeys and built at Imperial College[26], but the system only really gained a major presence in the construction market in the 1980s with the development of the modern welded shear stud and profiled metal formwork decking[27].

2.2.2 Shear Lag and the Concept of Effective Width

As introduced in the previous chapter (Section 1.4.4) the shear lag effect is a mechanical response shown by plate-type elements that are subjected to localised forces acting in the plane of the plate. The internal compression/tension that results from the external force is distributed across the width of the plate in a non-linear fashion, such that at the position of the applied load, the internal forces are highest, whilst reducing as distance along the plate edge increases – this is the shear lag effect. As an upper limit, a hypothetical system where the shear lag effect was negligible or non-existent would result in an effective width of half the spacing between parallel acting beams.

Zhou used numerical modelling to analyse the shear lag effect in box girders[28]. Beam elements were used that incorporated shear lag degrees of freedom. During the 1960s and 70s, Adekola[29–32], and Mackey and Wong[33] explored the issue of shear lag and effective width for concrete-steel composite beams. Effective width is now safely assumed in design to be equal to the span of the beam divided by 4 for internal beams, and span divided by 8 for edge beams[34].

The shear lag effect in timber was investigated by Amana & Booth in the 1960s. They looked specifically at stressed-skin panels, which are prefabricated units of timber joists acting as stiffening ribs to plywood sheeting. They developed a theoretical basis for estimating the amount of the plywood sheeting that can be assumed to contribute to the stiffness of the joists[35]. They also verified their theoretical work with laboratory testing, with good agreement[36]. Similarly, Milner & Peczkis incorporated the effect of shear lag and interlayer slip into their analysis of wooden boat hulls as box-girders[37]. They also noted that in the tension region, the presence of butt joints reduced the ability for shear forces to be transferred, meaning the effective width is less than that of the compressive side.

Effective width was explored by Davalos & Salim[38] in the context of stress laminated T-beam timber bridges. The stress-laminated deck is teamed with Glulam beams and is shown in Figure 2.1.
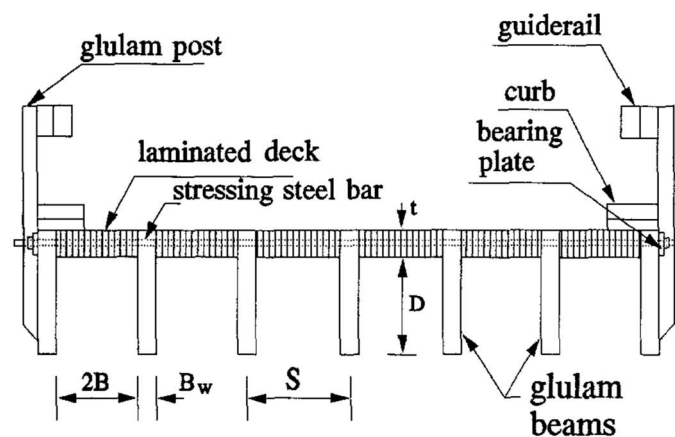
Figure 2.1: Stress-laminated T-beam bridge[38]

The European code of design for timber structures and elements, Eurocode 5, makes provision for the effective width of the sheathing material in stressed-skin panels. However, there is no corresponding method for solid panels.

The means with which the shear lag effect presents itself in CLT has so far not been extensively researched (the limited available literature on the topic was published after the project began[39–42]) - the anisotropy, laminated nature, glue-lines and slim-floor arrangement of a thick plate all combine to present a wide area of unexplored topics that are an opportunity for novel research.

2.2.3 Shear connectors:

Composite behaviour is very dependent on limiting the ability of the two component materials from bending independently from one another - the slip at the interface must be restrained. Restraint methods have developed over the course of history, but the established method in concrete-steel

composite systems is now the shear stud. Before shear studs were developed, metal loops or channel sections were embedded in the in-situ concrete to create the shear connection. Shear studs must transfer the load through the interface of the concrete and the steel through mechanical action, but must also prevent the concrete from lifting away from the beam – shear studs are flared at the top or headed for this purpose[4]. Their distribution along the beam will vary according to where shear forces and slip are greatest.

The nature of the shear connection will influence the degree of composite action between the two components. Broadly speaking, the interaction between components as a result of a connection can be categorised as fully composite, partially composite, or independent – in reality, all connections will fall into the "partially composite" category, but may be closer to one of the ideal cases. The degree of composite interaction (i.e. how much of the longitudinal shear force generated as a result of connecting two components can be transferred between the components) is often expressed on a linear scale with 0 being no interaction and 1 being the ideal case of full composite interaction.

One of the current research areas is in the development of shear studs that allow for deconstruction at end-of-life. High-strength bolts, placed in pre-drilled holes in precast units and the steel beam, are proposed as demountable shear connectors by Rowe & Bradford[43]. This type of connection was mooted some decades before[44,45], and results from this earlier research were used to calibrate a finite element model developed by Bradford & Pi[46]. Saveri & Lam[47] also developed and tested a demountable shear connector, finding that they could easily be disconnected after testing, that they had comparable mechanical behaviour to welded shear connectors, and also were more ductile than the welded variant.

2.2.4 SlimFlor as a composite construction system

The outer fabric of a multi-storey building represents one of the largest costs of the structure. Hence, reducing a structure's overall height, by even only a metre, can give significant savings, which also apply to vertically running services and plant equipment. Structural depth reductions offered by slimfloor systems also reduce the height of internal partitions, meaning lower cost and less load on the supporting system. In addition, in some areas such as central London, new buildings are subject to height restrictions to protect sight-lines of landmarks. If floor-to-floor heights are as small as possible, an extra storey of rentable space can be created whilst the overall building remains within acceptable limits. Whilst the initial development of the *Slimflor*[48] system had its origins in improving fire performance, the structural floor depth reduction remains a key selling point for the system.

As mentioned in Chapter 1, Lawson et al. opine that

> *"the key features of slim-floor construction are the steel beams, which are located within the slab depth, and the floor plate of either precast concrete hollowcore units or a composite slab using deep steel decking, which spans between the beams"*[7].

Slim floor beams are almost entirely contained within the floor slab depth, and when combined compositely with concrete, this gives a high degree of resistance in the case of fire.

Some of the earliest composite or hybrid floor systems were of a slim-floor arrangement. Brick arch floor construction entailed a masonry arch resting on the bottom flanges of steel I-beams, with a concrete topping[49] only just encasing the top flanges of the steel beams. Also known as jack-arches, they were the first type of floor to replace timber floors, from around 1790[27]. Clay tile arched systems, constructed using hollow clay tiles, were also in this arrangement and the benefits of the clay tiles in protecting the steel beams in fires were well known[50].

The SlimFlor® (precast units) and SlimDek® (composite deck) systems developed by TATA Steel (then British Steel) use rolled asymmetric steel beams(ASBs), though during the development of the system, fabricated beams were originally used. Rolled Hollow SlimFlor® Beams (RHSFBs), Rolled Hollow Sections (RHS) with plate welded to the bottom face, are used for the edge beams of the system, due to their torsional rigidity[51]. They are illustrated in Figure 2.2Figure 2.2: SlimFlor® and SlimDek systems®.
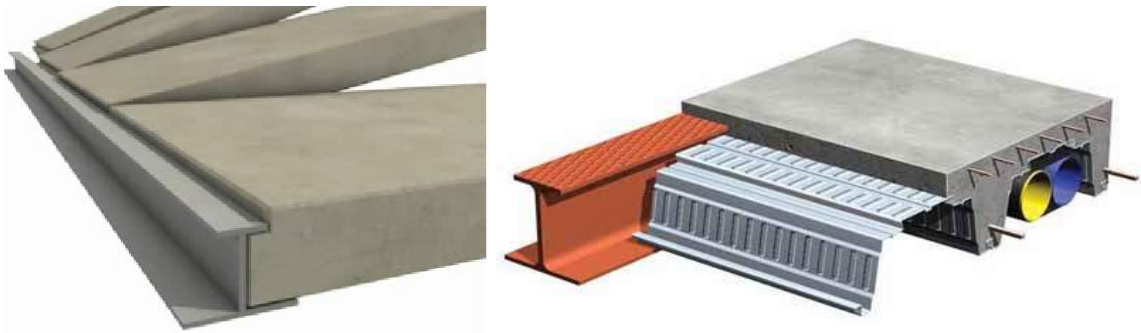
Figure 2.2: SlimFlor® and SlimDek systems®

Interest in slim-floor systems was reignited by developments in Scandinavia after advances were made in steel and concrete construction during the 1970s[52]. The `Thor' beam was fabricated from a plate with two channel sections welded together to form an open box, which was subsequently filled with concrete and closed with an additional plate[53].

The development of rolled ASBs in the late 1990s included the embossing of a raised pattern on the top flange of the beam - this allows the steel beam to act compositely with the concrete without the need for shear connectors[7,54]. A significant portion of research has centred on the fire performance of SlimFlor® beams[53,55,56], and they can achieve a 60 minute fire rating due to their inherent resistance[54].

Initially three sections were available[54], however the range has since been extended to ten[57], five of which are Fire Engineered with thicker webs to improve the inherent fire resistance of the ASB-Concrete composite SlimFlor system even further. Development of slim-floor systems has continued and documentation from The University of Stuttgart's workshop on Eurocode 4 details several new innovations in slim-floor and composite floors[58].

2.3   Timber behaviour

2.3.1 Microstructure of Timber as a construction material

The nature of timber is a by-product of the evolution of trees and plants into the most efficient structure to gain as much sunlight as possible, transport nutrients and store food[59]. As a natural material, it can therefore be considered on a variety of scales, with different behaviours becoming apparent. The natural structures that make up the growing tree determine the characteristics and anisotropy of the final timber.

There are approximately 30,000 tree species[59], each with distinct material properties, meaning timber is an incredibly variable material. This variability is also present *within* species, as the mechanical behaviour of structural timber is influenced by naturally occurring defects (e.g. knots) and how the biological structures of the parent tree manifest themselves, which can vary from tree to tree, and in different positions in a single tree.

The internal structure of the growing timber is geared around positioning the leaves as high as possible, to best collect sunlight for photosynthesis, the process used to generate energy. This means the structures within the timber are arranged to run up and down the length of the trunk – this is the "longitudinal" axis in the final construction material.

2.3.2 Mechanical Behaviour

Directionality

The timber in longitudinal axis (see Figure 2.3) must resist the wind forces exerted on a tree, requiring the bending resistance of the timber to be highest along this axis. In addition, as the tree supports itself through compression of the trunk, the structural timber has its highest compressive strength in the longitudinal axis. The structures that transfer water and food around the tree are fibrous, and it is these structures that provide tensile resistance. As these structures tend to run in the longitudinal direction, tensile strength is also highest in this axis, a necessary characteristic to resist bending.
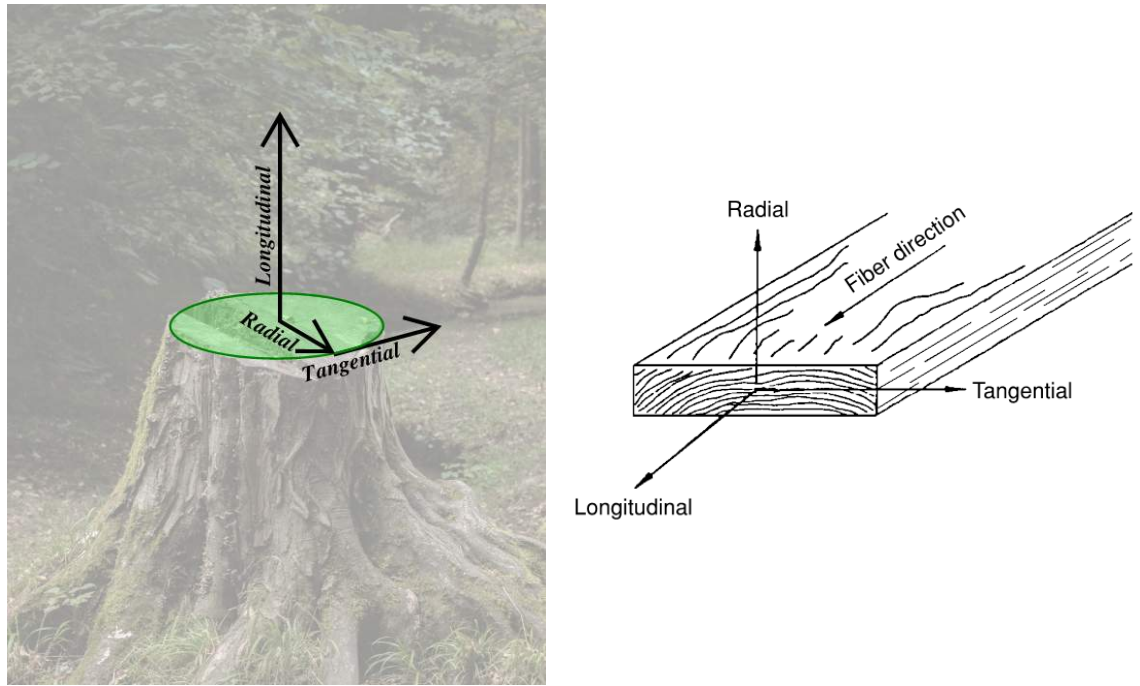
Figure 2.3 - Mechanical axes of wood when part of a tree (left) and in structural elements (right)

Failure and Defects

In the novel system investigated in this thesis, i.e. CLT panels acting compositely with asymmetric steel beams, the failure mechanisms are not well established. Timber failure, delamination, connection failure, or some combination, are the expected modes of failure but it is clearly important to understand how the CLT will act in failure. If ductile failure can be ensured, further economies can be made by utilising plastic design, but if (as is suspected) some form of brittle failure at the connection is the dominant mechanism, this has a profound impact on the design approach that can be applied.

Defects in timber include knots (locations of where branches connect to the main trunk), splits and shakes (cracks running parallel and perpendicular to the grain respectively, resulting from shrinkage of the timber as its moisture content reduces during seasoning), and grain defects resulting from how timber pieces are cut from the trunk. As described above, the structure of the living timber trunk supports the tree primarily against lateral wind load, meaning its strongest mode of resistance is in bending *parallel* to the grain, with the stiffest part of the timber being when the grain runs perfectly perpendicular to the imposed load. The defects described above all distort either the direction of the grain locally or affect the bond between fibres which allow the matrix of fibres to work together and from which timber derives its bending strength.

 A phenomenon seen in timber members is the size (or volume) effect. This is the fact that in general, smaller members can withstand higher stress conditions than larger ones[60]. CLT being a massive element but consisting of multiple small elements, presents an interesting case. The size effect phenomenon is often assumed to be related to the increased probability of a structural defect being present in a larger piece of timber. However, in *Fracture and Fatigue in Wood*[61], Smith, Landis & Gong

suggest that the size effect seen in timber is because of how damage progresses in the material rather than probability of defects, since defects are not evenly distributed through timber elements. According to their understanding, the cracks inherent in timber propagate by transfer of the strain energy stored in the member. Larger members can store a greater amount of strain energy and hence cracks can extend further, leading to complete member failure.

Cross Laminated Timber offers a conundrum for each of those theories. Slats with obvious defects, like knots, are removed or placed in sections of low stress during panel manufacture. This should mean the size effect, if due to the increased probability of defects, should not be present. However, if Smith, Landis & Gong's theory is correct, the preselection of timber in the manufacturing process should have no impact on the size effect. In fact, the presence of glue lines should present more failure planes and cracks/defects within the element.

Delamination is a phenomenon that occurs in layered composite materials[62,63]. Individual layers become separated, overcoming the strength of the fixing between them and hence reducing the capacity of the material. The strength and behaviour of the adhesive will have a role in the panel's susceptibility to delamination.

The connection of the CLT to the supporting steel beam is another area of concern. As has been discussed, timber failures originate in defects, or rather areas of lower strength in the non-homogeneous matrix. As such, failures could originate in the areas weakened by the connection technique - inevitably fibres will be damaged and cracks created as some mechanical fixing will be used rather than gluing in order to facilitate deconstruction.

Whilst it is clear that the connection may be a source of initial cracks, it may actually be of benefit by changing the post cracking behaviour. Borri & Corradi noted that, when performing flexural tests on timber beams reinforced with high strength cords, after failures had been initiated at defects, the presence of the steel cords in the tensile region "seems to arrest crack opening, confines local rupture, and bridges local defects", leading to an increase in tensile capacity perpendicular to the grain[64]. It may be possible to bestow this property on the connection zone of the CLT-to-Steel beam connection.

The complexity of timber extends to the way in which it fails. Under compression, failure arises as a result of the progressive collapse of cell-like structures and the subsequent compression of cellulose, and in load-displacement traces this shows an elasto-plastic relationship with strain softening occurring post yield (see Figure 2.4).
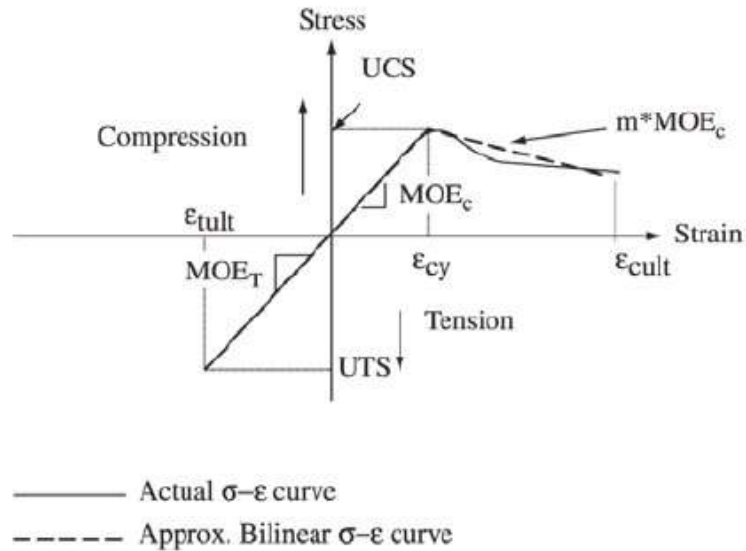
Figure 2.4 -Stress Strain relationship of timber in tension and compression[199]

In tension, however, things become yet more complex and a markedly different failure mechanism is apparent – one of brittle fracture. According to Dinwoodie[59], failure can be approached in two manners, that he terms the "Classical" and "Engineering" approaches. The Classical approach considers the strength of the material as a function of the constituent fibres and cells in the timber, with the theories of strength being based around these structures and adjusted to account for differences between the theory and reality. The Engineering approach disregards the internal structures of the material, and assumes that all timber contains defects that will be propagated under load and whose properties will define the ultimate strength of the material.

The tensile failure behaviour in the various axes again reflects the internal structures of the wood. In the radial and tangential directions, tension tends to separate the wood fibres, meaning resistance is only given by bond between fibres. Once this is surpassed, a sudden failure occurs. In the longitudinal direction, i.e. along the length of fibres, the fibres themselves resist tensile forces though extension. Timber shows the most strength in this direction, and failure comes about through the fibres reaching their limit of extension. In terms of shear, again there is variation depending on the directionality. Of particular importance is the phenomenon of rolling shear, as this is the loading scenario to which timber has the least resistance, and which some parts of a CLT panel will always be subjected to.

(a)   (b)
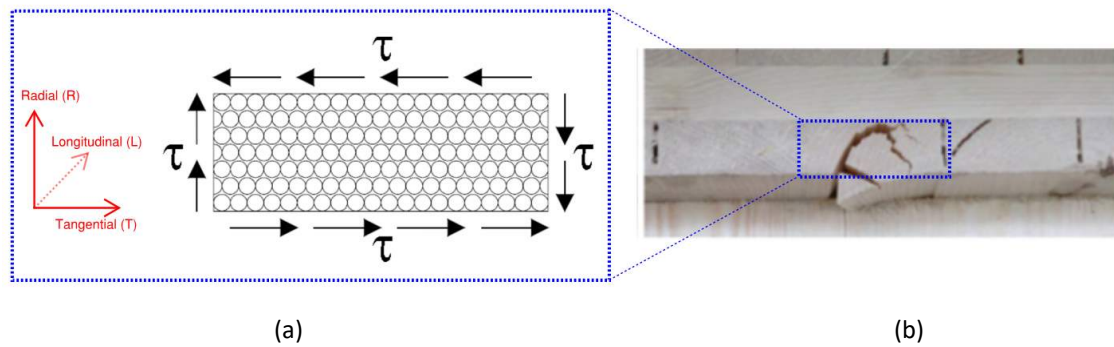
Figure 2.5 - a) Stress application subjecting timber to Rolling Shear[87] ; b) Rolling Shear failure in a CLT panel[65]

Rolling shear refers to shear acting in the Radial-Tangential (RT) plane. The fibres of the wood are roughly cylindrical, with the circular cross-section in the RT plane, as displayed in Figure 2.5. This means that when a shearing force occurs in that plane, the fibres have a tendency to "roll" past one another with reduced resistance, akin to sliding one's hand across a pack of straws. As Sandhaas notes in her thesis, rolling shear most often occurs in CLT[65], and this is because timber engineering has developed to avoid introducing load to the timber such that rolling shear could occur, however, this is unavoidable when using CLT as a floor panel.

2.4   Connections in Timber Resistance mechanisms

Connections in timber can be categorised into two major types, based on the manner in which the load is resisted by the timber – metal dowel type fasteners which resist and transfer load via 'dowel action' and those which resist through bearing or friction against the surface of the timber (e.g. nail plates)[60].

Connection choice will also raise other potential issues that need clarification. For example if simple screw connections or dowel like structures are used, this may lead to brittle failure mechanisms, due to connection groups[66,67] or due to splitting[68] especially in a material with existing potential failure planes like CLT.

Transfer of tensile forces is especially difficult as the grain of timber can be pulled apart relatively easily and in a brittle, progressive manner. In many cases, where tensile forces must be transferred, the timber is reinforced locally with steel plates or other components to reduce the tensile stresses being applied to the timber.

Further literature review of timber connections relating to the project can be found in section 5.2.2.

2.5 CLT as a Construction Material

2.5.1 History and Development

Plywood, which has been in use for almost a century, is an engineered timber formed from laminations of thin veneer sheets that are arranged with alternating grain orientations and glued together. CLT has been described colloquially as "jumbo-plywood"[12]. Plywood is, however, limited in thickness, thus restricting its use in structural engineering unless it forms part of a cassette system. A related product is GluLam, where beams and columns are formed from smaller pieces of timber glued together in layers but with a common grain direction[69]. The advent of GluLam elements was revolutionary for the use of timber framing in buildings, enabling much greater spans to be used.

CLT is a combination of approaches used in GluLam and plywood. Its precursor is a product called BrettStapel[70,71]. In this system, slats of timber are aligned in the same direction, in a similar manner as for GluLam, but rotated in 90-degrees in section. This system used nails or dowels to bind the individual pieces together to avoid the use of glues, which were not very environmentally friendly at the time. CLT's development has been centred about the academic institutions of Germany and Austria since its inception and has been growing in utilisation across Europe over the past two decades.

The initial patent was first granted in 1985[72], but more in-depth research and application of the panels did not begin in earnest until a decade later with the dissertation of Schickhofer in 1995[73]. Whilst the first project using the material was a multi-storey residence in Aichach (Bavaria, Germany) in 1995[74], it was not until 1998 that technical approval was first granted, in Germany and Austria[72]. A full research and development programme was initiated at TU Graz in 2003 from which the majority of best practice for design and capacity calculation was derived[15].

There are currently no prescribed design methods for CLT in Eurocode 5, and as yet no definitive design guide, however the CLT Handbook[75] (produced in 2013) collated a large amount of current best practice methods. Similarly, the UK Building Regulations are not suited to CLT structures which has required multi-storey CLT projects to seek other forms of certification in order to acquire insurance[76]. References to structural timber across the building codes and regulations across many countries relate to timber-frame construction, which has very different behaviour to CLT construction. However, the UK Building Regulations no longer put restrictions on the height of building specific to using structural timber, unlike in other countries such as the USA (6-storeys)[77], Germany (5-storeys)[77], Denmark (4-storeys)[78] and Finland (4-storeys)[78] where there are limits on the number of storeys, predominantly relating to fire performance.

This has allowed a series of multi-storey timber structures featuring CLT to be constructed over the past decade, furthering awareness and confidence in CLT structures at the same time. Murray Grove aka StadtHaus aka. Graphite Apartments (Hackney, London, 2008)[79] became the world's tallest timber structures upon its completion, a title it held for four years standing at 9 storeys (8 in timber with a 1-storey concrete podium). Bridport House (Hackney, London)[80] followed in 2011 consisting of 41 social housing apartments spread across 8 storeys. Banyan Wharf aka. Wenlock Road aka. The Cube building

(Hackney, London, 2015) combined CLT panels with steel framing in optimal locations to create a hybrid timber-steel structure.[81,82]

Forte Living[83], located in Melbourne (Australia), took over from Murray Grove as the world's tallest CLT building in 2012, standing at 10-storeys, though it has now been usurped by the 14-storey Treet (Norway) and other ,even taller, timber structures are in the pipeline[84]. Images of these buildings are shown in Figure 2.6.

Some of the highest profile CLT structures through the material's introduction into UK construction (Murray Grove, Bridport House, Banyan Wharf) are located in the London Borough of Hackney. A major reason for this is the policy of the borough council which has targeted sustainability as one of its core principles for further development and has time constraints on the construction phase of new developments as part of the planning application review process[76]. A by-product of these policies is that the characteristics of CLT construction were particularly suitable for these residential projects.
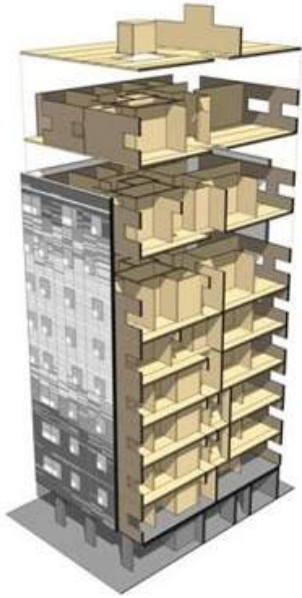
Figure 2.6 - Clockwise from top left - Murray Grove, London; Bridport House; Banyan Wharf; Forte living

2.6   Internal Structure & Mechanical Behaviour

Calculation of CLT panel deflections in bending is enabled through use of the shear analogy method developed by Kreuzinger,[85] a method that has become a standardised method included in the CLT Handbook[75]. The analogy involves aggregating the properties of the combined panel into two virtual "beams" whereby the elastic and shear moduli are taken into account. An example is shown in Figure 2.7. Essentially a means of simplifying the calculation process "Beam A" consists of a raw summation of the Moment's of Inertia for each layer, whilst "Beam B" contains the Steiner Points (the additional terms in the Parallel axis theorem that take into account the distance away from the composite neutral axis) as well as a term that factors in Shear deformations that result.
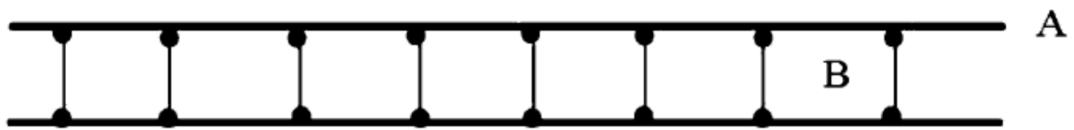
Figure 2.7 - Shear Analogy Method representation of a 3-layer panel[200]

In terms of failure of a CLT panel overall, some evidence of plastic behaviour has been reported in the literature for panels subject to in-plane shear[86] – this was postulated to have been a result of rupture taking place progressively through the laths rather than all at once, thereby allowing a ductile failure to occur.

Fellmoser & Blass[87,88] found that the design of CLT panels is greatly affected by the behaviour of timber in rolling shear. Through testing specimens of cross-layered timber of differing lay-ups, they found that due to the low rolling shear modulus, the depth of the layer(s) subject to rolling shear was of direct relation to the amount of shear deformation when subjected to out of plane loading. This work was also underpinned by Kreuzinger's Shear Analogy Method.

2.7   Timber Composites

2.7.1 Timber-Concrete composite behaviour

Combining timber and concrete is an interesting variation in composite floors. They are created either by supporting a concrete slab on timber beams/joists, or as a composite slab where the timber replaces the concrete in the tensile zone and the steel reinforcement, relying solely on the tensile strength/stiffness of the timber. This type of construction is by no means a new idea - as Cook noted in 1976, bridges were constructed in this manner in the 1930s[24].

Yeoh et al[89] have provided a thorough state-of-the-art on timber-concrete composites (TCC) and their development history. They see the main advantages of a TCC floor slab as rapid construction when making use of prefabricated timber sections, the ability of the timber to act as permanent formwork, the smaller superstructure mass (meaning reduced seismic response and reduced foundation loads), reduced environmental impacts and the opportunity to use the exposed timber decoratively. Their summaries of connections, testing, and FE modelling techniques for TCC systems give valuable insight into the complex issues that arise when using timber compositely.

Kuhlmann & Schänzlin[90] have proposed combining timber board stacks and concrete as a composite floor slab, together with an integrated shallow fabricated steel beam. The shallow beam supports the timber board stacks on the lower flange, with the concrete being cast over the whole arrangement and forming composite behaviour with both the steel and timber. With their system, they anticipate a 60% increase in column-free area compared to Reinforced Concrete (RC) slabs.

Blass & Schlager[91] tested a variety of connection systems (see Figure 2.8) between a concrete slab and timber beam. They found that connections created by casting concrete into grooves or notches into the timber gave a particularly plastic deformation characteristic and that if such connections are utilised, a load saring will occur between them, increasing the ultimate load of the composite beam[91].
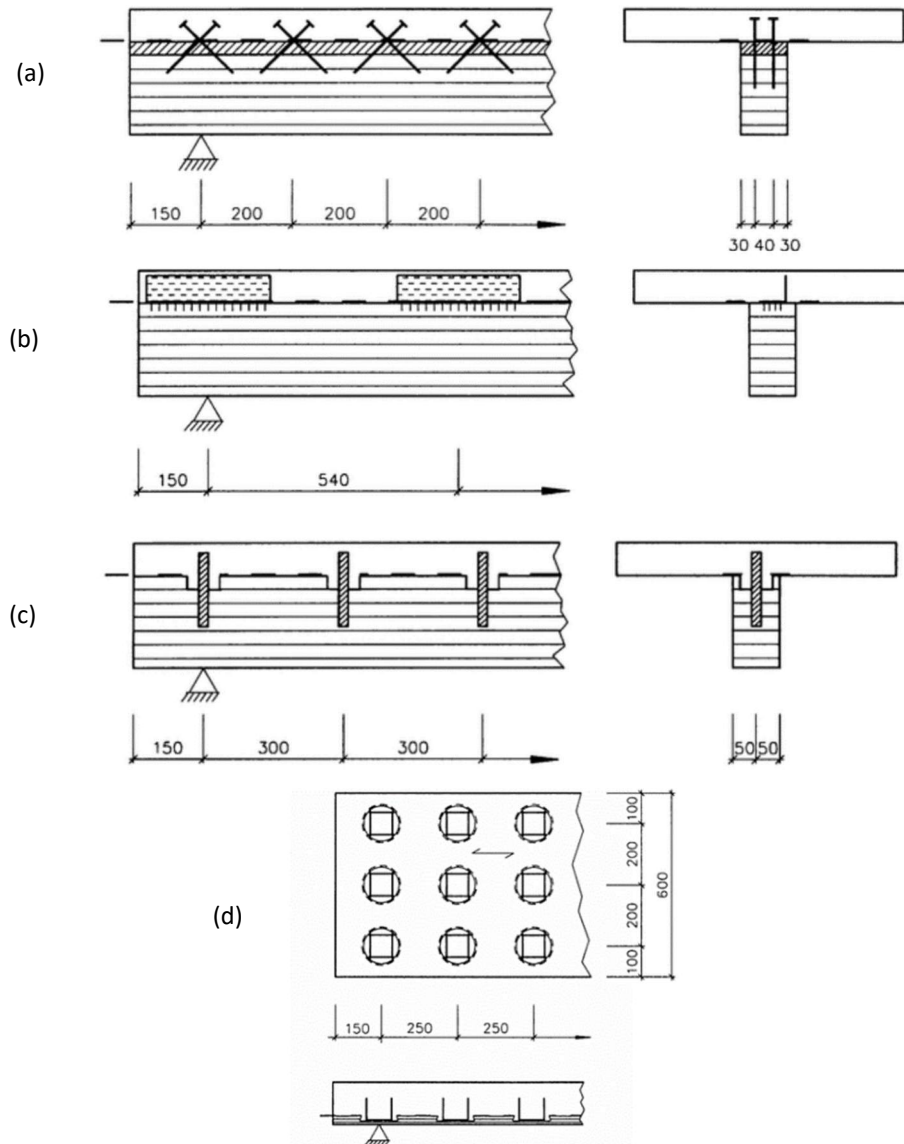
Figure 2.8 - Timber-Concrete composite connection systems tested by Blass & Schlager, including (a) crossed screws; (b) punched metal fasteners (Nail Plates); (c) grooved holes and dowels; and (d) grooved indentations in Laminated Veneer Lumber (LVL)

2.7.2 Timber-Steel composite behaviour

Replacing reinforced concrete slabs with CLT has been mooted in multi-storey construction by Asiz & Smith[92]. However, this did not take into account any potential composite behaviour, was not of a slim-floor arrangement, and mostly focussed on the responses to earthquake.

Historically, steel and timber have been used together, most notably in flitch beams. In timber construction, to allow beams that span larger distances, steel plates are bolted, screwed or nailed into either side of, or between, the members that are being connected to form a single beam. Initially formed by bolting, they fell out of favour due to the time consuming fabrication process, but more efficient and speedy manufacture processes allowed a resurgence in their use in the 1970s[93].

In 1973, Stern & Kumar[93] tested flitch beams. The flitch beams in the test were between 28% and 48% stiffer than similar beams without the plates, but found that defects in the timber such as knots and shakes (splits along the radial axis) had more of an effect on the performance of the beams than the presence of flitch plates.

Lantos[94] suggested, and tested, laminated timber beams that were reinforced with steel bars glued between laminations. He developed a composite beam theory for the beams and performed tests to corroborate the theory. The beams were found to behave as perfectly composite for practical purposes when they were of length greater than around 15 feet (4.57 m), and that if the rod diameter was above 0.5 inches (12 mm), early bond failure between the steel and timber would cause collapse.

The effect of nail density on flitch-plate flexural behaviour was investigated by Alam & Ansell[95] in 2012. Increasing the density of the nails in this configuration did not change the deflection response (the benefit of the presence of steel plates was maintained at the lowest nail density), but did alter the manner of crack propagation and failure. This will hold significant bearing on the connection design, where increasing joint stiffness through use of more connectors must be balanced against maintaining ductility in the connection and prevention of group failure which occurs when connectors are too closely spaced.

2.7.3 Research of CLT-Steel Construction

The connection between the CLT slab and steel section is critical to developing composite action and ensuring the robustness of the structure. Asiz & Smith[2] determined that it is possible to secure CLT slabs to steel beams with simple screw connectors, and that their sufficient ductility meant withstanding the horizontal forces experienced in a multi-storey building is just a question of specifying an appropriate number of these connectors. What is not certain is whether this type of connection will be enough to induce composite behaviour. Some form of reinforcement or gasket may be necessary, as explored by Guan & Rodd[96–99], to prevent excessive damage of the timber, especially in case of cyclic loading that may cause the fasteners to loosen.

Cristiano Loss of the University of Trento is developing a system incorporating CLT panels as floors and as wall infills in a steel-framed structure. The research programme aims to provide a lightweight, environmentally friendly structural solution to increase housing provision in a manner suitable to resist

seismic action that is prevalent in parts of Italy. As such, the behaviour of connections features heavily. Published research has covered the in-plane behaviour of steel frames (as both walls and floors) with CLT panel infills[100], experimental testing of a large range of potential shear connectors and inter-panel connections[101,102], finite element modelling of the system components and assembly[103], and most recently development of the system to incorporate cold formed sections to form a composite element with the CLT floor panels[104].

In this system, CLT panels are connected compositely on top of cold-formed hollow section beams, and the entire composite element sits within the depth of the hot rolled steel framing elements[104]. The research at Trento aims to provide suitable structures for earthquake regions and, hence, the performance of the connections in the system are of primary focus. Loss's system uses composite action to enhance the spanning capabilities of the CLT (rather than vice-versa), with the CLT panel sited on top of cold-formed beams with a shear connection to create a composite assembly. These units sit within the depth of larger hot rolled steel sections with connection being made between the cold-formed and hot-rolled steel members. Because there are a series of assemblies adjacent to one another, panels are not especially wide, and the effect of shear lag is limited., meaning exploration of effective width has not been taken.

2.7.4 Existing Timber-Steel Structures

Scotia Place, in Auckland, New Zealand employed glue-laminated timber floors on the top flange of a steel supporting frame. It is a 12-storey residential building that was completed in 2000. In Mark Moore's case study of the structure[105], he noted that there was a cost advantage over the concrete floor options for the project, and that due to the light weight of the structure, wind became the dominant lateral load case for the global vertical stiffening elements (in this case a concentrically braced frame) rather than seismic action which needs to be considered in New Zealand. Earthquake loads did dominate for the design of the floors themselves, as their performance in this design case as a diaphragm structure, along with the connections between timber and supporting steel, were most critical.

2.8   Robustness and Diaphragm Action

For any new construction system, ensuring sufficient robustness is critical not just to the system performance, but to meeting the requirements of the law. In the wake of the disproportionate collapse at Ronan Point in 1968, it was seen as imperative to ensure buildings were designed against such catastrophes leading to changes in the design codes and building regulations[106].

The robustness requirements are essential to prevent a progressive collapse of a structure as happened at Ronan Point. This means the structure must be capable of redirecting loads around structural elements that are damaged. The amount of measures that must be taken varies depending on building type and size[107], but multi-storey structures will require horizontal, and sometimes vertical, tying elements. Horizontal tying can be ensured by the steel frame, but may also be transferred by the floor plates given sufficient connection strength. Designers of existing multi-storey CLT structures in the UK

have struggled with meeting the requirements of the Building Regulations[107] relating to multi-storey residential or office buildings above 4 storeys (5 storeys for single occupancy houses), particularly regarding disproportionate collapse[81,108].

Linked to this subject is diaphragm action. The floor plates in a multi-storey structure are necessary to transfer horizontal loads (namely wind loads and notional horizontal loads) from the facade to the shear walls or steel bracing frame. Timber floor systems are known to be capable of doing this, however, the performance of CLT panels in this regard is less well known. Skidmore Owings & Merrill's report on timber skyscrapers suggests that the connection between the individual slabs is critical in diaphragm performance[19]. The timber floor slab must be able to transmit in-plane and lateral shear forces, with particular attention paid to fixings and nailed or screwed interfaces[109].

Any construction in the proposed hybrid system may initially be required to meet more stringent conditions in the design codes on the issue of robustness - Appendix B of Eurocode 1,Part 1-7 determines that unconventional structures, such as those using new materials, must go through an in depth Risk Assessment process during design to demonstrate that sufficient robustness is supplied[110].

2.9   Conclusion

In this chapter, literature review has been performed on the subject area as an overall system, exploring the established knowledge on the topics of composite action in multi-storey buildings, timber as a construction material, the known behaviour and implementation of CLT, existing structural composites involving timber, and robustness.

From this, it can be surmised that

- composite action as a principle is well understood and has been successfully used with steel-concrete composites for several decades.
- CLT as a more novel material has a growing rate of implementation, though a more limited knowledge basis.
- with the exception of the research of C. Loss[100–104], composite action of steel and timber have not been explored in any great way, though the behaviour of connections when using CLT in seismic zones offers the closest topic of interest. Where research has been done, it has not investigated the effective width of CLT in such a way as to determine the contribution of the CLT to a composite 2nd moment of area. This has certainly not been established for a slimfloor arrangement alternative to concrete flat-slab construction.

From this, the remaining questions are regarding how the composite contribution from CLT in the slimfloor arrangement can be quantified, and the means with which to maximise this through the connections. Further literature review on these topics are found in chapter 4 and 5, where development on these specific topics can be found. With the structural background of the system established, further clarity on the potential environmental benefit of a timber-steel composite method will be explored.

Chapter 3. Environmental Impacts

3.1   Chapter Introduction

In this chapter, the characteristics of the proposed system are discussed and developed, to determine how its performance may differ from the commonly used building methods of reinforced concrete and composite steel frame. The changing significance of environmental performance and impact is discussed, and a comparative study of embodied energy and carbon is reported. Finally, the potential for recycling or reuse of structural elements is explored in more detail. As a whole, this chapter aims to answer the first research question, "Can the substitution of CLT floors in place of concrete slabs be justified by a reduction in environmental impact?".

3.2   Technical Literature Review A: Environmental Performance

3.2.1 Context

The premise that global climate change is occurring and being exacerbated by human activity is an accepted reality by the vast majority of climate scientists and 84% of the general public[111]. Emissions of carbon-dioxide (CO_2) through the burning of fossil fuels in transport and industry, (along with methane emissions from livestock) and deforestation of rainforests that absorb CO_2 are contributing to the increase in average global temperatures that threatens to irreversibly alter how our climate functions and inundate coastal cities and settlements due to rising sea levels.

In 2011, UK Greenhouse Gas (GHG) emissions were 549 $MtCO_2e$, of which buildings contributed 186 $MtCO_2e$, which is approximately 35% of all emissions[112,113]. The majority of this (83% in 2008[114]) is associated with the operation and use of the buildings i.e. lighting heating, heating etc., however work is progressing rapidly to reduce these figures and meet government targets. As part of the Climate Change Act 2008[115] and subsequent statutes[116,117], the UK government has set in law strict national carbon emission targets known as carbon budgets each encompassing a 4-year period. Decreasing progressively, these limit carbon emissions aiming towards a 20% reduction by 2020[118] and further to an 80% fall by 2050[119] (compared to 1990 levels). The latest carbon budget order, made law in 2016, limits total GHG emissions across the years 2028-2032 at 1725 $MtCO_2e$[120] (57% of 1990 emissions in by 2030[121]), an average of 345 $MtCO_2e$ per year requiring a 37% reduction compared to the 2011 emissions alone.

The Low Carbon Construction report[119] additionally set the targets for buildings and construction specifically – it mandated for all new residential and non-domestic buildings to be Zero Carbon by 2019 and reductions of emissions (compared to 2008) of 29% from residential buildings and 12% for non-domestic properties. It also called for companies involved in construction to reduce their carbon usage and provide owners and users with buildings, whether existing or new, "that emit less carbon in their

construction, operation and decommissioning". Requirements were introduced through changes to the Building Regulations, initially covering commercial buildings, with a view to covering residential buildings later– within Approved Document L of the Regulations, sustainability of the building and construction materials used are scrutinised. The targets for zero-carbon housing have now been removed as it was felt the measures that would need to be implemented placed too high a burden on developers and would slow down the construction of new housing stock[122], however the requirements on commercial buildings are already in place and revised requirements are to be established by 2018[122].

Whilst the UK is currently meeting the emissions targets set out in the First Carbon Budget[123] (with the period of the Second Carbon Budget not yet complete), most research and government initiatives have focussed on reducing the operational carbon emissions, which is understandable as they represent such a large proportion currently. However, as the targets become ever stricter and operational carbon emissions reduce towards being carbon neutral (associated emissions offset by on-site energy generation or connection to renewable energy sources), the impact of the chosen building material and construction method will become critical for continuing improvement[124]. The definition of "Zero Carbon" was not initially determined but in England has come to mean meeting air-tightness and energy efficiency in heating and cooling, the limiting of CO_2 emissions on location, and restrictions on energy sourcing if it cannot be generated via low carbon means on-site[125].

As well as carbon emissions and embodied energies directly related to the manufacture of the building materials, the structural format of a building affects the environment in other ways. Taking a "whole-life" perspective of the environmental impacts, the choice of structural system will affect aspects of the construction process, the performance of the building in operation, and the deconstruction process.

3.2.2 Sustainability in Construction

The Principles of Green Urbanism[126], as set out by Steffen Lehmann, effectively summarises the key issues that the current thinking suggests must be considered in developing and re-developing sustainable human settlements. There are 15 principles in total, but the justification of this research lies in the meeting of Principle 3 (the Zero Waste City), and Principle 7 (Local and Sustainable Materials with Less Embodied Energy). Figure 3.1 demonstrates how these issues fall into 3 categories or "Pillars". This project predominantly falls within the pillar of Energy and Materials.

It is useful to examine environmental impacts of construction in the context of the Building Life Cycle, shown in Figure 3.2 and taken from the UK Government's Low Carbon Construction report.

GREEN URBANISM

ENERGY and MATERIALS	WATER and BIODIVERSITY	URBAN PLANNING and TRANSPORT
• Embodied energy • Material specification • Supply chain • Renewable energy solutions • Energy sources and consumption • Construction systems • Prefabrication and recycling • Energy efficiency • Resource management	• Urban water management • Water recycling and irrigation • Urban Farming • Urban landscape typologies • Ecosystems' biodiversity maximized • Grey water recycling • Storage of urban stormwater • Climate change impact management • Waste management	• Urban design • Social sustainability • Ecological city theory • Health and walkability • Mobility, public Transport • Infrastructure • Energy efficient buildings • Mixed land use • Housing affordability • Reducing car dependency • Subdivisions

Interaction between three main pillars

Figure 3.1: The Three Pillars of Green Urbanism[201]

Design → Materials or Product Manufacture → Distribution → Assembly on site → In Use → Refurbish/Demolish

Figure 3.2 - Phases of the Building Life Cycle[119]

Taking each part in turn:

- **Material /Product Manufacture**: Includes material extraction, transportation of raw materials to the factory, and processing towards the creation of the finished and packaged product.
- **Distribution**: Environmental impacts of the transportation of products from their respective factory gates to the construction site i.e. the shipping and road/rail haulage. This phase is often included within the Assembly-on-site phase.
- **Assembly on site**: The total impact of the machinery, lighting and personnel involved in the construction process.
- **In Use**: Operation and maintenance of the building from the point of handover to the owners/tenants.
- **Refurbish/Disassembly/Demolition**: The process of repurposing the structure or taking it down and clearing the site for another use, including all machinery, personnel and transportation required.

Sitting outside the Eurocode framework but within the European Standards is EN 15804 Sustainability of Construction Works[127]. This document details how to set up analyses of the environmental impact of construction, and the requirements of manufacturers to declare the associated impacts of their products. The building life-cycle phases are broken down into modules, and the different aspects are designated as mandatory or optional. The mandatory modules all relate to the product manufacture, requiring manufacturers to produce an Environmental Product Declaration (EPD) that designers can use to help make decisions on sustainability.

3.2.3 Assessment of sustainability in construction: Life Cycle Analysis

A Life Cycle Analysis (LCA), the process of quantifying and comparing environmental impacts, can be performed with regards to a material or for an entire structure. The salient measure in an LCA could be anything from ozone depletion potential to reduction in biodiversity. However, for this project the most relevant characteristics are Global Warming Potential (i.e. embodied CO_2 specifically) and Embodied Energy (the amount of energy used to produce the material/building). These two parameters are linked by the extent to which energy production is through burning of fossil fuels, however they offer complementary insight.

An important factor in the usefulness of LCA figures is the extent of the LCA. For a construction material, this is the associated emissions and energy usage involved in the production of a unit quantity up until the point that it leaves the factory (referred to as a "Cradle-to-Gate" LCA); for a building it is more complicated. Using the Innovation and Growth Team's approach[119], a true whole Life Cycle Analysis begins at the onset of Design and concludes with the building's Demolition, encompassing Manufacture (Cradle-to-Gate of materials), Transportation (of materials and personnel), Construction, Operation, and Maintenance in between. This is often termed a "Cradle to Grave" approach. It is only

through this depth of analysis that a true reflection of the impacts of a building or development can be assessed and compared with another.

3.2.4 Assessment of sustainability in construction: Dealing with the Phases

Quantifying to this degree of detail is a sizeable undertaking and thus in most cases only one or two phases are investigated at a time. It is notoriously difficult to calculate the values of each phase quantitatively with a high degree of confidence, as much depends on case studies of past projects which may or may not have other specification details that affect the performance. Even identical structures may have different whole Life Cycle Analysis impacts when situated in a different location, which will become more apparent by the end of this section.

There are, however, more qualitative predictions that can be made in sufficiently informed circumstances about what can be of relative positive or negative effect on the environmental impact of a particular phase of the building life cycle. It is possible to make estimates of some phases with more confidence and accuracy than others.

- **Material/Product Manufacture**: In most cases this constitutes the Cradle-To-Gate figure, and is a phase upon which more confidence can be placed on the available data from EPDs. The companies that manufacture construction materials are incentivised by code requirements in EN 15804 to perform their own analyses of the extraction, associated transport and manufacture processes. As the data declared by manufacturing companies must be acquired through prescribed methods, even where there is inaccuracy in the methods, these inaccuracies will be across all products and materials and will thus still allow useful comparisons to be made.

- **Transportation & Construction**: The accuracy of this phase in estimations for the future is quite variable and depends on the scope of information about the sources of construction materials and the required actions in construction. If the quantities of material required and the locations they will be transported from are known, it is straightforward to calculate the number of deliveries necessary and the environmental impact of those lorries. The actual construction processes are more difficult to state outright and will vary according to the particulars of a site or project. Qualitatively, the use of large numbers of personnel will bring the associated impacts of those staff traveling to site each day, and the need to provide suitable welfare facilities. Use of heavy machinery adds to the environmental impact and if they require skilled operators, they may travel from further away. Impacts from personnel and machinery are multiplied by the number of days that they are required, meaning anything that increases the duration of construction has a detrimental effect. Deep foundations, for example, require extensive excavation (quite apart from the material requirements) so will have a higher environmental cost.

- **Operation & Maintenance**: as mentioned in section 3.2.1, the current focus of global research is, perhaps understandably, on reducing the impacts relating to the Operational phase of the life cycle. Whilst this phase has the biggest overall effect, it is very difficult to predict, being as dependent as it is on future behaviours and energy generation practices. Huge variations arise from what the structure is to be used for, hence any future redevelopments (e.g. from offices to residential) may affect the outcome. Usually the nature of the building envelope will have a greater influence on the operational energy than the framing material, with the caveat that the use of exposed thermal mass combined with Passive Design strategies can reduce operational costs when harnessed successfully[128].

- **Refurbishment/Disassembly/Demolition**: This is not often considered by designers, but it does contribute to the environmental impact of a building, especially if the measure being considered is Landfilled Waste. There are two aspects to this Life Cycle phase, namely the disassembly or demolition process itself, and the outcomes of the building's component parts. If a structure can be easily dismantled and the structure reused, recycled, or the biomass used for energy generation, this reduces the environmental impact compared to a building that requires high energy demolition and wholesale sending of construction waste to landfill. The practice of reuse, recycling and energy recuperation has created debate in how to properly incorporate this into the analysis and accounting process. At present, the most appropriate mechanism appears to be to amend the values of embodied energy, carbon, etc. to reflect the potential for reuse, recycling and energy recuperation in the headline Cradle-to-Gate figure, as these are most often used when comparing construction materials.

3.2.5 Quantification: Sustainability of materials

As has been explained in the preceding section, an analysis of the environmental impact of CLT will start with the Cradle-to-Gate figures of embodied carbon and energy, as this data can be most relied upon quantitatively. In Table 3.1, the values for CLT, reinforced concrete and structural steel have been collected.

Table 3.1: Selected environmental properties of construction materials

	Density (kg/m^3)	Embodied Carbon (kgCO$_2$e/kg)	Embodied Energy (MJ/kg)
Cross-Laminated Timber[129]	417	0.169	7.98
Reinforced Concrete[130]	2500	0.113	0.78
Structural Steel[130]	7800	1.53	21.5

From this data, the comparison can immediately be drawn between the density of concrete and the greatly reduced density of CLT.

Datasets

When performing a lifecycle analysis, careful consideration must be taken in selecting data sources to use when allocating the environmental impact of a particular material or construction method. Independent data sources should be used wherever possible. In the context of the environmental impacts of construction materials, one such independent data set that is often used is the Inventory of Carbon & Energy (ICE)[130] produced by The University of Bath. Whilst a useful tool that has an extensive catalogue of construction materials and their embodied carbon and energies, it is merely a collation of the best available data, of which many are from manufacturers rather than EPDs and are without independent verification. Notwithstanding, it remains a very useful and respected dataset, which is utilised within this project. The ICE does not include values for CLT, only for Glulam, but figures were sourced from an independent Environmental Product Declaration for a Canadian CLT product[129].

Whilst the LCA approach is a helpful and appropriate means of assessing and quantifying environmental performance, there are a multitude of different criteria that could be explored and each would take significant work to determine the performance of a particular material. This makes it impractical to deliver quantitative comparisons of "sustainability" as a whole between materials. However, it is possible to make qualitative inferences based on related information that is available when combined with the quantitative cradle-to-gate embodied impacts as outlined earlier.

As well as embodied carbon and energy, sustainability also encompasses the renewability of the source material, the impact of the extraction and manufacture processes, and how increased utilisation of a material (and hence increased extraction /devotion of land to creating that material) would affect other human activities such as food growth.

3.3   Quantification: Material efficiency

3.3.1 Proponents of the Environmental Credentials of Structural CLT in the Literature

There have been several recent articles and reports highlighting the potential of CLT in multi-storey construction. Lehmann advocates the use of solid wood panel construction systems like CLT aligned with Design-for-Disassembly principles to meet sustainably the need for new urban dwellings in the urban environments of Australia[22]. Residential buildings of between 4 and 10 storeys were suggested.

Structures made purely of CLT do already exist up to 10-storeys (e.g. Forte Apartments) but there is a movement towards combining CLT panels with other construction materials to enable even taller structures and to reap the greatest efficiencies.
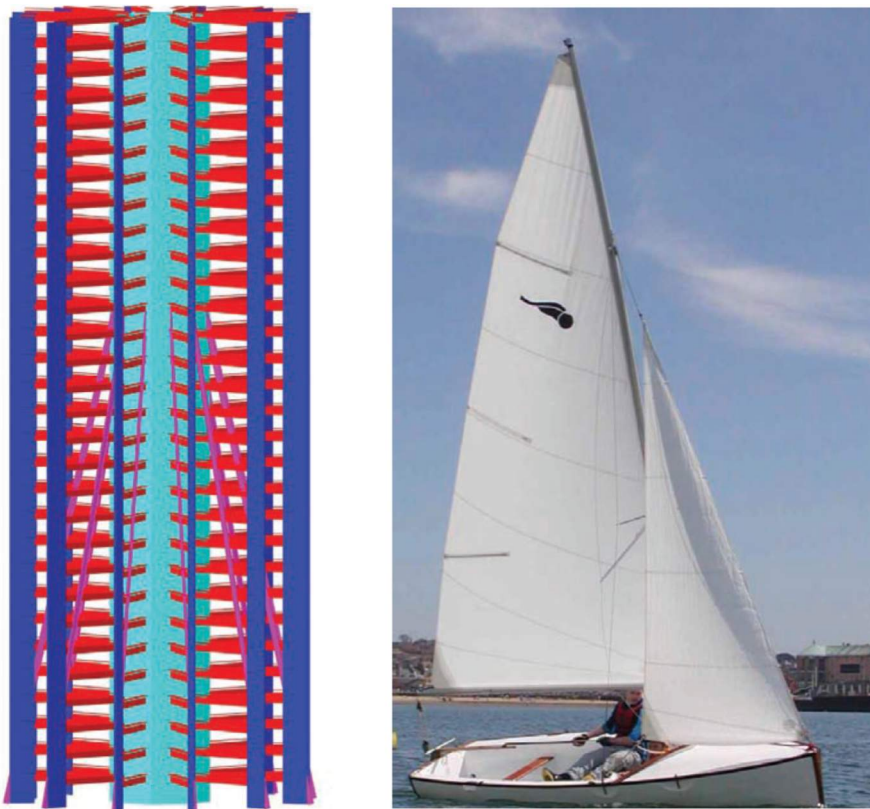
Figure 3.3 - Multi-Storey CLT structure using outriggers[131]

Chapman proposes a system using CLT panels in a tube formation for a central core (with inclined Universal Column stays giving assistance under wind loads, analogous to those of a yacht mast), aligned vertically for the outer columns, and as floor beams by cutting the panels along their length (see Figure 3.3). Reinforced concrete is used to form shear-transferring connections between CLT panels in the core, in outer "hoop" beams at the building perimeters, and compositely with the CLT beams as a Timber-concrete floor[131].

Skidmore, Owings & Merrill, renowned for designing some of the most recognisable tall structures in the world, produced a report investigating how structural timber can be used for tall buildings[19]. They found that using timber in composite systems was the best course of action, as

Figure 3.4: Skidmore Owings & Merrill's Timber Tower structural system[19]

materials such as reinforced concrete and structural steel are better suited for critically stressed members, and using timber compositely produced more efficient and economic structures, which are therefore more likely to be specified by clients. It was also noted that although foundations for timber structures would be much smaller there is the potential requirement for tall timber structures to have uplift restraint in the foundations, which would be a complicating factor. A potential structural system was developed, using a concrete-jointed timber frame, and is shown in Figure 3.4. This timber tower, combined CLT floor panels, with glulam beams and columns, and a coupled-shear-wall lateral support system of CLT. Reinforced concrete spandrel beams were also included. From a sustainability perspective, in their comparative study, they concluded that this tower had a 60 to 75% reduction in Embodied Carbon footprint against a benchmark structure, though it must be noted that this included carbon sequestration within values for the wood products.

The characteristics of the proposed system fit well with the recommendations of future development of tall structures incorporating timber, and suggest that a construction system with significantly reduced environmental impact may be possible in this way. In the next section, this reduction will be quantified.

Table 3.2 shows the depths of slabs required for floor systems under a 2.5kN/m^2 imposed load (suitable for office loading) and various spans, and the dead loads that these floor slabs produce. The significant reduction in dead loads compared to the current concrete floor systems offers potential reductions in the size of members in a steel frame and large reductions in the loads going down to the foundations. This is because for equivalently spanning slabs, the CLT panels are of similar depths to precast concrete panels, but are of lower density.
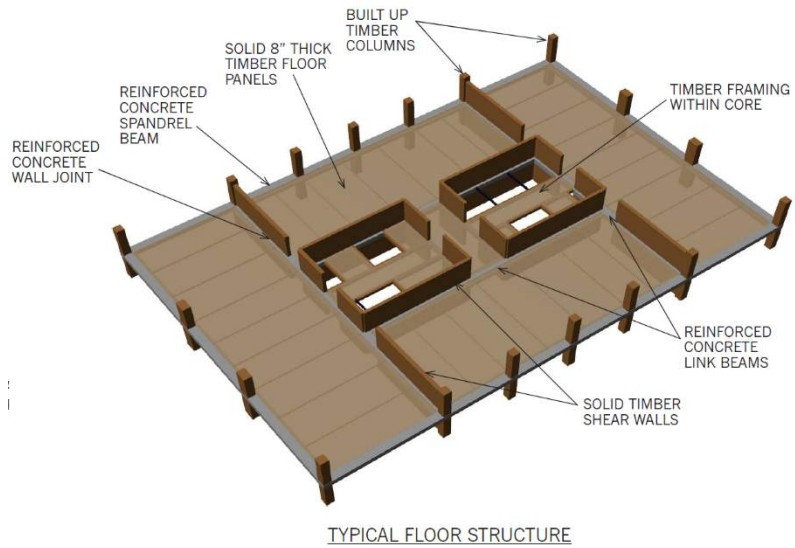
Table 3.2: Comparison of dead loads associated with various floor systems

q_k = 2.5kN/m²	Span = 4m		Span = 6m		Span = 8m		Span = 10m	
Floor Material	Slab Depth (mm)	Dead Load (kN/m²)	Slab Depth (mm)	Dead Load (kN/m²)	Slab Depth (mm)	Dead Load (kN/m²)	Slab Depth (mm)	Dead Load (kN/m²)
CLT[13]	125	0.59	182	0.86	208	0.98	300	1.41
Concrete Flat Slab[132]	200	4.70	206	4.84	250	5.88	343	8.06
Pre- Cast Concrete[133]	200	3.6	200	3.6	250	4.2	300	4.5
Composite Deck[134]	215	3.1	215	3.1	305	7.3	N/A	-

Foundations are often extensive, and carry significant embodied carbon and energy, both from their materials (Reinforced Concrete) and their construction. Previous work by the author[135] deduced that if the axial force sent to a pad footing was scaled by a given ratio, λ, then the volume of the pad foundation would be scaled by the approximate ratio $\lambda^{3/2}$. In the case of using a CLT floor rather than a composite deck to span 4m, the ratio between the axial loads to foundations will be approximately 0.58 – this translates to a pad footing volume ratio of 0.44 i.e. the volume of foundations could be more than halved by substituting a composite deck for CLT panels.

Reductions of this magnitude in the foundation volumes has a significant effect, not solely on the material quantities and embodied carbon and energy, but also the cost of foundations due to easier design and integration with existing ground features and increased speed of construction. Furthermore, the volumes of excavation required will be lower, which will allow construction on sites that may not have been viable with existing construction systems due to poor soil characteristics or because a prohibitively large amount of contaminated soil would need to be removed and treated.

3.3.2 Design for deconstruction

Low carbon design of structures will have a key role in meeting the carbon emissions targets outlined in Section 3.2.1. Reusing structural elements allows the embodied carbon and energy to be distributed between the working lives of the product[136], but one of the reasons element reuse is uncommon is that structures (and notably connections) are not designed to facilitate its dismantling at the end of life.

Design-for-Deconstruction (DfD) is a methodology that puts this idea at its core.

Lehmann offers a comprehensive study into the potential for CLT panels to form part of a construction system where elements can be reused[22], as well as outlining some of the other aspects of CLT's suitability in the context of residential housing.

Densley-Tingley & Davison summarise some of the strategies that need to be taken during structural design and decision making to enable and facilitate deconstruction[136]. These include (but are not limited to): using connections that are easy to remove, avoiding adhesives and coatings where possible; having deconstruction in mind from the outset of the design process; using standard structural grids to allow the maximum number of potential projects that members can be reused in; making sure connection points are easily accessible; using as few connection types as possible; making use of prefabrication and mass production; and choosing materials that are easy to separate and readily reusable.

Figure 3.5: The 2012 Olympics Basketball arena[202]

Notable examples of structures designed for deconstruction could be seen at the Olympic Games. In the 2012 games in London, the basketball arena (Figure 3.5), capable of holding 12,000 spectators and spanning 100m, was not designed to be permanently in place at the Olympic Park, but rather to be sold and relocated or recycled[137]. Similarly, the handball arena for the Rio Olympics of 2016 will be dismantled and reconfigured to create four separate schools. Parts of the steel structure, façade,

concrete circulation and disabled access ramps, visible in Figure 3.6, will be reused and evident in the buildings to serve a total of 2000 pupils[138].

According to representatives of the masterplanning team for both the London and Rio Olympics, the strategies exploited for these so called "nomadic venues" included standardised structural elements (steel beams/columns and concrete slabs) and prefabrication of modular parts that are now feasible due to advances in material technology[139].

Figure 3.6 - Rio 2016 Olympic venue, "Future Arena", designed for repurposing after the event[138]

3.4   Environmental impact Case Study

3.4.1 Canadian studies

A reduced environmental impact compared to conventional construction methods would be a powerful benefit of the proposed construction system. However, whilst the environmental credentials of the system are presumed through the employment of timber, those credentials must be confirmed as rigorously as possible to be considered credible. Hence a comparative study of construction systems including the proposed hybrid has been devised.

The investigation undertaken here takes inspiration from a study by Robertson, Lam & Cole[140]. In their study, an existing reinforced concrete building was redesigned to be functionally equivalent, but made from engineered timbers (a combination of Glue-Laminated Timber and CLT). Subsequently, the materials associated with the designs were summated, and the embodied environmental impacts calculated.

3.4.2 Design Process

The author has previously performed a comparative design study of CLT panels supported by ASBs against a conventional slim-floor system, but only in the context of a single bay[135]. Here, the scope of comparison is extended significantly. The superstructure (slabs, beams and columns) of a case study building has been designed in the proposed hybrid system, as well as in reinforced concrete and conventional composite construction. The chosen building, the residential StadtHaus building (Murray Grove, London – see Figure 3.7), was until recently the tallest CLT building in the world, standing at 9 storeys tall (8 storeys in timber). The compared structures are designed to be functionally equivalent, and the material quantities for each case can then be summarised and the environmental impacts calculated.

Software from the SCI (BDES[141]) and The Concrete Centre (Concept V3[142]) were used for the conventional composite and reinforced concrete structures to ensure impartiality in the design process.

3.4.3 Findings

Figure 3.7: StadtHaus[21]

As previously stated, a whole life cycle approach is how competing systems ought to be compared, however the complexity and scale of such a task is prohibitive. Quantifying the operational phase of such a building is beyond the scope of this research, but the other phases of the building life cycle are more readily quantifiable. (The building fabric was assumed to be consistent in all cases, so that the associated operational energies would be similar in any case.) Included in this analysis are cradle to gate embodied carbon and energy, taking into account recycling and reuse of the elements that can be dealt with in this way. Shear walls were also assumed constant.

Initially designed as non-composite and using the slim-floor configuration, the timber-steel hybrid system was found to have less than a third the mass of the steel-concrete composite (257.8 tonnes against 966.7 tonnes), and approximately one-fifth that of the reinforced concrete structure (1215.5 tonnes). This would have a significant effect on the size of the foundations required. Figure 3.8 demonstrates the substantially different masses associated with the superstructure for each construction method.

During the course of the calculations for the hybrid system, it became clear that the stock ASBs were oversized for the purpose of supporting a timber floor. Hypothetical, smaller beams were sized, and their employment was calculated to reduce steel usage in the structure by almost a quarter.
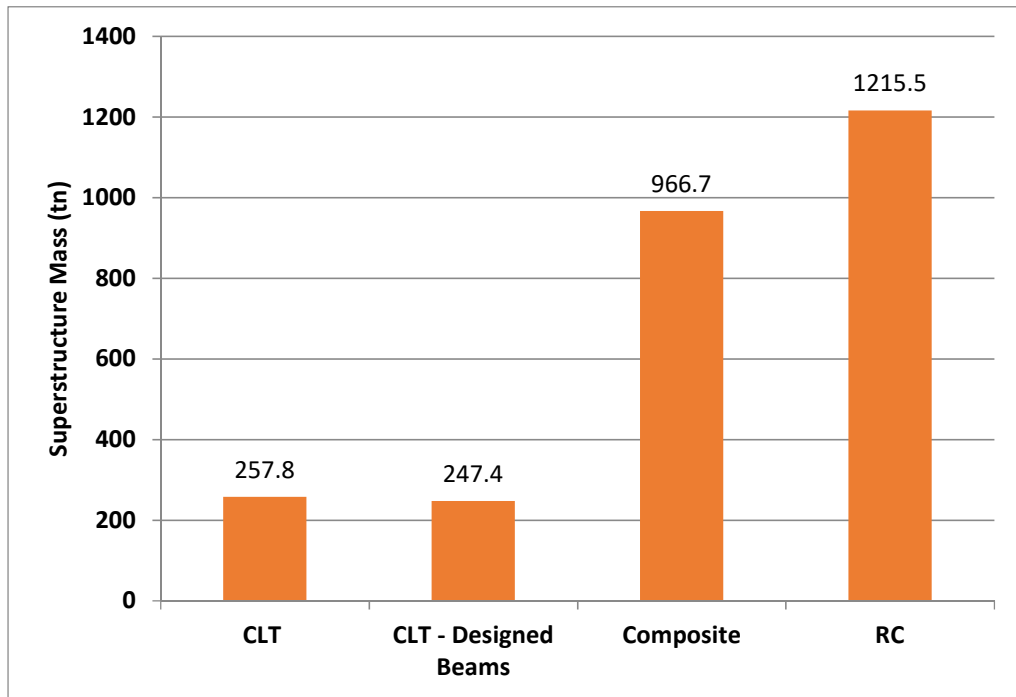
Figure 3.8: Construction system comparison – Superstructure Mass (Tonnes)
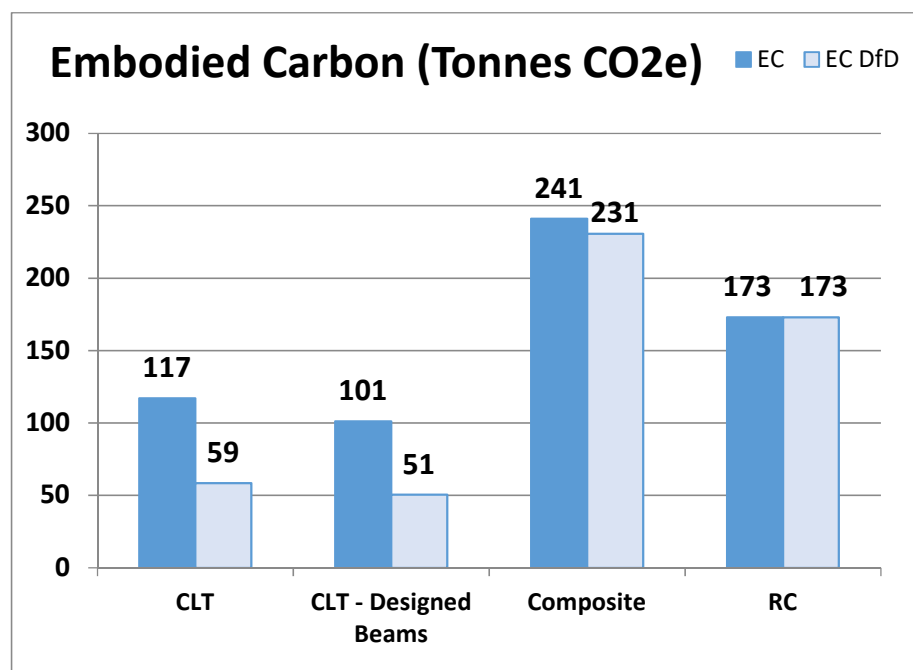
Figure 3.9: Construction system comparison – Total Embodied Carbon (Tonnes CO_2e)

Assessment of the embodied carbon and energy of the systems was made using Bath University's *Inventory of Carbon & Energy*[130], a well-known dataset with the CLT data coming from the EPD of a Canadian product, Nordic X-Lam[129]. Sakura, a web based tool developed at the University of Sheffield[143], was used to incorporate the effect of potential for material reuse on the impacts. The results show the impact Design-for-Deconstruction has on the environmental impacts of the building frame (Figure 3.9 and Figure 3.10). For the proposed hybrid, the nature of the materials and the envisaged connection system should allow all elements of the superstructure to be reused, allowing the embodied carbon and energy to be shared across the service lives, and hence halving the embodied impact figures here.

What is also apparent from Figure 3.10 is the remarkably high embodied energy in the CLT system before DfD is incorporated, compared to the established framing methods. This result is contrary to the popular thinking of timber as automatically of greater green credential. In mitigation, the embodied energy is only of concern if non-renewable sources are used in energy generation. There is also the difficulty in whether CLT should be credited for the fact it could eventually be burned to produce energy. What is certain is that the manufacturing process of CLT warrants further scrutiny to establish why the energy usage is so high.
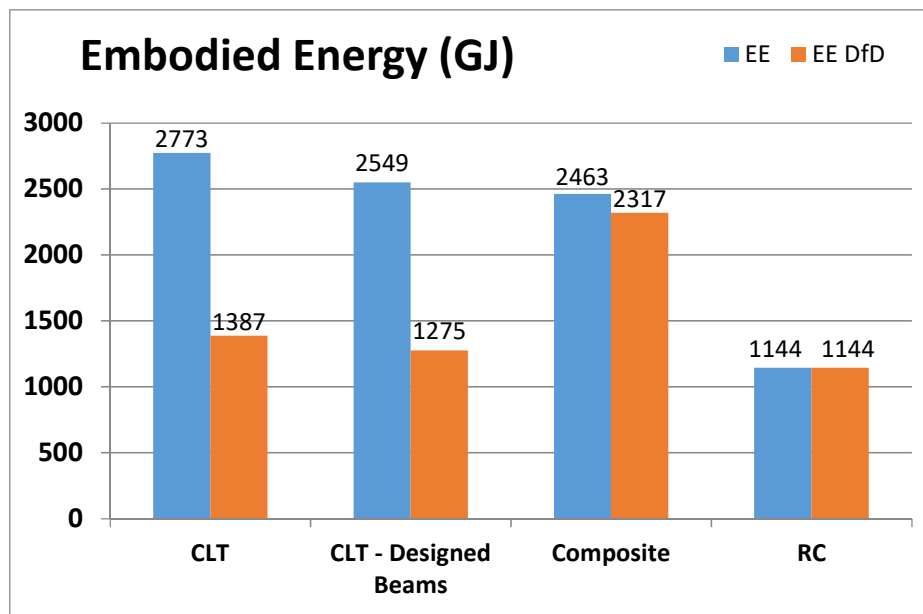
Figure 3.10: Construction system comparison – Total Embodied Energy (GJ)

Figure 3.11 and Figure 3.12 show how the environmental impacts are distributed across the different materials in the superstructure of the compared systems.

Embodied Carbon, CLT Design (kgCO2e/m²)

- CLT: 16.0
- Steel: 39.2

Total = 55.2 kgCO2e/m²

Embodied Energy, CLT Design (MJ/m²)

- CLT: 757.4
- Steel: 550.7

Total = 1308 MJ/m²

Embodied Carbon, CLT - designed beams (kgCO2e/m²)

- CLT: 16.0
- Steel: 31.7

Total = 47.7 kgCO2e/m²

Embodied Energy, CLT - designed beams (MJ/m²)

- CLT: 757.4
- Steel: 445.2

Total = 1203 MJ/m²
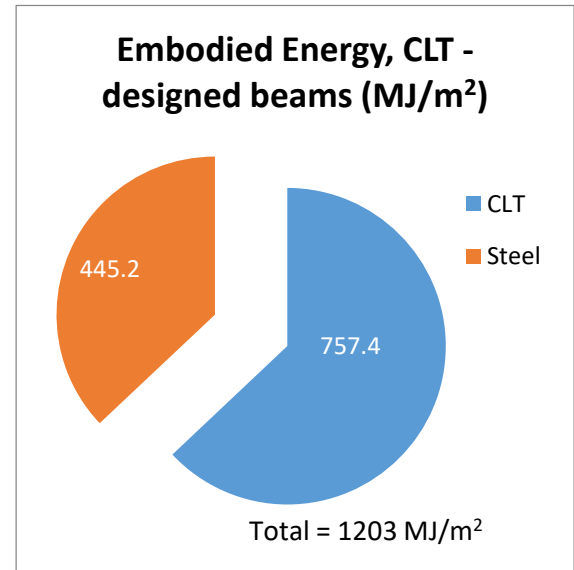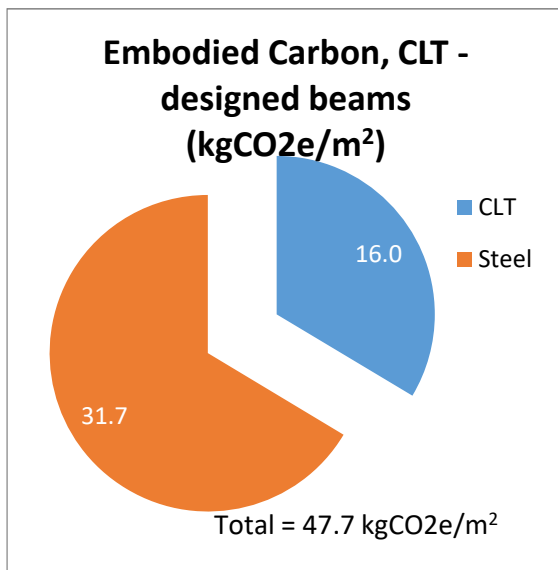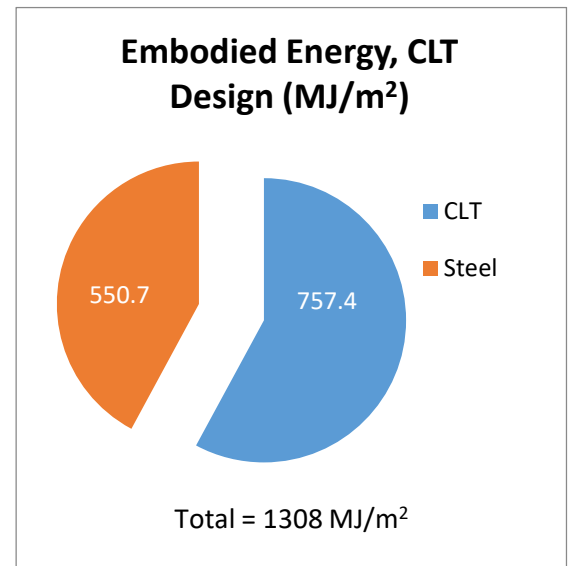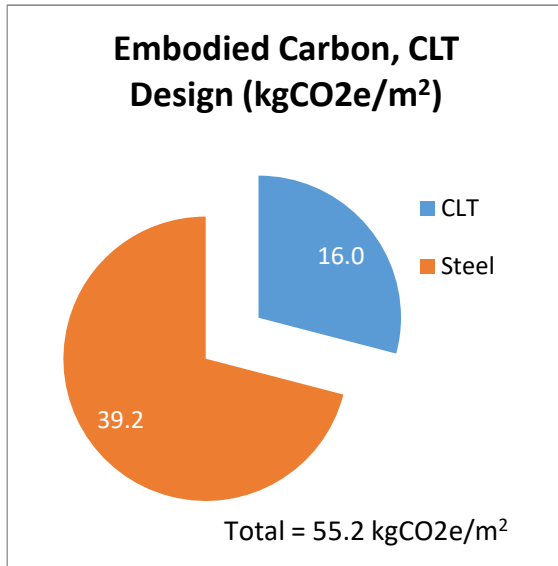
Figure 3.11: Embodied Carbon and Energy for CLT Hybrid Systems (per m²)

Embodied Carbon, Steel Composite Design (kgCO2e/m²)

- Steel: 31.2
- Concrete: 47.4
- Mesh: 3.1
- Steel Deck: 20.6

Total = 102.4 kgCO2e/m²

Embodied Energy, Steel Composite Design (MJ/m²)

- Steel: 438.1
- Concrete: 327.5
- Mesh: 38.6
- Steel Deck: 302.8

Total = 1106 MJ/m²

Embodied Carbon, Concrete Design (kgCO2e/m²)

- Concrete: 64.7
- Reinforcement: 1.5

Total = 66.2 kgCO2e/m²

Embodied Energy, Concrete Design (MJ/m²)

- Concrete: 446.3
- Reinforcement: 18.9

Total = 465 MJ/m²

Figure 3.12: Embodied Carbon and Energy for conventional construction methods (per m²)

43

3.5   Discussion of LCA Outcomes

The case study gives a demonstrable example of how the use of a CLT-ASB hybrid system can reduce the embodied environmental impact of the superstructure elements, even when taking into account the relatively large embodied energy of the CLT panels. In this section, the results are explored and their relative significances established.

3.5.1 Influence on Operational energy

This section mostly relates to how the construction material affects the need for temperature control and ventilation. The need for heating/cooling and ventilation is related to the fluctuations in internal temperature, and this is greatly affected by the thermal mass of the building structure, particularly the floor slab[144]. Thermal mass smooths out the fluctuations in internal temperature, hence reducing the amount of heating and cooling. Thermal mass also helps drive convection currents that allow passive ventilation systems to function. Concrete has high thermal mass, which enables it to perform these functions well. CLT has much lower thermal mass so will not be able to fulfil these roles in the same way.

3.5.2 Construction, Maintenance and Demolition

The potential improvements to the construction and/or demolition processes could be significant. Because of the CLT panels' light weight, it will be possible to use smaller, more efficient cranes, and as timber can be secured using simple connections, the construction process can be sped up considerably. Existing CLT structures have been built in a matter of weeks e.g the CLT superstructure of Bridport House (41 social housing apartments across 8 storeys) was completed in 10 weeks[80], which compares very favourably with all-concrete or composite structures which are limited by the curing time of cast-in-situ concrete. Steel frames, if bolted, are similarly speedy to construct. The CLT panels themselves are self-contained and factory-made meaning there is no need for specialist trades such as reinforcement fixers etc. and generally less construction staff overall. Alongside this, delivery of the panels (providing the panels are subsequently stored correctly) can be contained to a concentrated set of lorry deliveries at the beginning of the construction. The increased cleanliness extends to the structural elements themselves – machinery used to make modifications to the panels whilst in place can be lower powered, less noisy, and create less dust as the fixings can be readily made. As outlined in the previous section, the reduction in the number of construction staff, the number of delivery lorries and the timescale of construction will all reduce the environmental impact of the construction phase for the ASB-CLT system.

Maintenance-wise, the system should provide a flat soffit, allowing services to be more easily integrated, which facilitates quick and easy maintenance. If further services need to be added or modified, the fixtures to be changed are not difficult to deal with as timber fixtures are relatively simple to remove. For the timber itself, it will be important to protect the panels from insect attack and potential exposure to water. The environmental impact of the products used for this task must be accounted for, though this may be tempered by the fact their use will contribute to the reuse of the panels.

The demolition process, if the system is utilised appropriately, should become more of a dismantling process, with the construction phase being performed in reverse. Unlike current structures, there should be no high disruption, high energy destructive processes that then leave a large amount of leftover material to be dealt with. From an environmental perspective, this means less construction waste going to landfill, fewer emissions from machinery, and the ability to reuse or recycle large portions of the superstructure.

3.5.3 Foundation simplifications

Whilst the superstructure dead weight is not the only loading supported by the foundations, and the contribution of imposed load is clearly important, the degree of reduction in superstructure mass when using the CLT-ASB system rather than existing construction methods is significant.

The proposed system is envisaged to be supported by conventional foundations. Here the low weight of the superstructure has a threefold benefit - firstly compared to current systems, foundations could be smaller or have less reinforcement, simplifying and accelerating that phase of construction. Secondly, it allows for multi-storey construction in locations where the ground quality is too poor for existing systems. Thirdly, the combination of these factors will mean a reduced cost associated with foundations, a similar conclusion to that found in the Skidmore Owings & Merril report[19].

In previous work of the author, a simplified means of approximating comparative foundation extents was used[135]. Considering only vertical compression loads, and assuming pad foundations supporting columns, when the ratio of one superstructure method to another is given by λ, the ratio of the foundation volumes will be approximately $\lambda^{3/2}$. This method would give foundations in the proposed system that are a mere 15% of the size of that for a conventional composite structure. However, this is a very crude estimation method – the influence of additional loading, the need to resist moments, and practicalities such as re-bar detailing will serve to bring the relative foundation sizes closer together in required extents. This area is worthy of further study and refinement, especially as the foundations will represent a significant portion of the cost, construction time, and environmental impact of a multi-storey building.

3.5.4 Optimisation of beams

Over the course of the design process in the LCA, it became clear that the available ASBs in the catalogue were overdesigned for the situations and geometries under consideration. To improve utilisation of the beams and provide more efficient material usage (of the material with the highest embodied carbon and energy density), hypothetical slimflor beams were designed and the LCA performed again. Using these beams rather than the smallest ASB, the environmental performance improved by 14% in embodied carbon and 8% in embodied energy. This is an area for further potential development, though a balance must be drawn between designing the most materially efficient beam for a situation and maximising the potential to reuse the beam in a different structure. It would appear prudent to design a selection of beams that are smaller than the smallest catalogue ASB, and are standardised but more appropriate for CLT-ASB structures. Likewise, it may be advantageous and appropriate to use fabricated sections in the system, rather than rolled sections that require huge

investment to develop the mills. Using fabricated sections also give the potential to control distribution of steel within the beam section for optimal section design for the system. Taking the beam optimisation further, embodied environmental impacts could be reduced through the use of cold-formed sections. Cold formed sections have a reduced embodied energy and carbon per kg as they are created from steel sheeting, so the energy required is limited to the manufacture of the sheets alone rather than a hot rolling process.

3.5.5 Reusability

Taking into account the potential for reuse improves the performance of the CLT-Steel Hybrid significantly. The results, taking into account design for deconstruction and reuse, shown in Figure 3.9 and Figure 3.10, are predicated on all major structural elements being available for use for a second building's life cycle. With suitable connections between the CLT panels and the ASBs, combined with the use of bolted connections in the steel frame, a relatively simple disassembly process should result, with little wastage. Whilst not assessed here, the embodied carbon and energy associated with construction and disassembly phases will be reduced as construction will be quicker, cleaner, and require less manpower. The design of the shear connections will be key to maintaining this property. In ideal circumstances, the connector will not induce damage to the CLT that will significantly weaken the timber, either in installation, use, or disassembly. If the connector zone does become damaged, reuse of the panel would only be possible after those sections are removed – hence introducing extra processing as well as wastage and a limitation to the spans that the panels can be used.
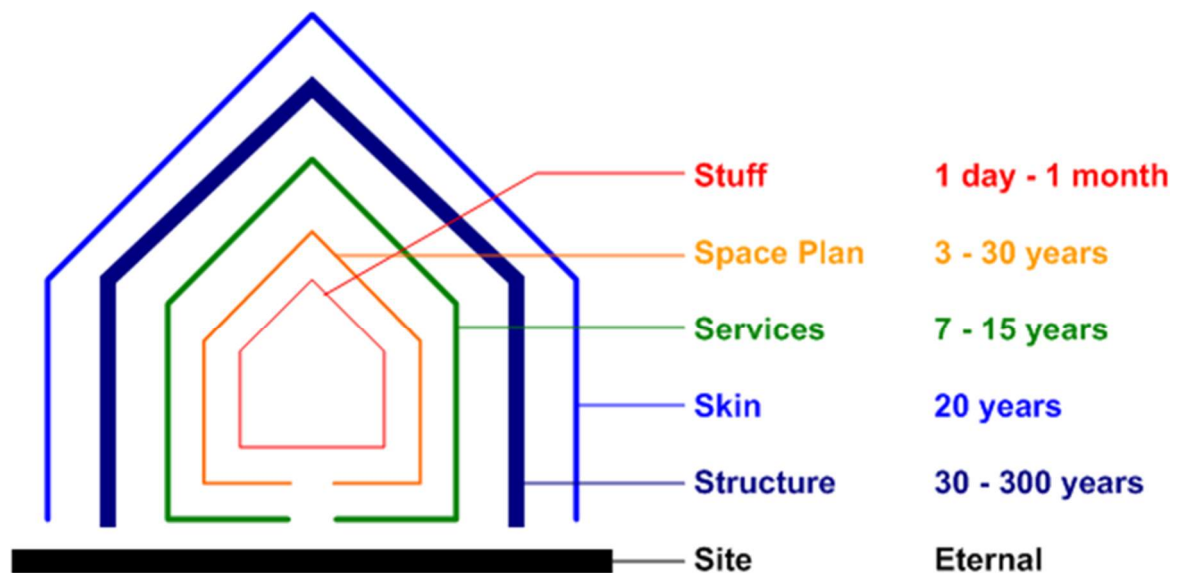
Figure 3.13: Stewart Brand's 6 S's approach to interpreting building make-up[145]

The principles of design-for-deconstruction will need to have been followed during fit out to obtain the most reuse potential out of the building and also to facilitate maintenance of services and non-structural

finishes. This will involve taking into account the differing layers and their respective service lives and, as outlined by Guy and Ciarimboli[145] and visualised in Figure 3.13, considering these components as "shearing layers of change" is a means of doing this.

3.6   Chapter Conclusion

From the study performed in this chapter, it suggests that in answer to research question 1, yes, the substitution of CLT floors for concrete slabs can be justified by environmental by a reduction in environmental impact. This chapter has explored a combination of qualitative and quantitative assessment, and hence the exact reduction cannot be estimated in general, but this is the case when considering any structure as so much depends on the specific site characteristics and requirements of the structure. This is not an unequivocal answer though.

In this case study explored here, a mixed picture is found whereby the embodied carbon reductions are stark but the embodied energy is higher for the CLT-steel hybrid. This certainly deserves further scrutiny. However, the qualitative assessments of the other contributing factors such as construction works and reusability do compound the environmental benefits of the embodied carbon reductions and may offset the embodied energy figures.

Chapter 4. Finite Element Modelling 1: CLT

4.1   Synopsis

This chapter covers the development of finite element modelling methodology that produces a representation of the mechanical behaviour of CLT suitable for the simulation of the ASB-CLT system. It collates and reviews the existing extent of relevant research that uses the finite element method applied to similar issues, before detailing the stages of development of a CLT model including verification against physical tests performed on CLT panels from the literature.

4.2   Technical Literature Review B: Modelling of Timber and CLT

4.2.1 Finite Element Modelling of Timber

Guan & Rodd[96–99] researched the reinforcement of dowel connections for timber structures with Densified Veneer Wood (DVW). Their research has relevance to research into the connection method for the system as their aim was to reduce the risk of brittle failures. In their studies, timber in tension was orthotropic elastic, and in compression it was modelled as elastic-perfectly-plastic[96]. The reinforcing plates were modelled as elasto-plastic. The models were verified with laboratory testing[99]. However, because their models were of a setup that had already been established to prevent brittle failure, and one in which the dowels and reinforcing DVW dominated the overall behaviour, there was no need to incorporate brittle failure of the timber into their models. The approach adopted was sufficient to simulate the real-world deformations and rotations in the joint in question.

Failure of timber beams around a fastener hole has been simulated in the ABAQUS software by Williams et al[146], exploring the capabilities of timber sections that are to be reused. A multi-step approach was taken, with removal of failed elements and re-meshing accordingly to approximate the crack propagation and load redistribution. This produced good agreement with mechanical tests.

Timber beams strengthened by Carbon Fibre Reinforced Plastic (CFRP) were modelled in ANSYS by Kim & Harries[147]. Mechanical properties were input to simulate the timber's anisotropic behaviour, but only a simple failure criterion (i.e. when longitudinal stress levels exceed the modulus of rupture) was incorporated, neglecting crack propagation as beyond the scope of the research. This may account for the discrepancies encountered between the model predictions and the experimental results.

In 2012, O'Loinsigh et al[148] used a combination of these approaches to model Glulam beams made with driven wooden dowels. Timber in tension was modelled as orthotropic elastic with a brittle failure criterion added. Van der Put[149] quantified the energy available for crack propagation in timber.

In 2006, Ellegaard modelled nail plates in timber knee-joints in a bespoke MATLAB finite element formulation[150]. Zhou & Guan[151,152] have also modelled nail plates in timber, but in much more detail.

Their study related to the embedding strength of the nails and resulted in a detailed model and sound methodology for simulating the behaviour of the nail and timber to predict embedding strengths.

In her 2012 PhD thesis, Sandhaas[65] produced a comprehensive development of finite element representation of timber for use in modelling the behaviour of timber connections using dowels with an intermediate steel plate, similar to the flitch plate configuration. This study involved the development of a bespoke subroutine in the FE analysis software, ABAQUS, collating mechanical properties from previous work, and validating against physical tests. Alongside this, a series of physical tests on the joint in question were performed, and the test configuration created in ABAQUS to determine the success of the modelling approach. Sandhaas's formulation successfully implemented the anisotropy and post-yield behaviour of spruce, including stable strain softening, however this was not able to reflect redistribution of stresses after the failure of overstressed elements.

4.2.2 Modelling CLT

The modelling of Cross-Laminated Timber can be split into two aspects – the modelling of the constituent timber, and the modelling of a CLT panel.

Existing CLT Models

The CLT handbook[75], produced in the United States in 2013, has a useful collection of the main aspects relating to using CLT in construction, and includes sections on modelling CLT in bending and in-plane shear (lateral loading on walls). Unfortunately, however, the methods collated are not appropriate for this research project – bending is approximated using the shear analogy method which, whilst giving good predictions of the bending of a CLT element, cannot be used to develop an effective width or be easily modified to incorporate a stiffening steel beam. Similarly, the lateral performance of walls assumes CLT panels to be rigid bodies and instead focusses on the behaviour of the connections rather than the internal mechanics of the panels subject to in-plane shear. The CLT handbook guidelines are based on the findings of Blass and Fellmoser in 2004[88] and Gliniorz, Mosalam & Natterer[153]. Whilst this presents a methodology for calculating stiffness and subsequent deflection, this does not transfer readily into the effective width and shear lag question.

In the development of his timber-steel hybrid floor system, Loss[103] has devised a means of modelling the influence of CLT panels on the composite section. In contrast to the work in this thesis, Loss used the analysis software SAP with CLT panels represented by plate elements. For this, the gross properties of layered CLT have been homogenised into its overall stiffnesses in the two planar axes. This simplification is possible because in this arrangement of elements, with the CLT above the steel member with which it is acting compositely (see Figure 4.1), the entire depth of the CLT is in compression.

In addition, quantifying the effective width of the CLT was not a key part of the research process. Suitability of the connections in this system was determined through an extensive testing regime rather than an FE study.

(i) Elements to be assembled

(ii) Assembly of elements

① CLT panel ② Steel thin cold formed beam ③ I-B-7 beam-to-panel connections ④ I-A-1 beam-to-panel connections
⑤ Panel-to-panel connections [FE] Floor composite elements [BE] Bracing wall composite elements
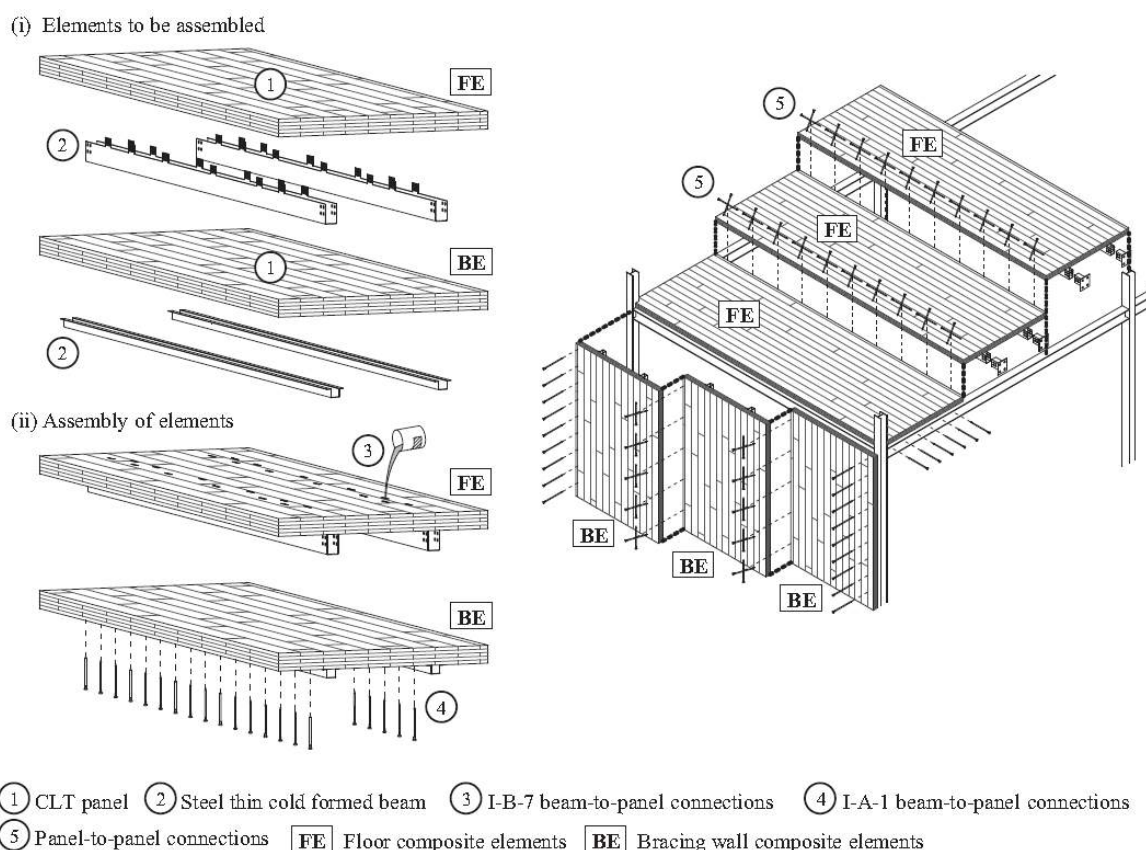
Figure 4.1 - Hybrid CLT-Steel system in development by Cristiano Loss[103]

The research paper of Mestek, Kreuzinger & Winter[154] detailed techniques for the design of uniaxially spanning CLT panels, whilst also performing theoretical and experimental investigation into panel twisting. In it, they made comparison between the shear analogy method of Kreuzinger[85] (the basis of design given in the CLT Handbook and Annex D of DIN 1052) and FE simulation using quadratic shell elements that were cross-linked manually. Using this approach, they found that whilst there were inconsistencies of shear stress results in the locality of the load when a concentrated load is applied, the more critical parameter of rolling shear can be reflected by the shear analogy method beyond a distance equal to the plate thickness away from the load.

In 2010, Mestek and Winter[155] investigated the reinforcement of CLT panels with inclined screws to enhance the strength of the panels in situations where rolling shear failure is induced. In this paper, the CLT was modelled in the FE software, Sofistik, and using a "girder-grid" approach in an attempt to gain more accurate responses to concentrated loading than volumetric or shell elements. The paper highlighted that the approach was more suitable for CLT elements that had layers of equal thickness. The investigation used the modelling approach to replicate experimental testing arrangements used to certify CLT panels in Europe, in order to simulate what the certified characteristics of a panel would be if reinforcing screws were used.

In 2011, Mestek, Kreuzinger and Winter collaborated again[156] developing the research of Mestek and Winter[155] detailed above. Physical tests were performed on the reinforced panels and the results

compared, this time to FE models comprising of solid elements and analysed in ANSYS. With the test setup of a panel simply-supported on all sides and subjected to a central patch load (inducing biaxial bending of the panel), the FE simulation was used to derive the rolling shear stresses, however, the calculated stresses were 70% higher than the rolling shear capacities of the panel that had been determined via 4-point bending tests.

Thomas Bogensperger has been involved with some of the most advanced work on modelling the behaviour of CLT. Since 2006 at TU Graz, development has been taking place into a bespoke CLT element that encompasses all the shear mechanisms appropriately[157–159]. In 2010, Bogensperger's collaboration with Moosbrugger, and Silly[158] developed (and verified through testing) a means of numerically modelling the in-plane shear behaviour of multi-layer CLT using Representative Volume Elements and Sub Elements (RVEs and RVSEs). With this approach it was possible to account for two components of shear deformation that arise – a direct shearing component and the torsional component – such that the influence of lateral gluing within layers of CLT boards could be taken into account.

In 2011, in conjunction with Augustin and Shickhofer, the behaviour of CLT under compression perpendicular to the plane of the panel was investigated by Bogensperger, and subsequently modelled in FE software[160]. Whilst this was a very complete and well formulated exercise, deformation of this kind is not of significant interest in the context of composite action between CLT and a steel beam. However, the methodology of modelling the timber as an elastic-plastic material has been adopted, and the orthotropic material parameters suggested in [160] were used for the first stage of modelling in this research, detailed in section 4.3.3.

Gubana[86] studied composite sections formed of CLT panels joined to GluLam beams in 2008. In her study, the proposed system comprised of 3-layer CLT panels positioned above the glulam beam section, joined by metal dowel connectors. As part of her investigation, CLT panels were subject to physical testing in compression, tension and shear and concluded that joining CLT panels compositely to timber beams showed potential as a restorative technique, and were able to transfer seismic forces through diaphragm action.

4.3   Analysis using Finite Element Software (Initial Model Development)

4.3.1 FE using Commercial Software

FE modelling was performed using version 14.5 of ANSYS, a well-known and established software for finite element analysis. This version includes the Workbench interface which makes setting up the 3D geometry of the problem less time consuming as the Graphical User Interface makes modelling fairly intuitive. It is possible to create user defined materials, and it supports anisotropy and plasticity. ANSYS allows composite materials with different meshes to be assembled together, and also has a Crack

Modelling feature that could be applied for investigating delamination, though the crack position must be manually input[161].

However, there is debate over the ability of ANSYS to handle non-linear problems and the ease with which the user can input a bespoke element[162]. There is also a maximum of 256,000 nodes permissible in Structural models under the Academic license. Lastly, the software cannot define a negative stiffness at any point of the stress strain curves, therefore strain softening cannot be modelled completely.

Other commercial software e.g. ABAQUS has been used to model timber for construction, and ABAQUS, in particular, has greater utility and has yielded greater success in the modelling of timber in the literature.

4.3.2 Aims

Initial simple models were created to approximate the contribution of CLT to a composite section. The desire was to keep models as simple as possible and reduce the duration of the solving process.

4.3.3 Material Characteristics

The CLT was initially modelled with solely elastic behaviour incorporated as deflection in service is the pertinent property being investigated rather than the ultimate load and failure mechanisms. Disregarding post-yield behaviour is also beneficial to the solving process, decreasing the time of solution.

In a previous study (the MSc thesis of the author[135]), data from KLH for the bending of CLT panels was assumed to calculate the modular ratio – a Young's modulus, E, of 12GPa. The panel manufacturer, KLH, specifies its products as having the mechanical properties given in Table 4.1. The axis subscript "0" refers to the spanning direction of the panel, which is consistent with direction of the longitudinal axes of the laths in the top and bottom layers; subscript "90" refers to the direction planar-orthogonal to the panel span direction.

This data is insufficient to represent the shear lag response of the panel. When considered in the axis system shown in Figure 4.2, the moduli of elasticity, $E_{0, mean}$ and $E_{90, mean}$, are E_z and E_x respectively.

Table 4.1 - CLT panel mechanical properties, from KLH[13]

Modulus of Elasticity	
– Parallel to the direction of the panel grain $E_{0, mean}$ --------------------------	12 GPa
– Normal to the direction of the panel grain $E_{90, mean}$ -------------------------	370 MPa
Shear modulus	
– Parallel to the direction of the panel grain G_{mean} ----------------------------	690 MPa
– Normal to the direction of the panel grain (rolling shear), $G_{R, mean}$ --------	50 MPa

Similarly, the shear modulus, G_{mean}, relates to shear forces acting in the yz-plane, and $G_{R, mean}$ relates to shears in the xy-plane. The shear lag effect is concerned with responses to differential shear in the xz-plane, for which the CLT manufacturer datasheets do not cover.
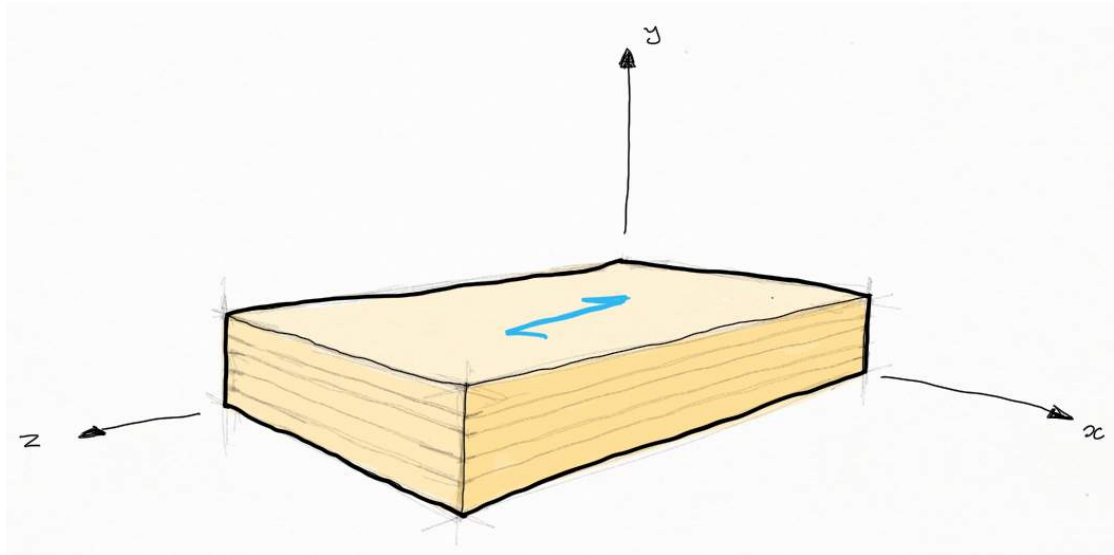
Figure 4.2 - CLT Panel Axis Reference

When making analogies to solid timber elements, the main span direction of the panel is equivalent to the longitudinal axis of solid timber. In modelling solid timber, a common simplification is to make the properties of the radial and tangential axes equal, and this was also done by Bogensperger et al.[160] modelling CLT subjected to compression perpendicular to the plane.

For the preliminary set of models, the parameters used by Bogensperger et al. were used. This involved dividing the panels in the FE model into the required layers and the layers are given differing reference axes to show the alternating orientations of the wood.

4.3.4 Model Setup

The primary aim was to establish the upper limit of composite benefit and an estimate of the quantitative benefit of connecting the slab to the steel beam. Under consideration is the smallest ASB section (280ASB74) in combination with timber floor slabs of KLH's 7ss-230 CLT section (a 5-layer panel but with double thickness outer layers, hence the "7-ss" designation).

The slabs rest on the bottom flange of the beam, with the slabs modelled as either rigidly fixed to the beam or with a friction contact (representing the zero-composite-action case). The influence of the connection between beam and slab is explored in detail in subsequent chapters (sections 5.3 and 6.3). The models created during this part of the study use a single part to represent each layer of the CLT panel, with the full length of the beam, along with half the span of the floor slabs is modelled. A line of symmetry is used on the centreline of the beam. Figure 4.4, Figure 4.3 and Figure 4.5 show the initial model mesh and arrangement. The region near the CLT-ASB connection was to be of interest, so the mesh refinement was increased in this zone (see Figure 4.3).

ASB section

CLT panels, with mid-span constraints modelling central symmetry
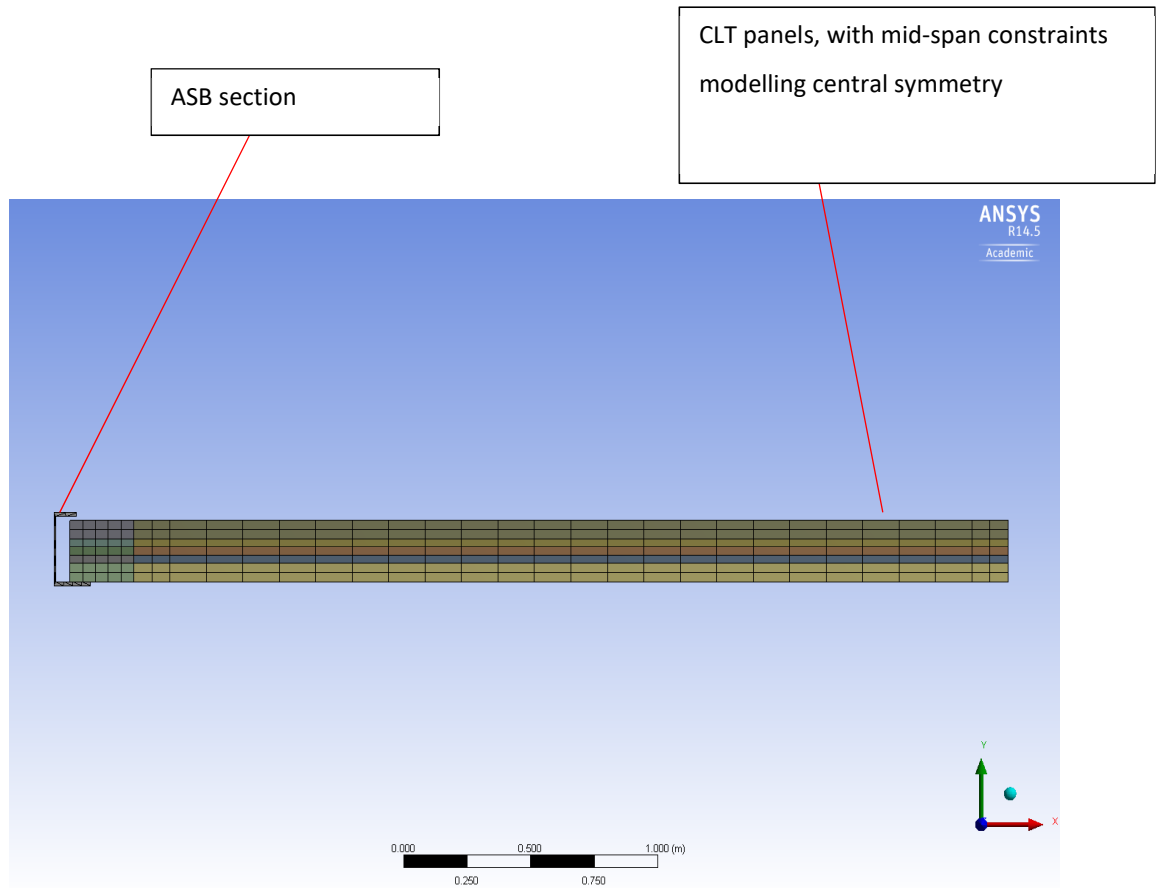
Figure 4.4: Preliminary FE model - extents

Half of ASB section, with symmetry constraint applied

Increased mesh density in connection zone for greater detail in area of interest

ASB-CLT interface
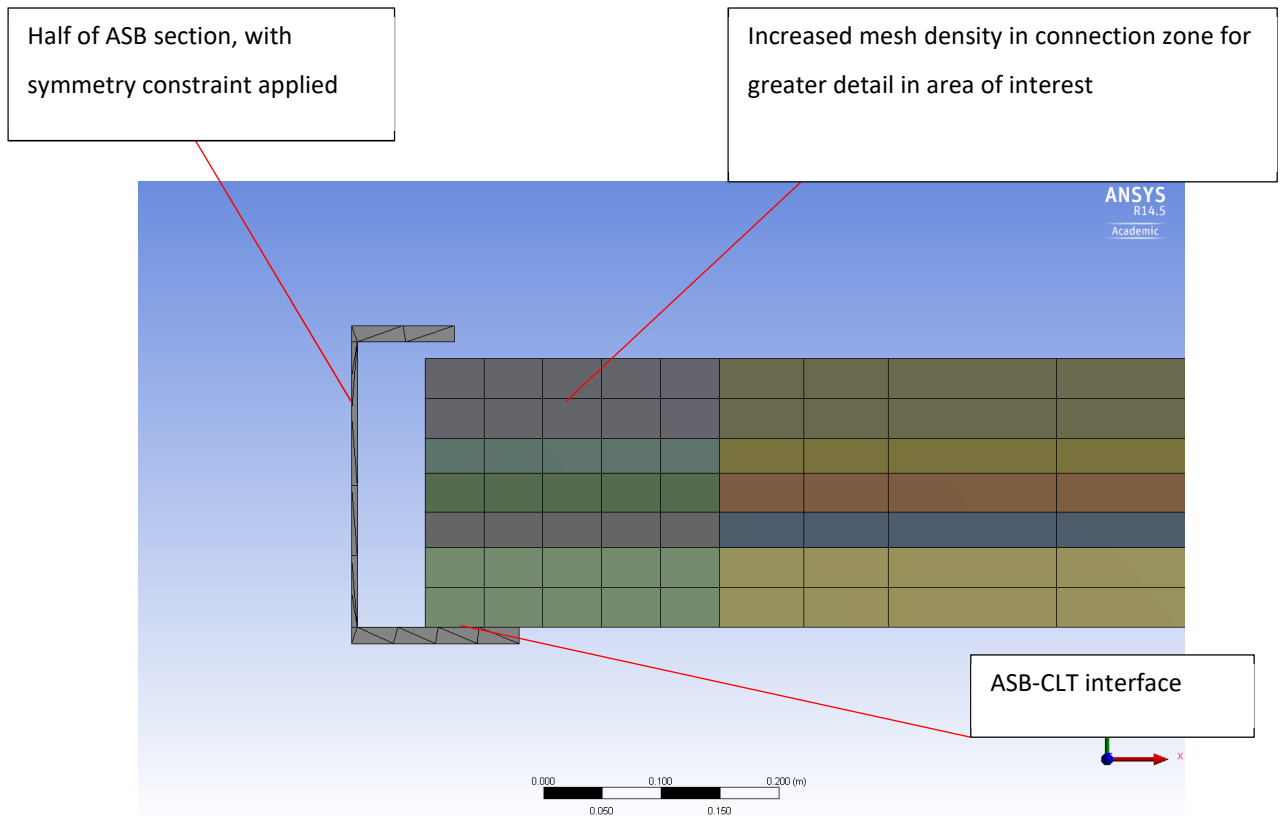
Figure 4.3: Preliminary FE model – connection zone

The beam consists of solid elements, with displacement constraints at the nodes at the ends to represent the simply supported condition. In these analyses, the CLT panels span 9m (4.5m modelled), and the beam spans 7.5m. An imposed load of 2kPa was applied, and permanent loads (self-weights) are included. A measurement of deflection was taken as the maximum vertical displacement of the nodes at the mid-line of the beam; the change in this output parameter was used to determine the degree of benefit arising from composite action.

At first, the interfaces between the panels were assumed to be completely unbonded, with the contact defined by a friction coefficient of 0.6. This high value of friction coefficient was chosen as the concern was that the friction forces, when combined with the compression on the upper faces of the timber, could induce localised over stressing of the wood causing failure of the system. Using a high friction coefficient aimed to highlight whether this was a possibility.
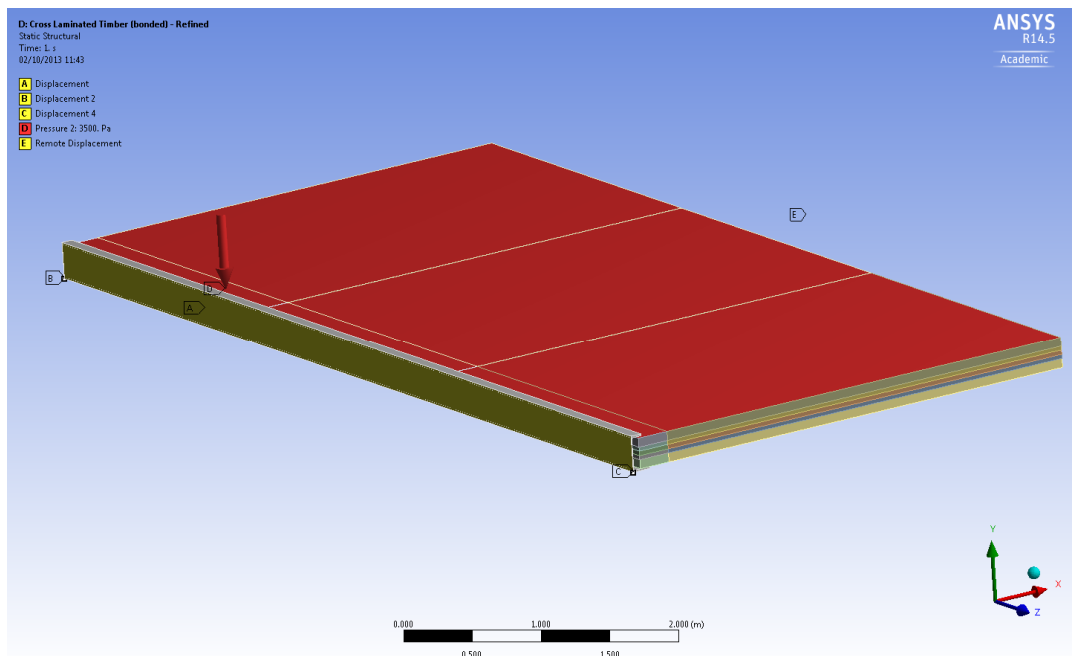
Figure 4.5: Preliminary FE model – Loading and constraints arrangement

4.3.5 Findings:

A series of analyses were run with variation of the connectivity between the timber panels to each other and to the ASB section. The goal was to provide an upper limit on the potential composite enhancement. The results of this are summarised in Table 4.

The initial finite element models show the potential for composite action to have a modest impact on deflections. Comparing against the "non-composite" case, where the timber slabs rest on the beam lower flange (δ=20.3mm), the use of a bonded connection between the slabs and the ASB leads to a 6.5% reduction in (δ=18.98mm).

Table 4.2: Summary of preliminary FE model results under 2kN/m² area load (beam: 280 ASB 74, span = 7.5m; panels: KLH 7ss-230, span = 9m)

CONNECTION LAYOUT	DETAILS	BEAM DEFLECTION
	• Panels resting on flange (non-composite) • Panels independent from each other	20.3 mm
	• Panels fixed to flange (fully composite) • Panels independent from each other	18.98 mm
	• Panels fixed to flange • Full-depth bond between panels	16.41 mm
	• Slab fixed to flange • Tension-zone only bond between panels	16.8 mm
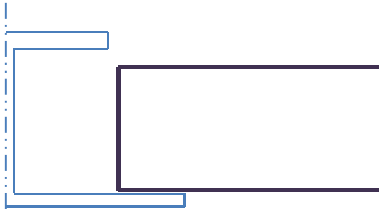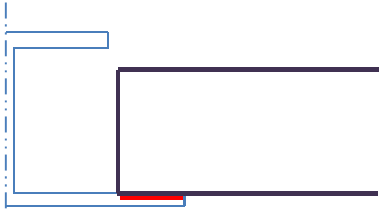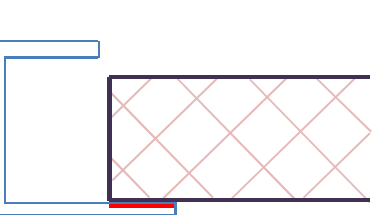
In conventional composite construction in the SlimFlor arrangement using precast concrete panels, the panels are connected to each other by a cast in situ concrete topping. As concrete has negligible tensile strength, there is no connection at the bottom of the planks. When using timber panels, the situation can be done differently – the timber has much greater tensile capacity than that of concrete, and which is much larger relative to the compressive strength than is the case for concrete. Hence, there is further capacity that can be drawn by connecting the panels together more substantially.

The results in Table 4 show that if the panels are fully connected to one another, the magnitude of deflection improvement rises to 19% (δ=16.41mm). If just the bottom two layers are bonded (the upper interfaces have frictional contact assumed) then the improvement is 17% (δ=16.8mm), showing that the majority of the difference is due to the engagement of the tensile stiffness of the CLT section.

This work shows the importance of the panel-to-panel connection, particularly in the tension zone. For an appreciable improvement in stiffness, the tensile strength of the timber must be induced and tensile forces transferred across the interface of panels in some way. The design of the inter-slab connection will therefore also be of high importance for composite behaviour between CLT slab and steel beam to be developed.

4.3.6 Revisions

Up to this point, the models applied the material properties used by Bogensperger et al.[160] in their investigation of CLT subjected to compression perpendicular to its plane. They simplified their FE material model so that the properties in the radial and tangential directions of the constituent timber were equal. This is a suitable (and computationally efficient) simplification for compressive loading perpendicular to the plane as the main resistance to the loading is not from the radial and tangential directions. This means it can be assumed the response in these axes are similar, however this is not the case for this research. The fact that the panels have an odd number of layers (see illustration in Figure 4.6) means the response to in-plane loading will be different depending on the direction of action, as more or fewer of the layers will be orientated with their strong axes offering resistance, and the depths of the layers are not equal.
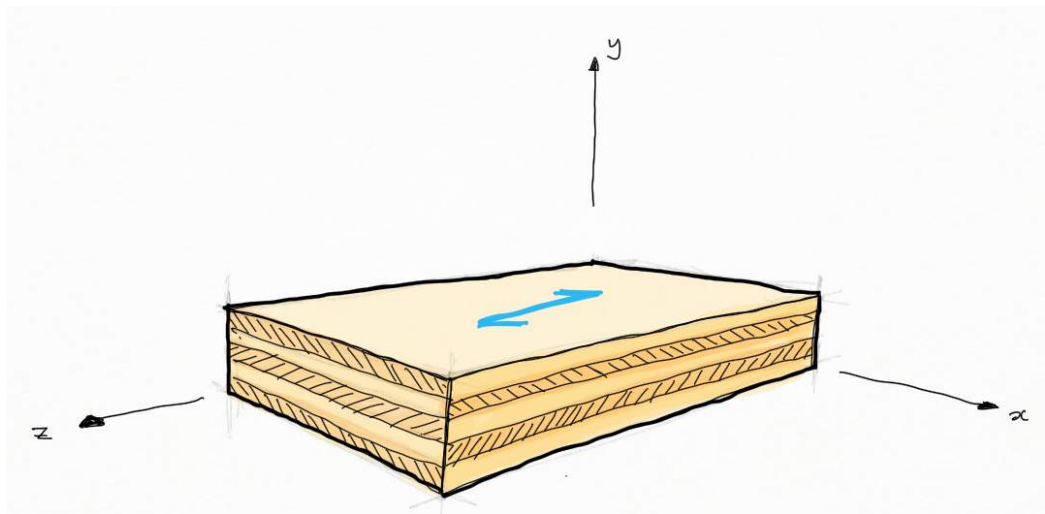
Figure 4.6 - CLT Panel, showing layer build-up

This necessitates, as a minimum level of detail, the incorporation of the layers of the CLT as independent pieces rather than the entire panel, as well as independent properties in the two weaker axes.

In making the revisions to the material model, the following characteristics were assumed:

- Documents from CLT manufacturers suggest that Spruce is most often used for the panels, so data for this species of wood is used.
- Grade C24 timber is assumed.
- Moisture content of 12% is assumed. The mechanical characteristics of timbers fluctuate according to the moisture content of that timber, but 12% is used as this is the manufacture target, and the design value used in calculations. The slats are left to dry to this moisture content before panel manufacture.

The material model, Spruce1, developed for this purpose was given the properties in Table 4.3, which were derived using Ch. 4 of "Wood handbook: wood as an engineering material"[163], compiled by the United States Department of Agriculture (USDA) Forest Service.

Table 4.3 - Properties of Sitka Spruce for use in FE analysis (derived from Tables 4.1 to 4.3 of the reference[163])

Property	Symbol	Value
Young's Modulus (Longitudinal)	E_L	10.89 GPa
Young's Modulus (Radial)	E_R	0.849 GPa
Young's Modulus (Tangential)	E_T	0.468 GPa
Shear Modulus (L-R)	G_{LR}	0.697 GPa
Shear Modulus (L-T)	G_{LT}	0.664 GPa
Shear Modulus (R-T)	G_{RT}	0.033 GPa
Poisson's Ratio (L-R)	v_{LR}	0.372
Poisson's Ratio (L-T)	v_{LT}	0.467
Poisson's Ratio (RT)	v_{RT}	0.435

4.3.7 Material Failure – Mechanisms, Detection and Practicalities

The CLT panel is a composite element in its own right, a composite of a series of timber laths connected to one another by glue layers. Failure of the panel can arise in the timber, in the glue, or at the interface between the two. Similarly, the connectors (inter-panel or shear connectors) can fail in the timber, in the connector, or by a combination of the two through loss of interaction. Timber failure is a deeply complex topic, to which this entire thesis could be devoted. This is partly due to the anisotropic nature of timber that extends beyond the elastic properties but also to the manner failure, and is covered more deeply in Chapter 2. To minimise computational expense as much as possible, whilst capturing all relevant parameters, the yield stresses in compression and tension for all three material axes need to be integrated. In this manner, despite the orders of magnitude difference in yield stresses in the different timber axes, and between timber and the connection, one can simply interpret any plasticity found in the model as failure of the system. The material model was updated to include yield stresses from a variety of sources, which are presented in Table 4.4.

Table 4.4 - Parameters used to define boundary of elastic behaviour in FE material model for spruce (LR = Longitudinal – Radial plane; LT = Longitudinal-Tangential plane; RT = Radial-Tangential plane)

Parameter used	Value
Ultimate tensile strength (tangential)[163]	2.6 MPa
Ultimate tensile strength (radial)[163]	2.6 MPa
Ultimate tensile strength (longitudinal)[163]	59.3 MPa
Compressive *yield* stress (longitudinal)[163]	35.7 MPa
Compressive *yield* stress (tangential)[160]	2.1 MPa
Compressive *yield* stress (radial)[160]	2.1 MPa
Shear *yield* (LR)[164]	4.17 MPa
Shear *yield* (LT)[164]	2.98 MPa
Shear *yield* (RT)[164]	0.93 MPa

In direct compression, the failure process is one of progressive crushing resulting from the cellular structure of the native timber, and hence has a degree of plastic deformation and strain softening. This can be captured fairly readily by the FE software given appropriate parameters.

Detection of failure in such a system requires more elaborate techniques than the usual features of most commercial software. In this case, it is useful to identify failure of the material by outputting a plot of

plastic deformation, allowing visual verification of where failure may occur. The aim is not to understand or recreate the actual failure mechanisms, but rather to ascertain whether the components remain elastic and hence undamaged after loading. As such, though the material yield process can be captured in more detail by using the multilinear approach (see Figure 4.7), this is unnecessary, and a bilinear implementation suffices for this purpose. ANSYS is not able to capture a negative gradient in such a defined stress-strain curve, which will have relevance in the sections on connections in Chapter 5.
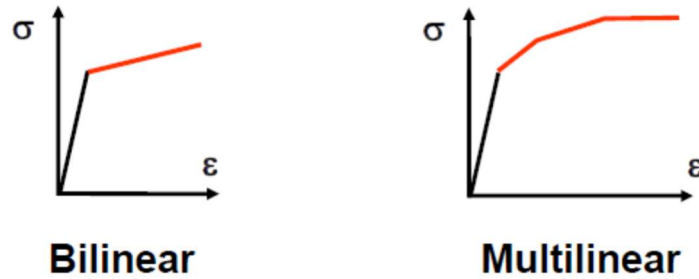
Figure 4.7 - Options for post-yield modelling in ANSYS

The finite element method is most suited to application with isotropic materials, and thus their failure can be defined by the Von Mises, Tresca or Drucker Prager criteria. The use of timber and its inherent anisotropy complicates matters as the anisotropy is not limited to stiffness but also to yield stresses in the different axes, along with having different properties in tension and compression. The more standard features of ANSYS are designed for materials that may have anisotropy of Young's moduli, or anisotropy of yield stress or dissimilar behaviour in tension and compression, but not all three aspects. The first difficulty arises in trying to define anisotropic properties for failure. Elastic stiffnesses in various directions are simple to input. There are two material features that can be used to model anisotropic behaviour – "Anisotropic Elasticity", which was initially chosen, and "Orthotropic Elasticity". Only the Orthotropic Elasticity function is currently compatible with post yield modelling.

Inputting plasticity and failure characteristics which differ between axes of action is more complex. Working within the constraints of Workbench and ANSYS, it is necessary to incorporate features from the older setup of ANSYS (APDL) which are not available within the Workbench environment. APDL is a programming language and environment for the setup and specification of finite element analysis that was previously the main way to use ANSYS, in contrast to the predominantly graphical user interface of Workbench, the modern replacement for APDL. The use of the older features is made possible by using a command input within the tree in the Workbench Mechanical program, which then opens the APDL structure from which the bespoke mechanical properties can be defined.

A feature called "Generalised Hills Criterion" (function TB,ANISO) allows the Young's moduli to be defined in the 3 axes independently, and combined with Bi-Linear plasticity within the same command space. Using the TB,ANISO code may require the use of a legacy element (those that have been superseded by more advanced element types) in certain versions of ANSYS Workbench. The suitable legacy elements, SOLID45 and SOLID65 are both linear elements without mid-side nodes, meaning their

deformation may give less accurate results. In the version of ANSYS used in this research, the contemporary elements (2nd order) were compatible with the use of TB,ANISO.

The revised material formulation was tested through application of load in different directions to a simple block of material, and determining that the displacements vary in the expected manner, however a particular drawback of the Hill's criterion is that it must apply the yield stress equally in tension and compression.

Tensile failure is a brittle failure mechanism that instantaneously removes the contribution of the fibres connected, and stress redistribution must occur. Whilst the tensile failure is modelled as a yielding process, it would be more appropriate if the elements that failed in tension were removed from the model. The feature of "Element Death" would fulfil this concept, and allow greater insight into the capacity of the system and load redistribution after initial failure. It was not possible to successfully include this process without detrimental impacts on the solving process, however this could be an interesting area of further development of the material model.

As the preliminary models did not have plasticity included, one would have to check the levels of stress in the model against material limits. Whilst this is a simple task for isotropic materials such as steel, the anisotropy of timber extends to the yield stresses in each axis. It is not straightforward to determine the stress occurring in a particular axis in a specific piece of timber within a CLT panel, especially as they are alternating in orientation through the layers. However, the approach followed in this project makes use of the plastic deformation result output in ANSYS Workbench. With the material models set up using TB,ANISO and yield stresses incorporated, this allows the use of the conservative approach detailed above of interpreting any plasticity in the analysis model as failure, with those varied properties in each axis. It will also highlight where "failure" may have occurred through combined actions from different axes combining to breach the failure criterion.

This approach has similarly been used by Xu, Bouchaïr & Racher in their investigation of glued in steel rod reinforcement to timber beams[165]. They went a stage further by combining Hill's criterion which defines yield with the Hoffman failure criterion which both allows dissimilar tensile and compressive ultimate stresses and incorporates damage evolution in their analysis, thus enabling some representation of strain softening in the moment-deflection curves.

4.4 CLT Validation Data & Development

4.4.1 Recognition of need for further verification

The desire to match the model performance against further data was driven by two concerns:

1) Concern over hidden failure within the system

Having incorporated the elasticity material boundaries of section 4.3.7, attempts to define an upper bound of composite benefit suggested there was risk of inducing failure in the timber at the connection if a bond was assumed (an insufficiently ductile connection). Further, without the individual laths explicitly modelled, concentration of stresses at the corners of the pieces could not be determined, which may or may not have led to localised failures occurring. Hence the author did not wish to argue the benefit of composite action in a situation where the panel had actually failed. The concern over hidden failure also extends to the connectors by the same logic; a connector failure would lead to a system failure so composite benefit in an arrangement that caused this would be unreliable.

2) Concern over estimation of quantitative composite enhancement

The preliminary models took material properties from the KLH catalogue, though the catalogue data does not have data for behaviour in longitudinal shear. Hence, the author was wary of having overestimated the composite enhancement through the contribution of an inadvertently over-stiff panel. Likewise, as the behaviour of the shear and inter-panel connections have direct influence over the system composite action, it was important to model their stiffness appropriately.

The optimal means of verifying and tuning the model would be a series of full-scale tests, to assess the behaviour of various elements of the system, however this was prohibitively expensive within the scope of available funding for this project. Therefore, a combination of data from literature and small-scale connector tests was used, as will subsequently be discussed.

4.4.2 Primary Verification

The most important behaviour to capture is the in-plane shear response of CLT. This parameter is critical in determining how much of the CLT contributes to the composite section, as it influences the effective width through the phenomenon of shear lag and therefore has a bearing on the degree of composite action that can be determined.

There was limited experimental data available in the literature covering this aspect of CLT's mechanical behaviour. Ashtari[166] faced a similar issue in seeking to use ANSYS to model the in-plane behaviour of CLT panels to assess the diaphragm capabilities of a CLT floor slab consisting of multiple panels, and to reproduce the behaviour observed in experimental testing. The mechanical properties used in her formulation were based on the properties derived by Gsell in 2007[167]. However, these homogenised properties were derived through modal analysis of the panels and verified by out-of-plane bending tests alone, leaving the in-plane properties unverified by experimentation. As such, these research projects were unsuitable for use as sources of CLT panel property data or for verification in this project.

Modelling the reported timber properties as closely as possible permits the identification of timber failure in the complex internal loadpaths of the CLT, highlighting failures that may occur in the radial or tangential axes of the timber pieces, which would otherwise be overlooked.
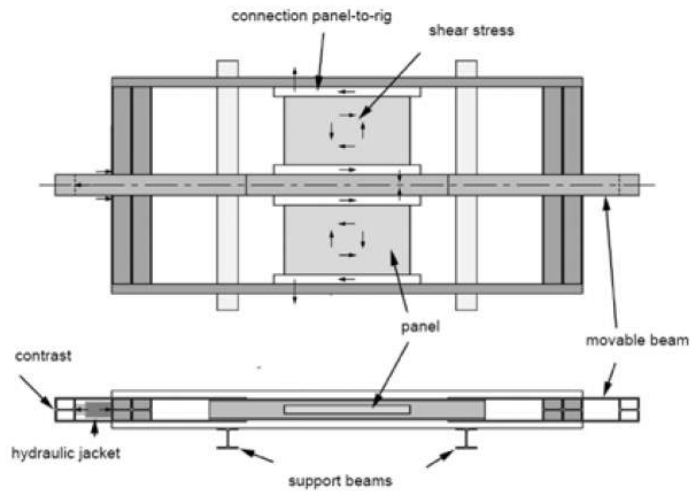
Figure 4.8 - Test setup used in Gubana's research study [86]

Direct testing of in-plane shear properties can be found in the research projects of Gubana[86] and of Bosl[168]. As part of a study into the capabilities of CLT panels to enhance the seismic performance of ancient timber floors, Gubana tested 20 samples of CLT panels in shear, with each test consisting of a pair of CLT samples arranged in a bespoke rig that applied shear to the two panels simultaneously (see Figure 4.8). Each panel tested was built up of 3no. 20mm thick board layers. Whilst Gubana's project investigated the relevant properties in a comprehensive manner and provides a useful comparison, reproduction of the test setup is made difficult by the lack of available information regarding the samples and rig, and the format of test results as stress-strain curves is more challenging to convert. Further the coupling effect of the two panels adds additional scope for erroneous setup in the Finite Element simulation.

The project conducted by Bosl[168], proved to be more suitable for reproduction in a computer model. In Bosl's PhD thesis, a series of tests on CLT were performed to derive test data to incorporate into a numerical formulation. One such test format was of CLT in planar shear. A square piece of CLT, was subject to diagonal tension in a custom made rig. Details of the CLT panel dimensions and the test rig were included, and the outputs are in the format of load-displacement. This, combined with the simplicity of the test setup led to its use as a validation tool in this research.

As can be seen in Figure 4.9, this diagonal tension is resolved into an equivalent shearing force on the panel. This testing provided a useful comparison for the FE models.

The first iteration of the validation model produced in ANSYS replicated the 1200mm x 1200mm panel area and 5-layer characteristics of the panels used in Bosl's investigations, but did not model glue or individual slats. This was the level of detail that had been applied in the model development at the end of section 4.3.

For simplicity, the panel was modelled using the global axes of ANSYS, so that the edges of the panel run parallel to the unit vectors of the global co-ordinate system. The tests performed by Bosl applied tension at 45° to the planar vertices of the panel. In order to apply the load in the same manner within ANSYS, the load had to be decomposed into the equivalent component vectors in the planar axes to define the vectors of loading through each timestep of the analysis. Fixed constraint was applied in one planar corner of the virtual panel (representing the fixity at the corner at the base of Bosl's test setup), with the tension load applied in the corner diametrically opposite. The fixture and loading were initially applied to the edges running along the thickness of the panel, however this produced extreme localisation of stresses in the model that were not representative of the panel behaviour in reality. To counteract this, both the fixed constraint and load application points were instead applied to the shorter faces of the laths that connected to these main edges of constraint or load application (3 faces in one planar direction, and 2 faces in the other planar direction, per constraint).
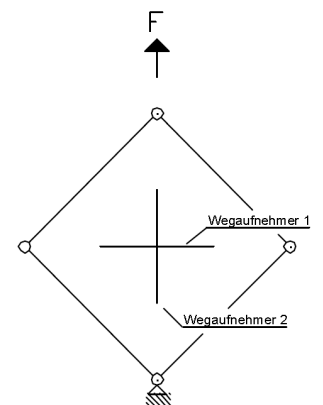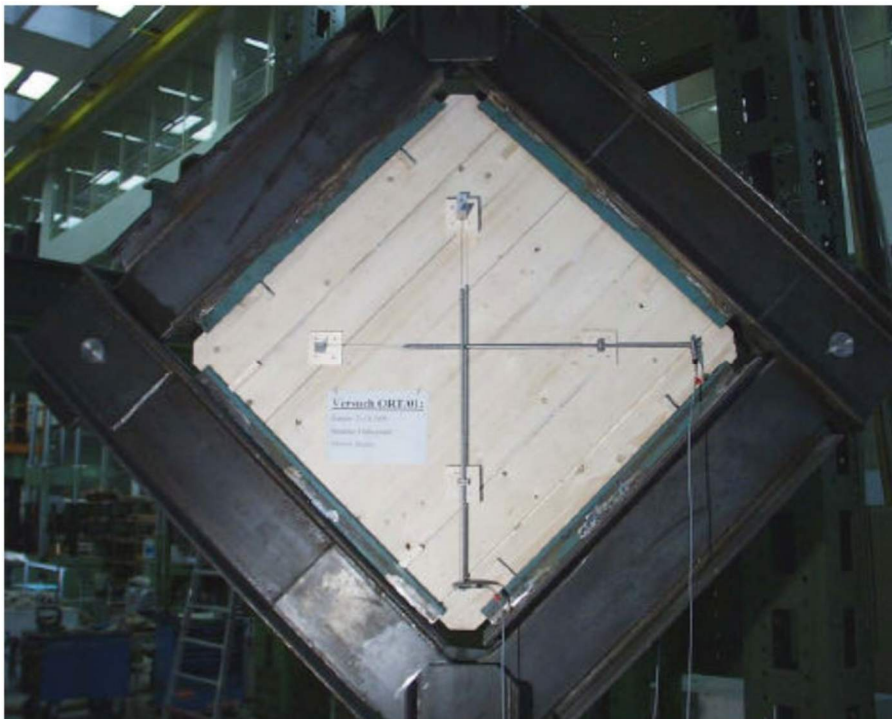
Figure 4.9 - Testing Rig from Bosl's research project [168]

Once the constraints were applied in this manner, the issue of localised stress concentration was resolved. As a further constraint to replicate Bosl's setup, the corners with neither loading nor fixity had constraints applied to prevent movement out of plane, as is provided in the real testing by the steel frame. This was so as not to lose applied load to non-shearing effects. With this setup defined the investigation of the panel modelling could progress.
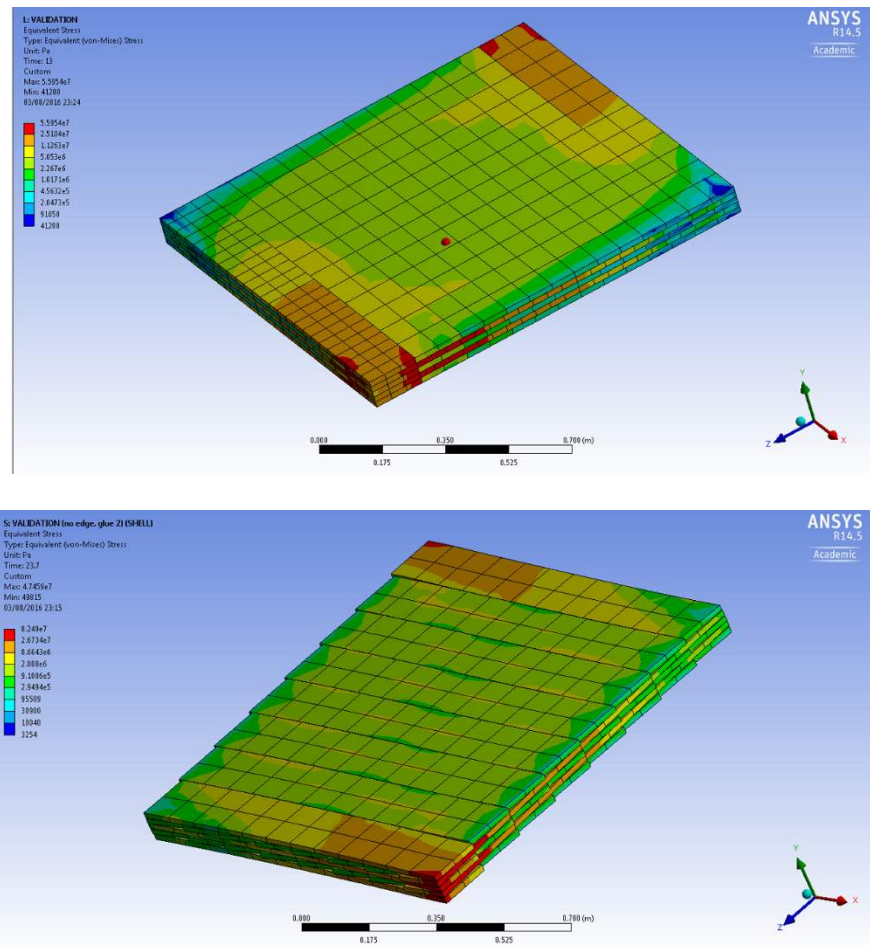
Figure 4.10 - Validation Models for shear, Initial model (top) and resultant model (bottom)

This model displayed more localised shear in comparison to the physical tests. This is shown in Figure 4.10. As well as this, the mechanical response to the shearing load was much greater than those resulting from physical tests – in the elastic zone, the initial FE output slope was approx. 47 kN/mm compared to approximately 15kN/mm from the physical tests.

Inclusion of Individual boards

A variant was tried with the slats within each layer modelled individually. This version showed more reasonable distribution of the internal stresses, capturing stress concentrations as predicted. The inclusion of individually modelled slats did reduce the shear stiffness of the panel, though was still markedly stiffer than those from Bosl's tests, at approximately 34kN/mm (see Figure 4.11). The next

development was to incorporate the glue layers to determine if this was the missing element that caused panel shear stiffness to be lower.

Inclusion of Glue layers

Timber Engineering STEP 1[169] explains that for crosswise jointing with adhesives, as is the case in CLT panels, the adhesive needs to have consistent shear strength parallel to the grain and similar tensile strength in the transverse direction. This should mean that the glue will not be likely to fail before the timber. It is noted, however, that due to the crosswise nature of the bonded connection, there is potential for the glue to be subject to the tensile forces that the timber can withstand in its *longitudinal* axis, which is much stronger than that in the transverse direction.

Glues in FE modelling are most often represented by a perfectly-plastic relationship once the yield stress has been exceeded. Whilst this is appropriate for determining failure of glues, this does not serve the purpose of demonstrating the flexibility that occurs in CLT panels as a result of the glue layers. For this reason, the glue layer included in the models was elastic. The glue used in the most modern CLT panels are of the polyurethane (PU) type. A technical report by Julia de Castro San Roman detailed mechanical properties of glues, including polyurethane, through physical tests[170]. These showed a mean tensile Young's modulus of 571 MPa, and shear modulus of 355MPa. However, using these values raised some issues. Firstly, the shear modulus had to be reduced for the assembled analytical model to behave comparably with Bosl's experimental results. The decision was made to sacrifice the accuracy of the glue properties rather than manipulate the mechanical properties of the timber – the area of focus is the timber at the medium scale (material failure etc) and how the overall composite element behaves on a macro scale. A key factor in making this decision is that the results of de Castro San Roman's testing is for the glue on its own, rather than the glue-timber joint. Further, the behaviour of the timber is of more consequence in this investigation. As such the glue interface is used as tuning mechanism for validation purposes.

The reduced stiffness of the panel in shear compared to the initial models with explicit planks may be a result of the low rolling shear resistance of the timber as described in Chapter 2. The FE modelling technique does not include this directly, hence the need for glue to act as a softening interface in the model when under shear may be due the need to reflect the rolling shear in some way.

Each level of further detail, added to the model by the necessity of the validation process, leads to an increase in computational cost – the addition of non-linear materials and the introduction of many frictional contacts have the most pronounced effect, and require many more intermediate solution steps to secure convergence. To counter this, two modelling efficiencies have been deployed. Symmetry has been used to facilitate the modelling of just one quarter of a floor bay rather than the whole area, and shell elements have been used to model the glue layers. Investigations representing the timber layers or shear connection with shell elements in ANSYS were unsuccessful, though this would give further computational benefits in terms of cost (albeit at the expense of reducing the scope of information that could be output)

The second issue arising from the initial glue properties is that of the assumption of isotropy. The development process of validation occurred concurrently with incorporation of the required modelling changes into the full-scale FE-model. Addition of more elements (and their associated contacts) increases the complexity of the model and the solution time, so initially, the glue was modelled as an isotropic material, as this was deemed the least computationally expensive method, and was implied by the outputs of de Castro San Roman's study. When the glue parameters had been tuned to correspond to the test data, glue layers were introduced into the full scale model, However, when the changes were included, the composite benefit reduced to zero because in reducing the material stiffness to mimic the shear behaviour, the layers of CLT could bend independently of one another by lifting off one another. The issue was resolved by changing the glue to an orthotropic material model, with a stiffness in the vertical direction similar to that of the timber. It further demonstrates that the use of the glue properties in isolation is inadvisable as they will not necessarily reflect the behaviour of the glue within a joint where it interacts with the joined element's material characteristics and geometry.

The final glue parameters applied are presented in Table 4.5 and a summary of the outputs of the development stages of the validated model can be seen in Figure 4.11. With the glue layers included as shell elements, the slope of the shear load-displacement graph in the elastic region reduced to 15.05 kN/mm, matching up much more closely with the test data than those without the glue layers.

Table 4.5 - Parameters used in material model for Glue layers

Property	Symbol	Value	Units
Young's modulus X direction	E_x	2.5	GPa
Young's modulus Y direction	E_y	290	MPa
Young's modulus Z direction	E_z	160	MPa
Poisson's Ratio XY	ν_{xy}	0.372	
Poisson's Ratio YZ	ν_{yz}	0.435	
Poisson's Ratio XZ	ν_{xz}	0.467	
Shear Modulus XY	G_{xy}	230	MPa
Shear Modulus YZ	G_{yz}	11	MPa
Shear Modulus XZ	G_{xz}	0.332	MPa
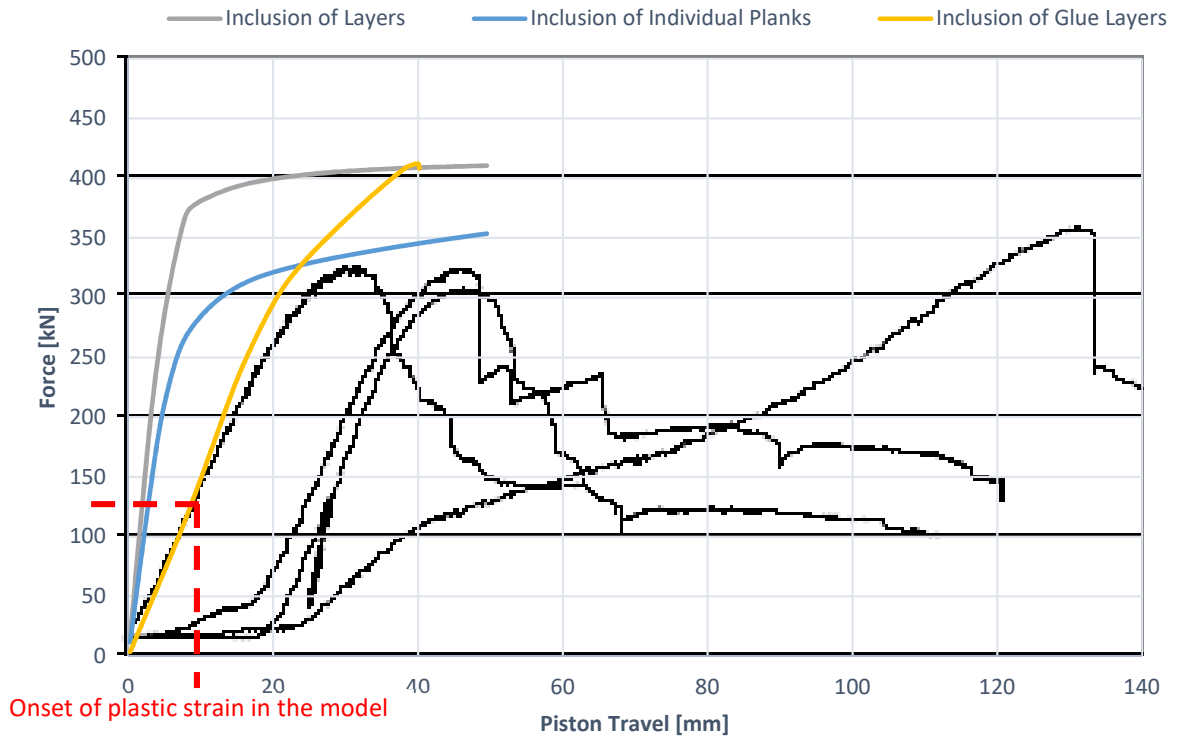
Figure 4.11 - Shear Force-Displacement of CLT panels Validation (Physical data generated by Bosl[168])

4.4.3 Secondary Validation

In addition to replicating the mechanical behaviour observed by Bosl, the new material model and modelling approach was applied to a test setup used by Hochreiner et al[171]. In this work, a square panel of CLT, fixed on four sides was subjected to a central patch loading. The deflection at the centre was measured against the imposed load. In a setup such as this, the central deflection is linearly related to the imposed load - Figure 4.12 shows the central deflection (y_{max}) for the equivalent situation involving a thin, flat homogenous plate (where maximum deflections are less than one third of the thickness, t) and where W is the point load, E is the young's modulus of the plate material, and α is a coefficient relating to the aspect ratio of the plate.

Whilst the CLT panel's properties lie outside the pre-requisite assumptions for the formula given in Figure 4.12, one can still infer that deflection and imposed load will have a linear relationship and thus, that the onset of non-linearity in the load-deflection trace is the onset of plasticity (which is assumed as failure) in the system. Therefore, in an FE model of the setup, matching the slope of the load-deflection curve and the onset of plasticity should be an effective capturing of failure behaviour.
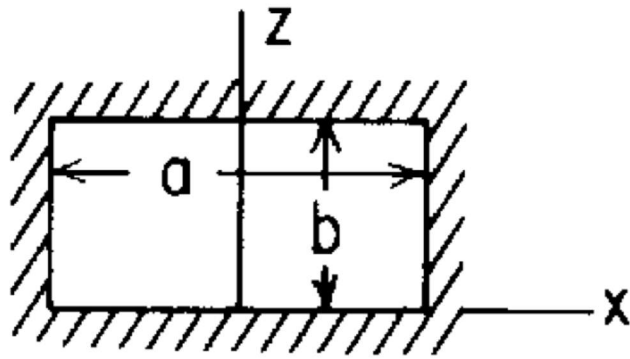
$$y_{\max} = \frac{\alpha W b^2}{E t^3}$$

Figure 4.12 - Central deflection of a flat rectangular plate that is fixed on all sides and subject to a concentrated load[203]
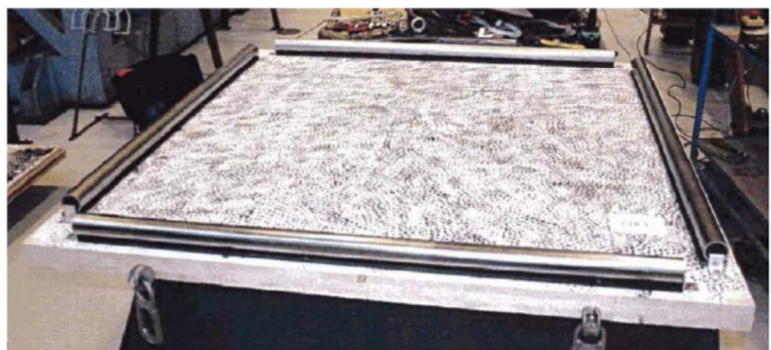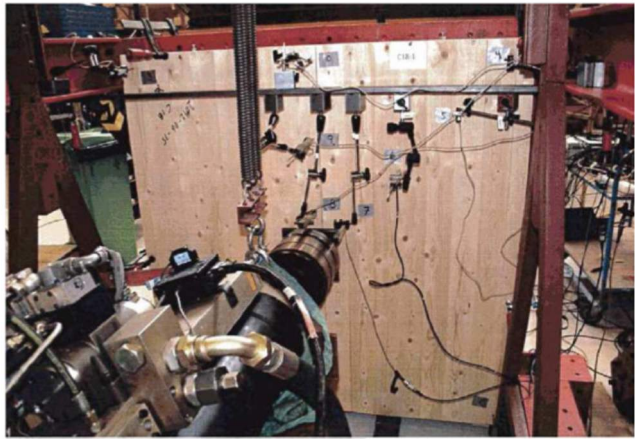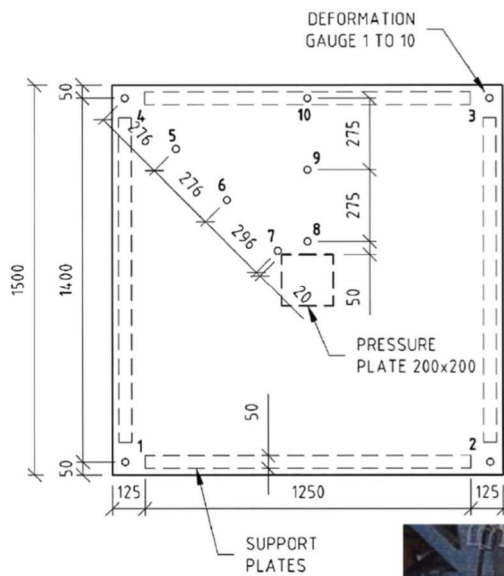
Figure 4.13 - Setup of Hochreiner experimentation[171]

Hochreiner's setup was modelled in ANSYS, and was able to replicate the deflection slope without further tuning (shown in Figure 4.14). It was not able to capture the post-yield behaviour though, as can be seen in Figure 4.15. Rather than demonstrating an overall plateau in the panel load-displacement curve, the load continues to increase with, in fact, an increase in gradient. This is most likely a result of redistribution of stresses into the glue as the timber in the model reaches its capacity – the glue layers do not have a yield point in the model, therefore will attract more and more load preventing capture of the collapse.
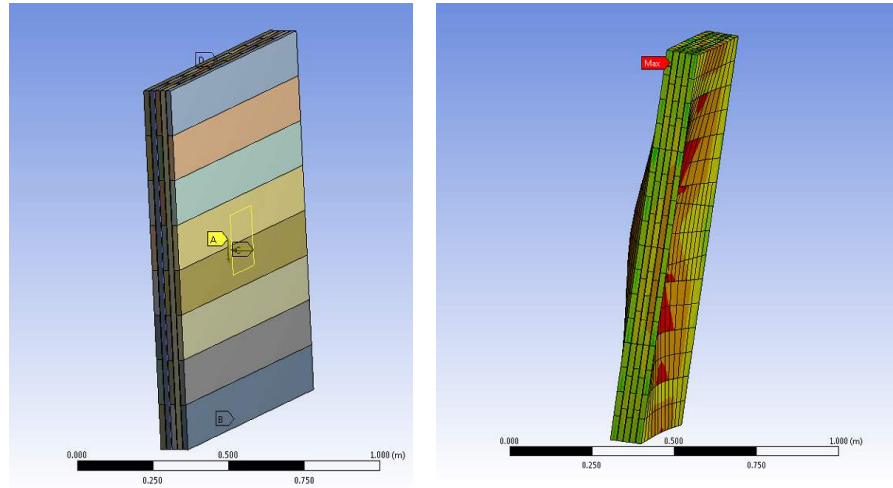
Figure 4.14 - a) Finite Element model for bending validation b) the resultant deflected shape after simulation

In spite of this drawback, since in the CLT models is any plastic deformation constitutes overall failure, over-estimation of the system capacity should not be an issue. Observing the pattern of plastic deformation through the loading process, the plastic deformation under the loading plate is replicated and the point of tensile plasticity (failure) corresponds to the 1st yield shown in Hochreiner's testing (or is at a lower load, and is hence conservative). With the use of this CLT modelling technique, failure in the system is associated with the shear connector and timber in the region of that interface.
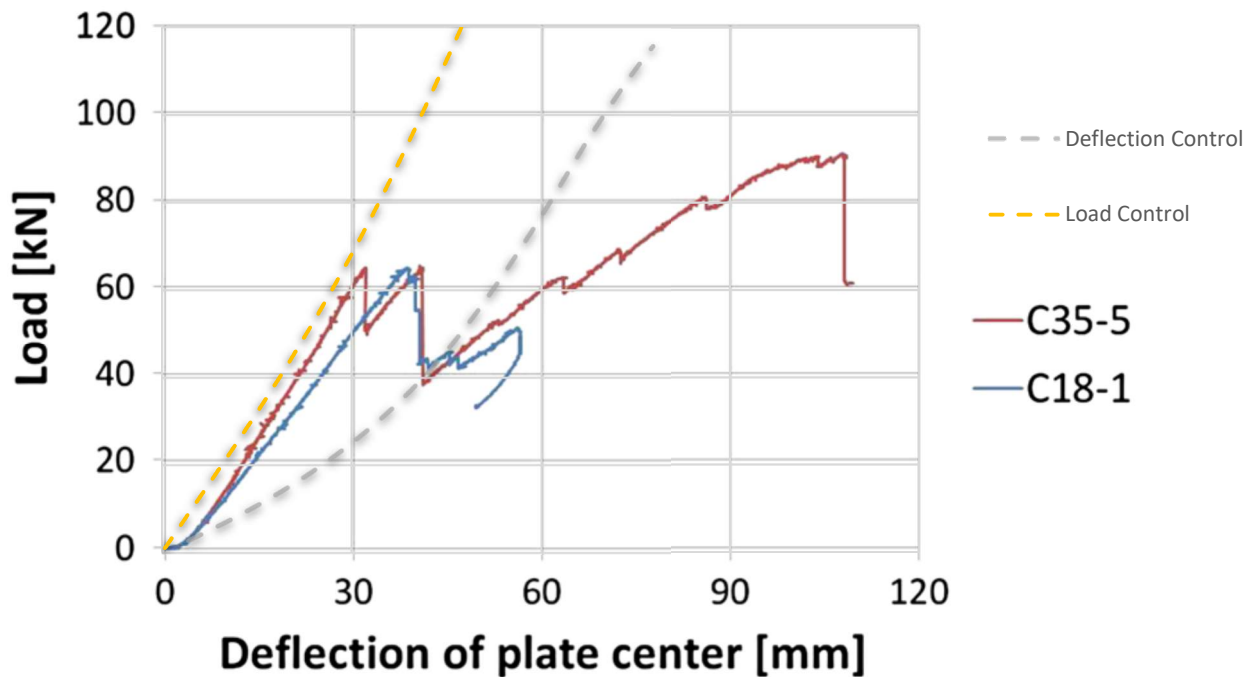
Figure 4.15 - Test data from Hochreiner et al. of simply supported CLT panels subjected to bending[171], overlaid by the results of the FE representation

4.5 Summary & Conclusions

This chapter has covered the full scope of developing a material model and modelling approach for CLT, from the available knowledge and previous work at the outset of the project, through initial modelling and establishment of important system elements, modelling technique refinements and finally validation.

Key findings from this chapter are:

- In order to maximise the contribution from the timber slab, ensure the panels are connected in the tensile zone (below the neutral-axis) to make use of the tensile strength inherent in timber.
- It is inadvisable to use Young's modulus values reported by CLT manufacturers when calculating composite section properties from FE models – they are insufficient to define the panel's shear lag response which determines the effective width. The panel layers must be modelled and their orientation included. Use properties for the relevant timber.
- Yield stresses have been incorporated in order to highlight locations of material failure in the CLT, so that composite benefit is not unintentionally reported to occur in situations where the CLT would have failed. Hill's criterion is applied to take into account the anisotropy of the material and the in both stiffness and strength.

As a result of the validation process, the following advisory notes and recommendations can be given:

- Modelling panels that are subdivided only into layers rather than the individual boards (analogous to edge-glued CLT) will over-estimate the panel stiffness when subjected to in-plane shear.
- It is crucial to model the individual planks explicitly, and include the glue layer.
- Some computational savings can be made by representing the glue layers with plate elements instead of solid elements, but care must be taken to have consistent meshes so nodes that form the plate elements correspond to nodes that define the timber solid elements.
- Glue properties may be changed to tune the gross panel behaviour.
- It is imperative that the glue is modelled as an orthotropic material – capturing the slip between layers must be combined appropriately with the inter-layer separation strength which, if omitted or underestimated, prevents the modelled panel behaving as an (internally) composite structural element. The consequence of this is instablility in the analysis, and isolation of the shear connector from all but the bottom layer of the panel.

In conclusion, CLT has been successfully modelled and validated in Finite Element form, and the modelling approach and parameters established in this chapter have been directly applied to the models used to investigate the ASB-CLT system in the parametric study of Chapter 6. However, before this, Chapter 5 applies a similar methodology and format to this one in developing approached for the connections that form part of the ASB-CLT system.

Chapter 5. Finite Element 2: Connections

This chapter reports the stage of development that tied the modelling philosophy (commercial software, simple modelling techniques, practical solution times) to the available data on the mechanical behaviour of CLT. A means of incorporating the behaviour of the connection types into the system for a more detailed prediction of the overall system performance has been developed.

5.1   Connections in Timber

As discussed in Section 2.3.2, the failure behaviour of timber is complex and dependent on grain orientation and load direction. When dealing with a material prone to brittle failure, such as concrete or timber, it is imperative to provide ductility within the connection and maintain the predisposition of ductile failure modes. As the differential of strength between the orthogonal axes of timber is so large, the connector often has to transfer stresses generated by the stronger longitudinal axis, but must be transferred and withstood by one of the timber's weaker axes. As a result, timber connections are often realised with multiple points of connection, with relatively large spacing between connection points. The high number of connection points is to reduce the stress of the timber surrounding each connector, and the subsequent risk of local timber failure, by distributing the load across more points. The spacing is to reduce the likelihood of group failure, which when combined with the large number of points needed, often becomes the key determinant of the overall dimensions of structural timber elements. Connection methods of this form include nails, screws, dowels, and glued-in-rods.

5.1.1 Connector Type: Dowels & Screws

Screws (and nails, which also fall into this group) are a long-established connection connecting method for timber construction. They provide fixity through a combination of resistance to withdrawal, tension, bending, and shear.

In timber design it is more important to refer to the behaviour of the joint rather than the connector alone, as it is the combined action that governs how well or poorly a connector works. Depending on the configuration of a connection, a connector may behave or fail in a different manner, and this is especially true for joints formed using screws or dowel type connectors. The spacing and embedment length determine how the connector interacts with the timber around it, and hence influences the stiffness and strength of the joint.

In their very nature, the connector points are locations where stress/load is concentrated to allow transmission across whatever interface. This can be problematic for timber especially compositely, because the magnitudes of loads that one would like to transmit or transfer may be very large. It becomes necessary to distribute the loads across many points of connection to prevent localised failure around the connectors. Conversely, if there are too many connection points and they are too closely spaced, group action can occur, where a failure happens through the surrounding material, taking a

series of connectors at the same time. Whilst there are established rules and guidance covering these phenomena for standard timber connections, this area is more complex for CLT and for creating a shear connection

Asiz & Smith[2] investigated the performance of simple screw connectors for joining steel and timber in multi-storey buildings. Their study was not investigating composite action between the two materials, and hypothesised CLT panels resting on the top flange of a conventional steel beam, but they did find the screw connectors were suitable for use in the system and offered sufficient ductility for hybrid CLT-steel structures to work in seismic regions.

A further option is the HELIX type screw connectors. They are characterised as having a more loosely packed thread than conventional wood screws.

The helical connector was initially developed to create a more effective wall tie for securing masonry to timber frames and other remedial uses. Research performed by Coste[172,173] demonstrated using a physical testing program that under lateral shear, timber connections using helical connectors show greater ductility than conventional screw connectors.

5.1.2 Connector Type: Nail Plate

Nail-plates (also known as "punched metal plate fasteners" or "truss plate connectors" - see Figure 5.1) are described in a technical declaration as "galvanised mild steel plates with rows of integral nails pressed out approximately at right-angles to one face of the plate"[174].

 Nail-Plates are a timber connector typically used to connect, or reinforce the connections of, timber elements in trusses. Simply described, they are sheets of metal with spikes projecting from one face, with the spikes having been created by partial punching that leaves the nails connected to the parent plate. To ensure rigidity, the nails are shaped during the punching process. Connections are made by hammering the plate teeth into the timber across the join between the two elements – the nails are embedded into both elements whilst the plate itself provides tensile strength across the join. The load
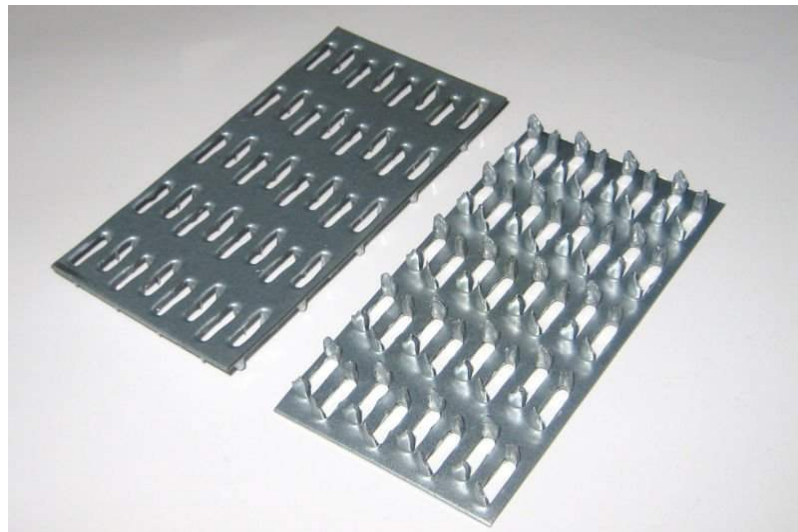
Figure 5.1: Punched Metal Fasteners (nail-plates)

path in nail-plate joints is from one timber element into the teeth, then through the teeth, the plate, and a second set of teeth (having crossed the joint interface) into the second timber element[175]. In conventional timber frames, the use of nail-plates is limited to the creation of butt-joints.

Nail plates have been investigated for suitability as a shear connector in the past, particularly for timber-concrete composite structures. In attempting to develop a prefabricated timber-concrete composite beam, they were proposed as a connecting device cast into the concrete slab, to be then pressed into an LVL beam to provide slip resistance. In the study of Blass & Schlager[91], single shear tests were performed on the joint, finding that the connection typically exhibited a slip stiffness of 50kN/mm per connector and an average maximum load of 48kN per connector. The overall load-slip behaviour was observed as elastic-plastic. Failure was seen to occur via withdrawal of the nails from the timber, with some cases of tensile failure of the nails themselves.

In 2014, with support from the IStructE, testing was performed to determine the potential of Nail-Plate connectors as a shear interface connection, which is detailed in section 5.3. During the same time period, Jacquier & Girhammar were testing double-sided nailplates as a shear connection between CLT floor panels and GluLam beams[176].

5.2   Shear Connection - Background

5.2.1   The need for a shear connection
A shear connection is fundamental for the development of composite action; it is the means by which the deformation of one part of the desired composite system can be linked to other parts of the system and allow load sharing between elements. In the context of composite beams, the shear connectors run along the length of the beam. Where two materials of non-trivial thickness are to be joined, the shear connection will always have an incomplete interaction i.e. at the interface between the parts to be connected, the deformation of one will not exactly match that of the other. This discrepancy can be referred to as "slip", and whilst this is evidence that the composite benefit achieved is less than the theoretical maximum, slip between the two elements results from deformation of the connector and introduces ductility into the system. This much needed ductility prevents brittle failure mechanisms that are possible in conventional composite construction using concrete and here using timber.

Due to the particular juxtaposition of CLT panel and steel beam in the slim floor system considered, the shear connection lies in an area of tension under gravity load. Timber fails in a brittle manner under tension, meaning the shear connector's behaviour is a critical factor. In preliminary investigations of section 4.3 when the CLT was modelled to the detail of separate layers but not individual laths, it was not possible to determine composite benefit with a complete shear connection in ANSYS because of the orientation of the layers in CLT, with the loads of the shear connection in the tensile zone pulling apart the timber along one of the weaker radial or tangential axes. The beam and panel were modelled as bonded together in ANSYS, but because of the lack of ductility offered by a bonded connection and the

large difference in Young's moduli, the deformation of the steel beam caused plasticity in the timber as it was forced to match the deformation. Although under bending the level of deformation in the steel resulted in stresses below the yield point in steel the equivalent deformation of the timber strained it beyond its yield point. It is worth remembering that timber tensile failure is a snapping of fibres, so when ANSYS displays "plastic strain" in the model, this represent sudden and complete removal of all composite benefit when tensile stresses are being applied. Whilst the introduction of individual laths in the CLT models meant the CLT panel was now more resilient to the deformations dictated by the extension of the steel beam in the tensile zone (through increased separation of laths rather than stretching of timber), the experiences of inducing failure by too stiff a bond highlighted the influence the shear connection can have on the behaviour of a composite system in ways that may not be first envisaged. Similarly, this also highlighted the benefit to including the stress limits of the timber in the different axes and a means of reporting when they are exceeded.

Another factor to consider is the anisotropy of timber. At the level of the shear connection, the timber is orientated with the grain direction (longitudinal axis) in the direction of span of the panel i.e. perpendicular to the beam's longitudinal axis. Bending of the beam causes tension and compression running along the beam length. Because of the relative orientations, the fixture of the CLT to the beam acts to pull the timber apart along its weaker axis resulting in plastic failure in the models very quickly.

Necessary Properties

- **Withstand Induced shear forces** - The magnitude of shear force to be withstood is a complex parameter that will be affected by a number of factors about the connector and the rest of the system. The amount of CLT slab that is engaged in assisting the beam to support the floor system (encapsulated by the effective width) is very important, as the relative stiffnesses of the beam and CLT within the composite section will determine the magnitude of the load at the interface. The effective width is itself dependent on the geometry of the setup (aspect ratio of the bay size, internal dimensions of the panels), whilst the longitudinal stiffness of the connection will impact on how much load is transferred between panel and beam.

- **Ductility** - As earlier mentioned, one aspect the connection assists with is introducing ductility into the system. Composite action is created by the compatibility of deformation of two elements of differing materials and, in the case of a timber-steel connection, the deformation the steel can undergo whilst still remaining elastic may induce failure in the timber, especially in the directions of the tangential and radial axes. The shear connection can provide a useful function by permitting the timber to remain elastic on one side, whilst enabling the deformation of the steel to proceed.

- **Demountable** - One of the grander aims of this research is to create a structural system that can be fully dismantled and elements re-used or recycled as appropriate. To allow this in composite

systems of any kind, the design of the shear connector is critical. In an ideal situation, the shear connector could be disconnected from both joined elements without having damaged either component in service or during disassembly.

5.2.2 Technical Literature Review C: Behaviour and FE Modelling of Connections in Timber and CLT

Existing studies on shear connections involving timber are most numerous in research focussed on timber-concrete composites. These date back beyond 20 years (e.g Blass & Schlager's experimental testing of nails, folded nail plates, dowels, and grooves as shear connections for composite elements of concrete slabs connected to GluLam beams[91]). The configuration of GluLam beams compositely connected to concrete floor slabs is a common one in the literature for this topic[177,178].

In 2012, Jacquier & Girhammar investigated a series of shear connector types for composite CLT elements, including shear studs, and a shear mesh on the concrete side, affixed by coach screws on the timber side. They found that providing sufficient spacing between the connectors on the timber side, a ductile failure mechanism could be induced with shear studs in the concrete for a maximum shear load of 56kN, but that with a mesh shear connector in the concrete, a ductile failure could be achieved with twice the number of connectors on the timber side, increasing the maximum shear load capacity to 129kN[179]. In later work performed in 2014 and 2015, the duo expanded their investigations to the suitability of double-sided nailplates (in combination with inclined screws) to act as the shear connection for the creation of a mass-timber cassette flooring consisting of CLT compositely joined to GluLam beams[176,180]. During physical tests of the shear connections, the double-sided nailplates were found to exhibit more pronounced non-linear behaviour than the screw connectors, and a certain amount of ductility, but little load carrying capability beyond the maximum load. Jacquier and Girhammar found that the nailplate characteristics are complemented by the inclined screws behaviour, allowing the combined joint to have ductility beyond that of inclined screws in isolation, but also higher capacity than the nailplates are capable of on their own[176].

In another example involving CLT, Gubana has investigated composite action of CLT panels on top of a GluLam beam[86]. In her study, 16mm steel dowels were used as shear connectors, inserted into predrilled holes, with varying concentration of connectors along the beam with more closely spaced dowels in the zones of greater shear stress. Experimental testing of the system managed to achieve composite enhancements of between 11% and 41%, with the more poorly performing specimens having been reused. This highlights a potential drawback to dowel-type connectors – observations of the samples after the testing showed the predrilled holes to have been widened due to localised crushing of the timber in the resisting of the generated shear forces in testing, which appears to have restricted the performance of the elements when re-used.

For connections between timber and steel, Schneider et al. explored the performance of CLT elements and their associated connections under seismic action to determine the suitability of CLT-steel hybridised construction, with the timber as wall infills to steel frames[181]. The focus was on the damage that would be induced to the CLT due to an earthquake, and assessed nailed and screwed connections for their ductility, whilst assuming the CLT panels to be rigid. The ductility of the connections was found to be satisfactory to dissipate the energy in an earthquake, but due to the amount of damage that would be caused to the panel, follow up work developing a novel tube-type CLT-steel connector was performed[182]. The philosophy and application of the tube type connector is shown in Figure 5.2, and demonstrates the successful achievement of isolating plastic deformations to the tube connector and leaving the CLT panel undamaged.
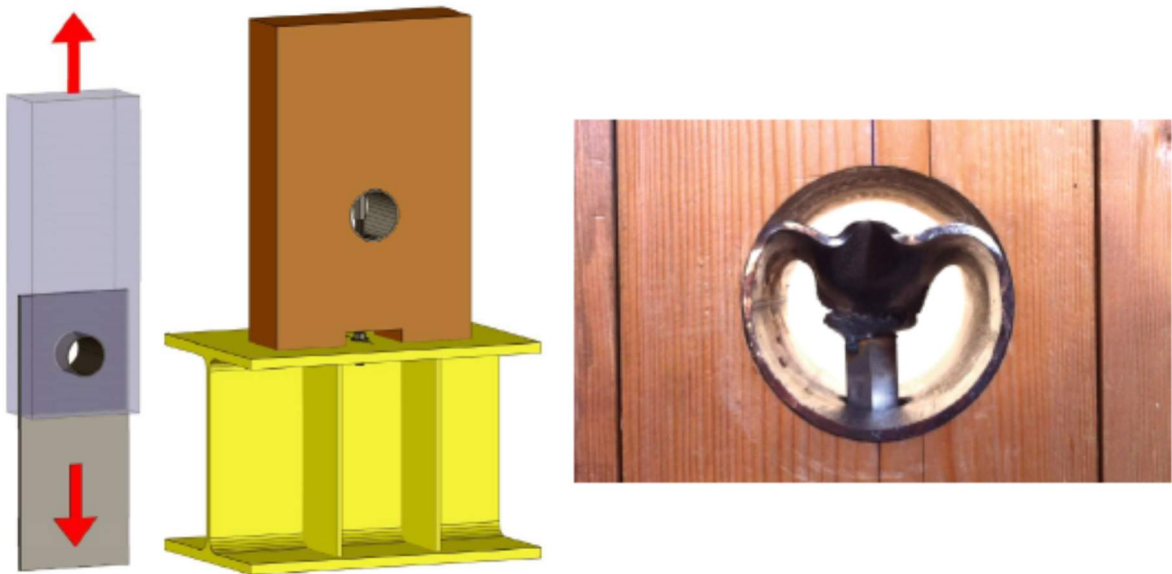
Figure 5.2 - Tube type connector in principle(left); in hypothetical practice (centre); and post-failure from experimental testing (right)[182]

The experimental testing found that under monotonic loading, the larger the diameter of tube, the lower the elastic stiffness of the connection and the lower the maximum load capacity, but each connector showed substantial ductility. As such, due to the characteristics demonstrated, the tube type connector appears to have great potential for use in timber-steel hybrid structures, and the ability to preserve the CLT panel against damage is an important feature for facilitating reuse of the structural elements.

In Asiz & Smith's research[2] referenced earlier, simple screws were tested for their suitability in connecting CLT panels to steel beams for the purposes of seismic resistance and this involved testing the connectors in shear, using a test setup based on the requirements of the American code ASTM D-5652-95[183]. They found that if the load was applied to the connection in a direction perpendicular to the grain, a higher ultimate load resulted (23.1kN per connector for long SFS screws) but with lower connection stiffness (1.32 kN/mm^2 per connector for long SFS screws) than that resulting from load

applied parallel to the grain (17kN per connector ultimate load; 2.96kN/mm² stiffness for long SFS screws). They also found that regardless of the direction of loading, ductile failure was prevalent, as can be seen in Figure 5.3).
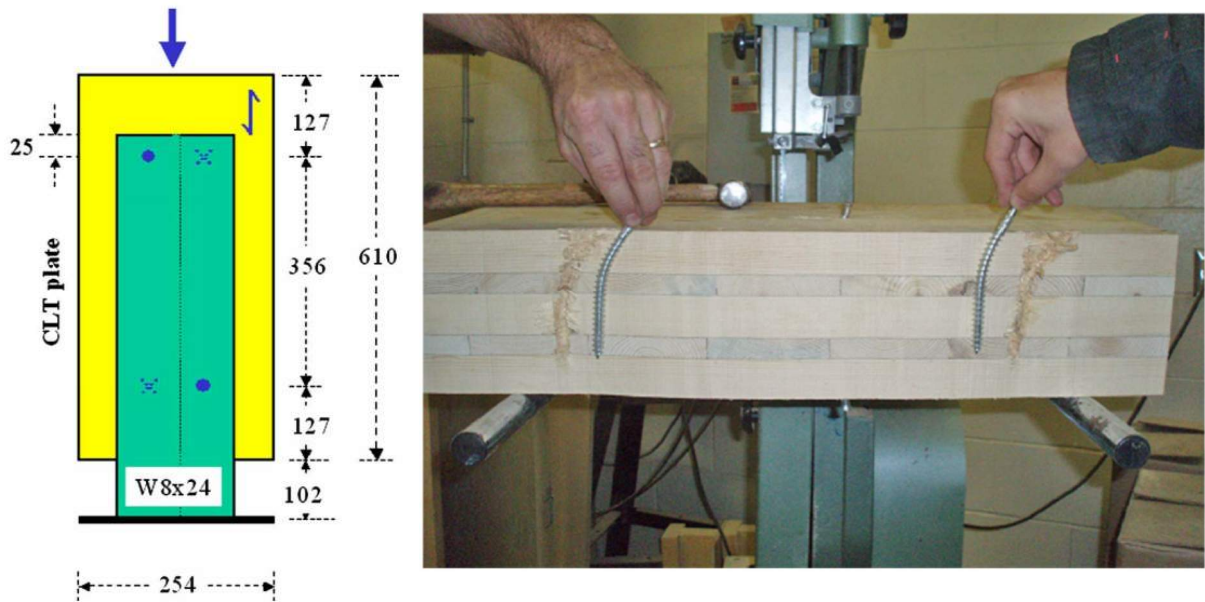
Figure 5.3 - Example test arrangement (left) and failure mode of screw connectors (right) for CLT-Steel hybrid by Asiz & Smith[2]

In some cases, when reviewing the literature for previous research on shear connections with CLT, the research focusses on the in-plane shear resistance offered by different types of inter-panel connection[184]. Studies of these connections are interested in determining the ability of CLT floor systems as a whole to transfer lateral loads via diaphragm action, and various groups have undertaken work on this area[166]

5.3 Shear Connection – Physical Testing & Inclusion into FE

5.3.1 Research Aims & Methodology

Interest in the use of nailplates was initiated by considering means of connecting CLT panels to the steel frame without the need for working at height. Nailplates are an established wood connector, and by positioning them on the bottom flange of the ASB, it was hypothesised that the timber slab could be dropped into place using a crane and the self-weight of the panel would cause the embedding of the nails into the timber matrix. It was further postulated that in forming a composite connection, the slip stiffness would be dependent on the embedment depth of the nails, and hence as more vertical load is applied, the embedment would increase, creating a stiffer connection in situations of higher load, where composite action is most helpful.

The aim of the testing regime was to determine the strength of nail plate joints in CLT, determine the slip stiffness to inform the level of composite interaction that can be determined, and to ascertain whether the failure would be ductile or brittle.

It is common practice to assess the behaviour of a shear connector via a slip test. In most cases this is arranged as either a single or double shear test (with two lines of connection for the double shear variant), and shear loading applied vertically, however a more representative and informative setup for this potential shear connector was established. One of the hypotheses of this part of the research was that in the proposed construction system, increased imposed load would drive the nails into the CLT, with the level of vertical load governing the embedment depth of the nails into the CLT, and hence the strength and stiffness of the joint. The presence of vertical loading is what induces the curvature and combined action of the beam and slab that defines composite action. Therefore, it is more reflective of the service condition to apply shear loading together with vertical compression. It would be most accurate to have the vertical and shear loads coupled together but this would require prior knowledge of the composite behaviour of which this thesis attempts to determine.

Subsequently, an arrangement of biaxial load was chosen, being most practical arranged in a similar fashion to the connection in service, with the shear load and line of connection running horizontally. Nail plates were welded to the outer face of the upper flange of small column sections, 4no. nail-plates per test sample. CLT panels (donated by KLH UK), were cut into sections of approx. 1m x 300mm, and placed onto the nail plates. To reflect the arrangement of elements in service, the bottom layer of the CLT was orientated orthogonal to the direction of shear load. The magnitude of preload was one of the parameters that changed, representing situations of different assumed panel spans.

The testing arrangement is shown in Figure 5.4, and the investigation is covered in greater detail in the Master's thesis of Chris Jarvis[185].
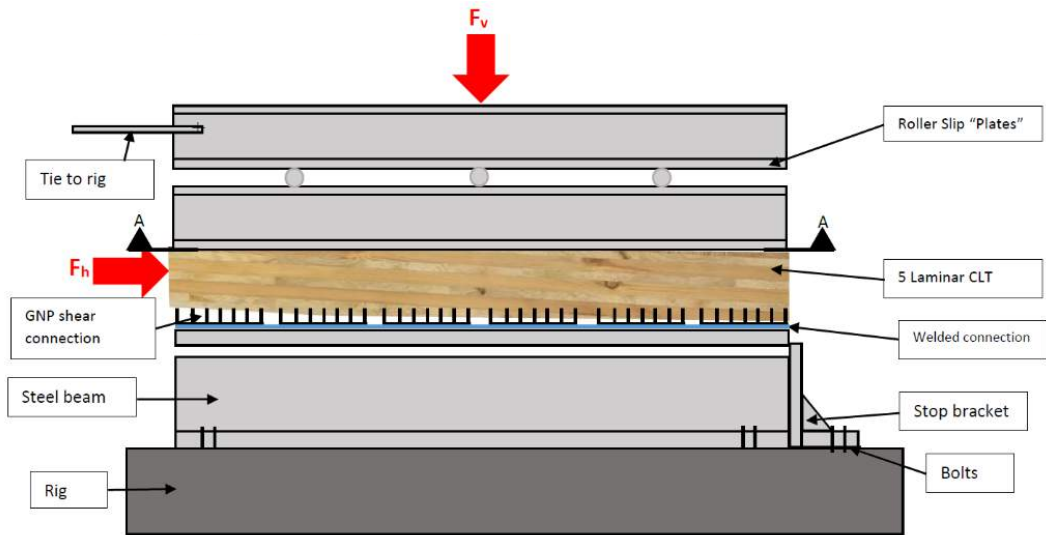
Figure 5.4: Test setup for Gangnail Shear Connection[185]

5.3.2 Testing Observations and Results

A preliminary test was carried out to assess the magnitude of resistance to expect from the connection and the method of failure. For this run, the nail plates were tack-welded to the beam for ease of setup and to reduce cost. During setup, the hypothesis that the self-weight of the panels would be sufficient to embed the nailplates was found to be incorrect. The pre-load, calculated to be equivalent to a full panel's self-weight, was insufficient to overcome the surface toughness of the CLT, and the sample had to be hammered down to form a viable slip connection for testing.

During the performance of the preliminary test, it became evident that it was the welds that were determining the slip behaviour, initially with buckling of the nail plate between welds, then by the shearing of the welds and pull-out of the plates from the weld. Consequently, the output of this run shows a load slip pattern comparable to standard welds, and the failure load is small.

This led to subsequent test setups using welds on all edges of the plate so that the determining factors of slip are related to the characteristics of the nailplate-CLT interaction rather than the properties of the weld. (The welding of cold-formed nail-plates to hot-rolled steel beams is an area of necessary investigation for a system of this configuration.)

Figure 5.5 - After slip test, showing bending of nails

The slip behaviour is initially through mechanisms of nail bending (Figure 5.5), and probably compression/bearing of the timber adjacent. As loads increase, a number of processes occurred – withdrawal of the nails at extreme angles (CLT begins to lift off the beam, which promotes this behaviour), shearing off of the nails which remain embedded in the panel (Figure 5.6), and cleaving of the timber between the bent-over nails. This led to chunks of timber being ripped out as strains continued.

Figure 5.6 - Nails still embedded in test sample, having sheared off

The load tests progress with the deformation occurring through the bending of the nails, which Is then followed by the withdrawal of the nails from the timber. Whilst these phenomena could be considered reversible or elastic deformation, further characteristics of load response can be seen. As the nails bend towards the horizontal, if they do not withdraw from the timber, they are either broken at their base from the steel plate, or "pinch" together around the timber fibres running perpendicular to the load direction. These phenomena were similarly occurring when Blass and Schlager applied them to Timber-Concrete composite floor beams[91]. This leads to a longer period of post-yield resistance, but both these other phenomena are non-reversible (Figure 5.7). Consideration of this is important due to the influence on the reusability of the panel after the use of this type of connection.

Figure 5.7 - Irreversible deformation/damage

The load-slip results are presented in Figure 5.9 and Figure 5.8. It is difficult, and inadvisable to draw definitive conclusions from such a small sample set, particularly for tests involving timber elements. The traces show elastic behaviour up to between 45kN and 55kN, before the onset of a degree of non-reversible deformation marked by a reduction in the gradient of the curve. The connection joint trace shows a peak load of approximately 80kN (on average), after which pronounced strain softening occurs down to a plateau of plastic deformations at a lower load of approximately 15kN. The strain softening observed in every test conflicts directly with the experimental findings of Blass & Schlager[91], detailed in section 5.1.2.
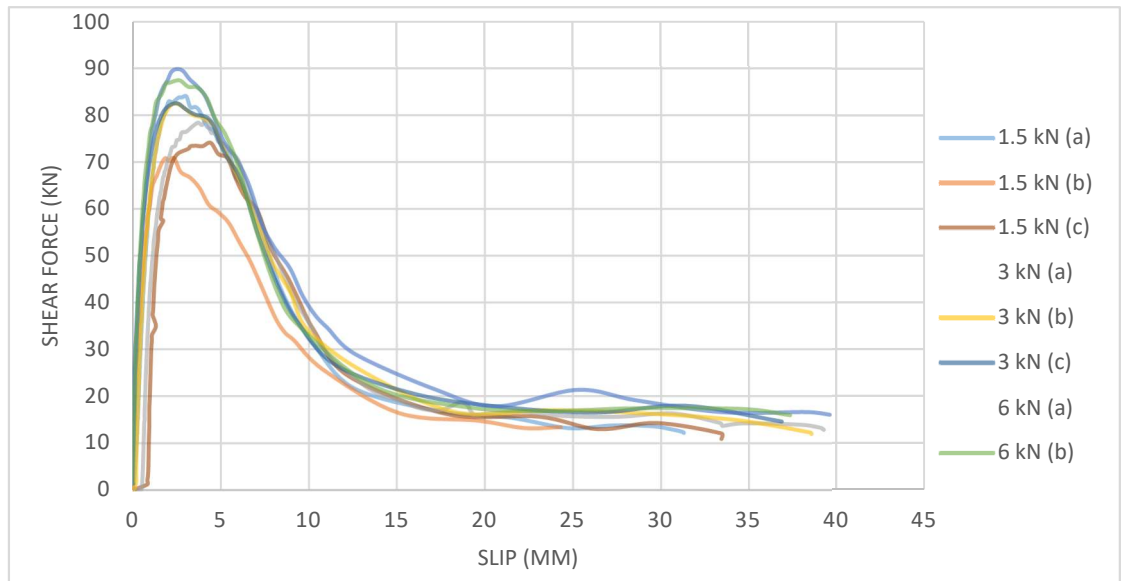
Figure 5.9 - Load Slip Trace of Nail Plate connection (defined according to vertical pre-load)
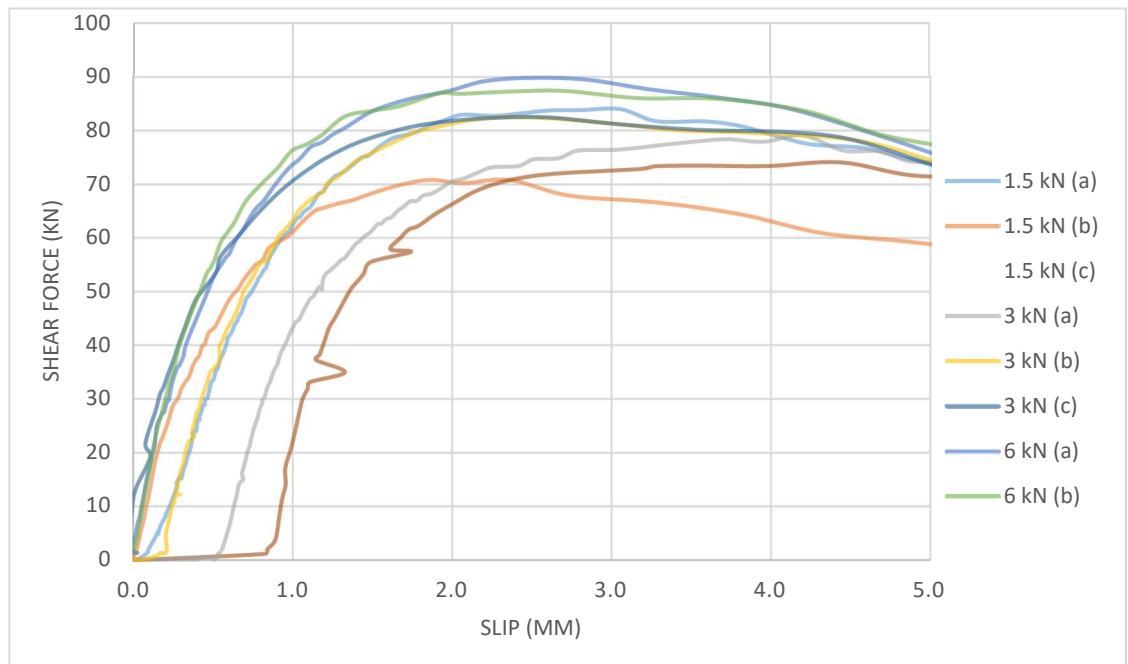
Figure 5.8 – Magnified view of load-slip load slip trace of Nail-plate connection

A notable testing phenomenon displayed by the results is a sometimes-present initial slip of up to approximately 0.8mm before the connection is engaged in shear. This is most likely a result of the test setup for example sample ends not being cut exactly vertically, meaning some displacement of the loading plate is necessary at the outset. Interpreting the load-slip graph and the condition of the nail plate and CLT panel after the test, one can match the stages of the graph to particular load resisting modes. In the, elastic region, deformation is characterised by the bending of the nails, with the reduction in slope being initially a result of withdrawal of the nails. As the load increases to its peak, the "pinching" of the timber fibres (which are running perpendicular to the direction the nails are deforming) engages a further mode of resistance from the internal binding of the timber fibres to one another. As the fibres

fracture, the inversion of the load-slip trace (strain softening) begins, with progressively lower load resistance. As timber fibres break, this leads to more localised stresses on the remaining embedded nails, where the degree of embedding strength of the particular nail determines whether the nail is sheared off in, or withdrawn from, the timber matrix.

It was not possible to determine conclusively how the amount of pre-load affected the behaviour of the nailplate-CLT connection; a more expansive testing regime investigating this would be required. The tests performed in this study potentially show that the higher the preload, the higher the limit of elastic deformation. This could be explained by the tendency of the samples to try to deform by hogging longitudinally, and lifting away from the central nailplates. In such an occurrence, the embedment depth of the nails reduces, making that part of the joint less stiff and leading to non-linear behaviour. With higher preloads, there is greater limiting of this effect, allowing the linear deformations to continue to higher loads. More detail on the effects of the pre-load can be found in Jarvis's thesis[185].

5.3.3 FE modelling of Nail Plate Shear connector

The tests performed in the earlier parts of this section provide data for inclusion of the nailplate shear connection within the FE models. As a real joint, the connection stiffness will be somewhere between zero (the "no-connection" case) and a hypothetical infinitely stiff connection ("Bonded connection" in ANSYS). Having real connection behaviour provides a particularly useful comparison, that allows a more representative characterisation of the overall system, and allows phenomena, potentially obfuscated in the "no-connection" and "full-connection" cases, to be revealed.

Modelling the individual nails or bolts within a shear connection would be too complex when on the scale of a slab and beam system, so a method was devised to replicate this behaviour in a simpler fashion. Since it was not possible to write a bespoke friction behaviour into the connections offered within ANSYS Workbench 14, it was decided that a "dummy material" approach would be used. In this method, a user generated material is defined that when loaded, would display the same overall deformation as experienced by the nail plate connection through careful specification of the material properties. This necessitates reproduction in FE software of the testing setup used to derive the behaviour to be incorporated, but avoids the need for highly complex geometries and contact behaviours to be modelled. This will pay dividends when modelling an entire bay of a structural frame.

The research of Hong and Barrett[186] provided guidance on the modelling technique for addressing the connection design. Investigating FE modelling of nailed connections in wood, they state that wood compression is not scalable, and that the localised crushing in nailed connections relates more to the contacting wood fibre performance than the overall compression behaviour of the wood. Hence it may be necessary to have a distinct material property definition for the region immediately surrounding the connection points in order to pick up the localised behaviour. Then the more general material model being developed can be used for the majority of the panel. This is a similar strategy to that employed by Hong and Barrett.

The behaviour and failure of the nail plate connection in Jarvis's work clearly demonstrates a distinct softening behaviour once the peak stress has occurred. As previously stated in section 4.3.7, this creates difficulties when modelling as ANSYS cannot incorporate this negative slope of the stress strain curve. This limitation prevents further investigation into the ultimate limit state of the system with the models in their current form.

Despite this, it is possible to incorporate the initial, elastic stages of the joint behaviour, and this is sufficient to assess the impact of the nail-plate connection on the composite stiffness of the system. Figure 5.10 displays the finite element representation of Jarvis's tests, with the dummy material displayed in full colour.
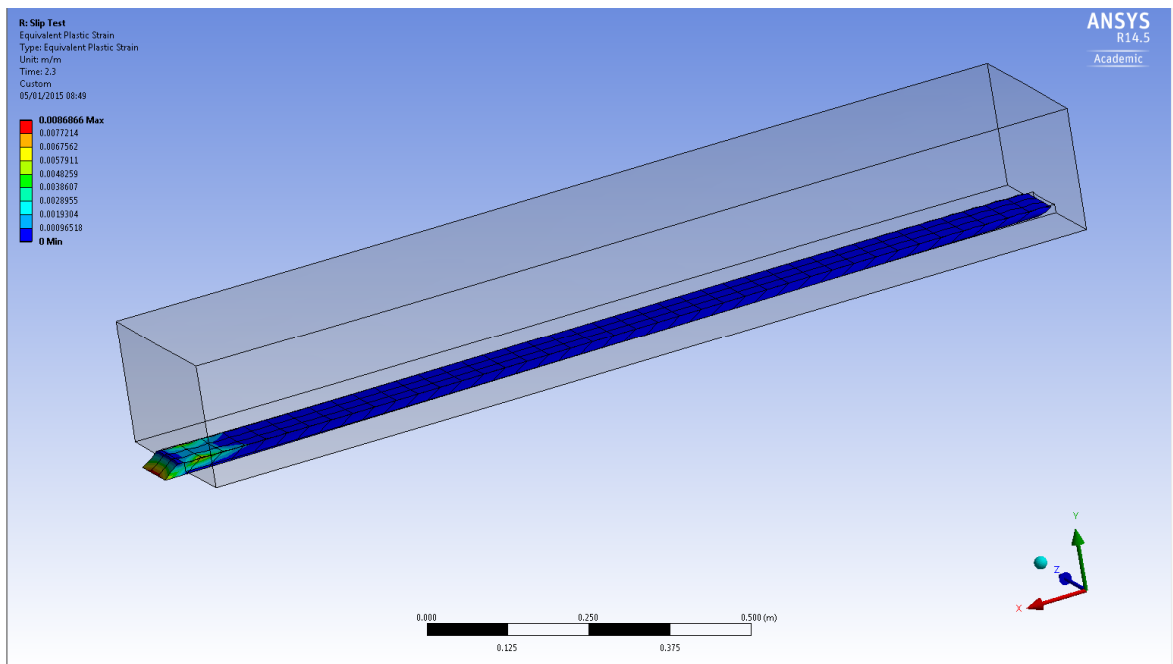
Figure 5.10 - Finite Element Model of the Nail-plate test, including "dummy" material

5.3.4 Properties and evaluation/Comparison

The nailplate was modelled as an isotropic material for simplicity, though it should be acknowledged that the behaviour of the connection in a direction perpendicular to the beam will likely be different, not least due to the difference in nail layout and orientation within the nailplate, as well as the behaviour of the timber in that direction being different. The properties used to match the longitudinal stiffness of the connection are shown in Table 5.1, below.

Table 5.1 - Mechanical properties of Nailplate shear connection "dummy material

Property	Symbol	Value	Units
Young's modulus	E	45	MPa
Poisson's Ratio (XY-plane)	ν	0.40625	
Shear Modulus (XZ-plane)	G	16	MPa
Yield Strength	σ_y	6	MPa

The resulting behaviour of the finite element representation of the nailplate joint can be seen in Figure 5.11, and in more detail over the elastic region in Figure 5.12. The yield strength of 6MPa corresponds to the onset of plasticity at 50kN load in the finite element reproduction, which is a representative, but conservative, figure and allows overcapacity in the nail-plate connection to be easily identified without impinging too much on the speed of solutions.
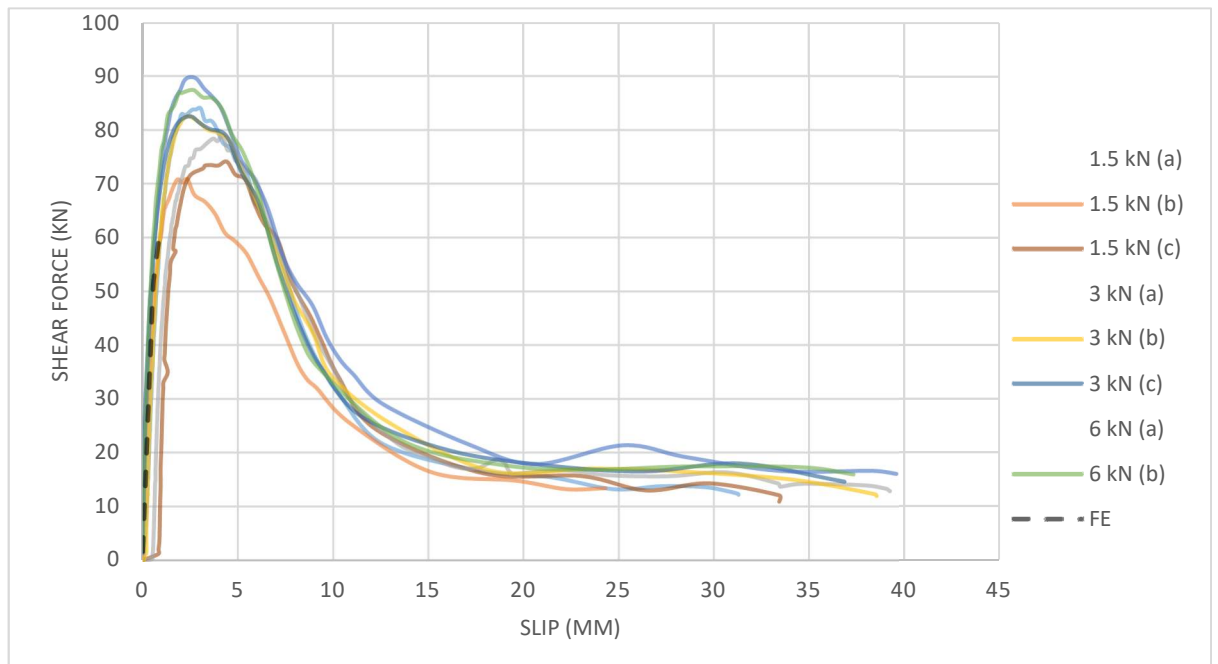
Figure 5.11 - Load Slip Trace of Nail Plate connection, with FE model trace. (letters in brackets designate repeat tests)
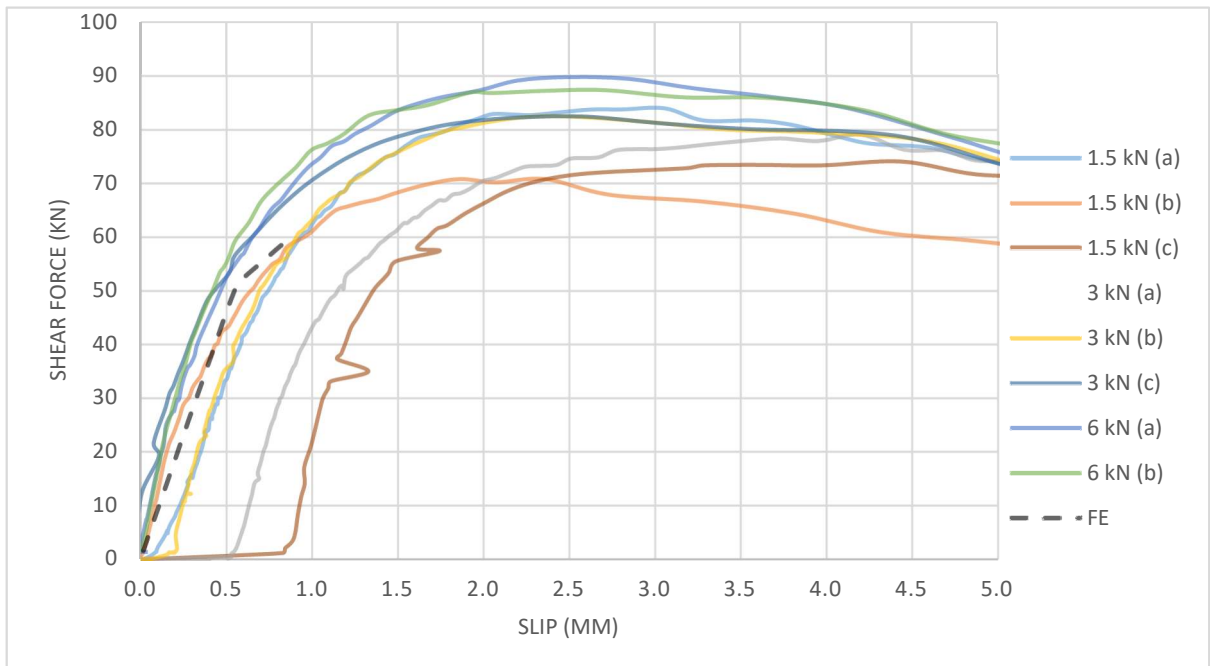
Figure 5.12 – Magnified view of load-slip comparison of Nail-plate testing and FE model

5.3.5 Incorporation into main model

Having set the geometry of the nail-plate dummy material in relation to the likely physical setup in the finite element model used in section 5.3.3, it was relatively simple to incorporate the nail plate into the full-scale finite element model. As shown in Figure 5.13, the nailplate dummy material was modelled as a part of the CLT panel at the interface with the ASB. The impact of this incorporation is discussed in Chapter 6.
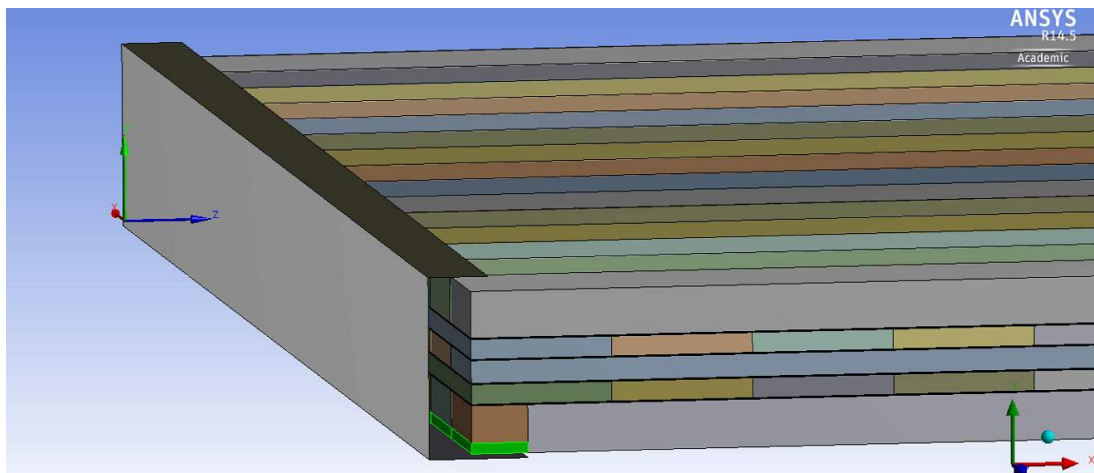
Figure 5.13 - Incorporation of Nail-plate dummy material (highlighted in green)

5.3.6 Helical Connector

Several aspects of the practicality and mechanical behaviour of the nailplate shear connection, as experienced through the testing regime outlined in the preceding sections, suggest this may not be a viable connection method for the system. The need for test samples to be hammered onto the nail plates for embedment to occur (rather than the simulated self weight) would be problematic in a construction context. Connecting to a steel beam in place within a frame, any impulsive load applied would likely result in the conversion of the energy to vibration of the beam, creating instability within the structure and a dangerous working environment for construction staff. In terms of mechanical response, the strain softening of the nailplate connection (discussed in section 5.3.2) is particularly problematic. As well as maintaining compatibility of curvature between the two elements, the shear connection must maintain the join between the floor slab and the steel frame to prevent disproportionate collapse, and requires a degree of ductility to do this in the accidental condition. The results of Jarvis' study[185] show that the nailplate connection loses its load carrying capabilities once the peak stress is reached and would therefore not withstand the tying forces necessary to maintain robustness. For these reasons, the use of a different type of connector was considered – the Helix connector.

Coste[172] researched the use of Helix connectors in timber structures and the background information and test data used in this section are sourced from his study. According to Helifix, one manufacturer of the connector, the helix connector is typically used in masonry associated with timber frame construction for strengthening and stabilisation purposes[187].

The helix connector can be seen compared to other timber connector types in Figure 5.14. Coste's study[172] tested and compared the behaviour of each of the types of connector shown in different loading conditions and arrangements. Of particular interest was the testing performed on the connectors with lateral loading. The behaviour of a single connector in single shear was tested and the load displacement trace shown in Figure 5.16, whilst the results are summarised in Table 5.2 – P_{max} is maximum load, δ_{max} is the slip under maximum load, P_y is the yield load, δ_y is the slip at yield, and R_D is the "ductility ratio" given by δ_{max}/δ_y .
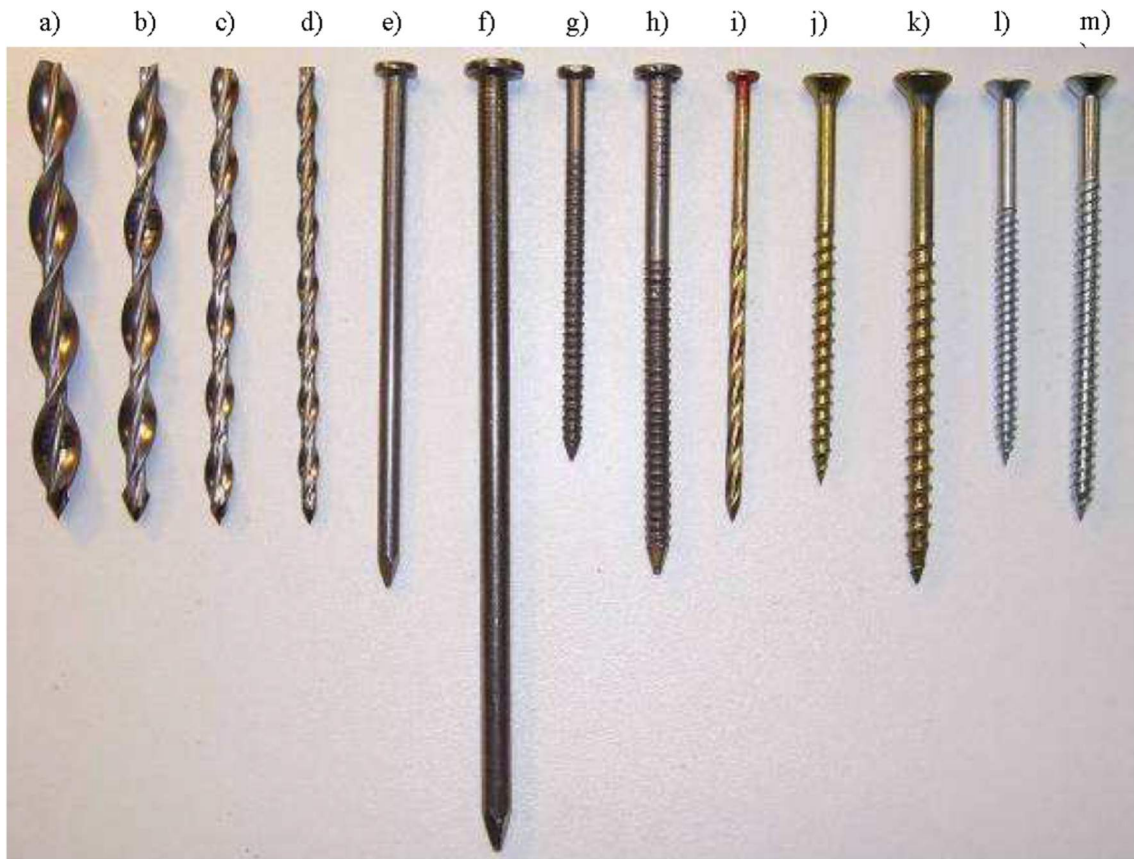
Figure 5.14 - Helix connectors of various specification (a. to d.) compared to round nails (e. & f.), annular threaded nails (g. & h.), a helically threaded nail (i.), and wood screws of various specification (j. to m.)[172]

(a)   (a)
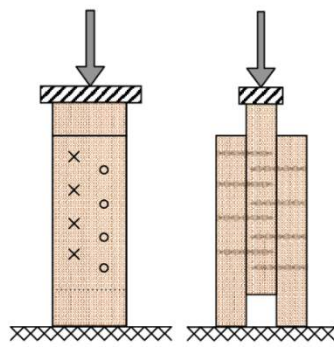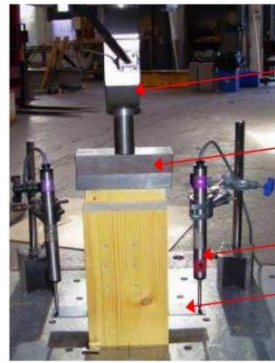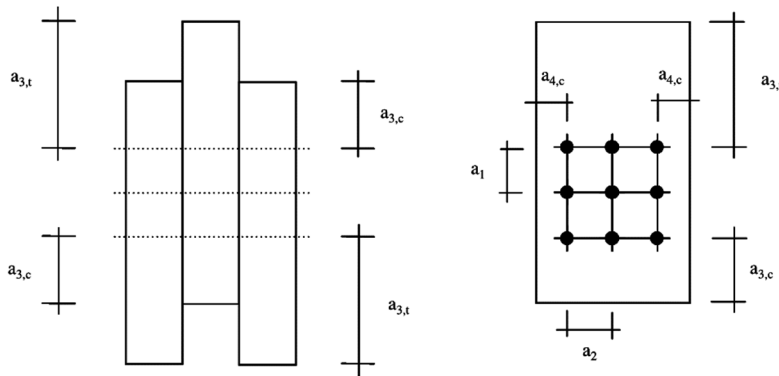
- Min spacing parallel to the grain, a_1 8d
- Min spacing perpendicular to the grain, a_2 5d
- Distance to loaded end, $a_{3,t}$ 80mm
- Distance to unloaded end, $a_{3,c}$ 30mm
- Distance to loaded edge, $a_{4,t}$ 25mm
- Distance to unloaded edge, $a_{4,c}$ 25mm

(c)

Figure 5.15 - Helical Connectors in Lateral Shear - (a) Testing arrangement; (b) Testing setup and components; (c) Connector spacings and end/edge distances (modified from Eurocode 5)[172]

Table 5.2 - Results of single fastener lateral load tests[172]

Single shear test results					
Fasteners	P_{max}	δ_{max}	P_y	δ_y	R_D
	N	**mm**	**N**	**mm**	
StarTie 10	4597.8	33.36	2814.5	3.50	9.52
StarTie 8	3828.1	33.56	2532.3	3.64	9.21
InSkew	3522.4	30.93	1969.7	2.57	12.03
TimTie	3260.0	29.25	1877.4	1.80	16.23
UMW5	3099.1	5.19	2001.0	0.97	5.33
BZP-10	3011.9	7.94	1674.3	1.07	7.44
BZP-12	4379.3	7.57	2291.1	0.84	8.98
ATN375	2619.1	12.79	1676.8	1.92	6.65
HTN3	2080.6	15.26	1671.0	1.95	7.83

As shown in Figure 5.16, joints formed with the helical connectors (StarTie 10, StarTie 8, InSkew and TimTie) all show a high degree of ductility compared to the other connectors whilst also having similar stiffness against lateral loads, both key characteristics for application as a shear connector in the proposed ASB-CLT composite system. The most suitable connector from these tests is the StarTie 10, which has the highest yield stress (2.8 kN) combined with good ductility (R_D = 9.52). This behaviour was represented in the finite element method.
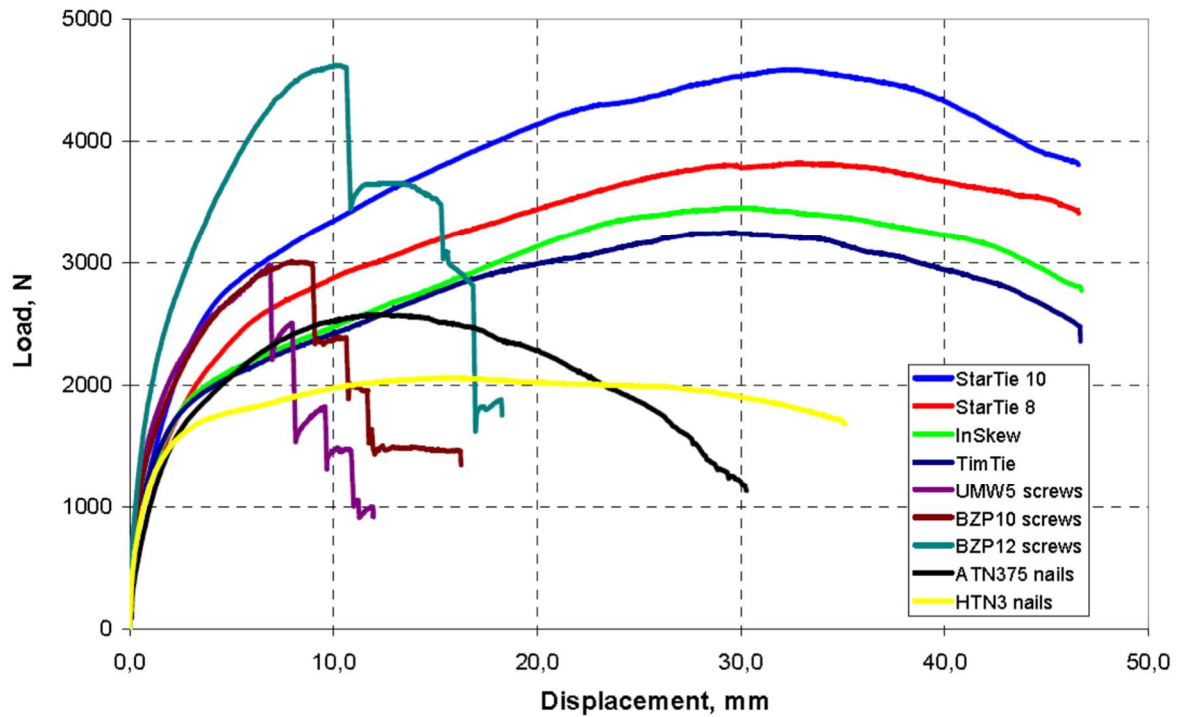
Figure 5.16 -Comparative load-displacement traces for timber connectors loaded laterally[172]

The "dummy material" approach used in the nailplate modelling was utilised for the helix connector too. The single shear connector test was recreated in finite element format, with the interface of the joined pieces and the behaviour of the helix connector being represented by an intermediate body – shown in orange in Figure 5.17. To facilitate the use of the same modelling geometry in the bay-scale models, the intermediate dummy material of the shear test is modelled with the same depth as the shear connector body in the main models, meaning the material model, once tuned, can be directly applied.
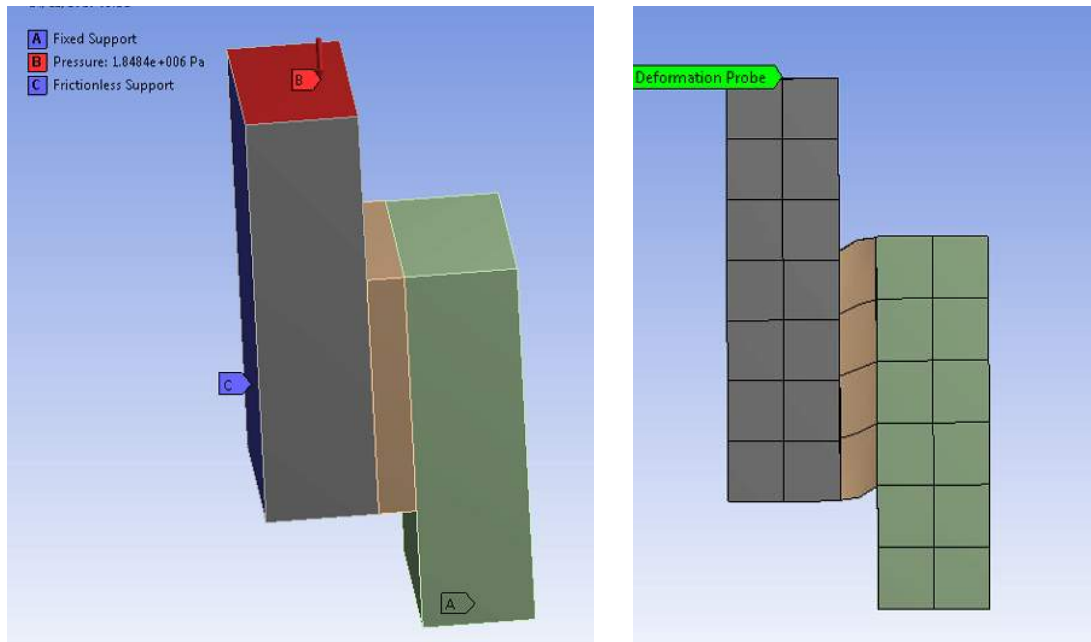
Figure 5.17 - Finite Element model of the single shear test showing loading/constraints (left) along with the mesh and deformation mode (right)

The parameters of the dummy material were tuned to the target of 3.5mm of slip under a 2.8kN load, at which point the deformation should become plastic. This target is taken from the yield point results experienced in the physical tests of the StarTie 10 (highlighted in Table 5.2). The behaviour was tuned through manipulation of the material parameters by trial and error, which are reported in Table 5.3 and Figure 5.19.

Table 5.3 - Helix material model trial parameters

	Young's Modulus [Pa]	Poisson's Ratio	Shear Modulus [Pa]	Yield Strength [Pa]
Trial 1	3.9e6	0.3	1.5e6	n/a
Trial 2	7.8e7	0.3	3e6	5e5
Trial 3	1.56e7	0.3	6e6	5e6
Trial 4	8e6	0.33	3e6	5e6
Final Parameters	1.6e7	0.33	6e6	6e5
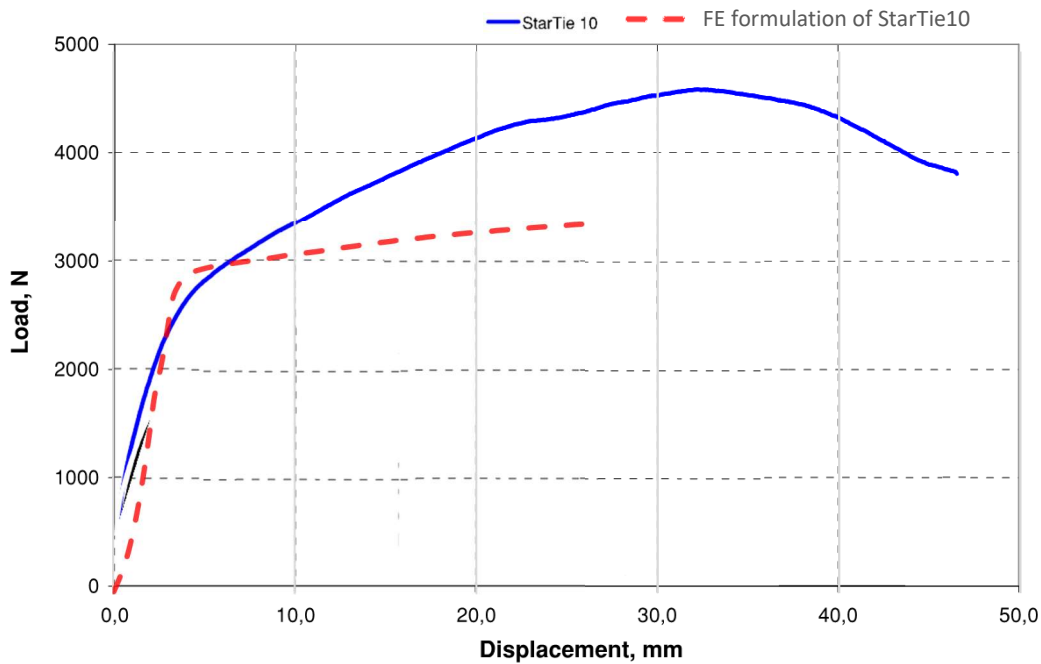
Figure 5.18 – Lateral Load-displacement behaviour of simplified FE representation, representing StarTie10

The load-slip trace goes passes close to the target point of 2.8kN, 3.5mm (P_Y, δ_Y from test results), however onset of plasticity in the ANSYS model is in fact at 1.8kN, 2.34mm. This is symptomatic of one of the drawbacks of material formulations in ANSYS and simplifications in the modelling approach. The real-world behaviour of the joint shows the onset of *non-linearity* at approximately this point (1.8kN, 2.34mm), however the deformation is likely still elastic, however in ANSYS, any change in slope of the young's modulus behaviour is taken as plastic deformation (and therefore post-yield). This means that whilst the joint behaviour shows relatively well the transition from pre- and post-yield, using the onset of plastic deformation in the ANSYS model will be a conservative assessment of the connection strength.

A comparison of the FE model output and the physical testing is shown in Figure 5.18. From this figure it can also be seen that that the initial slope of the FE representation is less than that of the physical tests, suggesting that the stiffness of the connection will be underestimated in the main FE models where the Helix connector is applied, and is hence conservative in both stiffness and strength.

Figure 5.20 - Typical failure of helical fastener in single shear test[172]

The major drawback of the implementation of these results is that the data is from timber-timber slip tests, and therefore is not directly comparable to the envisaged usage of the helix connector. As can be seen in Figure 5.20, in timber-timber slip testing, deformation is distributed between the two pieces being joined, whereas for a timber-steel configuration, the deformation distribution will be markedly different. Whilst the deformation characteristics cannot be predicted for the helix connector, it is likely that the increased stiffness of the steel piece compared to the timber will alter the deformation mode to one similar to that found by Asiz & Smith[2] (shown earlier in Figure 5.3), however there is also the potential for the failure mode to become more prone to shearing of the connector which is a less ductile mode.
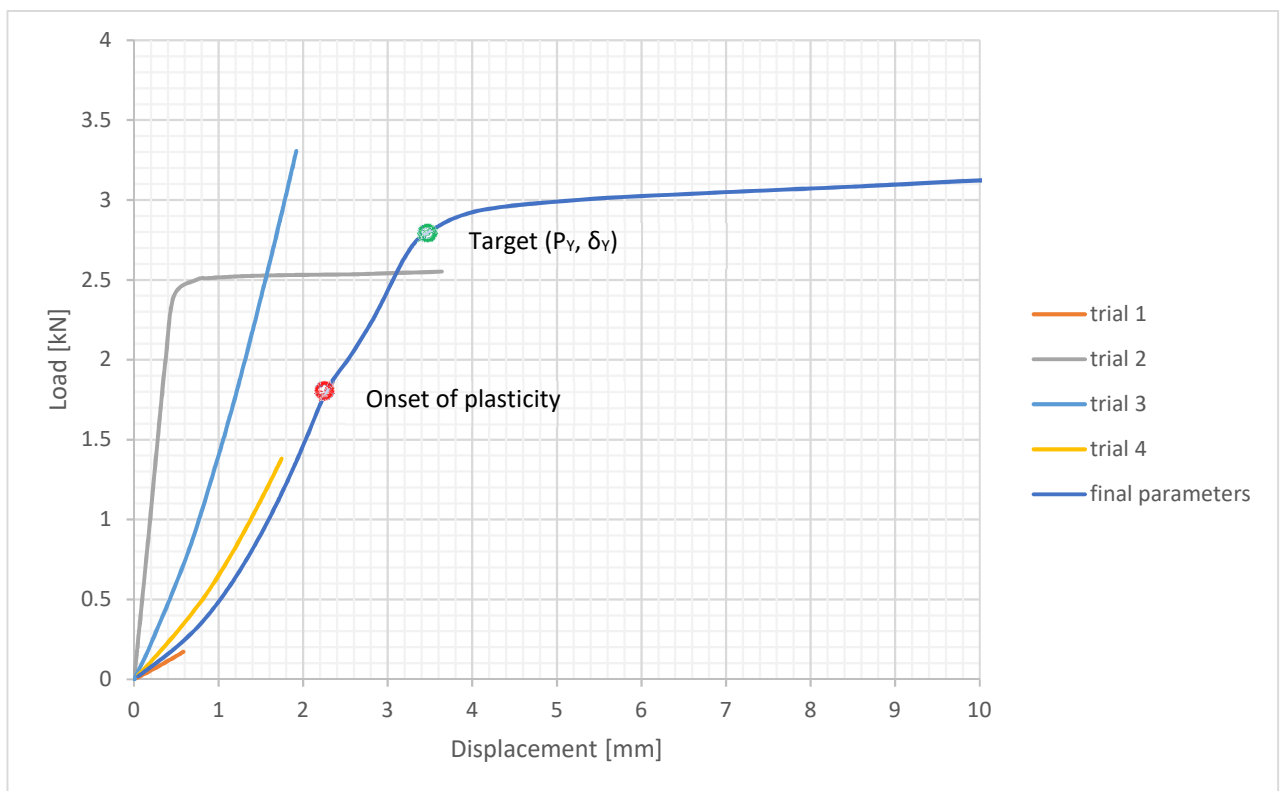
Figure 5.19 - Helix Connector Load-Displacement outputs of FE trials

Group action was not considered as this is unlikely to be issue due to the practical spacings between connectors envisioned. Closer grouping would allow for a stiffer connection in the system if needed for more highly loaded structures, at which point group failure may become more impactful.

In terms of practical use of a helix type connector in CLT steel construction as a shear connector, this would require a redeveloped helical tie to be more suited to the application. This includes the addition of a countersunk or bolt head along with a section of blank shaft to more effectively bear against the inside of the hole through the steel and resist lateral movement. The opening in the steel would need to be predrilled off-site and it (along with the unthreaded portion of connector shank) would need to be of larger dimension to the helical section to allow clearance when fixing into timber through the hole.

5.4 Panel-to-Panel Connection

5.4.1 Need for Connectors

Whilst initial models (sections. 4.3.4 and 4.3.5) were unsuitable (overly stiff), a key output from that study was the potential influence of connection in the regions of the CLT panels that are below the neutral axis. Where in conventional concrete-steel SlimFlor systems, the concrete below the neutral axis is ignored and assumed to have no tensile capacity, timber has significant capabilities under tension. Ignoring this would be to waste section depth and material, which impacts both the cost and environmental impact of the structure, and therefore the tensile zone of the CLT slabs must be engaged to generate composite action most successfully.

The models showed an improvement in reduction of deflections (from 6.5% to 17%, see section 4.3.5) as a result of tying together the lower-most faces of the panels, and suggests a suitable connection must be found that, in connecting the panels together, transfers tensile forces across the joint and engages the tensile regions of the panels. This connection also plays an important role in ensuring the robustness of the structure and in transmitting loads to the lateral stiffening structures (cores/bracing etc.). Loss has been working concurrently on the suitability of CLT as floor diaphragms in this way, and performed a programme of tests on a variety of inter-panel connectors[102].

An MSc project within the department investigated the performances of panel-to-panel connection types[188]. In that study, the joints were constructed and subjected to bending and shear forces along the panel-panel interface. An overview of the testing regime, approach and findings is presented in 5.4.2. Panel-to-panel connections are already employed in CLT structures, though little mechanical behaviour data for the joints was available at the beginning of the project. The tests performed in the MSc project aimed to assess the mechanical behaviour of two types of joint so their load responses could be incorporated into the overall system model. Butt joints and half-lapped joints were investigated due to their relative simplicity to create. To allow for load transfer across the interface, screws are used across the join, and also to give some local reinforcement.

5.4.2 Testing Regime

In the CLT–ASB floor system, vertical load induces curvature in both the beam and the panels perpendicular to their span direction. To mimic this an experiment was set up as a 4-point bending test to subject the joint to pure moment, with the CLT pieces arranged to join the top and bottom layers in the weaker radial-tangential direction. This is an important point – in the internal structure of the CLT panel, it is the 2nd layer from the bottom that has significant tensile strength and stiffness when loading is applied in this orientation. This means load transfer has to occur between these layers running parallel to the beam in each panel and the screw connectors need to interface with these parts effectively.

The testing regime was informed by the research of Hossain et al[184], performed at University of British Columbia Vancouver. In their study, 3-point bending tests were performed on joints formed by self-tapping screws between CLT panels. This was in essence a push-out test, but configured to prevent crushing of the CLT from being the dominant deformation mode. With 60 specimens tested and three joint configurations compared (spline joint, lap joint and butt joint) they concluded that whilst the self-tapping screws have a large degree of ductility in and of themselves, butt joints formed with them are stiffer and stronger than would be expected when deformation of the screws is dominant.

In the test performed as part of this project, self-tapping screws were adopted as envisioned metal fasteners for the panel-to-panel connection. Half-lapped joints were tested alongside butt joints with both using self-tapping screws as ties/local reinforcement. As well as a three-point bending test, arranged to subject the connection to shearing loads, the joints were also tested in 4-point bending, in order to approximate the loading and orientations that would occur in service in a manner more relevant to the system behaviour of interest. As such, the joints for testing were assembled as a strip cut out of a panel (see Figure 5.21). The arrangements of the shear and bending tests can be seen in Figure 5.22 and Figure 5.23 respectively.
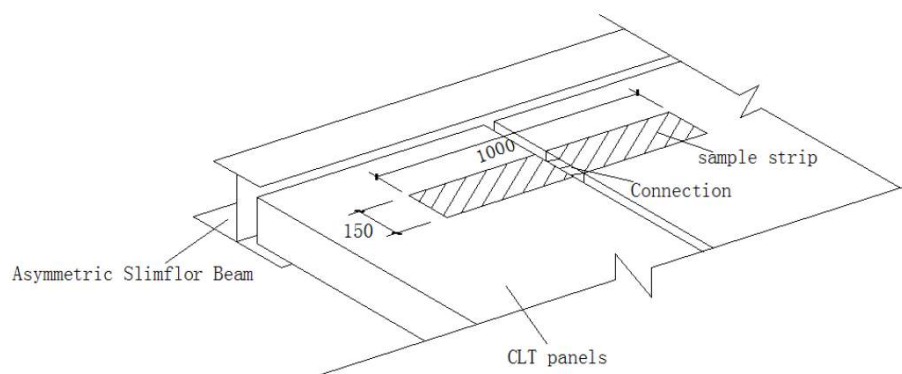
Figure 5.21 - Panel-to-Panel Connection - Test Sample Strip[188]
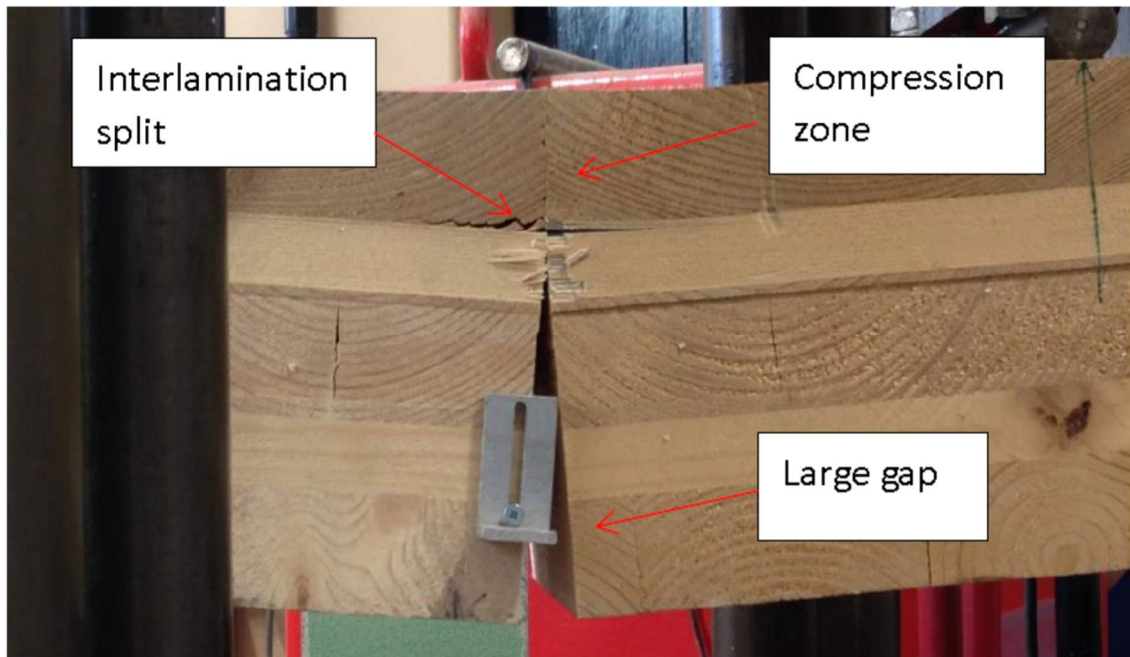
Figure 5.23 - Butt-joint in 4-point bending test - connection subject to bending parallel to the steel beam[188]

Figure 5.22 -Half-lapped joint in 3-point bending test - connection subject to shear between CLT panels[188]

Whilst the above figures show the end state of the tests after failure has occurred and the mechanisms involved, for the purposes of modelling, it is the stiffness and limit of elastic behaviour that are of greater importance.

The full details of the testing can be found in Peng's report, *Cross Laminated Timber Panel-to-Panel Connections for Timber-Steel Hybrid Construction*[188]. In total, 8 tests were performed; in both bending and shear, the half lapped connection was tested with and without additional reinforcing screws, and the butt joint test was performed twice in each loading configuration. The trace of load against deflection for the bending tests is reproduced in Figure 5.24, and it can clearly be seen that the butt joint offers a generally stiffer connection between panels, with satisfactory ductility and a clearer transition from elastic to plastic behaviour, when compared to the half-lapped joints.
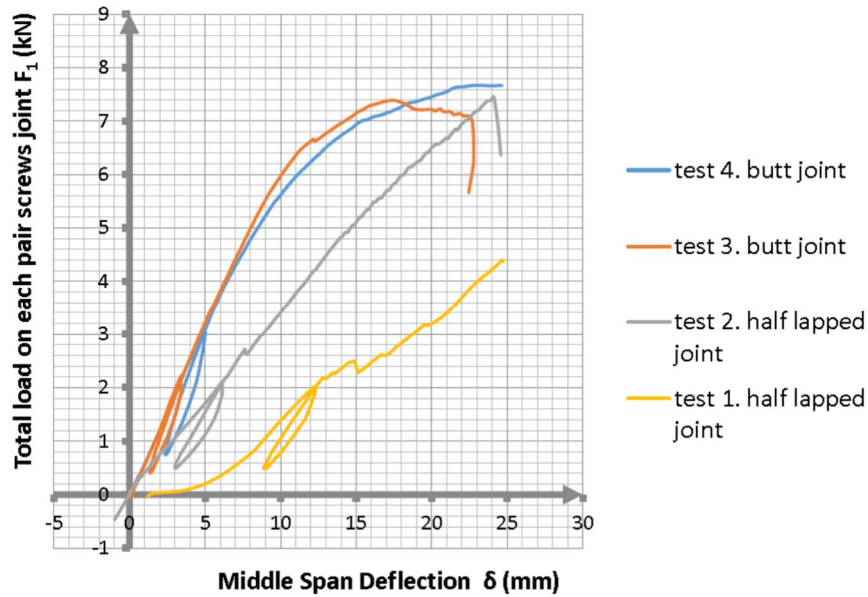
Figure 5.24 - Load-deflection diagram of test strips under bending[188]

In terms of resistance mechanisms, the arrangement of the screws in the butt joint induces them to withstand the bending forces by tensile extension of the screws, and the withdrawal strength of the thread in the timber. This appears to be a stiffer mechanism than for half lapped joints where the screws are subject to shear with bending, and the timber acts in bearing.

As the butt joint offers a more effective prospect for the panel-to-panel connection, this was the behaviour introduced to the overall system finite element model. In order to do this, the test setup was replicated in ANSYS, in much the same manner as for the nail plate connection.

5.4.3 FE modelling of tests

As was the case with the shear connection, modelling of the detail of the self-tapping screws and its interaction with the timber would be overly time consuming and computationally intensive. Instead, the "dummy material" approach was used again.

Figure 5.25 - Butt-joint testing sample geometry[188]

The geometry of the butt-joint bending test setup is shown in Figure 5.25. This geometry was recreated in ANSYS in order to tune the behaviour of the model to match that of the test. The CLT formulation used was that developed for the main investigation i.e. including glue layers and individual laths. The key aspect of the behaviour to capture is the response in the tensile zone. Where previously the contact behaviour between the lower laths of the two CLT pieces were set as bonded, here a "splicing" solid element is added that spans the gap between the CLT panels, and is bonded to the lower most laths of each panel. In this way, the properties of the splicing piece can be manipulated until the response of the model mimics that of the butt joint in the physical tests performed. The formulation of the model can be seen in Figure 5.26.

Figure 5.26 - ANSYS model replicating butt-joint bending test configuration

For simplicity, just the elastic stiffness was sought to be replicated. Through tuning of the properties the stiffness of the connection could be replicated appropriately. The behaviour of the ANSYS model is shown in Figure 5.27, and was generated using the material properties shown in Table 5.4.
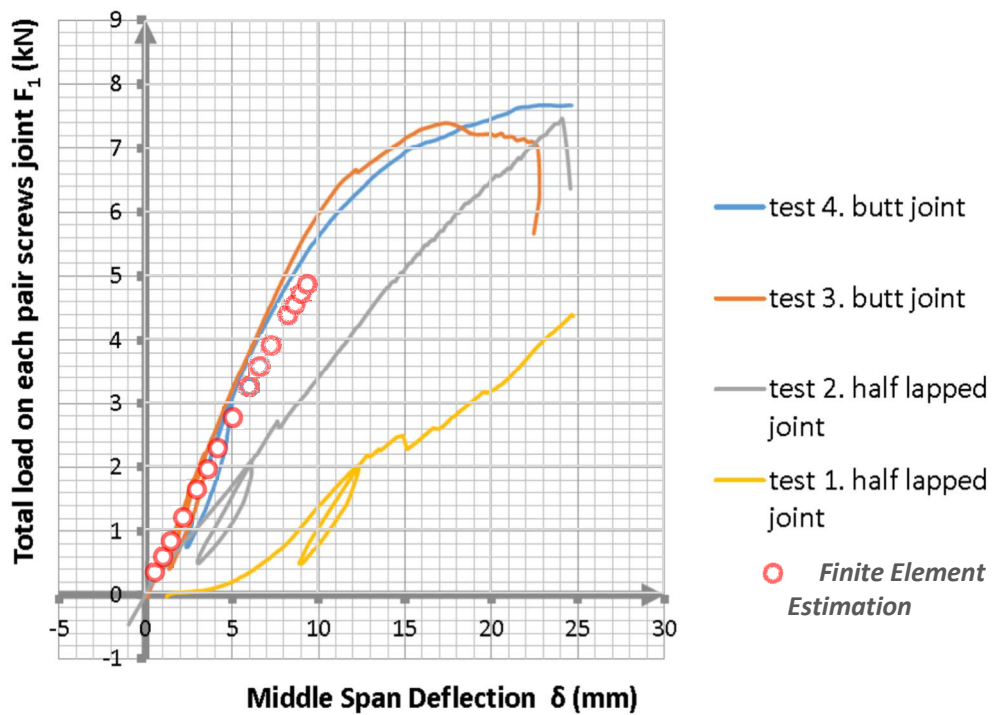
Figure 5.27 - Load-deflection diagram comparing FE approximation to Test Results

Table 5.4 - Mechanical properties of butt-joint dummy material

Property	Symbol	Value	Units
Young's modulus X direction	E_x	3.5	GPa
Young's modulus Y direction	E_y	20	MPa
Young's modulus Z direction	E_z	160	MPa
Poisson's Ratio XY	v_{xy}	0.3	
Poisson's Ratio YZ	v_{yz}	0.35	
Poisson's Ratio XZ	v_{xz}	0.467	
Shear Modulus XY	G_{xy}	230	MPa
Shear Modulus YZ	G_{yz}	11	MPa
Shear Modulus XZ	G_{xz}	0.332	MPa

With this behaviour established from testing, the implementation of the behaviour into the main models is achieved by means of introducing the splicing element and its mechanical properties at the interface between panels of the main model in the same manner as the test configuration model. The splicing element can be seen implemented in the main system model highlighted in green in Figure 5.28. The impact of the panel-to-panel connection is discussed in section 6.5.
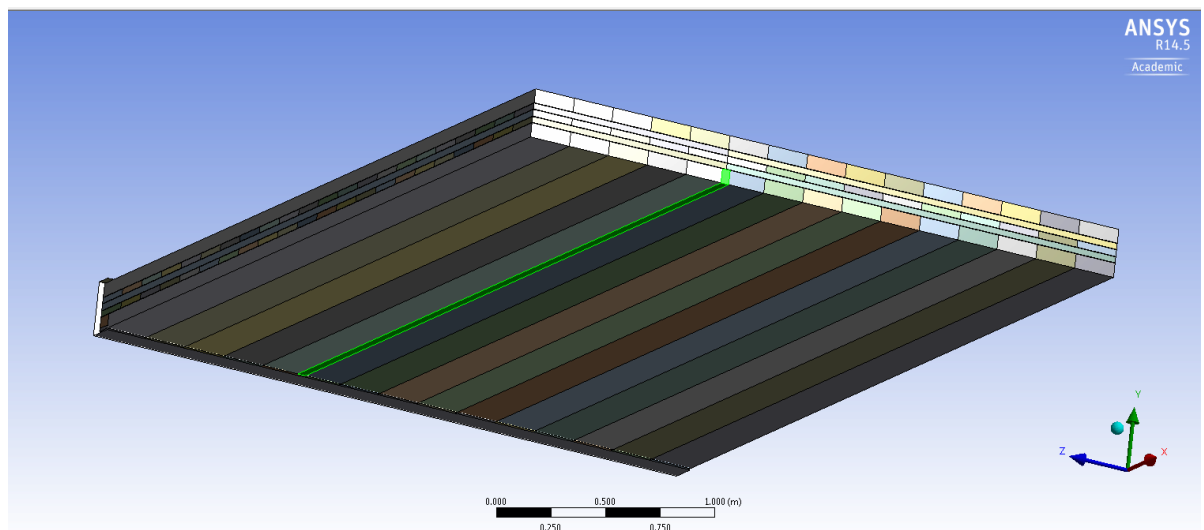
Figure 5.28 - Implementation of Panel-to-Panel connection (highlighted in green)

5.5 Conclusion

This chapter has reported the culmination of the development process of representing Cross-Laminated timber panels in a finite element formulation, and through the validation against physical testing performed in the literature, answers research question 2 in the affirmative – the mechanical behaviour of CLT can be modelled accurately using the finite element method. Whilst this answer has caveats (validation has been performed for bending and in-plane shear only), it is suitable for the application of the modelling methodology in analysing the effective width and associated composite benefit of CLT panels in a composite system.

Capturing the mechanical behaviour necessitates modelling to a level of detail that includes modelling the individual laths within the layers of the timber, and the representation of the glue layers as interstitial elements between the timber layers.

Supplementing the development of the CLT modelling, physical testing and finite element representation of the key system connectors have been performed, namely the shear connection (defining interface slip behaviour) and the inter-panel connection (affecting load carrying capacity, as detailed in Chapter 4).

The modelling methodology developed here, combined with the material properties derived for the connections, provide analytical tools for the investigation and determination of the composite benefit provided by a composite CLT-ASB system.

This investigation will be reported in chapter 6.

Chapter 6. Parametric Study – Application of Finite Element Modelling Philosophy

6.1   Synopsis

This chapter presents the application of the modelling methodology, developed through Chapters 4 and 5, towards answering Research Question 3:

 "Is it possible practically to generate composite behaviour between steel and timber, and can the degree of benefit be quantified?"

Further analysis and discussion of the implications of these findings within the wider context of the system will follow in Chapter 7.

6.2   Introduction and Reference Case

6.2.1 Scope of Study

With the developed FE modelling process, it is now possible to explore the effects of various parameters within the system. This allows further analysis to take place and the quantification of the impacts of various changes to the setup of the system.

The study considers the following aspects:

a.   Bay dimensions – beam length, slab span, aspect ratio
b.   Panel position – above the top flange of the beam or sitting on bottom flange
c.   Shear connection
d.   Inter-panel connection
e.   CLT panel make up and layout – standard panels vs. designed panels

The remainder of this chapter will cover the findings of the parametric study analysed with a focus on different subject areas.

6.2.2 Further Model Development – Implementation Process

Following on from the preliminary models described in section 4.3.3, and the validation and development that is discussed through the remainder of Chapter 4 and Chapter 5, a modelling approach has been developed to explore the quantification of composite action. The key changes from the models used in Chapter 4 are:

- Modelling individual laths in CLT
- Modelling of the glue layers in the CLT panels, represented as shell elements (see Figure 6.1)
- Inclusion of yield points in the material model to make material failure visible

The type of shear connection (nail plate and the hypothetical helix connector) as well as the panel to panel connection have been incorporated into the model for use and comparison in investigations.
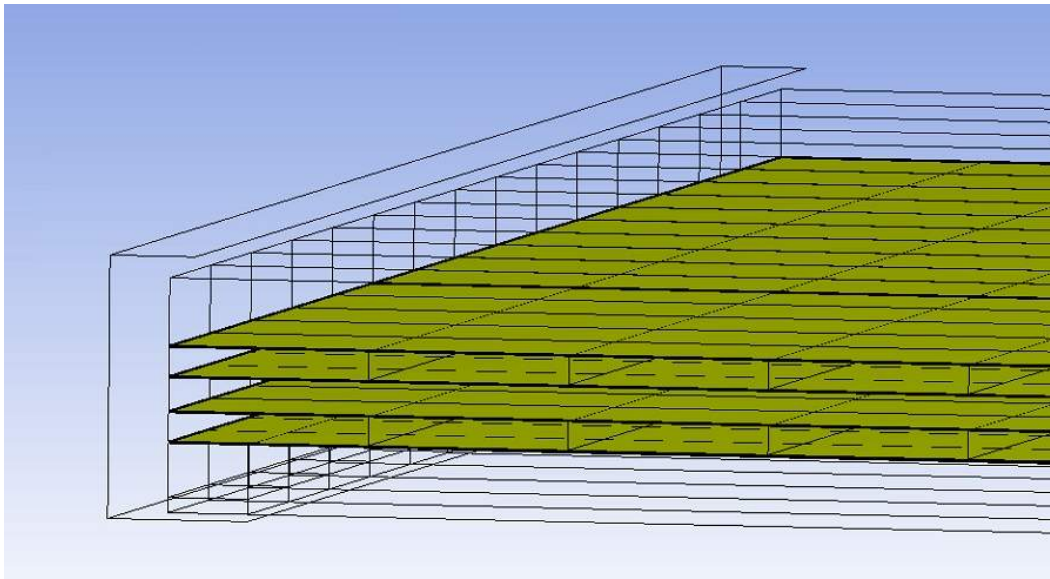
Figure 6.1 - Shell element representation of glue layers in parametric FE model

As the complexity of the models increases in order to take into account a variety of features of the system, the analysis times increase exponentially. Inclusion of the glue layers, the plasticity of timber and the shear interface, the discrete modelling of the panel slats, and the large number of associated frictional contacts that must be modelled all increase the solution time significantly. To counter this, it is advantageous, from a computational cost perspective, to use symmetry in order to halve or quarter the required number of elements and contacts. This was done during the modelling of the CLT-ASB system. In the system being analysed, symmetry is utilised at the centre of the beam (both along the centre of its cross-section and at the midspan point), and the centre of the span of the CLT panel. At these positions, the equivalently behaving system has a restraint on the rotation of the elements and the translation of the element along one of the horizontal axes, but allows vertical deflections to occur, i.e. a roller-moment support (see Figure 6.2)
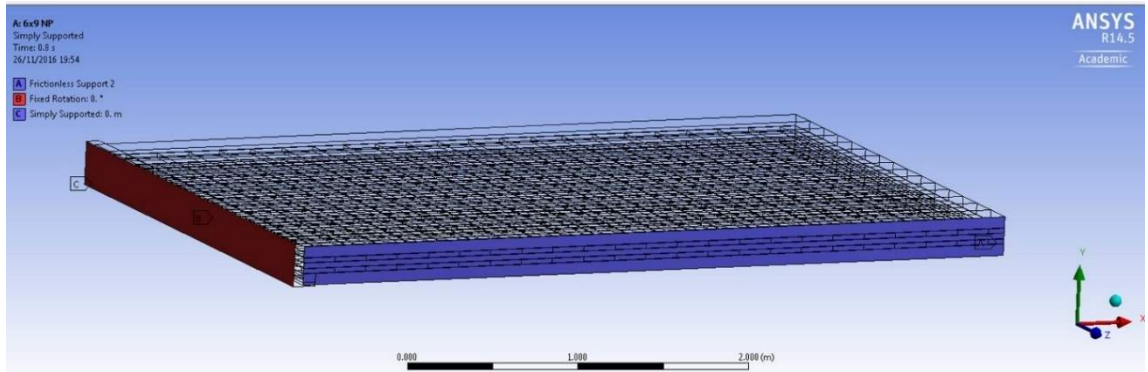
Figure 6.2 - support conditions

Within ANSY there are a number of potential methods of restraining parts of the model, and one such method, the "Remote Displacement" constraint, appears to allow these rotations and translations to be defined exactly as necessary. However, the experience of the author is that whilst the nature of the definitions suggests it will behave as desired, in actual fact the rotations are not constrained as expected; deformation in other axes are affected which can lead to the solution not converging and plasticity to develop in unusual locations and in an erratic manner. A more effective option is to use the "Frictionless Support" constraint, which behaves in a more predictable manner, though horizontal movements of the overall system must be controlled by other constraints.

6.2.3 Reference Case - Effective Width Determination

To provide a comparison point against which the effect of changes and variations in the system characteristics can be measured, a reference case setup was selected, and is outlined here. Each subsequent model created for the study of the effect of different parameters will have the same characteristics as this case, save for the parameter under consideration. The one exception to this is the study of slab position, where the shear connection was assumed as bonded instead of the nailplate, and compared to the reference case with a bonded shear connection.

The response is sought against an imposed load of 2kN/m^2 applied as an area load in the model, whilst the effect of gravity is omitted to limit the number of variables – the large deflection option (which allows for 2nd order effects in ANSYS) is utilised, meaning the inclusion of gravity loads may obscure deflection relationships by enhancing deflections. This will allow repeats of the finite element study to be performed with larger or smaller imposed loads and comparison to be made without needing to compensate for the gravity induced deflections and stresses.

The beam ends were modelled as simply supported, with fixity in the horizontal plane of its mid-span (due to the symmetry constraints, as detailed in section 6.2.2), and freedom to move longitudinally at the end. This was to prevent further stresses being induced or the deflection (taken at mid-span) being reduced because of restricting the curvature and movement of the beam.

The "reference case", as it will from hereon be referred to, is of the following configuration:

- Beam span: 6m
- CLT panel: KLH 230ss, spanning 9m, one-way
- Shear Connection: nail plate
- Inter-Panel Connection: Assumed infinitely strong/stiff bond between panels in tensile zone
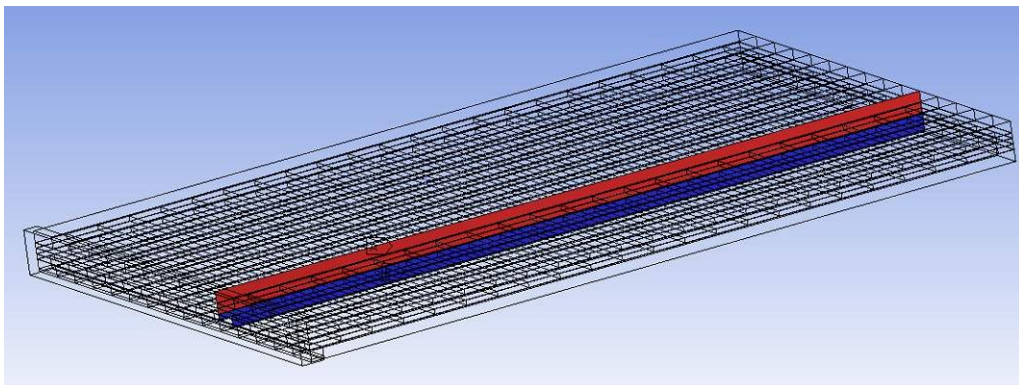
Figure 6.3 - Constraint approach between panels; Red Zone = friction constraint, Blue Zone = bonded

The nailplate shear connection was assumed, included as a single part at the interface of the ASB bottom flange and the CLT panel. A 280ASB74 section was modelled, in conjunction with a series of 7ss230 KLH CLT panels. Between the panels, an inter-panel connection was modelled as a perfectly bonded tensile zone only connection – in practice this means the bottom two layers of the 5-layer panels were joined together using a bonded contact, as shown in Figure 6.3.

The concept of an effective width is a means of simplifying the design and analysis of a composite beam section. It helps quantify how much of the floor slab contributes stiffness to the composite section, and therefore is a key part of addressing Research Question 3. As described in detail in section 2.2.2, the effective width is derived from the distribution of longitudinal stress (or strain) in the floor slab. The set-up of ASB and CLT panels was replicated in a finite element model (shown in Figure 6.4) from which the response of the system in terms of stress distribution could be extracted.

To extract the stress trace from the finite element model results in ANSYS, a linearized stress output was utilised. The trace gives evidence of the actual effective width computed by the simulation, with sampling points taken from equally spaced locations along a defined path. The magnitude of the stresses should be related to the ability of the shear connection.

The laminar nature of CLT combines with the anisotropic character of the parent timber to the result that the only layers giving meaningful contribution to the composite section are those with planks running parallel to the beams. These layers have their stiff axis in the correct orientation to contribute.

The position of sampling was selected as just below the extreme fibre of the CLT layer in the compression zone with its longitudinal axis running parallel to the beam – if the layers in a CLT panel are numbered consecutively from bottom to top, then layers 1, 3, and 5 are orientated perpendicular to the beam, whilst layers 2 and 4 run parallel to the beam and contribute to the composite section.
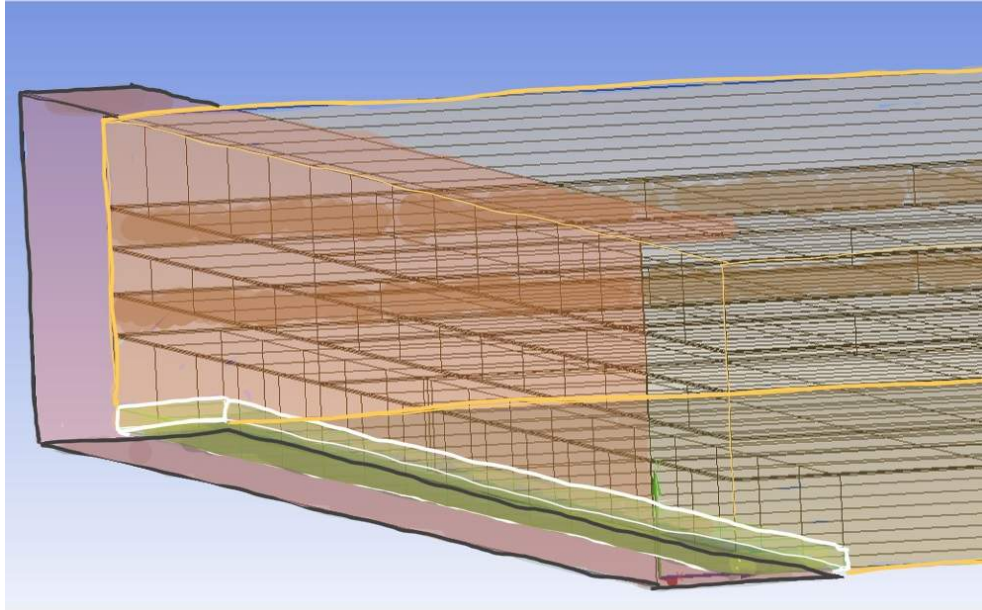
Figure 6.4 - Components of finite element model, with false colour highlighting: ASB (red), shear connection (green) and CLT panels (yellow)

The extreme fibre of layer 4 was selected so the largest stress the CLT was subjected to could be extracted. However, the stress result is affected by the edge effects, meaning it was more representative to take measurements at an offset from both the top faces of the longitudinal oriented CLT layers (by 1mm) and the *centre* of the beam span (the boundary of the model as formulated). These characteristics are the same for all effective width outputs detailed in this section

Figure 6.5 shows an example ANSYS output of longitudinal stress when taken across the CLT panel at the midpoint of the beam span, whilst Figure 6.6 shows the same output at an offset of 100mm from the model edge. Comparing the two figures one can see that end effects are playing some role, as both the shape of the stress curve and the magnitude of the maximum stress measured are different, with the larger stress occurring in the trace taken at an offset. Further, the maximum stress in the trace taken at the model edge does not occur at the first sampling position (denoted by a white tag containing the number "1") which is the value used to compute the effective width approximation. As such, these two factors have a distorting effect on the calculated effective width and the effect is not consistent, meaning sampling at an offset is a more appropriate data set for calculating effective widths. This methodology is followed for the remainder of the parametric study.
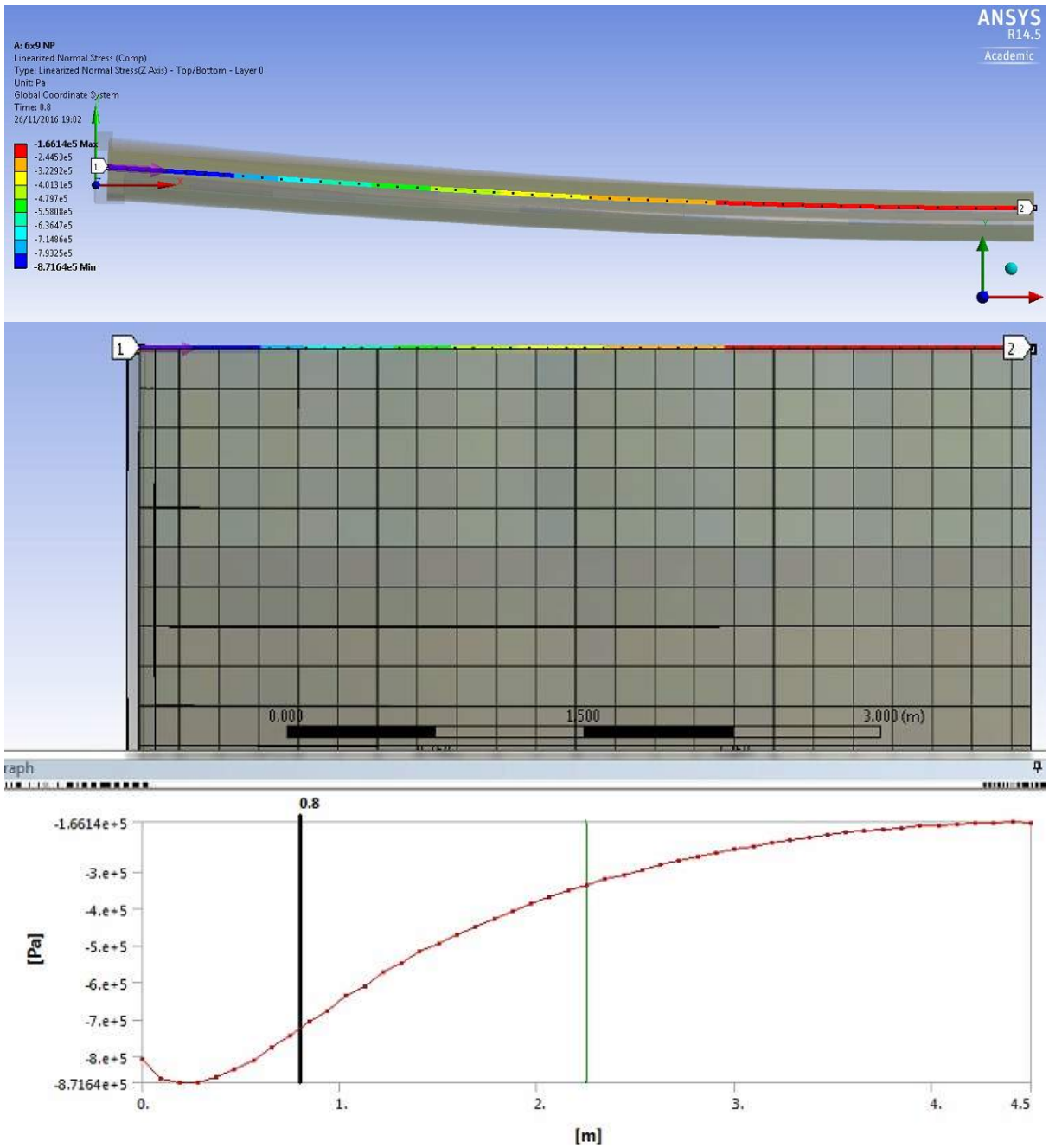
Figure 6.5 - Longitudinal stress output, measured at centre of beam span
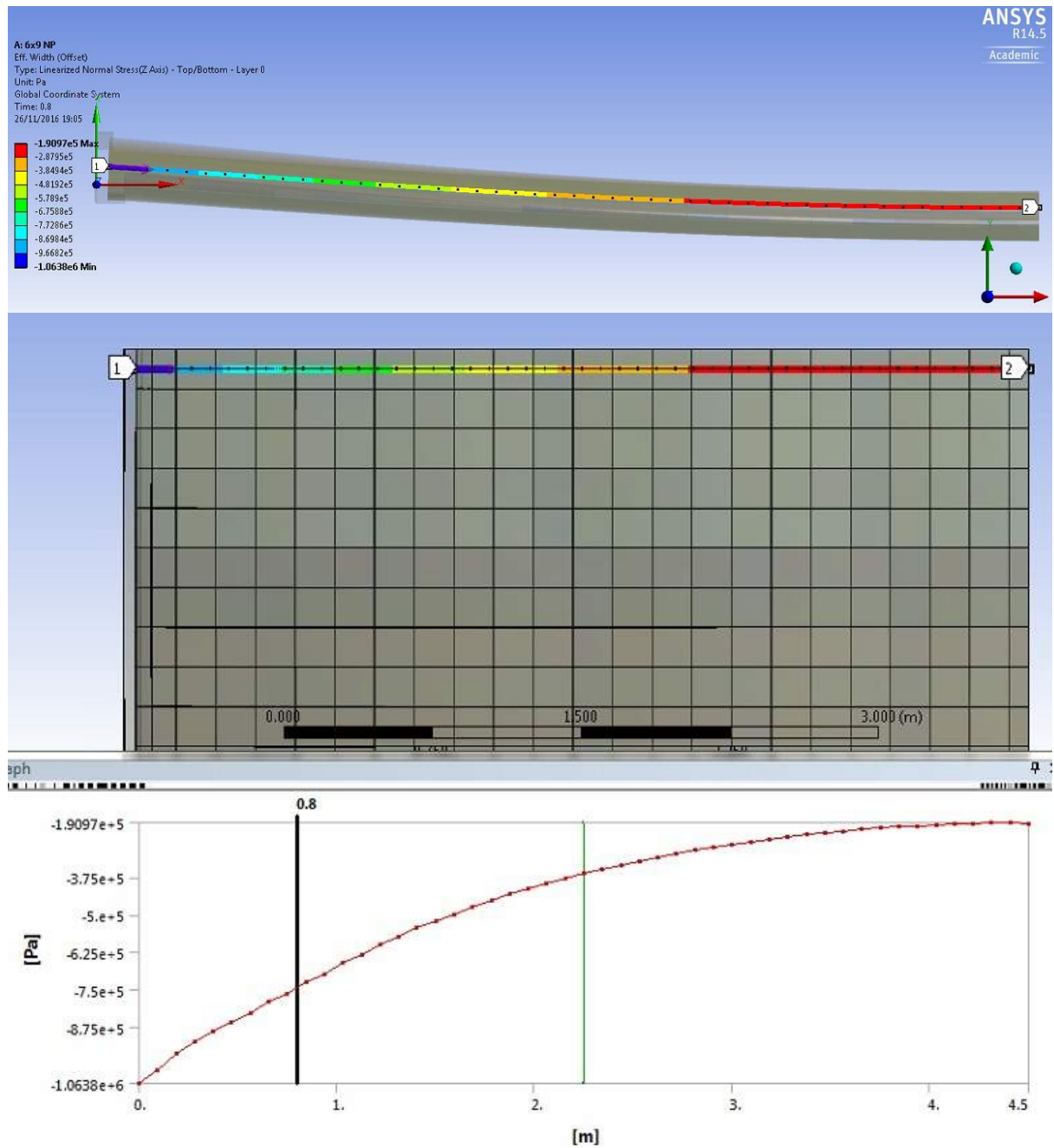
Figure 6.6 - Longitudinal stress output, offset from edge constraints by 100mm

The output trace of stresses for the reference case is given in Figure 6.7 as the blue circles. Also shown is the derived effective width, computed as detailed in section 1.4.4. For this, case the effective width has been calculated as **2.99m** (noting that the trace only displays one side of the beam, whilst symmetrical stress distribution is present). This result set will be used as a reference for comparison to determine the impact of various design changed. Deflection was found to be **12.39mm** under the defined loading. This compares to **13.12mm** that was found when the shear connection was removed and replaced with frictional contacts to represent the non-composite case. In these results, "composite benefit" is defined as the reduction of beam midspan deflection when compared to this non-composite case, expressed as a percentage of the non-composite deflection. For example, the result for the

reference case represents a composite benefit of **5.6%** using a nail-plate shear connection, rather than a non-composite connection.

A maximum stress was found at the edge of the CLT panel closest to the beam, with a value of **1.06N/mm²**.

Longitudinal Compression Stress
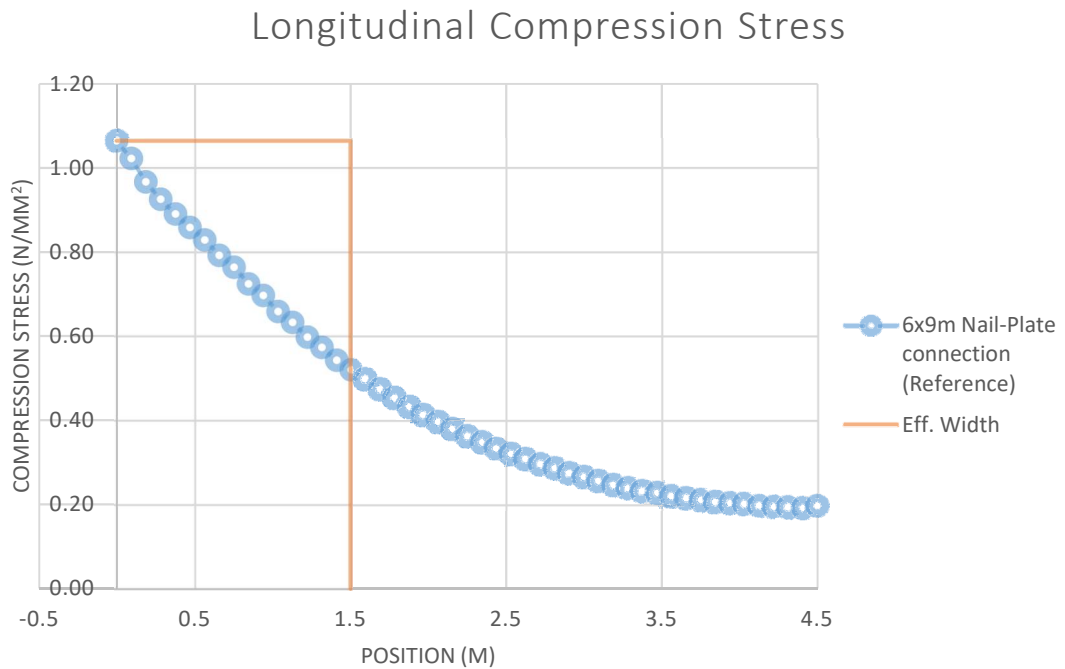
Figure 6.7 - Reference Case effective width determination

Concrete-Steel composite sections show a complex relationship between effective width, the beam span, and the position at which the measurement is taken. This appears to also hold true for CLT-ASB composite floors. Figure 6.8 shows a plot of the longitudinal stress in the CLT layer subject to mostly compressive loads, and demonstrates how the level compressive stress is at its maximum at the centre of the beam span (disregarding the visible end effects), and reduces towards the supports. However, the situation is more complex as can be seen in Figure 6.9.

Figure 6.9 displays the same data as regions of longitudinal compression and tension, and what is clear is that large portions of the CLT layer that are in the "compression zone" of a composite section are experiencing tension. The equivalent plot of layer 2, the contributing layer in the tensile region shows a corresponding compression in the same region which demonstrates that the panel is hogging in those areas rather than sagging under the distributed imposed load. The plate is deforming into a saddle shape that is characteristic of an elastic plate that is supported on two opposing sides only.
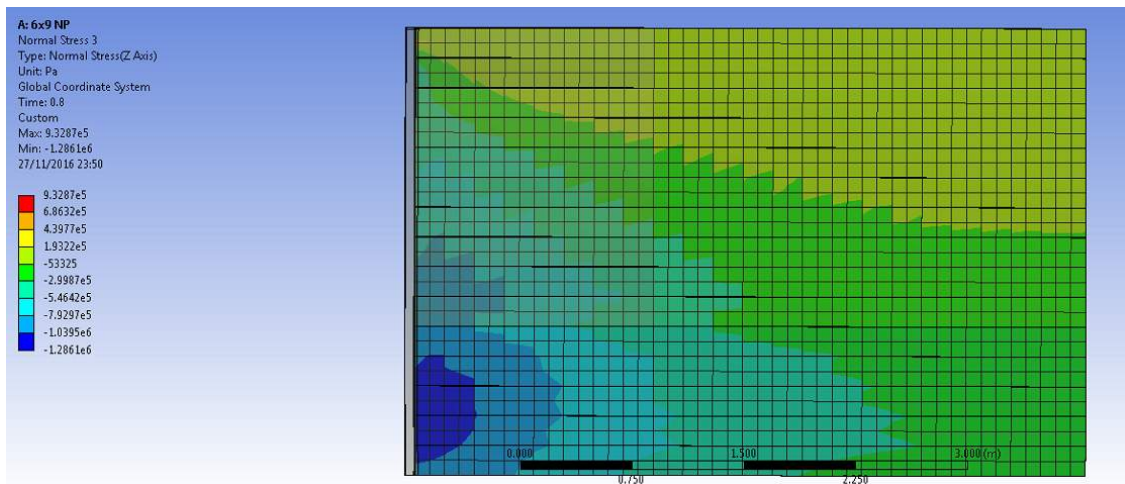
Figure 6.8 -Plan view of longitudinal stress plot in layer 4 (parallel to the beam)
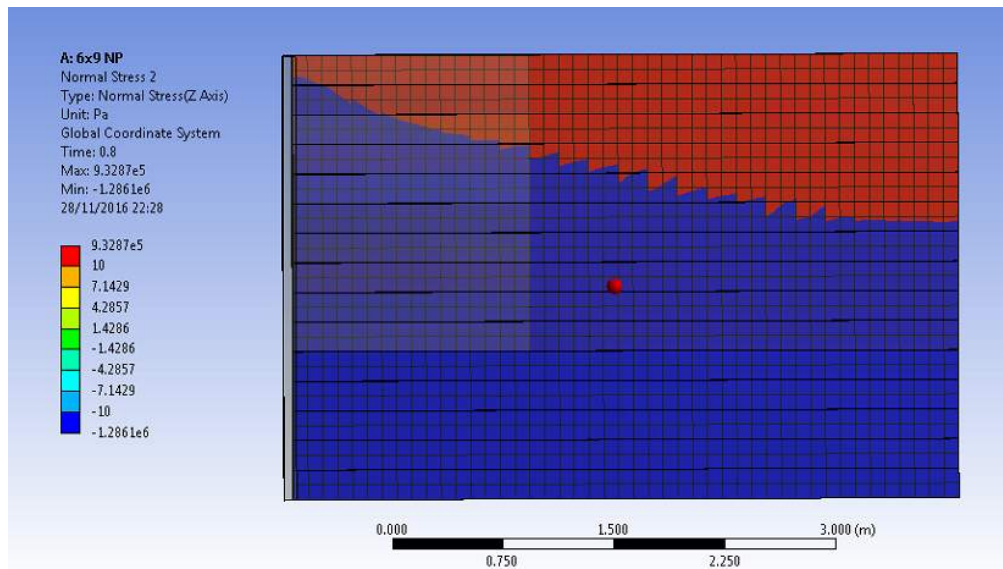
Figure 6.9 - Longitudinal stress plot in layer 4 (blue = compression, red = tension)

Whilst this deformation is reasonable, it has the effect of obscuring the measurement needed to determine the effective width closer to the supports – the tensile stresses when included in the calculation will disrupt the summation, and it is not possible to separate the stresses due to composite action from those due to the edge support conditions. A further complication is that, rather than matching the standard result from plate theory of a plate simply supported on two sides, the supports (steel beams) are in fact flexible, and have variable stiffness (from the perspective of the floor plate) along the sides.

6.3   Shear Connection Influence

In this section the effect of the shear interface connection is reported. Comparison is made between the reference case (which has a nail-plate shear connection) and an idealised bonded shear connection. These are subsequently compared to the helix connection. The mechanical behaviour of these connection methods has been covered in section 5.3.6

The nail-plate connector material was implemented by incorporating an intermediate body between the CLT panel and the bottom flange of the ASB section, forming the reference case as described in section 6.2. The connector is modelled as a solid body that runs along the length of the beam with a width of 80mm (corresponding to the bearing width of precast panels on ASBs) and a height of 15mm, which is the approximate height of the nail plate's vertical dimension and embedment depth.

For the ideal composite connection, the intermediate body was removed, and the bottom laths of the CLT panel allowed to continue and bear onto the ASB bottom flange directly (see Figure 6.10). Contacts were then used within ANSYS to bond the CLT panel to the ASB, representing a hypothetical perfect composite connection. In this way, it is possible to both determine the success of the nailplate as a shear connection and approximate an upper bound to the potential composite benefit that can be achieved.
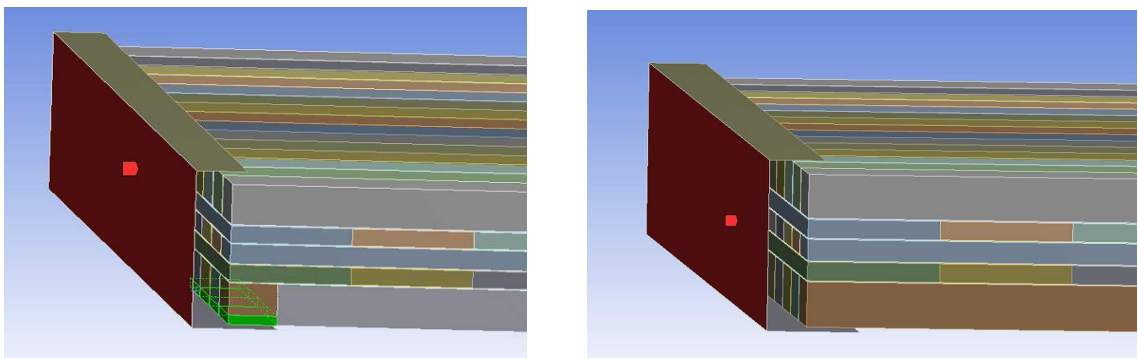
Figure 6.10 – FE model shear connection zone for nailplate/Helix connector (left) and bonded case (right)

6m Beam x 9m Panels - Longitudinal Compression Stress
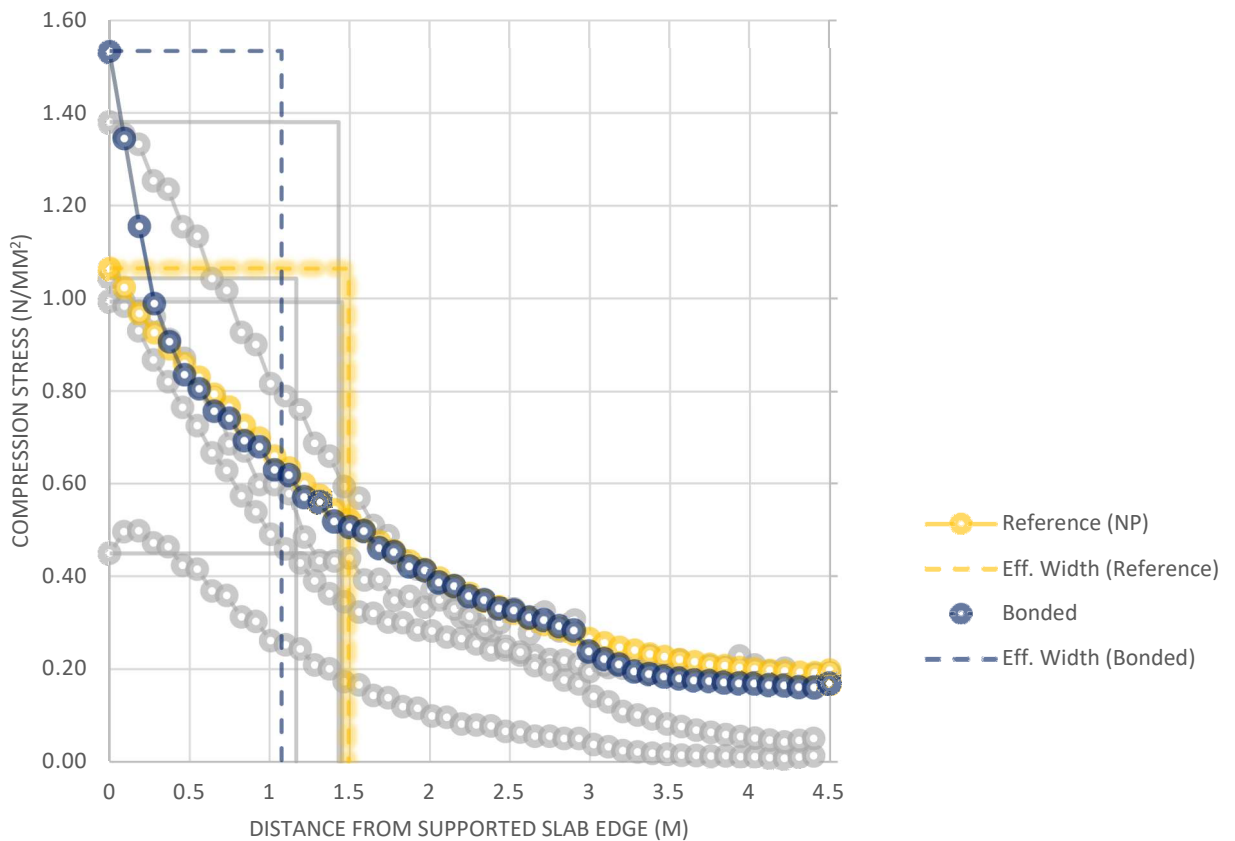
Figure 6.11 - effective width: shear connection effect (NP=NailPlate)

The trace of longitudinal compressive stress is reported in Figure 6.11, and includes the derived effective widths for the reference case (nailplate shear connection, in yellow) against the idealised bonded shear connection. As can be seen by comparing the traces of the bonded and nail-plate connections, there is little difference in the generated stresses in the majority of the panel span. The difference lies in the peak stress induced above the panel-beam interface. With a stiffer connection, this increases the peak stress induced, and because this effect is limited to the zone close to the shear connection, this *reduces* the effective width. This is because, as detailed in section 1.4.4 the effective width is the width of panel that would capture an equivalent cumulative force if the longitudinal stress was constant and equal to the stress at the beam interface. As it is just the stress level above the connection that is different between the two cases, the effective width must be reduced for the bonded connection in order for the cumulated forces (calculated from the area under the curves) to remain equivalent. The result of this is the **reduction** in effective width observed from that of the less capable shear connector, when from a design calculation perspective an increase in composite action should result in a larger effective width. This finding brings into question the validity of applying this definition of effective width for CLT composite section calculations.

In terms of deflection, applying a perfect shear connection gives a deflection of **11.35mm**, which constitutes a composite benefit of **13.5%** over the non-composite deflection**,** compared to the reference case's 12.39mm (5.6% composite benefit). Importantly, this suggests the simpler modelling methods that were initially used in chapter 4, in fact *under*estimate the potential impact of using composite action in the system, where a 5.6% composite enhancement was found with a bonded shear connection.

Note the fact that this result reflects the use of the nailplate at a particular distribution along the beam (250 mm centres). This performance may be enhanced through use of closer centres or nailplates of different configuration, but this would require verification through further study into this area through an expanded testing regime.

As noted in the detailed testing of the nail-plates, the installation and implementation of a nailplate connection may not be the most practical, and also does not offer the kind of ductility that would be preferable in such a system. In section 5.3.6, a second shear connector candidate offering more ductility and (potentially) more straightforward installation, the helix connector, was modelled and validated against physical tests. The derived material properties for the helix connector were implemented into the parametric study models, replacing the nail-plate material model and the results are shown in Figure 6.12.

6m Beam x 9m Panels - Longitudinal Compression Stress

Legend:
- Reference (NP)
- Eff. Width (Reference)
- Bonded
- Eff. Width (Bonded)
- Helix
- Eff. Width (Helix)
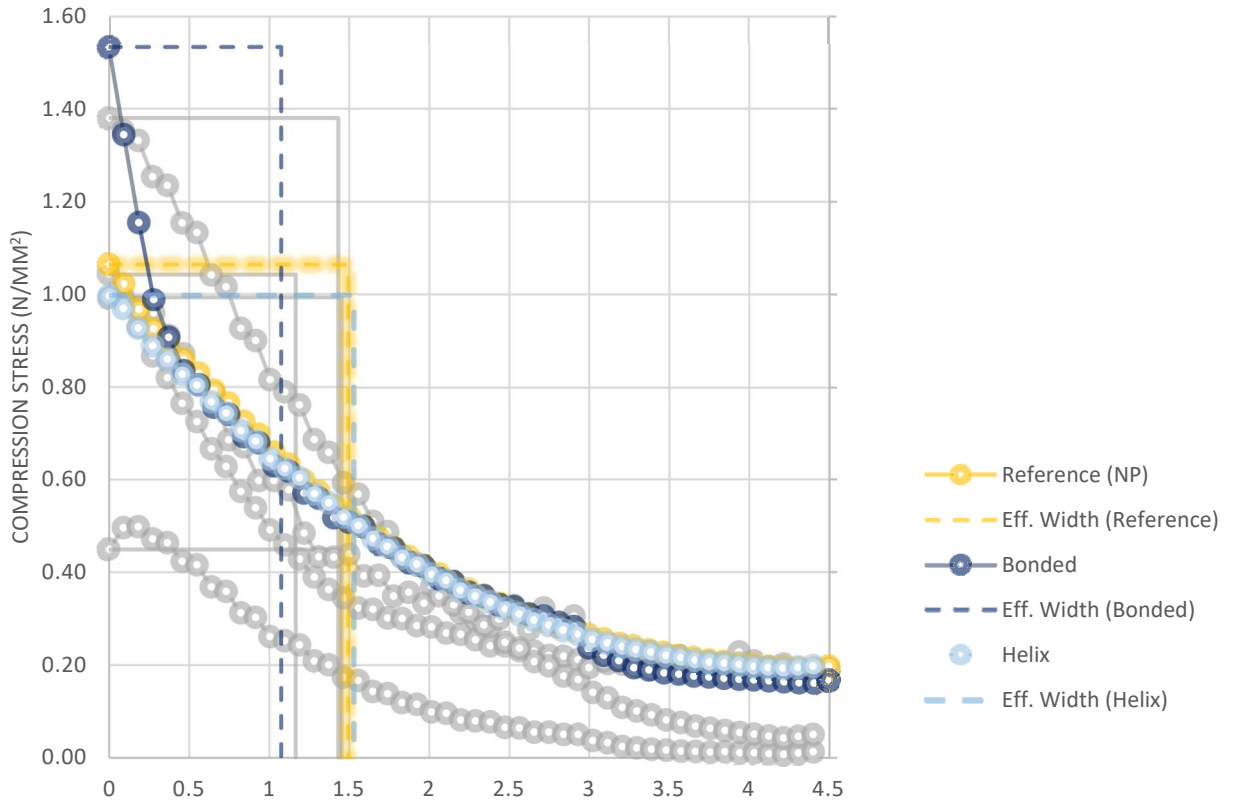
Figure 6.12 - effective width: shear connection effect, Helix connector

The longitudinal stress distribution for the helix connector shows similar behaviour to the reference case of a nail-plate connector. The peak stress at the beam is **1.0N/mm²** (lower than the 1.06N/mm² in the reference case) illustrating a less stiff connection, whilst the effective width is 3.06m (increased compared to the 2.99m of the reference case). This gives more evidence to the concept of the peak stress influence on effective width in this system as the longitudinal stresses beyond 500mm either side of the beam are very similar between the helix and nail-plate connector results.

Overall, the peak stress reduction and effective width increase result in a deflection result of **12.53mm**, representing a **4.5%** composite enhancement over the non-composite deflection (lower than the nailplate reference enhancement of **5.6%**)

At first glance, the helix connector as modelled does not appear to be as beneficial as the nailplate, however, one must remember as detailed in chapter 5, the that helix connector offers much greater ductility, meaning that by closer spacing of the connectors than was assumed in the modelling, a higher stiffness connection could be derived whilst maintaining a plastic failure mechanism. The nailplate does not have this potential, contrastingly.

6.4 Slab Position Influence

An area of interest is whether the position of the CLT floor slab, relative to the steel beam, has an effect on the effective width behaviour, and the impact on deflection. This section compares the behaviour of the reference case compared to when the CLT panels are positioned on the top flange of the beam rather than the bottom flange. Whilst it is clear that having the slab above the beam will increase the composite 2nd Moment of Area (by moving more material away from the neutral axis) this will remove the practical benefits of using a slim-floor arrangement, as was discussed in Chapter 2.

For the purposes of this comparison, the beam modelled remained a 280ASB74, to give a direct comparison. In a real world situation, the beam would be unlikely to be an asymmetric section, but here it provides a direct comparison so the determining factors are limited to the shift in position of the slab. The model arrangement is shown in Figure 6.13. Finally, a bonded shear connection was applied
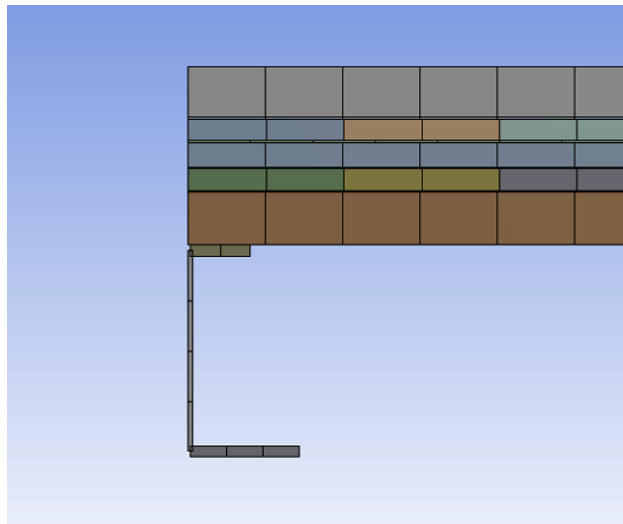
Figure 6.13 - FE model arrangement for non-slimfloor case

6m Beam x 9m Panels - Longitudinal Compression Stress
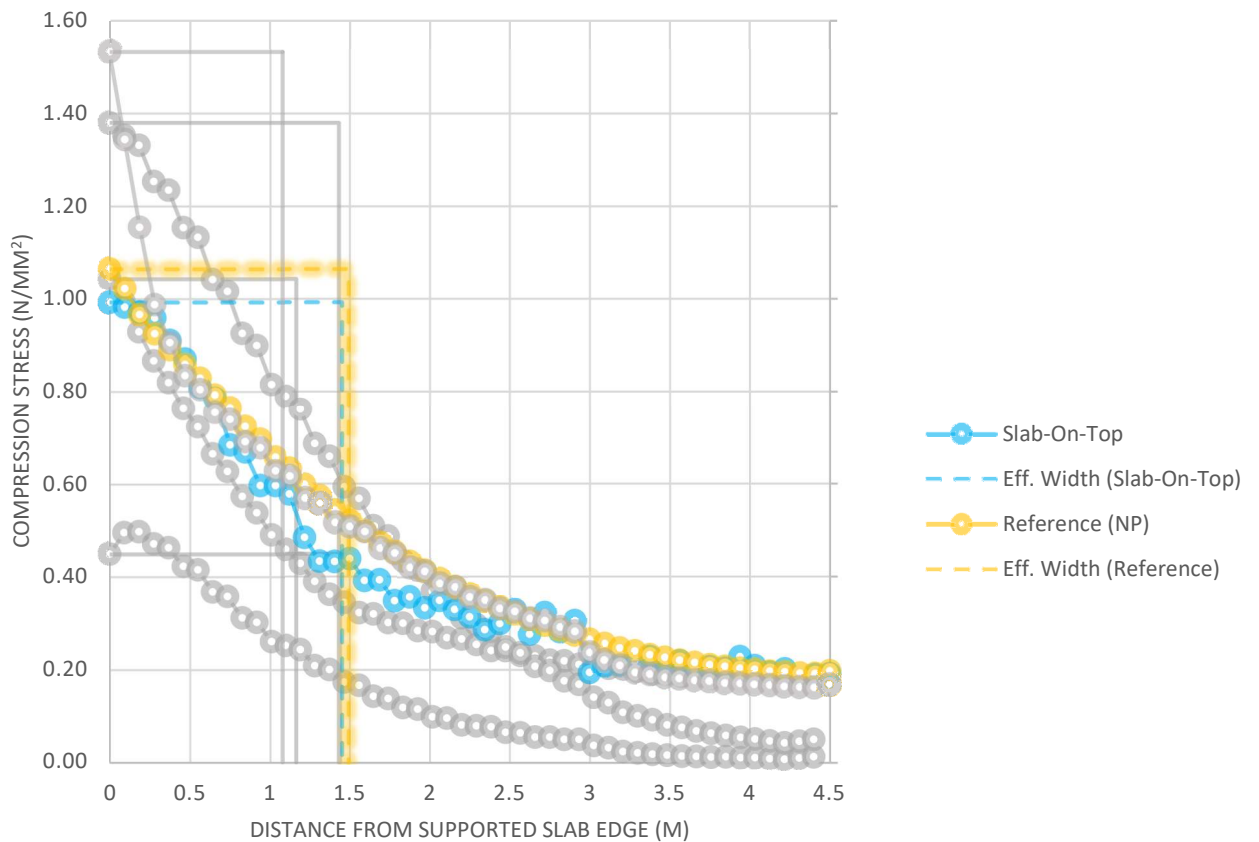
Figure 6.14 - effective width: slab position influence

As can be seen from the longitudinal stress trace displayed in Figure 6.14, the effective width is not significantly changed (2.88m) from the reference case (2.99m) through moving the CLT panel from the bottom flange to the top flange, and the peak stress follows this trend. The small discrepancies are likely down to the presence of extra CLT in the non-slimfloor case, which gives an added contribution to the longitudinal stress distribution. Interestingly, there increased peak stress is not observed at the position of the shear connection even though a bonded shear connection is applied – in fact the peak stress is lower compared to the reference case (0.9kN/mm^2 compared to 1.06 kN/mm^2). There may be counteracting phenomena occurring in this instance – whilst the shear connection is bonded (the stiffness of which appears to increase the loads to the CLT in section 6.3) the magnitude of the force induced in the upper contributing layer of CLT by the applied bending moment is lower due to the increased lever arm from the composite neutral axis and sharing of load with the lower CLT layer.

What the result of this analysis highlights is the sensitivity of the effective width determination on the peak stress value – in the bonded, slimfloor case, the effective width is reduced compared to the reference case as a result of a larger peak stress, whilst with the slab moving position as well, the peak stress is only affected to a small degree and the effective width does not change greatly. Hence, the effective width approximation appears to be contingent on appropriately evaluating the magnitude of

peak stresses at the shear connection location and certainly warrants further study for developing a design method.

For deflections, whilst the effective width is unchanged, the increase in composite section depth has, as expected, had a profound effect on the overall section stiffness – a deflection of **5.99mm** is recorded (a composite enhancement of **54%** over the non-composite deflection) which compares to 5.6% for the reference case, and 13.5% for the equivalent slim-floor case with a bonded shear connection.

6.5   Tensile Connection Effect

The preliminary modelling section of 4.3 found that connecting the tensile zone of the timber panels had a marked effect on the amount of composite action that could be generated, improving deflection reduction from 6.5% to 17%. In the reference model and in the general development phase, the inter-panel connection was assumed bonded to allow further investigation to take place.

As detailed in Section 5.4, physical testing of two methods of panel-to-panel connection was undertaken. The performance of the butt joint was found to be superior, and the testing arrangement and behaviour of the connection was replicated in finite element form. This connection was incorporated into the main model, shown in Figure 6.15, and this section reports the comparative behaviour of the more realistic butt-joint connection and the reference case in order to give a prediction of its impact.

As can be observed from the longitudinal stress trace displayed in Figure 6.16, the panel-to-panel

Figure 6.15 - FE model including panel-to-panel connection (highlighted green)

connection has no discernible impact on the peak stress experienced by the CLT panel at midspan. However, the overall stress generated along the panel span is reduced when compared to the reference case, and subsequently the effective width is reduced. This behaviour demonstrates the reduction in stiffness of the overall flooring system through the use of a butt-joint compared to a perfect bond at the panel interface, and is reflected in an increased beam deflection (**12.51mm** compared to the reference **12.39mm**). As a consequence, via the inclusion of the inter-panel connection, the composite enhancement potential is reduced by 18% (i.e. a multiplying factor of 0.82 on the composite enhancement expected through the use of a shear connection). This is an important factor to be aware of if a more comprehensive future programme of FE modelling is undertaken.
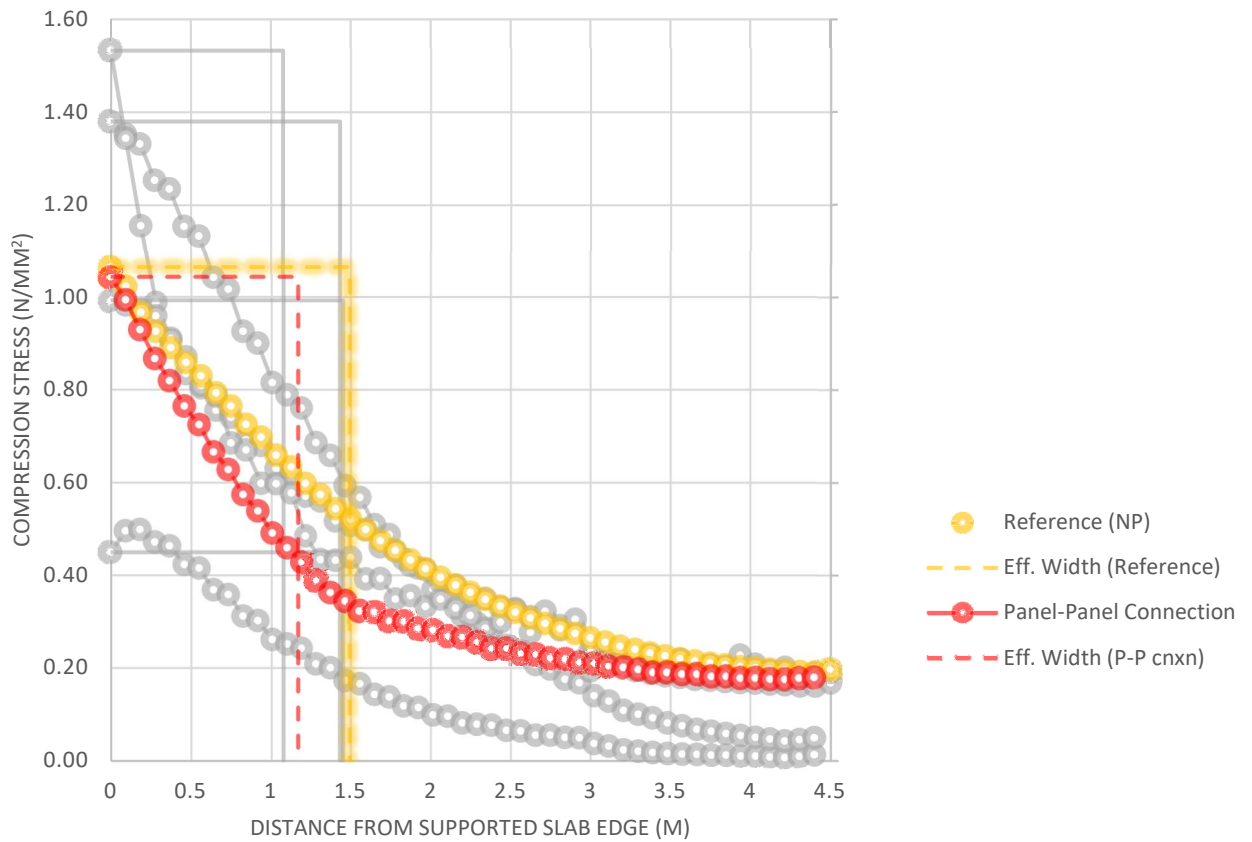
Figure 6.16 - effective width: tensile zone connection effect

6.6   CLT panel make up and layout – Standard panels vs. designed panels

Composite action is a complex interplay of the stiffnesses, both material and geometrical, of the components involved. This section explores how changing the stiffness of the CLT panel (by altering the internal design dimensions of the CLT panel) affects the effective width and composite action.

The standard design lay-up of CLT panels maximises the capability of the panel to span in the direction orthogonal to the beam, but this means the amount of panel that can usefully contribute to the stiffness of a composite section is limited to the two thin, "even-numbered" layers which run parallel to the beam. Addressing this through rearrangement of the panels is discussed in section 7.1.

Panel (and outer layer) spanning direction

| 68 mm |
| 30 mm |
| 34 mm |
| 30 mm |
| 68 mm |

| 38 mm |
| 60 mm |
| 34 mm |
| 60 mm |
| 38 mm |

Figure 6.17 - Layup dimensions of standard CLT panel (left) and designed panel (right)

The KLH 7ss230 panel, used in the reference analysis case, is notionally a 5 layer panel, however the outermost layers are in fact double thickness[13]. The FE model was adapted so that instead of the face layers being of double thickness, the depth of the layers running parallel to the beam are doubled instead. The overall panel depth is maintained at 230mm deep (see Figure 6.17). The inter-panel connection is maintained as bonded for the bottom two layers and frictional contacts for the upper layers, as can be seen in Figure 6.19.

Figure 6.18 - standard panel (left) and designed panel (right)

Figure 6.19 – Inter-panel contact behaviours, frictional (red) and bonded (blue)

The longitudinal compressive stress trace for the reference case and the revised panel design are presented in Figure 6.20. Two traces for the designed panels have been reported as the position of measurement has changed in significance. The depth of measurement in the darker green colour is at the same position as the reference case, however this is now in the middle of the CLT layer in the designed panel. The results at the new extreme fibre of the longitudinal layer are displayed in the lighter green colour of Figure 6.20.

The results show some interesting features – firstly the effective width has not been changed through the change in panel layer dimensions. This demonstrates that the interplay of the shear connector stiffness and the longitudinal stiffness of the panel material (presumably along with aspect ratio) has more bearing on the effective width than the build-up of the panel. This, however, does not mean that the deflection reduction is unaffected. The use of a designed panel increases the composite benefit from **5.6**% to **12.6**%.
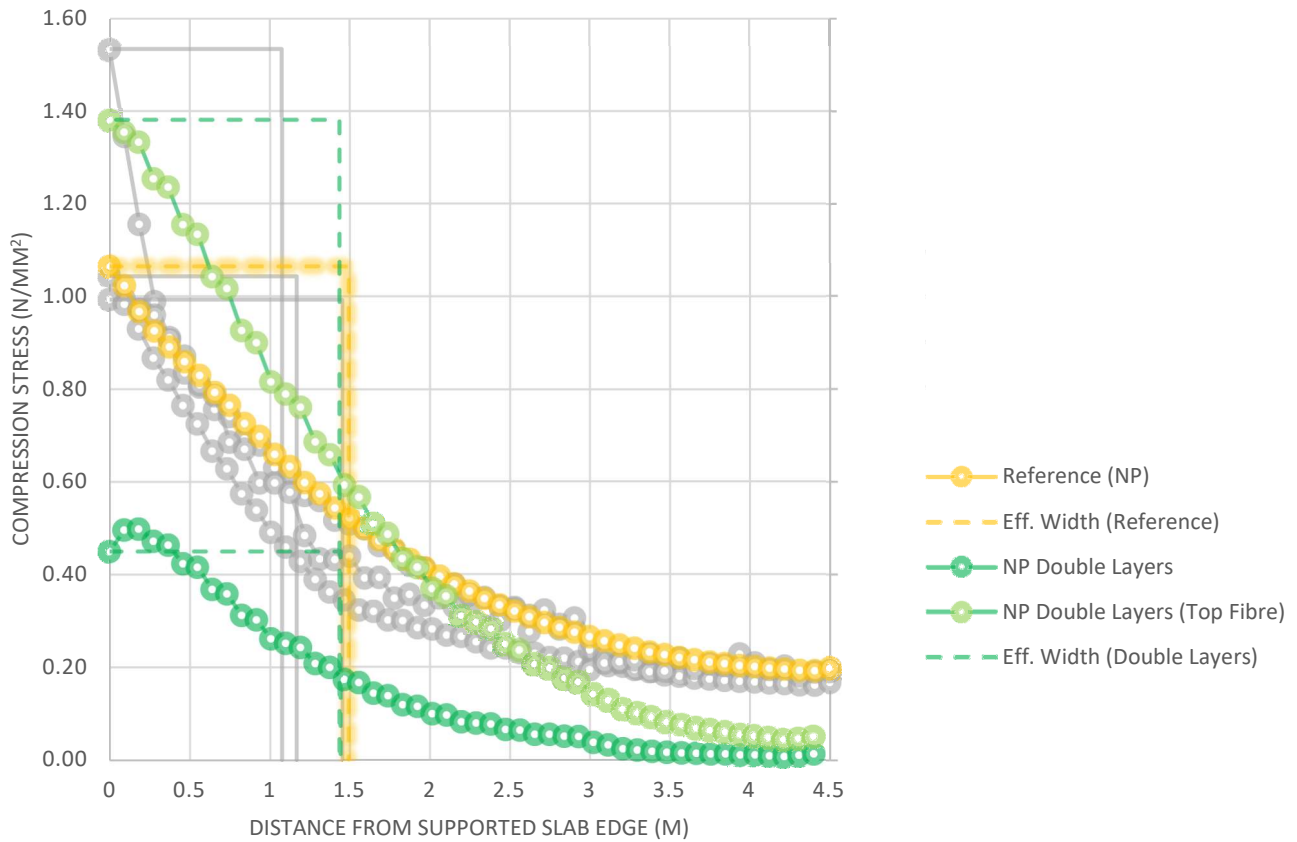
Figure 6.20 - Effective width: panel stiffness effect

The implications of the results are that manipulation of panel layers can greatly improve deflection of the beam. What must be determined is the limit of reducing the layers that run along the panel span so that it can still span the required distances without breaching deflection limits. If necessary, it may be feasible to add a layer to the top of the panel with laths running parallel to the beam to create a similar effect without affecting the span capabilities of the CLT panel. Care must be taken with this as the extra layer will shift the neutral axis upwards and affect the 2nd moment of area generated by the layers resisting panel deflection. This area of the design shows promise for optimising the system for greatest performance.

6.7 Aspect Ratio of the Bay

A selection of the previous analysis cases were performed with a 6m x 6m bay dimension. The Reference case was repeated along with the two variants that have the potential to enhance composite action the most – the designed panel (double-layers) and the bonded shear connection. The effective width outputs are shown in Figure 6.21.
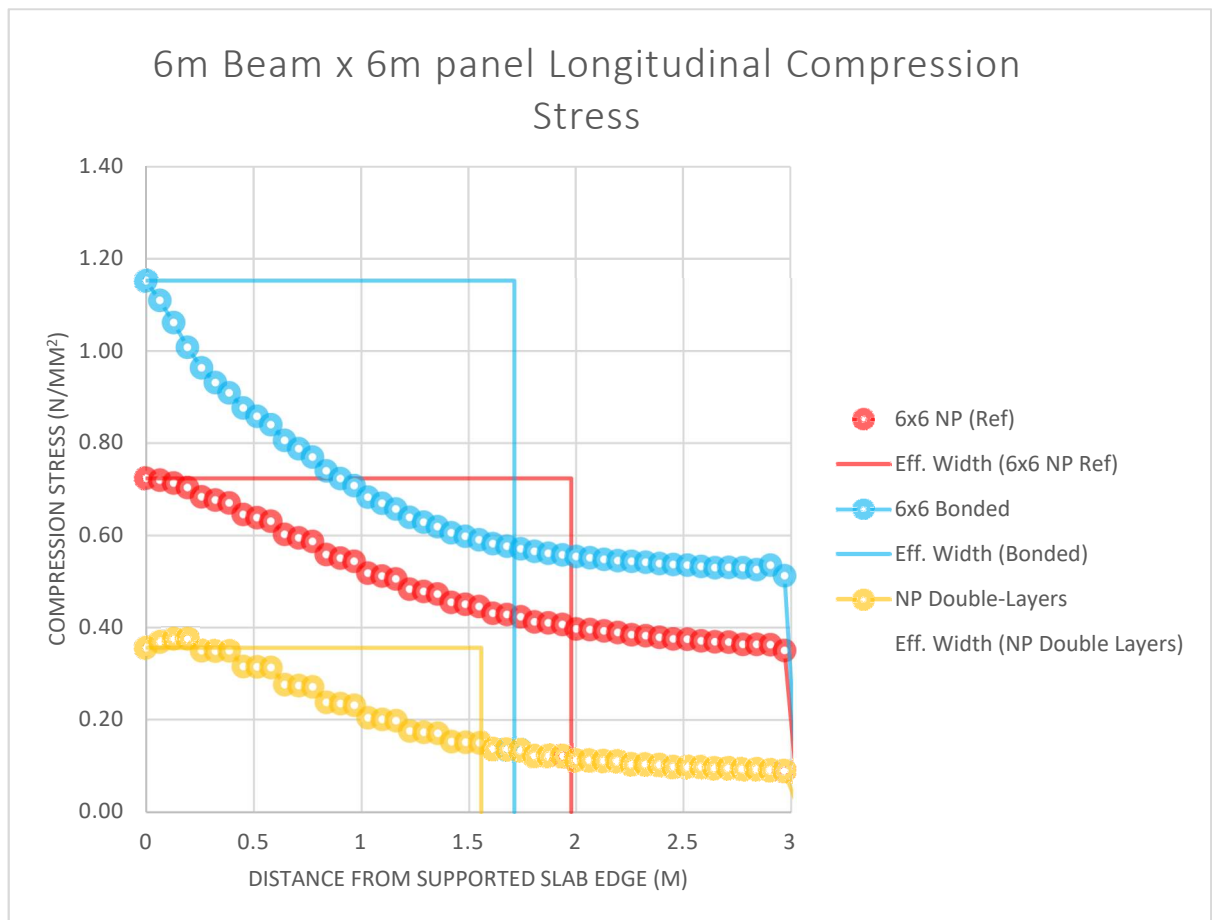
Figure 6.21 - effective width: aspect ratio effect

As can be seen, there are some features that carry over from the 6m x 9m panel case – The stiffer connection leads to an increase in peak stress above the connection (thus narrowing the effective width), and the designed panel has a reduced peak stress, likely due to sharing of load across a greater area of contributing CLT cross-section. Where things differ are the magnitudes of loads further away from the beam position. Whilst the relationship between the in-span stresses of the reference and the designed panels is qualitatively unchanged, the effective width has reduced markedly, meaning load is more concentrated towards the beam in the 6mx6m case compared to the 6mx9m case.

For deflections, compared to a non-composite deflection of 8.43mm, the reference case with Nail-plate connection resulted in a deflection of 8.26mm (**2%** reduction), the bonded connection resulted in a

deflection of 6.67mm (a **20.9%** reduction) and the designed beam gave a result of 7.68mm (**8.9%** reduction). Note that the two results for the nailplate are worse than for the 6mx9m situation, however the relative impact of using a designed beam has increased significantly. These results suggest that there is potential for greater benefit to be derived from a composite connection and/or generated by using a designed panel for the smaller bay dimension of 6m x 6m, but it may be more difficult to transfer the forces into the system efficiently as the shear connection appears to work less well.

6.8   Summary

Collating the findings from the different parts of the parametric study, one can infer –

- The position of the CLT slab does not have a bearing on the effective width, but placing the slab on top of the beam leads to composite enhancement of greater than 50%, compared to the 13.5% composite enhancement given by the equivalent case (bonded shear connection) in the SlimFloor arrangement..

- The shear connection impacts on the composite action through by the magnitude of stress induced into the timber above the connection position. There is an associated impact on the effective width derived, which appears to be highly sensitive to the peak stress in CLT panels.

- The configuration used in this study does not allow the determination of the variation in effective width along the beam due to the occurrence of plate bending that obscures the longitudinal stresses due to composite action.

- The actual behaviour of the inter-panel connection is important to include, scaling any predicted composite enhancements by a factor of 0.82.

- While the distribution of layers within the panel does not affect the effective width in the 6m x 9m case, this does not hold true for square bays.

- Compositely joining CLT to an ASB has greater potential for augmenting the section stiffness in a 6m x 6m bay than for a 6m x 9m bay, but the shear connection must be stiffer to do so.

Chapter 7. Further Areas of Development

7.1   Bay layout options and the problem of incompatible bending

Composite action is a complex interplay of the stiffnesses, both material and geometrical, of the components involve – in this case, the beam, floor slabs, and the shear connection. Getting the beams and slab to work together demands forcing the panel into behaviour it does not necessarily want to do. This is made more complex by the anisotropic behaviour of the panel. Consider first a series of generic floor panels spanning in a floor bay – these can be arranged in several orientations.

Assuming the same arrangement as was used in the parametric study, the panels span perpendicular to the primary beams, with assumed ties between columns. In this arrangement, the panels have their short dimension parallel to the span of the beam. The beam, as well as being subjected to more load than each individual panel, is significantly longer so it is induced into a curvature that will greatly exceed that of the panels in their short dimension.

The upshot of this is that the panels end up spanning between their corner points – their 2nd moment of area is large due to their large "width" (into the panel spanning direction), for bending parallel to the beam, meaning they would need to have a very low young's modulus to conform to the curvature of the beam. It is precisely this stiffness that the concept of connecting the slab to the beam is trying to harness.

To get the largest composite benefit from the slab, the panel stiffness in bending should be as high as possible. The standard panels have odd numbers of layers with the outermost layers having their strong, longitudinal, axis running in the direction of the slab span. The layers running parallel to the beam are thinner and have a smaller lever arm between each other meaning the couple of resistance they form is small. This is the source of the different bending stiffness of the panel axes. In section 6.6, increasing the dimension of these layers contributed to large increases in the developed composite action compared to when a standard panel was used.

Suggestions have been made that it may be more practical, when using CLT, to run the extant CLT panels (rather than designed panels) parallel to the beam to get the composite benefit from the CLT's axis of greatest bending resistance. However, in the opinion of the author, this would either necessitate the use of secondary beams to support intermediate panels (those not connected directly to the primary beam) or having a primary beam between every panel. In both cases, this leads to an increase in steel usage, bringing with it an increase in the large associated embodied carbon and energy.

Another argument against this arrangement is that in trying to boost the stiffness of the slab so that it gives greater composite benefit to the beam, there reaches a situation where the panel, with its large width dimension, becomes stiff enough to span the distance on its own, rendering the use of the steel beams redundant, and leading to the initial setup being recreated on primary beams.

7.2   Vibration and semi-rigid joints

Vibration of timber floors is a challenging area to satisfy in multi-storey construction as the combination of the spans required and the lightness of the floor plate means there is proportionally much less inherent damping from the floor slab mass than for an equivalent composite floor slab. Reducing the perceptibility of floor vibration to the human occupiers of a structure is based around controlling the natural frequencies of the floor system, to ensure it is high enough so as not to allow vibration of the floor to be induced by the movement of people. Figure 7.1 shows an extract from The Structural Engineer's Pocket Book[189], giving the expression for the natural frequency of a beam.

Simply supported, sagging, mass and stiffness distributed
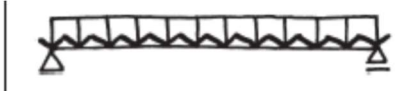
$$f = \frac{\pi}{2}\sqrt{\frac{EI}{mL^4}}$$

Figure 7.1 - expression for the natural frequency of a simply supported beam subject to a UDL[189]

Given such an expression, and the aim of increasing the natural frequency as much as possible, one can see that increasing the 2nd moment of area of the beam, such as by joining it compositely to the floor slab, can increase the natural frequency. The natural frequency of a floor system is influenced by the interaction of the dynamics of the floor slabs themselves with that of the supporting beam. Whilst analysis of structural systems usually incorporates the simplification of supports either being pinned (simply supported) or fixed (moment or encastre support), the reality is that all real-world connection or joint will be somewhere between these two extreme conditions i.e. semi-rigid. If the end connections of a beam have capacity to resist moment, this has the effect of redistributing the moment from the beam to the connections, thus reducing the magnitude of moment the beam must withstand, and consequently reducing the vertical deflections at mid-span. Nethercot[190] provides a comprehensive review of the features of joint design needed to appropriately harness the potential benefits of moment redistribution and how having composite beam sections affects this.

Siditan Zagani performed research at The University of Sheffield investigating how modelling semi rigid joints in a *hybrid* CLT-ASB floor system affected the natural frequency of the beam and it's suitability for different bay dimensions[191]. This was done in finite element software through modelling the joint behaviour in Abaqus and incorporating the behaviour into beam models produced in SAP2000.
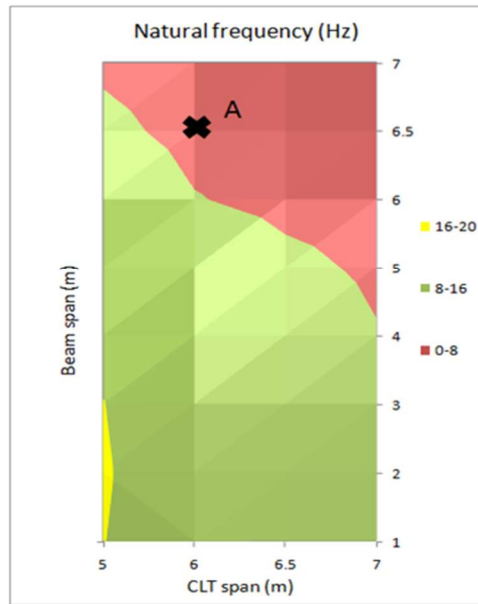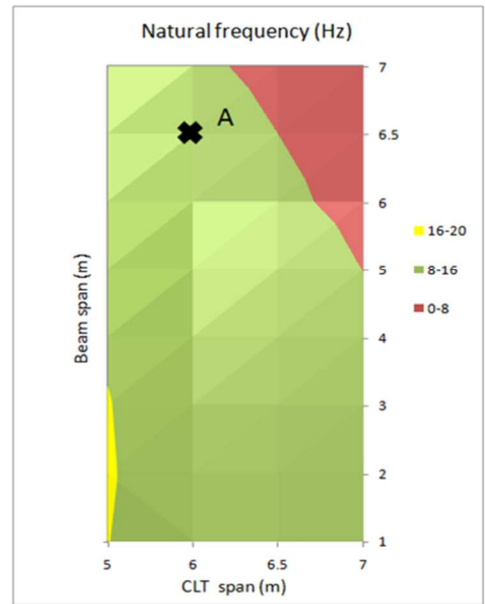
a) k=0 kNm/rad   b) k=11330 kNm/rad
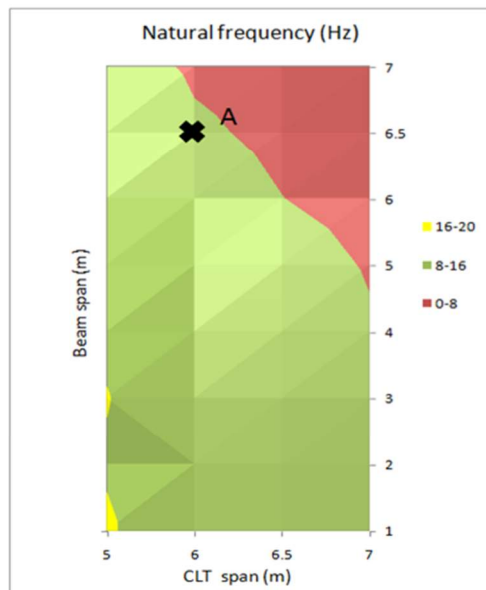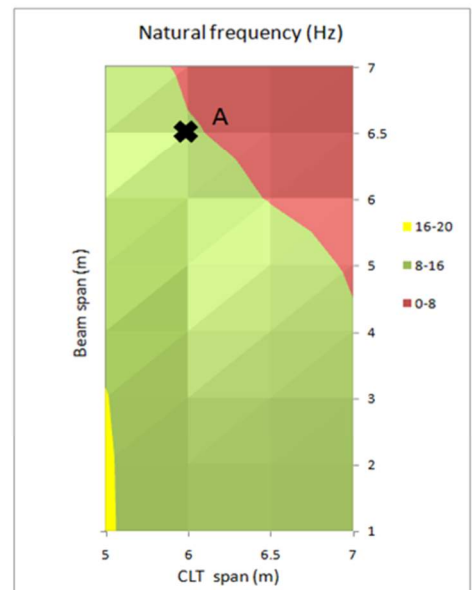
c) k=5400 kNm/rad   d) k=4130 kNm/rad

Figure 7.2 - Fundamental frequencies of CLT-ASB hybrid bays with varying rotational connection stiffnesses[191]

Against a recommendation of minimum natural frequency of 8Hz from Eurocode 5, a 6m (CLT) by 6.5m (beam) floor bay was calculated not to meet the recommendation when simply supported (7.36Hz), but became compliant when a moment connection of 4 bolts or more was used. Figure 7.2 shows the bay dimensions and joint stiffness combinations that result in natural frequencies above the Eurocode 5 recommendation (the red regions of the plots). They suggest that a 7m x 6m bay can work dynamically if semi-rigid joint design is taken into account.

Zagani's study did not include the impact of having a composite connection between the slab and the beam, which means it may be possible for the composite action to enhance the vibration performance further for larger spans, and similarly that the use of semi rigid joints in the design can allow for further improvements in limiting midspan deflection through moment redistribution. Hence this would be an interesting are of further study combining and codifying the two beneficial effects.

7.3   Fire performance & Robustness

Fire performance of structural systems involving timber is a topic that causes concern among prospective end-users[77,192] (likely due to numerous fires involving timber-frame buildings during construction[193]) and is difficult to contend with structurally and in terms of the building codes. It has already been established that providing appropriate inter-laminar glues are used[194], CLT performs well in fire due to the predictability of its charring rate, and the large volume to surface-area ratio makes it difficult to ignite[195,196].

For the CLT-steel hybrid proposed in this thesis, whilst the inherent performance of CLT is established and the requirements for building codes can be met through detailing of the inter-panel joints (discussed in previous work of the author[135]), the protection offered to the steel beam and, most critically, the behaviour of the connections in the fire condition necessitate close scrutiny.

In the "accidental" loading condition, which covers the incidence of fire, the structural system needs to meet robustness requirements for resisting progressive collapse. Robustness rules for the UK are internationally respected. They call for the structure to be able to withstand the loss of a key element, notably a column. In this situation, the floor system needs to adjust to span across the location where the column once stood, and requires the connection between floor slab and beam to take the tying forces generated.

A key basis of this is that the floor system can act as a catenary in accidental conditions and therefore must maintain a minimum tying resistance across the whole floor. The interface between timber floor panels and steel beams must therefore be able to transfer this tensile force. What must be carefully considered is that any connection between the CLT panel and steel beam will likely metallic and therefore able to transmit the heat from a fire and reach very high temperatures. These temperatures will certainly be sufficient to cause deterioration of the timber in contact with the connector, and hence,

will lead to a weakening of the joint overall. It is therefore crucial to prevent the connectors from being exposed to the heat from a fire.

Similarly, the floor system including the beam-panel connection and the panel-panel connection need to have the ability to transfer lateral forces (wind, out-of-straightness) back to the shear walls or stability structures. This is also a key robustness requirement.

The testing of the panel-panel connector included lateral shear to give an estimation of the performance in this area. Sepideh Ashtari's Master's thesis researched the behaviour of CLT panels subjected to in-plane loading and the influence of the panel-to-panel connection on this behaviour[166].

7.4   Further Work

7.4.1 Full Scale Testing

The findings of chapter 6 suggest there is potential for some composite benefit to be found in connecting the currently available CLT panels to steel beams. However, the estimations of the finite element models can only be verified by implementation of the system where it can be tested and analysed. This would be beneficial for verifying the in-plane shear behaviour and effective width's induced, as well as the performance of different shear connectors. Further, with full-scale testing, there would be scope for including the influence of the joint stiffness on the vibration of the system. As such, a full-scale testing scheme would be a most appropriate next step for confirming that useful composite action can be generated, and some of the hypotheses around the system behaviour. If this were to take place, it would be prudent to test composite behaviour in both the slimfloor configuration and the conventional slab-on-top layout, as both arrangements may have benefit depending on the context of the structural application.

7.4.2 Fire Performance and Connections

The fire performance of the system as a whole requires further scrutiny. As well as the issues of robustness of the connection and durability of the CLT in a fire, discussed in section 7.3, the performance of the steel beam must also be considered. Steel elements are arguably the most susceptible to performance deterioration in fire as they will readily soften under high temperatures, becoming more prone to buckling. In conventional structural systems, steel beams have their top flange restrained by the concrete slab in normal composite buildings, and are protected from heat and buckling via encasement by the slab in slimfloor systems. As the CLT slab will deteriorate over time, however predictably, the encasement protection and buckling restraint to the beam will also deteriorate. The arrangement of beam and slab may make the addition of fire protection more difficult to incorporate effectively, thus a better understanding of the deterioration process for the combined system is crucial if a CLT-ASB composite system were used.

7.4.3 Beam & Section Optimisation -Practicality & Feasibility

Off the shelf rolled ASBs were designed for use with concrete slabs. Their dimensions suit the demands of supporting a concrete slab and their depth is able to be relatively shallow as the composite action reduces the bending stiffness burden of the steel section. The upper and lower flanges, are thicker to improve the section fire resistance.

A result of this is that if CLT panels are specified for use as floor slabs supported by ASBs, the steel section is significantly underutilised. To improve the material efficiency of the researched system, a different set of steel beam designs could be found that meet the particular requirements of CLT panels, but offer less wastage.

This endeavour can be helped by a greater understanding of the composite action effect, as the bending stiffness requirement would be a key parameter to be determined. It is envisioned that rather than being rolled, these designed sections would be fabricated, and the same study could be undertaken for cold-formed sections where applicable.

The beam design would need to consider the required bending stiffness for both construction and in-service cases, bending strength and buckling resistance, torsional rigidity, and local buckling especially of the flanges. Further to this, providing sufficient dimensions for steel frame connections to be formed requires consideration.

7.4.4 Further Connection Development

From the work of Chapters 5 and 6, helical ties may provide suitable characteristics as shear connectors, but would need to be developed and investigated for performance in this application – for example, the addition of blank shaft section and bolt or countersunk head are crucial for use as a demountable shear connector with steel, but this may be difficult to introduce considering the manufacture process of the ties.

For connectors of any type, it may be more beneficial to install shear connectors at an angle (longitudinally to beam) so the connectors are resisting in tension via embedment in the timber, rather than shear of the connector and bearing of the timber. This may be a stiffer joint less prone to fatigue failure, but may also have reduced ductility and must be verified. G Coste's thesis investigated the embedment behaviour of helical connectors in wood[172], and provides a good place to start.

From a robustness perspective, it may be necessary to have further connectors orientated diagonally into the span of the CLT panel to enhance the tying resistance of the beam-panel interface and prevent the fall-through of panels in the accidental condition.

7.4.5 Impacts on foundations

The desktop study of Chapter 2 (as well as previous work by the author) suggests the significant Dead Load reduction can have a notable impact of the foundations. Foundations support the structure and transmit any vertical and lateral forces the structure is subjected to into the ground. The magnitude of these forces, combined with the ground conditions, determine the type and extent of the foundations.

It must be noted that whilst dead load is important, often Live Load is the more onerous load type. That being said the floor slab contributes so much to the overall dead load, and the mass reduction through substituting concrete for CLT is so large that it is worthy of study in more detail.

7.4.6 Incorporation of Cold-Formed Steel.

In a system attempting to create a construction method with reduced impact on the environment, the embodied energy associated with the rolled steel sections is a factor that may have a significant benefit if it can be reduced. Methods of affecting such an energy intensive part of the system are:

- Reduce the energy intensity of the material
- Reduce the quantity of material used further

Whilst the latter is discussed in section 7.4.3, using Cold-Formed sections, a less energy intensive form of steel, could be a means of achieving the former. Cold formed sections are made from direct forming of steel sheets rather than having been formed and rolled from molten steel in a mill. The reduced energy involved in manufacture endows cold-formed sections with an environmental benefit. Whilst cold-formed sections are of equal strength and stiffness to an equivalently sized hot-rolled element, the forming process is typically limited to very thin gauge steel sheets which can limit the scope of the resulting section's applications[197].

Currently, cold-formed steel is used as profiled metal formwork for composite floor slabs, and cold-formed sections are commonly used as purlins supporting roof panels, and as intermediate structures supporting façade systems. However, more recently, the use of cold-formed sections for a more significant structural role is being researched and developed – Majdi, Hsu & Zarei[197] provide a useful summary of some recent development in the field, particularly the use of cold-formed steel sections compositely. Given further research, it may be possible and environmentally beneficial to pair the CLT floor panel with cold-formed sections of some kind may be the most energy efficient way of delivering the composite system, or alternatively to incorporate both cold-formed and hot rolled sections, as Loss & Davison purport[104].

One challenge would be to combine the material efficiencies of optimised, fabricated beam sections with cold-formed sections as the gauge of steel sections used is too thin to weld successfully and the heat induces thermal stresses that are not offset by internal thermal stresses as they are in hot-rolled sections.

Chapter 8. Conclusions

In concluding this thesis, one must first return to the research questions from the 1st Chapter. Taking each one in turn:

1)   Can the substitution of CLT floors in place of concrete slabs be justified by a reduction in environmental impact?

Through the course of Chapter 3, the scope of the environmental challenges and the place of CLT as a construction material within that challenge were reported and further developed. By collating the available data on various construction materials and performing a comparative design study, it was shown that the use of CLT in place of concrete greatly reduce the environmental impact of the structural system both directly and indirectly. The embodied carbon of the slab is much reduced, and the knock-on effects of having a structural system of 1/3 the mass are sure to be experienced in the foundation extents, and the construction phase, if not calculated quantitatively here. The inherent properties of CLT mean it can facilitate reuse of the structural frame too, helping to close the material cycle in this sector.

There remain aspects where CLT performs less well – the embodied energy of the material is very high, and the reduction in thermal mass by swapping CLT for concrete needs to be explored – however from the research performed in this project, there **is** justification for using CLT floor panels instead of concrete due to environmental impact benefits

2)   Can the mechanical behaviour of CLT be modelled accurately by numerical means?

At the start of this research project, there had been no published research into the finite element modelling of CLT in order to determine the workings of the effective width in that material. The research and development reported in Chapter 4 has resulted in a finite element modelling approach that captures the anisotropy of the parent timber in bending and limits of elasticity, and reflects the interior mechanics of the CLT panel in order to reproduce the mechanical behaviour in bending and in-plane shear that was observed in laboratory testing. This can provide the basis of a powerful analysis tool to investigate the structural behaviour of CLT without the limitations on applicable situations that there are with some of the stick or planar numerical models. There is certain need to validate the model behaviour in more situations that reflect how CLT will be used in service, but one can determine that the output traces of longitudinal stresses generated by the modelling approached developed in this thesis are reasonable compared to what one might expect, and the established relationships for concrete-composite sections. In answer to this research question, **yes,** but more work needs to be done for greater confidence in the results generated.

The answer to this research question is less straightforward based on the investigations of the project.

Taking the results of this project, using existing CLT panels in a slimflor arrangement and realistic connections, yes, composite benefit was encountered but it appears to be a small benefit, less than 5%. However, the investigations have highlighted what developments could bring about more sizeable gains – restructured panels, better shear and inter-panel connections, or having the panels on top of the beam all appear to create more sizeable composite action.

The results of the parametric study in Chapter 6 showed that much depends on the nature and performance of the connections within the system. The research and FE model development of the connections in chapter 5 have shown that practicality remains a significant challenge- the shear connectors included in this study are not ready for application and the joint configurations will require development to bring the performance closer to that of a bonded connection whilst maintaining ductility.

Given more validation of the developed finite element model, more authority could be put into the quantification of the composite benefit calculated in this work.

Combining these findings to answer the overarching question:

Is there a benefit in designing/constructing multi-storey steel-framed buildings using CLT floors instead of traditional concrete floors/slabs?

In the opinion of the author, **yes**, there is benefit in combining steel frame construction with CLT floors. Even if composite action cannot be generated to a worthwhile level, there are still many important positive characteristics from hybrid CLT steel construction, most notably the reduction in material usage and the associated environmental and cost benefits that will result. Chapter 7 highlights the range of interesting and critical topic areas of further development that are upshots of taking the concept forward, with the most important being the system characteristics in fire and for robustness.

REFERENCES

1. The British Constructional Steelwork Association Ltd. "Market Share." (2013). Available at: http://www.steelconstruction.org/resources/commercial/market-share.html.

2. Asiz, A. & Smith, I. "Connection System of Massive Timber Elements Used in Horizontal Slabs of Hybrid Tall Buildings." *Journal of Structural Engineering* p1390–1393 (2011). doi:10.1061/(ASCE)ST.1943-541X.0000363.

3. Rackham, J. W., Couchman, G. H. & Hicks, S. J. "*P300 COMPOSITE SLABS AND BEAMS USING STEEL DECKING□: BEST PRACTICE FOR DESIGN AND CONSTRUCTION*." (The Steel Construction Institute, 2009).

4. Johnson, R. "*Composite Structures of Steel and Concrete, Volume 1: Beams, Slabs, Columns, and Frames for Buildings*." **Vol.1,** (Blackwell Science Ltd., 1994).

5. Zou, B., Chen, A., Davalos, J. & Salim, H. "Evaluation of effective flange width by shear lag model for orthotropic FRP bridge decks." *Composite Structures* **Vol.93,** p474–482 (2011).

6. Lam, D., Elliott, K. S. & Nethercot, D. A. "Designing composite steel beams with precast concrete hollow-core slabs." *Proceedings of the ICE - Structures and Buildings* **Vol.140,** p139–149 (2000).

7. Lawson, R. M., Bode, H., Brekelmans, J. W. P. M. & Wright, J. "'Slimflor' and 'Slimdek' construction: European developments." *The Structural Engineer* **Vol.77,** p22–30 (1999).

8. Lam, F. "Modern structural wood products." *Progress in Structural Engineering and Materials* **Vol.3,** p238–245 (2001).

9. Mayr-Melnhof Kaufmann Group. "Cross-laminated timber panels M1 BSP crossplan M1 BSP crossplan." (2009).

10. Stora Enso. "Stora Enso Building and Living - Building Solutions." (2012). Available at: http://www.storaenso.com/products/wood-products/products/buildingsystems/Documents/Stora Enso Building Solutions CLT_EN.pdf.

11. Sutton, A., Black, D. & Walker, P. "IP17/11 Cross-Laminated Timber - An introduction to low-impact building materials." (2011).

12. TRADA. "WIS 2/3-61 Cross-laminated timber: introduction for specifiers." (2011).

13. KLH Massivholz GmbH. "Engineering Brochure." (2008). Available at: http://www.klhuk.com/media/16583/klh engineering en 2008.pdf.

14. Structurlam. "CrossLam - Cross Laminated Timber Design Guide."

15. Brandner, R. "Production and Technology of Cross Laminated Timber (CLT): A state-of-the-art Report." in *Focus Solid Timber Solutions - European Conference on Cross Laminated Timber (CLT)* p3–36 (2013).

16. Green, M. "Why we should build wooden skyscrapers." *TED* (2013). Available at: http://www.ted.com/talks/michael_green_why_we_should_build_wooden_skyscrapers.html.

17. Oliver, A. "Pushing the design envelope." *New Civil Engineer* p10–11 (2013).

18. Fountain, H. "Towers of Steel? Look Again." *The New York Times* (2013).

19. Skidmore Owings & Merill. "*Timber Tower Research Project.*" (2013).

20. mgb Architecture + Design. "*Tall wood - The Case for Tall Wood Buildings.*" (2012).

21. TRADA. "*Case Study: Stadthaus , 24 Murray Grove , London.*" (2009).

22. Lehmann, S. "Low carbon construction systems using prefabricated engineered solid wood panels for urban infill to significantly reduce greenhouse gas emissions." *Sustainable Cities and Society* (2012). doi:10.1016/j.scs.2012.08.004

23. Porter, L. "Local group pushing to expand use of cross laminated timber in the U.S." *Seattle Daily Journal of Commerce* (2013).

24. Cook, J. P. "Composite Contruction Methods." *Journal of the Construction Division, American Society of Civil Engineers* **Vol.102,** p21–27 (1976).

25. The Institution of Structural Engineers. "*Appraisal of existing structures.*" (IStructE, 2010).

26. Johnson, R. P. "Research on Steel-Concrete Composite Beams." *Journal of the Structural Division (ASCE)* **Vol.96,** p445–459 (1970).

27. Bussell, M. "*P138 Appraisal of Existing Iron and Steel Structures.*" (The Steel Construction Institute, 1997).

28. Zhou, S. "Finite Beam Element Considering Shear-Lag Effect in Box Girder." p1115–1122 (2010).

29. Adekola, A. A. O. "Effective widths of composite beams of steel and concrete." *The Structural Engineer* **Vol.46,** p285–289 (1968).

30. Adekola, A. O. "On Shear Lag Effects in Orthotropic Composite Beams." *International Journal of Solids and Structures* **Vol.10,** p735–754 (1974).

31. Adekola, A. O. "The dependence of shear lag on partial interaction in composite beams." *International Journal of Solids and Structures* **Vol.10,** p389–400 (1974).

32. Adekola, A. O. "THE DEPENDENCE OF SHEAR LAG ON Plan." **Vol.10,** p389–400 (1974).

33. Mackey, S. & Wong, F. K. C. "The Effective Width of a Composite Tee-Beam Flange." *The Structural*

Engineer **Vol.39,** p277–285 (1961).

34.　"*Steel Designers' Manual.*" (Blackwell Science Ltd., 2008).

35.　Amana, E. J. & Booth, L. G. "Theoretical and Experimental Studies on Nailed and Glued Plywood Stressed-Skin Componenets: Part 1. Theoretical Study." *Journal of The Institute of Wood Science* **Vol.4,** p43–69 (1967).

36.　Amana, E. J. & Booth, L. G. "Theoretical and Experimental Studies on Nailed and Glued Plywood Stressed-Skin Components: Part 2. Experimental Study." *Journal of The Institute of Wood Science* **Vol.4,** p19–34 (1968).

37.　Milner, H. & Peczkis, J. "Wooden ship hulls as box girders with multiple interlayer slip." *Journal of structural engineering* **Vol.133,** p855–861 (2007).

38.　Davalos, J. & Salim, H. "Effective Flange Width for Stress-Laminated T-System Timber Bridges." *Journal of Structural Engineering* **Vol.119,** p938–953 (1993).

39.　Masoudnia, R., Hashemi, A. & Quenneville, P. "Evaluation Of Effective Flange Width In CLT Composite T-Beams." in *WCTE 2016 - World Conference on Timber Engineering* p4507–4514 (2016).

40.　Bogensperger, T. "Darstellung und praxistaugliche Aufbereitung für die Ermittlung mitwirkender Plattenbreiten von BSP-Elementen (in German)." (TU Graz, 2013).

41.　Papastavrou, P., Smith, S., Wallwork, T., Mcrobie, A. & Niem, N. "the Design of Cross-Laminated Timber Slabs With Cut-Back Glulam Rib Downstands – From Research To Live Project." in *World Conference in Timber Engineering* (2016).

42.　Thiel, A. "ULS Design of CLT Elements – Basics and some Special Topics." p1–24 (2016).

43.　Rowe, M. & Bradford, M. A. "Partial Shear Interaction in Deconstructable Steel-Concrete Composite Beams with Bolted Shear Connectors." in *Design, Fabrication and Economy of Metal Structures - International Conference Proceedings* p585–590 (2013).

44.　Dallam, L. N. "High Strength Bolt Shear Connectors -Pushout Tests." *Journal Proceedings* **Vol.65,** (1968).

45.　Dallam, L. N., Harpster, J. L., Program., M. C. H. R., Missouri. & Department., S. H. "*Composite beam tests with high-strength bolt shear connectors.*" (Missouri State Highway Dept., 1968).

46.　Bradford, M. A. & Pi, Y.-L. "Computational Modelling of Deconstructable Composite Steel-Concrete Beams." in *Proceedings of the Eleventh International Conference on Computational Structures Technology* (Civil-Comp Press, 2012).

47.　Lam, D. & Saveri, E. "Shear Capacity of Demountable Shear Connectors." in *Proceedings of the 10th International Conference on Advances in Steel Concrete Composite and Hybrid Structures* (eds. Liew, J. Y. R.

& Lee, S. C.) (2012).

48.   Lawson, R. M., Mullett, D. L., Rackham, J. W. & Institute, S. C. "*P175 Design of Asymmetric Slimflor Beams Using Deep Composite Decking*." (Steel Construction Institute, 1997).

49.   Stuart, D. M. "Antiquated Structural Systems Series - Part 10 Masonry." *Structure Magazine* p24–28 (2010).

50.   Stuart, D. M. "Antiquated Structural Systems Series - Part 2 Clay Tile Arched Floor Systems." *Structure Magazine* p18–20 (2007).

51.   Rogan, A. L. & Lawson, R. M. "*Value and Benefit Assessment of Slimdek Construction (P279)*." (The Steel Construction Institute, 2001).

52.   Schleich, J.-B. "Slim floor construction: Why?" in *Composite constructive - conventional and innovative* p53–64 (1997).

53.   Newman, G. M. "Fire Resistance of Slim Floor Beams." *Journal of Constructional Steel Research* **Vol.33,** p87–100 (1995).

54.   Wright, P. "Slimdek: Development of an integrated floor system." *Composite construction-conventional and innovative. …* p343–347 (1997).

55.   Mäkeläinen, P. & Ma, Z. "Fire resistance of composite slim floor beams." *Journal of Constructional Steel Research* **Vol.54,** p345–363 (2000).

56.   SCI. "*Slimflor Compendium.*" (2008).

57.   Tata Steel. "*Slimdek Manual.*" **Vol.23,** (Tata Steel Europe Ltd, 2012).

58.   University of Stuttgart. "EN1994 Workshop: Slim-floor systems." (2012).

59.   Dinwoodie, J. M. in *Construction Materials - Their Nature and Behaviour* (ed. Illston, J. M.) (E & FN Spon, 1994).

60.   Porteous, J. & Kermani, A. "*Structural Timber Design to Eurocode 5.*" (Blackwell Science Ltd., 2007).

61.   Smith, I., Landis, E. & Gong, M. "*Fracture and Fatigue in Wood.*" (Wiley, 2003).

62.   Valipour, H. R. & Crews, K. "Efficient finite element modelling of timber beams strengthened with bonded fibre reinforced polymers." *Construction and Building Materials* **Vol.25,** p3291–3300 (2011).

63.   Johns, K. C. & Lacroix, S. "Composite reinforcement of timber in bending." *Canadian Journal of Civil Engineering* **Vol.27,** p899–906 (2000).

64.   Borri, A. & Corradi, M. "Strengthening of timber beams with high strength steel cords." *Composites Part B: Engineering* **Vol.42,** p1480–1491 (2011).

65.   Sandhaas, C. "*Mechanical Behaviour of Timber Joints With Slotted-in Steel Plates*." (2012).

66.   Tan, D. & Smith, I. "Failure in-the-row model for bolted timber connections." *Journal of Structural Engineering* p713–718 (1999).

67.   Johnsson, H. & Stehn, L. "A Linear Fracture Mechanics Evaluation of Plug Shear Failure." *Proceedings of the 8th World Conference on Timber Engineering* (2004).

68.   Murty, B., Asiz, A. & Smith, I. "Tests and models for engineered wood product connections using small steel tube fasteners." *Engineering Structures* **Vol.33,** p63–68 (2011).

69.   Cohen, D. H., Ellis, S. C., Kozak, R. A. & Wilson, B. "*A New Taxonomy of Wood Products*." (1996).

70.   Crespell, P. & Gagnon, S. "Cross Laminated Timber: a Primer." (2010). Available at: https://fpinnovations.ca/Extranet/Pages/AssetDetails.aspx?item=/Extranet/Assets/ResearchReportsWP/2779.pdf#.Vvi9fHrtjvw.

71.   Henderson, J., Foster, S. & Bridgestock, M. "What is Brettstapel?" (2012). Available at: http://www.brettstapel.org/Brettstapel/What_is_it.html. (Accessed: 14th November 2016)

72.   Weirer, W. "HISTORY AND DEVELOPMENT OF CLT USING THE EXAMPLE OF KLH." *www.woodworks.org* (2011). Available at: http://www.woodworks.org/wp-content/uploads/CLT-Weirer.pdf.

73.   Schickhofer, G. "Cross Laminated Timber (CLT) in Europe – from Conception to Implementation." (2010).

74.   Lowenstein, O. "How massive wood came to Britain." *Fourth Door Review* (2011).

75.   Karacabeyli, E. & Douglas, P. E. (Editors). "*CLT Handbook (US Edition)*." (FPInnovations, 2013).

76.   Miller, G. "Cross-laminated timber: the sky's the limit [online]." *The Guardian* (2012).

77.   Bo, X., O'Neill, T., Zuo, J., Skitmore, M. & Chen, Q. "Perceived obstacles to multi-storey timber-frame construction□: an Australian study." *Architectcural Science Review* **Vol.57,** p169–176 (2014).

78.   Jonsson, R. "Prospects for timber frame in multi-storey house building in England, France, Germany, Ireland, the Netherlands and Sweden." p31 (2009). doi:10.13140/2.1.1356.4486

79.   Wells, M. "Stadthaus, London: raising the bar for timber buildings." *Proceedings of the ICE - Civil Engineering* **Vol.164,** p122–128 (2011).

80.   Zumbrunnen, P. & Fovargue, J. "MID RISE CLT BUILDINGS – THE UK ' s EXPERIENCE AND POTENTIAL FOR AUS AND NZ." in *World Conference of Timber Engineering* (2010).

81.   Parker, D. "Timber structures□: Loaded lumber." *New Civil Engineer* p1–4 (2015). Available at: www.nce.co.uk/features/structures/timber?structures?loaded?lumber/8674614.article. (Accessed: 13th

January 2015)

82.   Frearson, A. "Hawkins\Brown pairs cross-laminated timber and steel for record-breaking apartment block." *dezeen.com* (2015).

83.   Lend Lease. "Forté." (2012).

84.   Unattributed. "Top of the tree." *The Economist* (2016).

85.   Kreuzinger, H. "Platten, Scheiben und Schalen – ein Berechnungsmodell für gängige Statikprogramme." *Bauen mit Holz* **Vol.1,** p34–39 (1999).

86.   Gubana, A. "EXPERIMENTAL TESTS ON TIMBER-TO-CROSS LAM COMPOSITE SECTION BEAMS." in *World Conference of Timber Engineering* (2010).

87.   Fellmoser, P. & Blaß, H. "Influence of rolling shear modulus on strength and stiffness of structural bonded timber elements." *CIBW18 Meeting* p1–8 (2004).

88.   Blass, H. & Fellmoser, P. "Design of solid wood panels with cross layers." in *8th World Conference on Timber Engineering* (2004).

89.   Yeoh, D., Fragiacomo, M., Franceschi, M. De & Boon, K. H. "State of the Art on Timber-Concrete Composite Structures: Literature Review." *Journal of Structural Engineering* **Vol.137,** p1085–1095 (2011).

90.   Kuhlmann, U. & Schänzlin, J. "Composite of board stacks and concrete with integrated steel slim-floor profile." in *World Conference of Timber Engineering* p1–6 (2004).

91.   Blass, H. J. & Schlager, M. "Connections for timber-concrete-composite structures." in *Composite construction - conventional and innovative* (International Association for Bridge and Structural Engineering, 1997).

92.   Asiz, A. & Smith, I. "Demands Placed on Steel Frameworks of Tall Buildings Having Reinforced Concrete or Massive Wood Horizontal Slabs." *International Association for Bridge and Structural Engineering* **Vol.19,** p395–403 (2009).

93.   Stern, E. G. & Kumar, V. K. "Flitch Beams." *Forest Products Journal* **Vol.23,** p40–47 (1973).

94.   Lantos, G. "The Flexural Behaviour of Steel Reinforced Laminated Timber Beams." *Wood Science* **Vol.2,** p136–143 (1970).

95.   Alam, P. & Ansell, M. "The Effects of Varying Nailing Density upon the Flexural Properties of Flitch Beams." *Journal of Civil Engineering Research* **Vol.2,** p7–13 (2012).

96.   Guan, Z. W. & Rodd, P. D. "A three-dimensional finite element model for locally reinforced timber joints made with hollow dowel fasteners." *Canadian Journal of Civil Engineering* **Vol.27,** p785–797

(2000).

97.   Guan, Z. & Rodd, P. "DVW-Local Reinforcement for Timber Joints." *Journal of Structural Engineering* **Vol.127,** p894–900 (2001).

98.   Guan, Z. . & Rodd, P. . "Hollow steel dowels — a new application in semi-rigid timber connections." *Engineering Structures* **Vol.23,** p110–119 (2001).

99.   Guan, Z. & Rodd, P. "Modelling of timber joints made with steel dowels and locally reinforced by DVW discs." *Structural Engineering and Mechanics* **Vol.16,** p391–404 (2003).

100.   Loss, C., Loss, C., Piazza, M. & Zandonini, R. "Innovative construction system for sustainable buildings Innovative construction system for sustainable buildings." (2015).

101.   Loss, C., Piazza, M. & Zandonini, R. "Experimental tests of cross-lamited timber floors for timber-steel hybrid structures." *WCTE 2014 - World Conference on Timber Engineering, Proceedings* (2014).

102.   Loss, C., Piazza, M. & Zandonini, R. "Connections for steel-timber hybrid prefabricated buildings. Part I:Experimental tests." *Construction and Building Materials* **Vol.122,** p796–808 (2016).

103.   Loss, C., Piazza, M. & Zandonini, R. "Connections for steel-timber hybrid prefabricated buildings. Part II: Innovative modular structures." *Construction and Building Materials* **Vol.122,** p796–808 (2016).

104.   Loss, C. & Davison, B. "Innovative composite steel-timber floors with prefabricated modular components." *Engineering Structures* **Vol.132,** p695–713 (2017).

105.   Moore, M. "Scotia Place – 12 Story Apartment Building A Case Study of High-Rise Construction Using Wood and Steel –." *New Zealand Timber Design Journal* **Vol.10,** p5–12 (2000).

106.   Way, A. G. J. "*P391: Structural robustness of steel framed buildings.*" (SCI, 2011).

107.   HM Government. "*Approved Document A.*" *The Building Regulations* (NBS, 2010).

108.   Yates, M., Linegar, M. & Dujic, B. "*Design of an 8 storey Residential Tower from KLH Cross Laminated Solid Timber Panels.*"

109.   The Institution of Structural Engineers. "*Practical guide to structural robustness and disproportionate collapse in buildings.*" (The Institution of Structural Engineers, 2010).

110.   "*BS EN 1991-1-7:2006/AC:2010.*" (BSI, 2010).

111.   Harvey, F. "British belief in climate change on the rise, research finds." *The Guardian* (2015).

112.   The Commitee on Climate Change. "*The Fourth Carbon Budget.*" (2010).

113.   The Commitee on Climate Change. "*Meeting Carbon Budgets – 2012 Progress Report to Parliament.*" (2012).

114. Department for Business Innovation & Skills. "*Estimating the amount of CO2 emissions that the construction industry can influence*." (2010).

115. HM Government. "*Climate Change Act*." (2008).

116. Ruddock, J. "*CLIMATE CHANGE - The Carbon Budgets Order 2009*." (Department of Energy and Climate Change, 2009).

117. Barker, G. "*CLIMATE CHANGE - The Carbon Budget Order 2011*." (Department of Energy and Climate Change, 2011).

118. HM Government. "*Implementing the Climate Change Act 2008*." (2011).

119. Innovation & Growth Team. "*Low Carbon Construction*." (Department for Business, Innovation and Skills, 2010).

120. "*The Carbon Budget Order 2016*." (2016).

121. Vaughan, A. "UK sets ambitious new 2030s carbon target." *The Guardian* (2016).

122. Ares, E. "*Zero Carbon Homes (Briefing Paper no.6678)*." (2016).

123. Department of Energy & Climate Change. "*UK Greenhouse Gas Emissions: performance against emissions reduction targets – 2012 provisional figures*." (2013).

124. Sansom, M. & Pope, R. J. "A comparative embodied carbon assessment of commercial buildings." *The Structural Engineer* **Vol.October,** p38–49 (2012).

125. Unattributed. "Zero Carbon Homes." *Designing Buildings Wiki* (2016). Available at: https://www.designingbuildings.co.uk/wiki/Zero_carbon_homes. (Accessed: 1st March 2017)

126. Lehmann, S. "*The Principles of Green Urbanism - Transforming the City for Sustainability*." (Earthscan, 2010).

127. "*BS EN 15804:2012+a1:2013*." (BSI, 2014).

128. Ramesh, T., Prakash, R. & Shukla, K. K. "Life cycle energy analysis of buildings□: An overview." *Energy and Buildings* **Vol.42,** p1592–1600 (2010).

129. FPInnovations. "*Environmental Product Declaration: Nordic X-Lam*." (2013).

130. Hammond, G. & Jones, C. "*Inventory of Carbon & Energy: ICE (V2.0)*." (2011).

131. Chapman, J. "30-level timber building concept based on cross- laminated timber construction." p36–40 (2012).

132. Goodchild, C. H., Webster, R. M. & Elliott, K. S. "Economic Concrete Frame Elements to Eurocode 2 A pre-scheme handbook for the rapid sizing and selection of reinforced concrete frame elements."

133.   Bison Manufacturing. "Hollow Composite Floors Load / Span Table." p817500 Available at: http://www.bison.co.uk/pdf/Bison-Hollow-Composite-Floors-Load-Span-Table.pdf. (Accessed: 15th January 2014)

134.   Using, W. & Load, K. "Load Tables Multideck 146 Load Tables." p59–64 (1994).

135.   Okutu, K. "Structural Implications of Replacing Concrete Floor Slabs With Timber in Composite Construction." (University of Sheffield, 2012).

136.   Densley Tingley, D. & Davison, B. "Developing an LCA methodology to account for the environmental benefits of design for deconstruction." *Building and Environment* **Vol.57,** p387–395 (2012).

137.   Nimmo, A., Wright, S. & Coulson, D. "Delivering London 2012: temporary venues." *Proceedings of the ICE - Civil Engineering* **Vol.164,** p59–64 (2011).

138.   Howarth, D. "Rio 2016 handball arena will dismantle to become four schools." *dezeen.com* (2016). Available at: https://www.dezeen.com/2016/07/25/rio-2016-olympics-handball-arena-dismantle-become-four-schools-brazil/. (Accessed: 1st December 2016)

139.   Lubell, S. "After the Games, Rio's Stadiums Won't Rot—They'll Transform." *wired.com* (2016). Available at: https://www.wired.com/2016/08/games-rios-stadiums-wont-rot-theyll-transform/. (Accessed: 1st December 2016)

140.   Robertson, A. B., Lam, F. C. F. & Cole, R. J. "A Comparative Cradle-to-Gate Life Cycle Assessment of Mid-Rise Office Building Construction Alternatives: Laminated Timber or Reinforced Concrete." *Buildings* **Vol.2,** p245–270 (2012).

141.   SteelConstruction.info. "Design software and tools." Available at: http://www.steelconstruction.info/Design_software_and_tools.

142.   The Concrete Centre. "Concept Version 3." Available at: http://www.concretecentre.com/online_services/design_tools/concept_v3.aspx.

143.   Densley Tingley, D. "About Sakura." (2012). Available at: http://dfd.group.shef.ac.uk/about_sakura.html.

144.   The Concrete Centre. "*Thermal Mass Explained*." (The Mineral Products Association, 2012).

145.   Guy, B. & Ciarimboli, N. "*Design for Disassembly in the built environment: a guide to closed-loop design and building*." (2008).

146.   Williams, J. M., Fridley, K. J., Cofer, W. F. & Falk, R. H. "Failure modeling of sawn lumber with a fastener hole." *Finite Elements in Analysis and Design* **Vol.36,** p83–98 (2000).

147.   Kim, Y. J. & Harries, K. a. "Modeling of timber beams strengthened with various CFRP composites." *Engineering Structures* **Vol.32,** p3225–3234 (2010).

148. O'Loinsigh, C., Oudjene, M., Shotton, E., Pizzi, A. & Fanning, P. "Mechanical behaviour and 3D stress analysis of multi-layered wooden beams made with welded-through wood dowels." *Composite Structures* **Vol.94,** p313–321 (2012).

149. van der Put, T. A. C. M. "Softening behaviour and correction of the fracture energy." *Theoretical and Applied Fracture Mechanics* **Vol.48,** p127–139 (2007).

150. Ellegaard, P. "Finite-Element Modeling of Timber Joints with Punched Metal Plate Fasteners." *Journal of Structural Engineering* **Vol.132,** p409–417 (2006).

151. Zhou, T. & Guan, Z. W. "A new approach to obtain flat nail embedding strength of double-sided nail plate joints." *Construction and Building Materials* **Vol.25,** p598–607 (2011).

152. Zhou, T. & Guan, Z. "DOUBLE-SIDED NAIL PLATE JOINTS." in *World Conference of Timber Engineering* (2010).

153. Gliniorz, K.-U., Mosalam, K. M. & Natterer, J. "Modeling of layered timber beams and ribbed shell frameworks." *Composites Part B: Engineering* **Vol.33,** p367–381 (2002).

154. Mestek, P., Heinrich, K. & Winter, S. "Design of Cross Laminated Timber (CLT)." *10th World Conference on Timber Engineering* p156–163 (2008).

155. Mestek, P. & Winter, S. "Cross Laminated Timber (CLT) – Reinforcements with Self-Tapping Screws." *World Conference in Timber Engineering* p2–4 (2010).

156. Mestek, P., Kreuzinger, H. & Winter, S. "Design concept for CLT-reinforced with self-tapping screws." *Working Commission W18 - Timber Structures* (2011).

157. Moosbrugger, T., Guggenberger, W. & Bogensperger, T. "Cross-Laminated Timber Wall Segments under homogeneous Shear — with and without Openings." in *World Conference on Timber Engineering* (2006).

158. Bogensperger, T., Moosbrugger, T. & Silly, G. "Verification of CLT-plates under loads in plane." in *World Conference of Timber Engineering* (2010).

159. Brandner, R., Bogensperger, T. & Schickhofer, G. "In plane Shear Strength of Cross Laminated Timber (CLT): Test Configuration , Quantification and influencing Parameters." p1–13 (2013).

160. Bogensperger, T., Augustin, M. & Schickhofer, G. "Properties of CLT-Panels Exposed to Compression Perpendicular to their Plane." in *44th International Council for Research and Innovation in Building and Construction, Working Commission W18 - Timber Structures* p1–15 (2011).

161. "ANSYS 14.5 Release Highlights." Available at: http://www.ansys.com/Products/ANSYS+14.5+Release+Highlights.

162. "Why ANSYS not ABAQUS?" Available at: http://imechanica.org/node/6711.

163. Green, D. D. W., Winandy, J. E. & Kretschmann, D. E. in *Wood handbook□: wood as an engineering material* (ed. Forest Products Laboratory) (1999).

164. Dahl, K. B. & Malo, K. a. "Nonlinear shear properties of spruce softwood: Numerical analyses of experimental results." *Composites Science and Technology* **Vol.69,** p2144–2151 (2009).

165. Xu, B. H., Bouchaïr, A. & Racher, P. "Analytical study and finite element modelling of timber connections with glued-in rods in bending." *Construction and Building Materials* **Vol.34,** p337–345 (2012).

166. Ashtari, S. "In-Plane Stiffness of Cross-Laminated Timber Floors." (University of British Columbia (Vancouver), 2012).

167. Gsell, D., Feltrin, G. & Schubert, S. "Cross-laminated timber plates: Evaluation and verification of homogenized elastic properties." *Journal of Structural Engineering…* **Vol.133,** p132–138 (2007).

168. Bosl, R. "Zum Nachweis des Trag-und Verformungsverhaltens von Wandscheiben aus Brettlagenholz." (Universität der Bundeswehr München, 2002).

169. "*Timber Engineering: STEP 1.*" (Centrum Hout, 1995).

170. Castro, J. de. "*Experiments on Epoxy, Polyurethane and ADP adhesives.*" *Composite Construction Laboratory. École …* (2005).

171. Hochreiner, G., Füssl, J., Serrano, E. & Eberhardsteiner, J. "Influence of Wooden Board Strength Class on the Performance of Cross-laminated Timber Plates Investigated by Means of Full-field Deformation Measurements." *Strain* **Vol.50,** p161–173 (2014).

172. Coste, G. "The Assessment and Applications of a New Connector Type for Use in Timber Structural." (Edinburgh Napier University, 2010).

173. Coste, G., Kermani, A. & Porteous, A. "Performance of helically shaped metal fasteners in timber." *Proceedings of the ICE -Construction Materials* **Vol.159,** p53–60 (2006).

174. Chamberlain, B. "GANG-NAIL GN20 PUNCHED METAL PLATE TIMBER FASTENERS." p1–12 (2010).

175. Abdulrahman, N. "Load transfer Mechanism in punched metal plate timber connections." (Napier University, 2002).

176. Jacquier, N. & Girhammar, U. A. "Tests on glulam-CLT shear connections with double-sided punched metal plate fasteners and inclined screws." *Construction and Building Materials* **Vol.72,** p444–457 (2014).

177. Stojic, D. & Cvetkovic, R. "Analysis of a composite timber-concrete structures according to the limit states: Design and innovative methods in coupling of a timber and concrete." *Facta universitatis-series: Architecture and Civil Engineering* **Vol.2,** p169–184 (2001).

178. Khorsandnia, N., Sch??nzlin, J., Valipour, H. & Crews, K. "Time-dependent behaviour of timber-concrete composite members: Numerical verification, sensitivity and influence of material properties." *Construction and Building Materials* **Vol.66,** p192–208 (2014).

179. Jacquier, N. & Girhammar, U. A. "Tests on shear connections in prefabricated composite cross-laminated- timber and concrete elements." *World Conference on Timber Engineering 2012: Architecture and Engineering Case Studies, WCTE 2012, July 15, 2012 - July 19, 2012* **Vol.3,** p441–450 (2012).

180. Jacquier, N. & Girhammar, U. A. "Evaluation of bending tests on composite glulam–CLT beams connected with double-sided punched metal plates and inclined screws." *Construction and Building Materials* **Vol.95,** p762–773 (2015).

181. Schneider, J., Stiemer, S. F., Tesfamariam, S., Karacabeyli, E. & Popovski, M. "Damage Assessment of Cross Laminated Timber Connections Subjected to Simulated Earthquake Loads." in *World Conference on Timber Engineering* (2012).

182. Schneider, J. *et al.* "Novel Steel Tube Connection for Hybrid Systems." *World Conference on Timber Engineering* (2014).

183. ASTM. "*Standard Test Methods for Bolted Connections in Wood and Wood-Based Products*." *Standard D5652-95* (2000).

184. Hossain, A., Lakshman, R. & Tannert, T. "Shear Connections with Self-Tapping Screws for Cross-Laminated Timber Panels." in *Structures Congress* p2251–2259 (2015).

185. Jarvis, C. "Can a Gangnail Plate be used as a shear connection in a composite beam of Cross-Laminated Timber and Steel." (University of Sheffield, 2014).

186. Hong, J. & Barrett, D. "Three-dimensional finite-element modeling of nailed connections in wood." *Journal of Structural Engineering* **Vol.136,** p715–722 (2010).

187. "Helifix Products." Available at: http://www.helifix.co.uk/products/. (Accessed: 1st December 2016)

188. Peng, C. "CROSS-LAMINATED TIMBER PANEL-TO-PANEL CONNECTIONS FOR TIMBER-STEEL HYBRID CONSTRUCTION." (The University of Sheffield, 2015).

189. Cobb, F. "*Structural Engineer's Pocket Book*." (Elsevier Ltd, 2009).

190. Nethercot, D. A. "Semirigid joint action and the design of nonsway composite frames." *Engineering Structures* **Vol.17,** p554–567 (1995).

191. Zagani, S. & Engineering, S. "SEMI-RIGID STEEL FRAMES WITH TIMBER CROSS-." (2014).

192. Schmidt, R. J. & Griffin, C. T. "Barriers to the design and use of cross-laminated timber structures in high-rise multi-family housing in the United States." *Structures and Architecture. - New concepts, applications and challenges* p2225–2231 (2013).

193. Dunton, J. "Uni fire rekindles debate on timber-framed buildings." *Architects Journal* p1–3 (2014).

194. Frangi, A., Knobloch, M. & Fontana, M. "Fire design of timber slabs made of hollow core elements." *Engineering Structures* **Vol.31,** p150–157 (2009).

195. Timber Trade Federation. "Positive Results for CLT in Fire Safety study Positive Structural Integrity Results for CLT in new Fire Study." (2014).

196. Stora Enso. "*CLT - Cross Laminated Timber - Fire protection*." (2016).

197. Majdi, Y., Hsu, C.-T. T. & Zarei, M. "Finite element analysis of new composite floors having cold-formed steel and concrete slab." *Engineering Structures* **Vol.77,** p65–83 (2014).

198. Lukaszewska, E. "Development Prefabricated Timber-Concrete Floors Timber-Concrete Composite Floors." (Lulea University of Technology, 2009).

199. Bazan, I. M. M. "Ultimate bending strength of timber beams." (Technical University of Nova Scotia, 1980).

200. Zhou, Q., Gong, M., Chui, Y. H. & Mohammand, M. "Measurement of rolling shear modulus of Cross Laminated Timber: Exploratory study using downscaled specimens under variable span bending tests." in *Proceedings of 2012 International Conference on Biobase Material Science and Engineering* p36–40 (Ieee, 2012). doi:10.1109/BMSE.2012.6466175

201. Lehmann, S. "Towards a Sustainable City Centre: Integrating Ecologically Sustainable Development (ESD) Principles into Urban Renewal." *Journal of Green Building* **Vol.1,** p83–104 (2006).

202. Architecture, P. "Interesting Olympic Architecture." (2012). Available at: http://phxarch.wordpress.com/2012/08/21/olympic-architecture/.

203. Young, W. C. & Budynas, R. G. "*Roark's Formulas for Stress and Strain*." (McGraw-Hill, 2002).

Appendix A

Loading & Initial Calcs

Beam and Column Designations for Steel-Timber and Steel-Concrete Designs
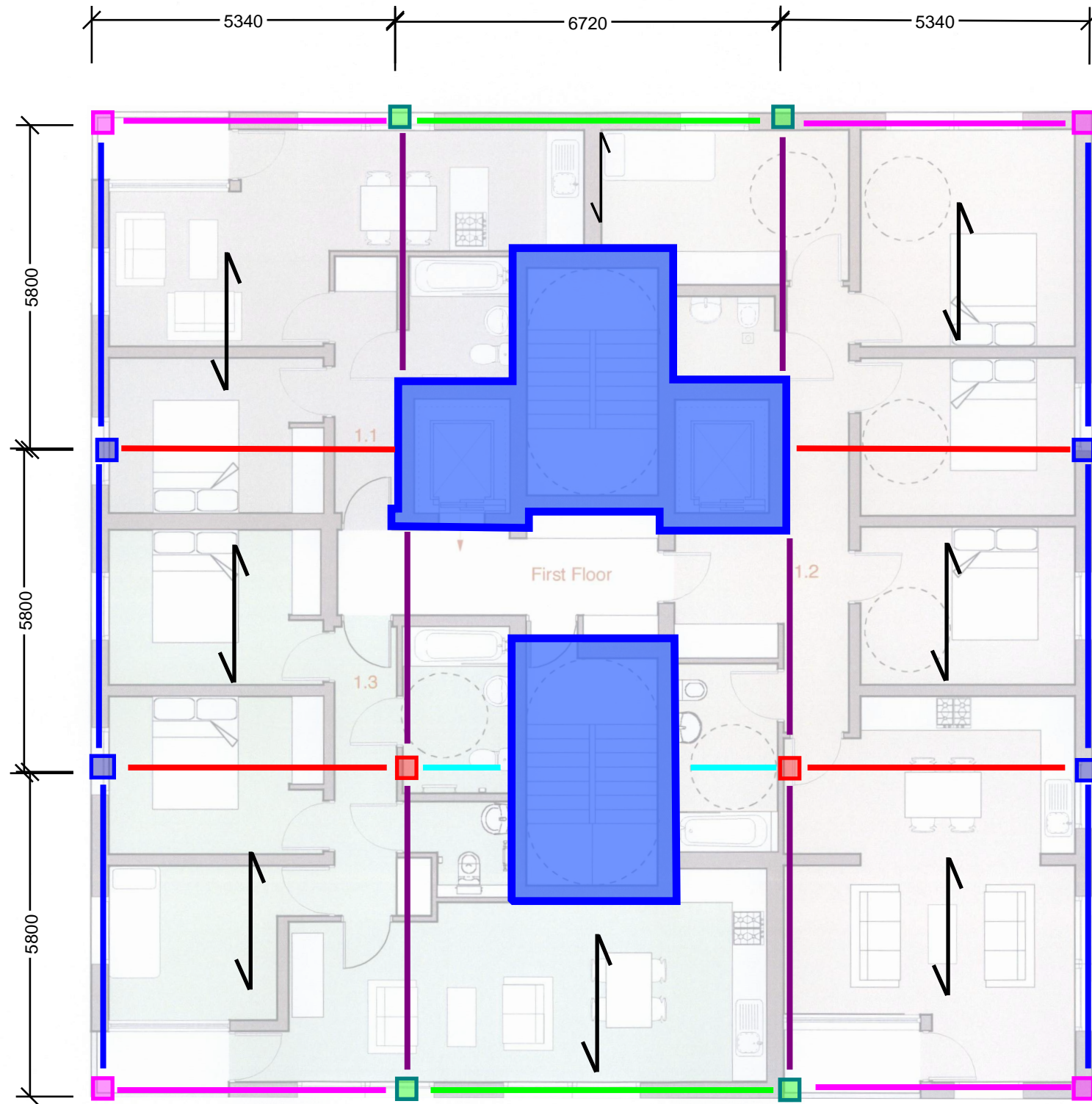
Legend:
- Beam 1
- Beam 2
- Beam 3
- Beam 4
- Edge Beam
- Tie Beam
- Column 1
- Column 2
- Column 3
- Column 4

Dimensions (horizontal): 5340 | 6720 | 5340

Dimensions (vertical): 5800 | 5800 | 5800

First Floor

1.1

1.2

1.3

1:100 FIRST FLOOR PLAN

1 / 101

REV	COMMENTS	DATE	CHK
A	Plans ammended to suit Telfords comments and apply structural grid. Lifts relocated and en-suite bathrooms omitted from all units except 3 beds from 5th floor up.	21.03.07	
B	Flat 1.3 balcony and bathrooms amended	29.03.07	

STATUS

PLANNING ISSUE

Job	MURRAY GROVE
Title	PROPOSED FIRST FLOOR PLAN
Date	APRIL 2007
Scale	1:50@A1, 1:100@A3
Drawn	CG
Approved	KH

1-285.101.B

Initial Calculations

- **Calculating Roof Snow Load**

Altitude, A		≈	22
∴ Zone, Z		=	3

- Characteristic Ground Snow Load…

  $$s_k = [0.15 + (0.1 \cdot Z + 0.05)] + \left(\frac{A-100}{525}\right)$$
  $$= [0.15 + ((0.1 \times 3) + 0.05)] + \left(\frac{22-100}{525}\right) = 0.351 \text{ kN/m}^2$$

  NA to BS EN 1991-1-3, NA.1

- Roof Shape coefficient, μ_1 = 0.8

  NA to BS EN 1991-1-3, Table NA1

- **Snow Loads**

s	=	$\mu_i \cdot C_e \cdot C_t \cdot s_k$	(persistent)	
	=	$\mu_i \cdot C_e \cdot C_t \cdot s_{Ad}$	(accidental)	

  Eq. 5.1, BS EN 1991-1-3

s_{Ad}	=	$C_{esl} \cdot s_k$	… where C_{esl} = 2.0		
	=	2 x 0.351		=	0.702

  Eq. 4.3, BS EN 1991-1-3

C_e	=	0.8	windswept, tall building
C_t	=	1.0	

  Secn. 5.2.8, BS EN 1991-1-3

∴ **$S_{persistant}$** =	**0.8 x 0.8 x 1.0 x 0.351**		=	**0.225 kN/m²**
$S_{accidental}$ =	**0.8 x 0.8 x 1.0 x 0.702**		=	**0.449 kN/m²**

- **Façade Loads**

  Assume **Façade load = 1.1 x timber mass** (taking into account cladding system)

γ_{CLT}	=	480 kg/m³	=	4.8kN/m³

Original building floor-to-floor height	≈	2.8m
	∴	Assume 2.6m clear height

  Allowing for 400mm for services, say floor-to-floor height, h = 3.0m

Wall panel thickness	=	128mm
BUT	Outer Walls are double-layered	
	∴	Assume thickness, t = 256mm

  ⇨ **Façade load = $\gamma_{CLT} \cdot t \cdot h$ = 3.0m x 4.8kN/m³ = 13.9 kN/m²**

- Internal Column

Tributary Area	=	5.8m x 6.05m	=	35.0m²
No. of floors			=	8 (+ roof)

Initial Calculations (Concrete)				

- Building usage: Residential
  - ∴   **Imposed Load (q_k)**   =   **1.5 kN/m^2**   *(BS EN 1991-1-1 Table NA.3)*

  -     **Superimposed Dead Load (SDL)**   =   **1.5 kN/m^2**   *(Services & Finishes; CCIP-025)*

- Assume flat-slab construction
  - ∴   Assume: Slab Depth,   d   =   235mm   *(CCIP-025, Table 3.7)*
    - Column Size   =   350x350 sq.   *(CCIP-025)*
    - Standard span Reinforcement   ≈   14 kg/m^2
    - Long span Reinforcement   ≈   20 kg/m^2

- Concrete slab dead-weight
  - Concrete density, γ_{conc} =   2400 kg/m^3
  -     =   24 kN/m^3
- Slab self-weight
  - = γ_{conc} x d
  - =   24kN/m^3 x 0.235m   =   5.64 kN/m^2

- **Dead Load (g_k)**
  - =   slab swt. + SDL
  - =   5.64 + 1.5   =   **7.14 kN/m^2**

- Load Factors

Dead Loads	γ_G	=	1.35	*Table NA.A1.2(B), BS EN 1990*
Imposed Loads	γ_Q	=	1.5	*Table NA.A1.2(B), BS EN 1990*
	ξ	=	0.925	*Table NA.A1.2(B), BS EN 1990*
	ψ_0	=	0.7	*Table NA.A1.1, BS EN 1990*

- **Design UDL (ω)**
  Combination 1
  - = $\gamma_G \cdot g_k + \gamma_Q \cdot \psi_0 \cdot q_k$ *Eq. 6.10a, BS EN 1990*
  - =   (1.35 x 7.14) + (1.5 x 0.7 x 1.5)   =   11.214 kN/m^2

  Combination 2
  - = $\xi \cdot \gamma_G \cdot g_k + \gamma_Q \cdot \psi_0 \cdot q_k$ *Eq. 6.10b, BS EN 1990*
  - =   (0.925 x 1.35 x 7.14) + (1.5 x 1.5)   =   11.116 kN/m^2
  - ∴   **Take   Design UDL   ω**   =   **11.2kN/m**

Concrete Design

Putting Above parameters into Concept V3 Software…

Solid Flat Slab	**225mm**
Internal Columns	**400x400mm square**
Edge Columns	**400x250mm**
Corner Columns	**275x275mm**

Initial Calculations (Steel)	

Max. Slab Span = 5.8m
Apply Kingspan MD146, gauge 1.5mm, with 225mm slab (max. span = 6.0m, unpropped)

∴   Assume: Slab Depth,   d   =   225mm

- Building usage: Residential

     ∴   **Imposed Load (q_k)**   =   **1.5 kN/m^2**

          Superimposed Dead Load (SDL)   =   **1.5 kN/m^2**

- Concrete slab dead-weight

          Concrete density, γ_{conc} =   2400 kg/m^3
                                                        =   24 kN/m^3
- Slab self-weight
     = γ_{conc} x d
     =   24kN/m^3 x 0.225m   =   5.4 kN/m^2

- **Dead Load (g_k)**
     =   slab swt. + SDL
     =   5.4 + 1.5   =   **6.9 kN/m^2**

- Load Factors

Dead Loads	γ_G	=	1.35	*Table NA.A1.2(B), BS EN 1990*
Imposed Loads	γ_Q	=	1.5	*Table NA.A1.2(B), BS EN 1990*
	ξ	=	0.925	*Table NA.A1.2(B), BS EN 1990*
	ψ_0	=	0.7	*Table NA.A1.1, BS EN 1990*

- **Design UDL (ω)**

     Combination 1
     = $\gamma_G \cdot g_k + \gamma_Q \cdot \psi_0 \cdot q_k$ *Eq. 6.10a, BS EN 1990*
     =   (1.35 x 6.9) + (1.5 x 0.7 x 1.5)   =   10.89 kN/m^2

     Combination 2
     = $\xi \cdot \gamma_G \cdot g_k + \gamma_Q \cdot \psi_0 \cdot q_k$ *Eq. 6.10b, BS EN 1990*
     =   (0.925 x 1.35 x 6.9) + (1.5 x 1.5)   =   10.87 kN/m^2
∴   **Take   Design UDL   ω   =   10.9 kN/m**

Using BDES software to size steel beams…

Beam Type 1   -   UB356x171x51
Beam Type 4   -   UB254x146x31

Assuming 2.6m clear height, 600mm for beam + slab…
Floor-to-floor = 3.2m   =>   façade load = 15.36kN/m^2 =>   3.93 kN/m

Beam Type 2   -   UB254x146x37
Beam Type 3   -   UB305x165x54

Edge Beam   -   RHS180x100x5
Tie Beam   -   UKT102x152x17

Appendix B

Slab Sizing References

Reference Pattern

Load on panel over 3 spans –
e.g. for floor in a residential
building
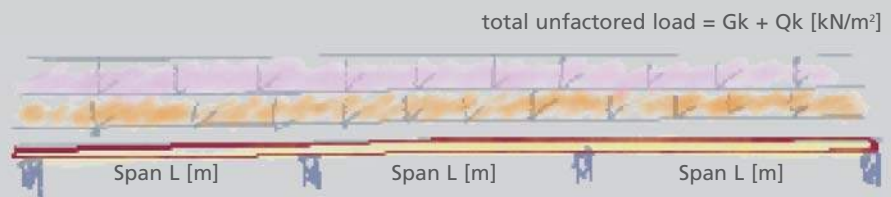
total unfactored load = Gk + Qk [kN/m²]

Span L [m]   Span L [m]   Span L [m]

**Triple-span beam for total unfactored load = Gk + Qk for L/400
unfavourably superposed Gk/Qk = 0.5 to 1.5**

— 3-s 108
— 5-s 117
— 3-s 95
— 3-s 90
— 3-s 78
— 3-s 60

**Triple-span beam for total unfactored load = Gk + Qk for L/400
unfavourably superposed Gk/Qk = 0.5 to 1.5**
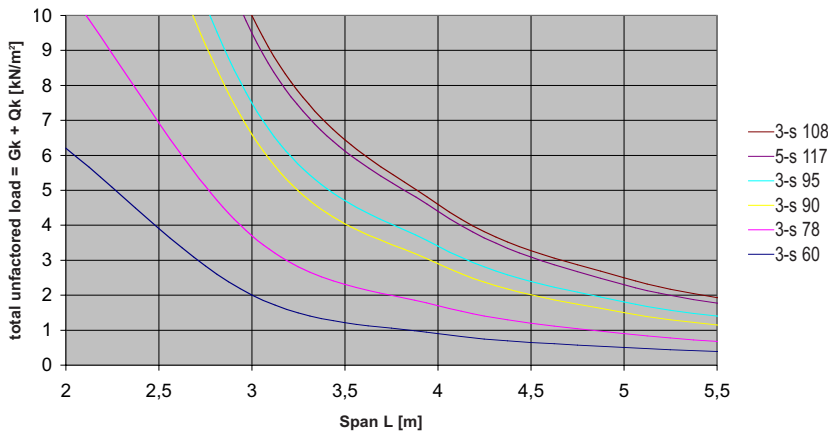
— 5-s 200
— 5-s 182
— 5-s 162
— 5-s 146
— 5-s 140
— 3-s 120
— 5-s 125
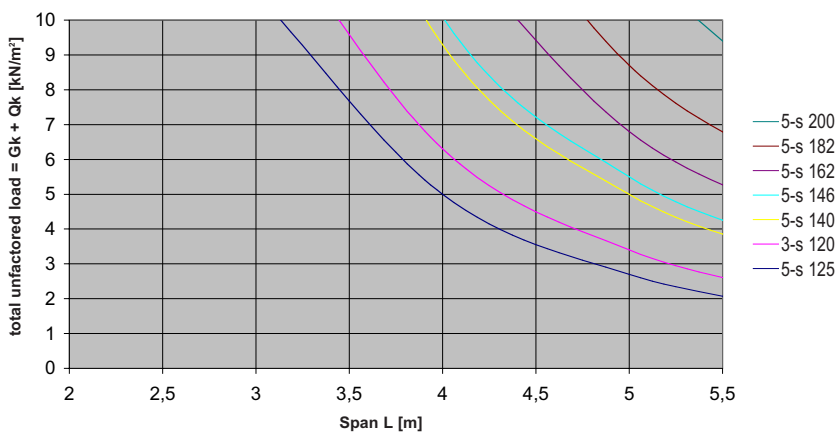
KLH AS A FLOOR

L/400, worst case total loads
considering variable actions on
full an alternate spans.

3-s panels with 34 mm thick
edge laminations are rated
REI 30 under normal loads.

5-s and 7-s panels are rated
REI 60 under normal loads.

For higher permissible deformations,
the chart values can be converted
using the following equation :

E.g. $u_{\text{, perm L/300}} = u_{\text{ perm L/400}} \times \dfrac{400}{300}$

CROSS-SECTIONAL VALUES OF DIFFERENT KLH CROSS-LAMINATED PANEL TYPES

FACING LAYERS ALIGNED TO PANEL TRANSVERSE DIRECTION TT

Nominal thickness in mm	Layers	Layer build-up (= / ⊥ / t)	A net [mm²]	A q [mm²]	I full [10⁴mm⁴]	I effective (depending on span length L) L=1000mm [10⁴mm⁴]	L=2000mm [10⁴mm⁴]	L=2950mm [10⁴mm⁴]	I effective / I full L=1000mm %	L=2000mm %	L=2950mm %
57	3 s	19 19 19	38000	57000	1543	1075	1354	1422	69.7%	87.8%	92.2%
72	3 s	19 34 19	38000	72000	3110	1626	2354	2567	52.3%	75.7%	82.5%
94	3 s	30 34 30	60000	94000	6922	3233	5169	5845	46.7%	74.7%	84.4%
95	5 s	19 19 19 19 19	57000	95000	7145	3129	4692	5168	43.8%	65.7%	72.3%
128	5 s	30 19 30 19 30	90000	128000	17476	6805	11446	13146	38.9%	65.5%	75.2%
158	5 s	30 34 30 34 30	90000	158000	32869	7869	15997	19911	23.9%	48.7%	60.6%

FACING LAYERS ALIGNED TO PANEL LONGITUDINAL DIRECTION TL

Nominal thickness in mm	Layers	Layer build-up (= / ⊥ / t)	A net [mm²]	A q [mm²]	I full [10⁴mm⁴]	I effective (depending on span length L) L=2000mm [10⁴mm⁴]	L=4000mm [10⁴mm⁴]	L=6000mm [10⁴mm⁴]	L=8000mm [10⁴mm⁴]	I effective / I full L=2000mm %	L=4000mm %	L=6000mm %	L=8000mm %
60	3 s	19 22 19	38000	60000	1800	1535	1663	1690	1699	85.3%	92.4%	93.9%	94.4%
78	3 s	19 40 19	38000	78000	3955	2814	3245	3341	3375	71.2%	82.0%	84.5%	85.3%
90	3 s	34 22 34	68000	90000	6075	5020	5707	5858	5913	82.6%	93.9%	96.4%	97.3%
95	3 s	34 27 34	68000	95000	7145	5629	6578	6795	6875	78.8%	92.1%	95.1%	96.2%
108	3 s	34 40 34	68000	108000	10498	7292	9113	9566	9736	69.5%	86.8%	91.1%	92.7%
120	3 s	40 40 40	80000	120000	14400	9752	12511	13227	13499	67.7%	86.9%	91.9%	93.7%
117	5 s	19 30 19 30 19	57000	117000	13347	6993	8585	8965	9107	52.4%	64.3%	67.2%	68.2%
125	5 s	19 34 19 34 19	57000	125000	16276	7892	9914	10410	10596	48.5%	60.9%	64.0%	65.1%
140	5 s	34 19 34 19 34	102000	140000	22867	14799	18416	19305	19638	64.7%	80.5%	84.4%	85.9%
146	5 s	34 22 34 22 34	102000	146000	25934	15761	20181	21307	21733	60.8%	77.8%	82.2%	83.8%
162	5 s	34 30 34 30 34	102000	162000	35429	18347	25181	27084	27822	51.8%	71.1%	76.4%	78.5%
182	5 s	34 40 34 40 34	102000	182000	50238	21608	31979	35161	36435	43.0%	63.7%	70.0%	72.5%
200	5 s	40 40 40 40 40	120000	200000	66667	27890	42995	47923	49938	41.8%	64.5%	71.9%	74.9%
202	7 s	34 22 34 22 34 22 34	136000	202000	68687	38927	49559	52243	53257	56.7%	72.2%	76.1%	77.5%
226	7 s	34 30 34 30 34 30 34	136000	226000	96193	45728	62232	66775	68533	47.5%	64.7%	69.4%	71.2%
208	7 ss	68 19 68 19 68	170000	208000	74991	43322	61508	66987	69167	57.8%	82.0%	89.3%	92.2%
230	7 ss	68 30 68 30 68	170000	230000	101392	45979	74100	84238	88534	45.3%	73.1%	83.1%	87.3%
260 *	7 ss	80 30 80 30 80	200000	260000	146467	62593	104691	120992	128094	42.7%	71.5%	82.6%	87.5%
280 *	7 ss	80 40 80 40 80	200000	280000	182933	64335	117634	141238	152124	35.2%	64.3%	77.2%	83.2%
248	8 ss	68 22 68 22 68 22 68	204000	248000	127108	66273	98047	108149	112241	52.1%	77.1%	85.1%	88.3%
300 *	8 ss	80 30 80 30 80 30 80	240000	300000	225000	92760	155646	179997	190606	42.1%	69.2%	80.0%	84.7%
320 *	8 ss	80 40 80 40 80 40 80	240000	320000	273067	92386	169137	203126	218802	33.8%	61.9%	74.4%	80.1%

* Special panel types, price upon request, all data refer to panel strips 1000 mm in width

A net	Cross-sectional value for calculating the compressive stresses in the direction of the face layer orientation
A q	Cross-sectional value for calculating the shear stresses for load transfer in the direction of the face layer
I full	Moment of inertia of the full cross section – reference value only
I effective	Moment of inertia for the composite cross section, including the percentage shear deformation for load transfer in the direction of the covering layers
I effective / I full	Ratio that indicates how much the transverse layers change the moment of inertia of the cross section.
W effective	Moment of resistance for calculating the stress resulting from bending moments $= $ I effective / (h* 0.5)
i effective	Radius of gyration of the composite cross section for calculating the slenderness $= $ root (I effective / A net)

Multideck 80-V2
Normal Weight Concrete Load Tables

Unpropped - Load/Span Table (Steel - 350N/mm²)

Span Type (Support Condition)	Slab Depth (mm)	Min Mesh Size	Gauge = 1.0 Total Applied Load (kN/m²) SLS					
			4.0	6.0	8.0	10.0	12.0	14.0
	130	A142	4.03	3.90	3.70	3.28	2.98	2.75
	140	A142	3.93	3.93	3.92 / 3.93	3.48 / 3.86	3.16 / 3.51	2.91 / 3.24
	150	A142	3.84	3.84	3.84	3.66 / 3.84	3.32 / 3.70	3.06 / 3.41
	160	A142	3.75	3.75	3.75	3.75	3.49 / 3.75	3.21 / 3.58
	175	A142	3.65	3.65	3.65	3.65	3.65	3.42 / 3.65
	200	A193	3.45	3.45	3.45	3.45	3.45	3.45
	250	A252	3.16	3.16	3.16	3.16	3.16	3.16
	130	A142	4.53	4.31	3.70	3.28	2.98	2.75
	140	A142	4.39	4.39	3.92 / 4.29	3.48 / 3.86	3.16 / 3.51	2.91 / 3.24
	150	A142	4.26	4.26	4.13 / 4.26	3.66 / 4.08	3.32 / 3.70	3.06 / 3.41
	160	A142	4.15	4.15	4.15	3.84 / 4.15	3.49 / 3.89	3.21 / 3.58
	175	A142	3.99	3.99	3.99	3.99	3.72 / 3.99	3.42 / 3.82
	200	A193	3.76	3.76	3.76	3.76	3.76	3.75 / 3.76
	250	A252	3.40	3.40	3.40	3.40	3.40	3.40

Propped - Load/Span Table (Steel - 350N/mm²)

Span Type (Support Condition)	Slab Depth (mm)	Min Mesh Size	Gauge = 1.0 Total Applied Load (kN/m²) SLS					
			4.0	6.0	8.0	10.0	12.0	14.0
	130	A142	★	★	★	★	★	★
	140	A142	4.56 / 4.90	★	★	★	★	★
	150	A142	4.73 / 5.25	★ / 4.52	★	★	★	★
	160	A142	4.87 / 5.42	4.21 / 4.69	★ / 4.19	★	★	★
	175	A142	5.08 / 5.65	4.41 / 4.91	★ / 4.40	★ / 4.02	★	★
	200	A193	5.36 / 5.98	4.70 / 5.24	4.22 / 4.72	3.87 / 4.33	★ / 4.02	★
	250	A252	5.81 / 6.49	5.16 / 5.77	4.68 / 5.24	4.31 / 4.83	4.02 / 4.51	3.78 / 4.24
	200	A193	★	★	★	★	★	★
	250	A252	★	★	★	★	★	★

Notes:

Total applied load referred to in the above table is a working load based on factored combinations of live loads, finishes, ceilings, services and partitions, divided by a load factor of 1.60 (excluding slab self weight).

Figures in red are maximum permissible spans in situations where there is one stud per trough.

Permanent Support ▲   Temporary Support ⬆

Multideck 80-V2
Normal Weight Concrete Load Tables

Unpropped - Load/Span Table (Steel - 350N/mm²)

Span (m) (see diagram page 27)

Span Type (Support Condition)	Slab Depth (mm)	Min Mesh Size	Gauge = 1.1mm — Total Applied Load (kN/m²) SLS						Gauge = 1.2mm — Total Applied Load (kN/m²) SLS					
			4.0	6.0	8.0	10.0	12.0	14.0	4.0	6.0	8.0	10.0	12.0	14.0
(single span)	130	A142	4.13	3.93	3.86	3.43	3.11	2.87	4.22	3.95	3.90	3.53	3.21	2.96
	140	A142	4.03	4.03	4.03	3.63 / 3.99	3.30 / 3.63	3.04 / 3.34	4.11	4.11	4.11	3.75 / 4.08	3.40 / 3.71	3.14 / 3.42
	150	A142	3.93	3.93	3.93	3.83 / 3.93	3.47 / 3.83	3.20 / 3.53	4.02	4.02	4.02	3.95 / 4.02	3.59 / 3.92	3.31 / 3.61
	160	A142	3.85	3.85	3.85	3.85	3.64 / 3.85	3.36 / 3.70	3.93	3.93	3.93	3.93	3.77 / 3.93	3.47 / 3.80
	175	A142	3.74	3.74	3.74	3.74	3.74	3.58 / 3.74	3.82	3.82	3.82	3.82	3.82	3.70 / 3.82
	200	A193	3.58	3.58	3.58	3.58	3.58	3.58	3.66	3.66	3.66	3.66	3.66	3.66
	250	A252	3.27	3.27	3.27	3.27	3.27	3.27	3.37	3.37	3.37	3.37	3.37	3.37
(double span)	130	A142	4.55	4.50	3.86	3.43	3.11	2.87	4.55	4.55	3.98	3.53	3.21	2.96
	140	A142	4.68	4.68	4.09 / 4.44	3.63 / 3.99	3.30 / 3.63	3.04 / 3.34	4.90	4.90	4.22 / 4.53	3.75 / 4.08	3.40 / 3.71	3.14 / 3.42
	150	A142	4.54	4.54	4.31 / 4.54	3.83 / 4.21	3.47 / 3.83	3.20 / 3.53	4.81	4.81	4.45 / 4.73	3.95 / 4.31	3.59 / 3.92	3.31 / 3.61
	160	A142	4.42	4.42	4.42	4.01 / 4.42	3.64 / 4.02	3.36 / 3.70	4.68	4.68	4.67 / 4.68	4.15 / 4.53	3.77 / 4.12	3.47 / 3.80
	175	A142	4.25	4.25	4.25	4.25	3.88 / 4.25	3.58 / 3.95	4.50	4.50	4.50	4.43 / 4.50	4.02 / 4.40	3.70 / 4.06
	200	A193	4.01	4.01	4.01	4.01	4.01	3.92 / 4.01	4.24	4.24	4.24	4.24	4.24	4.06 / 4.24
	250	A252	3.62	3.62	3.62	3.62	3.62	3.62	3.84	3.84	3.84	3.84	3.84	3.84

Propped - Load/Span Table (Steel - 350N/mm²)

Span (m) (see diagram page 27)

Span Type (Support Condition)	Slab Depth (mm)	Min Mesh Size	Gauge = 1.1mm — Total Applied Load (kN/m²) SLS						Gauge = 1.2mm — Total Applied Load (kN/m²) SLS					
			4.0	6.0	8.0	10.0	12.0	14.0	4.0	6.0	8.0	10.0	12.0	14.0
(double span, temporary supports)	130	A142	★	★	★	★	★	★	★	★	★	★	★	★
	140	A142	4.76 / 4.90	★	★	★	★	★	★	★	★	★	★	★
	150	A142	4.93 / 5.25	★ / 4.67	★	★	★	★	5.08 / 5.25	★	★	★	★	★
	160	A142	5.08 / 5.59	★ / 4.84	★	★	★	★	5.24 / 5.60	★ / 4.95	★	★	★	★
	175	A142	5.29 / 5.84	4.60 / 5.08	★ / 4.55	★	★	★	5.47 / 5.97	4.75 / 5.20	★ / 4.66	★	★	★
	200	A193	5.59 / 6.18	4.90 / 5.42	4.41 / 4.88	4.04 / 4.47	★ / 4.15	★	5.78 / 6.33	5.07 / 5.56	4.57 / 5.01	★ / 4.59	★ / 4.26	★
	250	A252	6.06 / 6.71	5.38 / 5.96	4.89 / 5.42	4.51 / 5.00	4.20 / 4.66	3.95 / 4.36	6.27 / 6.89	5.58 / 6.13	5.07 / 5.57	4.67 / 5.14	4.35 / 4.79	4.09 / 4.51
(multiple temporary supports)	200	A193	★	★	★	★	★	★	★	★	★	★	★	★
	250	A252	★	★	★	★	★	★	★	★	★	★	★	★

Notes:

Total applied load referred to in the above table is a working load based on factored combinations of live loads, finishes, ceilings, services and partitions, divided by a load factor of 1.60 (excluding slab self weight).

Figures in red are maximum permissible spans in situations where there is one stud per trough.

Permanent Support ▲   Temporary Support ↑

Kingspan

Multideck 80-V2
Normal Weight Concrete Load Tables

Unpropped - Load/Span Table (Steel - 350N/mm²)

Span (m) (see diagram page 27)

Span Type (Support Condition)	Slab Depth (mm)	Min Mesh Size	Gauge = 1.0					
			Total Applied Load (kN/m²) SLS					
			4.0	6.0	8.0	10.0	12.0	14.0
	130	A142	4.03	3.90	3.70	3.28	2.98	2.75
	140	A142	3.93	3.93	3.92 / 3.93	3.48 / 3.86	3.16 / 3.51	2.91 / 3.24
	150	A142	3.84	3.84	3.84	3.66 / 3.84	3.32 / 3.70	3.06 / 3.41
	160	A142	3.75	3.75	3.75	3.75	3.49 / 3.75	3.21 / 3.58
	175	A142	3.65	3.65	3.65	3.65	3.65	3.42 / 3.65
	200	A193	3.45	3.45	3.45	3.45	3.45	3.45
	250	A252	3.16	3.16	3.16	3.16	3.16	3.16
	130	A142	4.53	4.31	3.70	3.28	2.98	2.75
	140	A142	4.39	4.39	3.92 / 4.29	3.48 / 3.86	3.16 / 3.51	2.91 / 3.24
	150	A142	4.26	4.26	4.13 / 4.26	3.66 / 4.08	3.32 / 3.70	3.06 / 3.41
	160	A142	4.15	4.15	4.15	3.84 / 4.15	3.49 / 3.89	3.21 / 3.58
	175	A142	3.99	3.99	3.99	3.99	3.72 / 3.99	3.42 / 3.82
	200	A193	3.76	3.76	3.76	3.76	3.76	3.75 / 3.76
	250	A252	3.40	3.40	3.40	3.40	3.40	3.40

Propped - Load/Span Table (Steel - 350N/mm²)

Span (m) (see diagram page 27)

Span Type (Support Condition)	Slab Depth (mm)	Min Mesh Size	Gauge = 1.0					
			Total Applied Load (kN/m²) SLS					
			4.0	6.0	8.0	10.0	12.0	14.0
	130	A142	★	★	★	★	★	★
	140	A142	4.56 / 4.90	★	★	★	★	★
	150	A142	4.73 / 5.25	★ / 4.52	★	★	★	★
	160	A142	4.87 / 5.42	4.21 / 4.69	★ / 4.19	★	★	★
	175	A142	5.08 / 5.65	4.41 / 4.91	★ / 4.40	★ / 4.02	★	★
	200	A193	5.36 / 5.98	4.70 / 5.24	4.22 / 4.72	3.87 / 4.33	★ / 4.02	★
	250	A252	5.81 / 6.49	5.16 / 5.77	4.68 / 5.24	4.31 / 4.83	4.02 / 4.51	3.78 / 4.24
	200	A193	★	★	★	★	★	★
	250	A252	★	★	★	★	★	★

Notes:

Total applied load referred to in the above table is a working load based on factored combinations of live loads, finishes, ceilings, services and partitions, divided by a load factor of 1.60 (excluding slab self weight).

Figures in red are maximum permissible spans in situations where there is one stud per trough.

Permanent Support ▲   Temporary Support ↑

Multideck 80-V2
Normal Weight Concrete Load Tables

Unpropped - Load/Span Table (Steel - 350N/mm²)

Span (m) (see diagram page 27)

Span Type (Support Condition)	Slab Depth (mm)	Min Mesh Size	Gauge = 1.1mm						Gauge = 1.2mm					
			Total Applied Load (kN/m²) SLS						Total Applied Load (kN/m²) SLS					
			4.0	6.0	8.0	10.0	12.0	14.0	4.0	6.0	8.0	10.0	12.0	14.0
	130	A142	4.13	3.93	3.86	3.43	3.11	2.87	4.22	3.95	3.90	3.53	3.21	2.96
	140	A142	4.03	4.03	4.03	3.63 / 3.99	3.30 / 3.63	3.04 / 3.34	4.11	4.11	4.11	3.75 / 4.08	3.40 / 3.71	3.14 / 3.42
	150	A142	3.93	3.93	3.93	3.83 / 3.93	3.47 / 3.83	3.20 / 3.53	4.02	4.02	4.02	3.95 / 4.02	3.59 / 3.92	3.31 / 3.61
	160	A142	3.85	3.85	3.85	3.85	3.64 / 3.85	3.36 / 3.70	3.93	3.93	3.93	3.93	3.77 / 3.93	3.47 / 3.80
	175	A142	3.74	3.74	3.74	3.74	3.74	3.58 / 3.74	3.82	3.82	3.82	3.82	3.82	3.70 / 3.82
	200	A193	3.58	3.58	3.58	3.58	3.58	3.58	3.66	3.66	3.66	3.66	3.66	3.66
	250	A252	3.27	3.27	3.27	3.27	3.27	3.27	3.37	3.37	3.37	3.37	3.37	3.37
	130	A142	4.55	4.50	3.86	3.43	3.11	2.87	4.55	4.55	3.98	3.53	3.21	2.96
	140	A142	4.68	4.68	4.09 / 4.44	3.63 / 3.99	3.30 / 3.63	3.04 / 3.34	4.90	4.90	4.22 / 4.53	3.75 / 4.08	3.40 / 3.71	3.14 / 3.42
	150	A142	4.54	4.54	4.31 / 4.54	3.83 / 4.21	3.47 / 3.83	3.20 / 3.53	4.81	4.81	4.45 / 4.73	3.95 / 4.31	3.59 / 3.92	3.31 / 3.61
	160	A142	4.42	4.42	4.42	4.01 / 4.42	3.64 / 4.02	3.36 / 3.70	4.68	4.68	4.67 / 4.68	4.15 / 4.53	3.77 / 4.12	3.47 / 3.80
	175	A142	4.25	4.25	4.25	4.25	3.88 / 4.25	3.58 / 3.95	4.50	4.50	4.50	4.43 / 4.50	4.02 / 4.40	3.70 / 4.06
	200	A193	4.01	4.01	4.01	4.01	4.01	3.92 / 4.01	4.24	4.24	4.24	4.24	4.24	4.06 / 4.24
	250	A252	3.62	3.62	3.62	3.62	3.62	3.62	3.84	3.84	3.84	3.84	3.84	3.84

Propped - Load/Span Table (Steel - 350N/mm²)

Span (m) (see diagram page 27)

Span Type (Support Condition)	Slab Depth (mm)	Min Mesh Size	Gauge = 1.1mm						Gauge = 1.2mm					
			Total Applied Load (kN/m²) SLS						Total Applied Load (kN/m²) SLS					
			4.0	6.0	8.0	10.0	12.0	14.0	4.0	6.0	8.0	10.0	12.0	14.0
	130	A142	★	★	★	★	★	★	★	★	★	★	★	★
	140	A142	4.76 / 4.90	★	★	★	★	★	★	★	★	★	★	★
	150	A142	4.93 / 5.25	4.67	★	★	★	★	5.08 / 5.25	★	★	★	★	★
	160	A142	5.08 / 5.59	4.84	★	★	★	★	5.24 / 5.60	4.95	★	★	★	★
	175	A142	5.29 / 5.84	4.60 / 5.08	4.55	★	★	★	5.47 / 5.97	4.75 / 5.20	4.66	★	★	★
	200	A193	5.59 / 6.18	4.90 / 5.42	4.41 / 4.88	4.04 / 4.47	4.15	★	5.78 / 6.33	5.07 / 5.56	4.57 / 5.01	4.59	4.26	★
	250	A252	6.06 / 6.71	5.38 / 5.96	4.89 / 5.42	4.51 / 5.00	4.20 / 4.66	3.95 / 4.36	6.27 / 6.89	5.58 / 6.13	5.07 / 5.57	4.67 / 5.14	4.35 / 4.79	4.09 / 4.51
	200	A193	★	★	★	★	★	★	★	★	★	★	★	★
	250	A252	★	★	★	★	★	★	★	★	★	★	★	★

Notes:

Total applied load referred to in the above table is a working load based on factored combinations of live loads, finishes, ceilings, services and partitions, divided by a load factor of 1.60 (excluding slab self weight).

Figures in red are maximum permissible spans in situations where there is one stud per trough.

Permanent Support ▲   Temporary Support ↑

Appendix C

Steel-Concrete Composite Columns

Domestic residence, hence $\qquad \psi_0 := 0.7 \qquad$ UK NA to BS EN 1990, Table NA.1.1

floor-floor height, $\qquad h := 3.2 \ m$

density of CLT, $\qquad \gamma_{CLT} := 4.8 \ \dfrac{kN}{m^3}$

wall panel thickness, (double panel) $\qquad t_{wall} := 256 \ mm$

$\qquad$ Hence, approx. edge load $\qquad \omega_{edge} := 1.1 \cdot t_{wall} \cdot h \cdot \gamma_{CLT} = 4.325 \ \dfrac{kN}{m}$

Dead Load from slab $\qquad d := 175 \ mm$

$$\gamma_{conc} := 24 \ \dfrac{kN}{m^3}$$

$$g_{k.slab} := \gamma_{conc} \cdot d = 4.2 \ \dfrac{kN}{m^2}$$

Services and finishes $\qquad g_{k.services} := 1.5 \ \dfrac{kN}{m^2}$

Permanent Load $\qquad g_k := g_{k.slab} + g_{k.services} = 5.7 \ \dfrac{kN}{m^2}$

Imposed Load $\qquad q_k := 1.5 \ \dfrac{kN}{m^2}$

$\xi := 0.925 \qquad \gamma_g := 1.35 \qquad \gamma_q := 1.5$

$\qquad$ working UDL $\qquad f_d := \xi \cdot \gamma_g \cdot g_k + \gamma_q \cdot q_k = 9.368 \ \dfrac{kN}{m^2}$

BASE STOREY

$$\alpha_n := \frac{2 + (5 \cdot \psi_0)}{7} = 0.786$$

Occupancy reduction, BS EN 1991-1, Clause 6.3.1.2(11)

(1) Corner Column

Catchment Area
$$A := 7.74 \ m^2$$

Beam span, north
$$l_N := 5.8 \ m$$

Beam span, east
$$l_E := 5.3 \ m$$

Slab supporting beam reaction
$$R_{d.slab} := \left(\frac{l_N}{2}\right) \cdot f_d \cdot \left(\frac{l_E}{2}\right) + \left(\frac{l_E}{2} \cdot \omega_{edge}\right) = 83.454 \ kN$$

Wall supporting beam reaction
$$R_{d.wall} := \left(\frac{l_N}{2} \cdot \omega_{edge}\right) = 12.544 \ kN$$

Design Axial Load
$$N_{Ed} := \alpha_n \cdot 7 \cdot f_d \cdot A = 398.79 \ kN$$

TRIAL SECTION: UC 152x152x30

$$h := 157.6 \ mm$$
$$t_w := 6.5 \ mm$$

$$N_{b.y.3.0} := 1150 \ kN \qquad N_{b.y.3.5} := 1080 \ kN$$
$$N_{b.z.3.0} := 714 \ kN \qquad N_{b.z.3.5} := 592 \ kN$$
$$M_{b.Rd.3.0} := 72.4 \ kN \cdot m \qquad M_{b.Rd.3.5} := 67.9 \ kN \cdot m$$
$$N_{pl.Rd} := 1360 \ kN$$

Interpolation (as L=3.2m):
$$N_{b.y.Rd} := N_{b.y.3.0} - 0.2 \cdot (N_{b.y.3.0} - N_{b.y.3.5}) = 1136 \ kN$$

$$N_{b.z.Rd} := N_{b.z.3.0} - 0.2 \cdot (N_{b.z.3.0} - N_{b.z.3.5}) = 689.6 \ kN$$

buckling:
$$M_{b.Rd} := M_{b.Rd.3.0} - 0.2 \cdot (M_{b.Rd.3.0} - M_{b.Rd.3.5}) = 71.5 \ kN \cdot m$$

$$\therefore n := \frac{N_{Ed}}{N_{pl.Rd}} = 0.293$$
check <0.25 (if breached, used reduced resistances)

$$M_{c.y.Rd} := 70.3 \ kN \cdot m$$
$$M_{c.z.Rd} := 39.4 \ kN \cdot m$$

$$M_{Rd} := min(M_{b.Rd}, M_{c.y.Rd}) = 70.3 \ kN \cdot m$$

I - orientation

$$M_{y.Ed} := R_{d.wall} \cdot \left(\frac{h}{2} + 100 \cdot mm \right) = 2.243 \ kN \cdot m$$

$$M_{z.Ed} := R_{d.slab} \cdot \left(\frac{t_w}{2} + 100 \cdot mm \right) = 8.617 \ kN \cdot m$$

Interaction (<1): $i := \dfrac{N_{Ed}}{N_{b.z.Rd}} + \dfrac{M_{y.Ed}}{M_{Rd}} + 1.5 \cdot \dfrac{M_{z.Ed}}{M_{c.z.Rd}} = 0.938$

$$\frac{N_{Ed}}{N_{b.z.Rd}} = 0.578 \qquad \frac{M_{y.Ed}}{M_{Rd}} = 0.032 \qquad \frac{M_{z.Ed}}{M_{c.z.Rd}} = 0.219$$

H - orientation

$$M_{y.Ed} := R_{d.slab} \cdot \left(\frac{h}{2} + 100 \cdot mm \right) = 14.922 \ kN \cdot m$$

$$M_{z.Ed} := R_{d.wall} \cdot \left(\frac{t_w}{2} + 100 \cdot mm \right) = 1.295 \ kN \cdot m$$

Interaction (<1): $i := \dfrac{N_{Ed}}{N_{b.z.Rd}} + \dfrac{M_{y.Ed}}{M_{Rd}} + 1.5 \cdot \dfrac{M_{z.Ed}}{M_{c.z.Rd}} = 0.84$

$$\frac{N_{Ed}}{N_{b.z.Rd}} = 0.578 \qquad \frac{M_{y.Ed}}{M_{Rd}} = 0.212 \qquad \frac{M_{z.Ed}}{M_{c.z.Rd}} = 0.033$$

(2) Edge (Stair) Column

Catchment Area $A := 14.76 \ m^2 \ A_W := 7.74 \ m^2 \ A_E := 7.02 \ m^2$

Beam span, west $l_W := 5.8 \ m$

Beam span, east $l_E := 6.72 \ m$

East slab supporting beam reaction
$$R_{d.east} := A_E \cdot f_d + \left(\frac{l_E}{2} \cdot \omega_{edge} \right) = 80.296 \ kN$$

West slab supporting beam reaction
$$R_{d.west} := A_W \cdot f_d + \left(\frac{l_W}{2} \cdot \omega_{edge} \right) = 85.051 \ kN$$

Design Axial Load $\qquad N_{Ed} := \alpha_n \cdot 7 \cdot f_d \cdot A = 760.484 \ kN$

TRIAL SECTION: UC 152x152x37

$$h := 161.8 \ mm$$
$$t_w := 8 \ mm$$

$$N_{b.y.3.0} := 1420 \ kN \qquad\qquad N_{b.y.3.5} := 1340 \ kN$$
$$N_{b.z.3.0} := 889 \ kN \qquad\qquad N_{b.z.3.5} := 738 \ kN$$
$$M_{b.Rd.3.0} := 93.1 \ kN \cdot m \qquad M_{b.Rd.3.5} := 88.4 \ kN \cdot m$$
$$N_{pl.Rd} := 1640 \ kN$$

Interpolation (as L=3.2m): $\quad N_{b.y.Rd} := N_{b.y.3.0} - 0.2 \cdot \left(N_{b.y.3.0} - N_{b.y.3.5} \right) = 1404 \ kN$

$$N_{b.z.Rd} := N_{b.z.3.0} - 0.2 \cdot \left(N_{b.z.3.0} - N_{b.z.3.5} \right) = 858.8 \ kN$$

buckling: $\qquad M_{b.Rd} := M_{b.Rd.3.0} - 0.2 \cdot \left(M_{b.Rd.3.0} - M_{b.Rd.3.5} \right) = 92.16 \ kN \cdot m$

$$\therefore n := \frac{N_{Ed}}{N_{pl.Rd}} = 0.464 \qquad$$ check <0.25 (if breached, used reduced resistances)

$$M_{c.y.Rd} := 62.5 \ kN \cdot m$$
$$M_{c.z.Rd} := 43.9 \ kN \cdot m$$

$$M_{Rd} := min \left(M_{b.Rd}, M_{c.y.Rd} \right) = 62.5 \ kN \cdot m$$

<u>I - orientation</u>

$$M_{y.Ed} := 0 \ kN \cdot m$$

$$M_{z.Ed} := \left| \left(R_{d.east} - R_{d.west} \right) \right| \cdot \left(\frac{t_w}{2} + 100 \cdot mm \right) = 0.495 \ kN \cdot m$$

Interaction (<1): $\quad i := \dfrac{N_{Ed}}{N_{b.z.Rd}} + \dfrac{M_{y.Ed}}{M_{Rd}} + 1.5 \cdot \dfrac{M_{z.Ed}}{M_{c.z.Rd}} = 0.902$

$$\frac{N_{Ed}}{N_{b.z.Rd}} = 0.886 \qquad \frac{M_{y.Ed}}{M_{Rd}} = 0 \qquad \frac{M_{z.Ed}}{M_{c.z.Rd}} = 0.011$$

<u>H - orientation</u>

$$M_{y.Ed} := \left| \left(R_{d.east} - R_{d.west} \right) \right| \cdot \left(\frac{h}{2} + 100 \cdot mm \right) = 0.86 \ kN \cdot m$$

$$M_{z.Ed} := 0 \ kN \cdot m$$

Interaction (<1): $i := \dfrac{N_{Ed}}{N_{b.z.Rd}} + \dfrac{M_{y.Ed}}{M_{Rd}} + 1.5 \cdot \dfrac{M_{z.Ed}}{M_{c.z.Rd}} = 0.899$

$$\dfrac{N_{Ed}}{N_{b.z.Rd}} = 0.886 \qquad \dfrac{M_{y.Ed}}{M_{Rd}} = 0.014 \qquad \dfrac{M_{z.Ed}}{M_{c.z.Rd}} = 0$$

(3) Internal Column

Catchment Area $A := 19.62 \ m^2 \qquad A_W := 15.49 \ m^2 \quad A_E := 4.13 \ m^2$

East slab supporting beam reaction $R_{d.east} := A_E \cdot f_d = 38.689 \ kN$

West slab supporting beam reaction $R_{d.west} := A_W \cdot f_d = 145.108 \ kN$

Design Axial Load $N_{Ed} := \alpha_n \cdot 7 \cdot f_d \cdot A = \left(1.011 \cdot 10^3\right) \ kN$

<mark>TRIAL SECTION: UC 203x203x46</mark>

$$h := 203.2 \ mm$$
$$t_w := 7.2 \ mm$$

$N_{b.y.3.0} := 1890 \ kN \qquad\qquad N_{b.y.3.5} := 1820 \ kN$
$N_{b.z.3.0} := 1430 \ kN \qquad\qquad N_{b.z.3.5} := 1260 \ kN$
$M_{b.Rd.3.0} := 158 \ kN \cdot m \qquad\quad M_{b.Rd.3.5} := 151 \ kN \cdot m$
$$N_{pl.Rd} := 2080 \ kN$$

Interpolation (as L=3.2m): $N_{b.y.Rd} := N_{b.y.3.0} - 0.2 \cdot \left(N_{b.y.3.0} - N_{b.y.3.5}\right) = 1876 \ kN$

$$N_{b.z.Rd} := N_{b.z.3.0} - 0.2 \cdot \left(N_{b.z.3.0} - N_{b.z.3.5}\right) = 1396 \ kN$$

buckling: $M_{b.Rd} := M_{b.Rd.3.0} - 0.2 \cdot \left(M_{b.Rd.3.0} - M_{b.Rd.3.5}\right) = 156.6 \ kN \cdot m$

$$\therefore n := \dfrac{N_{Ed}}{N_{pl.Rd}} = 0.486 \qquad \text{\color{red}{check <0.25 (if breached,}}$$
used reduced resistances)

$$M_{c.y.Rd} := 100 \ kN{\cdot}m$$
$$M_{c.z.Rd} := 72.2 \ kN \cdot m$$

$$M_{Rd} := min\left(M_{b.Rd}, M_{c.y.Rd}\right) = 100 \ kN \cdot m$$

I - orientation

$$M_{y.Ed} := 0 \ kN \cdot m$$

$$M_{z.Ed} := \left|\left(R_{d.east} - R_{d.west}\right)\right| \cdot \left(\frac{t_w}{2} + 100 \cdot mm\right) = 11.025 \ kN \cdot m$$

Interaction (<1): $i := \dfrac{N_{Ed}}{N_{b.z.Rd}} + \dfrac{M_{y.Ed}}{M_{Rd}} + 1.5 \cdot \dfrac{M_{z.Ed}}{M_{c.z.Rd}} = 0.953$

$$\dfrac{N_{Ed}}{N_{b.z.Rd}} = 0.724 \qquad \dfrac{M_{y.Ed}}{M_{Rd}} = 0 \qquad \dfrac{M_{z.Ed}}{M_{c.z.Rd}} = 0.153$$

H - orientation

$$M_{y.Ed} := \left|\left(R_{d.east} - R_{d.west}\right)\right| \cdot \left(\frac{h}{2} + 100 \cdot mm\right) = 21.454 \ kN \cdot m$$

$$M_{z.Ed} := 0 \ kN \cdot m$$

Interaction (<1): $i := \dfrac{N_{Ed}}{N_{b.z.Rd}} + \dfrac{M_{y.Ed}}{M_{Rd}} + 1.5 \cdot \dfrac{M_{z.Ed}}{M_{c.z.Rd}} = 0.939$

$$\dfrac{N_{Ed}}{N_{b.z.Rd}} = 0.724 \qquad \dfrac{M_{y.Ed}}{M_{Rd}} = 0.215 \qquad \dfrac{M_{z.Ed}}{M_{c.z.Rd}} = 0$$

(4) Edge (Clear) Column

Catchment Area	$A := 15.48 \ m^2$	
Beam span, north	$l_N := 5.8 \ m$	
		$N_{Ed} := 7 \cdot f_d \cdot A = \left(1.015 \cdot 10^3\right) \ kN$
Beam span, south	$l_S := 5.8 \ m$	

East slab supporting beam reaction $R_{d.east} := A \cdot f_d = 145.015 \ kN$

North wall supporting beam reaction $R_{d.north} := \left(\dfrac{l_N}{2} \cdot \omega_{edge}\right) = 12.544 \ kN$

South wall supporting beam reaction $R_{d.south} := \left(\dfrac{l_S}{2} \cdot \omega_{edge}\right) = 12.544 \ kN$

Design Axial Load $\qquad\qquad\qquad\qquad$ $N_{Ed} := \alpha_n \cdot 7 \cdot f_d \cdot A = 797.581 \ kN$

$h := 170.2 \ mm$

$t_w := 11 \ mm$

$N_{b.y.3.0} := 1990 \ kN \qquad\qquad N_{b.y.3.5} := 1880 \ kN$

$N_{b.z.3.0} := 1260 \ kN \qquad\qquad N_{b.z.3.5} := 1050 \ kN$

$M_{b.Rd.3.0} := 138 \ kN \cdot m \qquad\quad M_{b.Rd.3.5} := 133 \ kN \cdot m$

$N_{pl.Rd} := 2310 \ kN$

Interpolation (as L=3.2m): $\quad N_{b.y.Rd} := N_{b.y.3.0} - 0.2 \cdot \left(N_{b.y.3.0} - N_{b.y.3.5} \right) = 1968 \ kN$

$$N_{b.z.Rd} := N_{b.z.3.0} - 0.2 \cdot \left(N_{b.z.3.0} - N_{b.z.3.5} \right) = 1218 \ kN$$

buckling: $\quad M_{b.Rd} := M_{b.Rd.3.0} - 0.2 \cdot \left(M_{b.Rd.3.0} - M_{b.Rd.3.5} \right) = 137 \ kN \cdot m$

$$\therefore n := \frac{N_{Ed}}{N_{pl.Rd}} = 0.345 \qquad \text{check <0.25 (if breached,}$$
$$\text{used reduced resistances)}$$

$M_{c.y.Rd} := 106 \ kN \cdot m$

$M_{c.z.Rd} := 67.6 \ kN \cdot m$

$$M_{Rd} := min \left(M_{b.Rd}, M_{c.y.Rd} \right) = 106 \ kN \cdot m$$

<u>I - orientation</u>

$M_{y.Ed} := 0 \ kN \cdot m$

$$M_{z.Ed} := \left| R_{d.east} \right| \cdot \left(\frac{t_w}{2} + 100 \cdot mm \right) = 15.299 \ kN \cdot m$$

Interaction (<1): $\quad i := \dfrac{N_{Ed}}{N_{b.z.Rd}} + \dfrac{M_{y.Ed}}{M_{Rd}} + 1.5 \cdot \dfrac{M_{z.Ed}}{M_{c.z.Rd}} = 0.994$

$$\frac{N_{Ed}}{N_{b.z.Rd}} = 0.655 \qquad \frac{M_{y.Ed}}{M_{Rd}} = 0 \qquad \frac{M_{z.Ed}}{M_{c.z.Rd}} = 0.226$$

<u>H - orientation</u>

$$M_{y.Ed} := \left| R_{d.east} \right| \cdot \left(\frac{h}{2} + 100 \cdot mm \right) = 26.842 \ kN \cdot m$$

$$M_{z.Ed} := 0 \ kN \cdot m$$

Interaction (<1): $i := \dfrac{N_{Ed}}{N_{b.z.Rd}} + \dfrac{M_{y.Ed}}{M_{Rd}} + 1.5 \cdot \dfrac{M_{z.Ed}}{M_{c.z.Rd}} = 0.908$

$$\frac{N_{Ed}}{N_{b.z.Rd}} = 0.655 \qquad \frac{M_{y.Ed}}{M_{Rd}} = 0.253 \qquad \frac{M_{z.Ed}}{M_{c.z.Rd}} = 0$$

xxxxxxxxxxxxxxxxxxxxxxxxxxxxxxxxxxxxxxxxxxxxxxxxxxxxxxxxxxxxxxxxxxxxxxxxxxxxxxxxxx

<u>4th Floor Column</u>

$$\alpha_n := \frac{2 + \left(3 \cdot \psi_0 \right)}{5} = 0.82$$ Occupancy reduction

<u>(1) Corner Column</u>

Catchment Area $A := 7.74 \ m^2$

Beam span, north $l_N := 5.8 \ m$

Beam span, east $l_E := 5.3 \ m$

Slab supporting beam
reaction $R_{d.slab} := \left(\dfrac{l_N}{2} \right) \cdot f_d \cdot \left(\dfrac{l_E}{2} \right) + \left(\dfrac{l_E}{2} \cdot \omega_{edge} \right) = 83.454 \ kN$

Wall supporting beam
reaction $R_{d.wall} := \left(\dfrac{l_N}{2} \cdot \omega_{edge} \right) = 12.544 \ kN$

Design Axial Load $N_{Ed} := \alpha_n \cdot 4 \cdot f_d \cdot A = 237.824 \ kN$

$$h := 157.6 \ mm$$
$$t_w := 6.5 \ mm$$

$$N_{b.y.3.0} := 1150 \ kN \qquad N_{b.y.3.5} := 1080 \ kN$$
$$N_{b.z.3.0} := 714 \ kN \qquad N_{b.z.3.5} := 592 \ kN$$
$$M_{b.Rd.3.0} := 72.4 \ kN \cdot m \qquad M_{b.Rd.3.5} := 67.9 \ kN \cdot m$$
$$N_{pl.Rd} := 1360 \ kN$$

Interpolation (as L=3.2m): $\quad N_{b.y.Rd} := N_{b.y.3.0} - 0.2 \cdot \left(N_{b.y.3.0} - N_{b.y.3.5} \right) = 1136 \ kN$

$$N_{b.z.Rd} := N_{b.z.3.0} - 0.2 \cdot \left(N_{b.z.3.0} - N_{b.z.3.5} \right) = 689.6 \ kN$$

buckling: $\quad M_{b.Rd} := M_{b.Rd.3.0} - 0.2 \cdot \left(M_{b.Rd.3.0} - M_{b.Rd.3.5} \right) = 71.5 \ kN \cdot m$

$$\therefore n := \frac{N_{Ed}}{N_{pl.Rd}} = 0.175 \qquad$$ check <0.25 (if breached,
used reduced resistances)

$$M_{c.y.Rd} := 87.9 \ kN \cdot m$$
$$M_{c.z.Rd} := 39.6 \ kN \cdot m$$

$$M_{Rd} := min \left(M_{b.Rd}, M_{c.y.Rd} \right) = 71.5 \ kN \cdot m$$

I - orientation

$$M_{y.Ed} := R_{d.wall} \cdot \left(\frac{h}{2} + 100 \cdot mm \right) = 2.243 \ kN \cdot m$$
$$M_{z.Ed} := R_{d.slab} \cdot \left(\frac{t_w}{2} + 100 \cdot mm \right) = 8.617 \ kN \cdot m$$

Interaction (<1): $\quad i := \dfrac{N_{Ed}}{N_{b.z.Rd}} + \dfrac{M_{y.Ed}}{M_{Rd}} + 1.5 \cdot \dfrac{M_{z.Ed}}{M_{c.z.Rd}} = 0.703$

$$\frac{N_{Ed}}{N_{b.z.Rd}} = 0.345 \qquad \frac{M_{y.Ed}}{M_{Rd}} = 0.031 \qquad \frac{M_{z.Ed}}{M_{c.z.Rd}} = 0.218$$

H - orientation

$$M_{y.Ed} := R_{d.slab} \cdot \left(\frac{h}{2} + 100 \cdot mm \right) = 14.922 \ kN \cdot m$$
$$M_{z.Ed} := R_{d.wall} \cdot \left(\frac{t_w}{2} + 100 \cdot mm \right) = 1.295 \ kN \cdot m$$

Interaction (<1): $\quad i := \dfrac{N_{Ed}}{N_{b.z.Rd}} + \dfrac{M_{y.Ed}}{M_{Rd}} + 1.5 \cdot \dfrac{M_{z.Ed}}{M_{c.z.Rd}} = 0.603$

$$\dfrac{N_{Ed}}{N_{b.z.Rd}} = 0.345 \qquad \dfrac{M_{y.Ed}}{M_{Rd}} = 0.209 \qquad \dfrac{M_{z.Ed}}{M_{c.z.Rd}} = 0.033$$

(2) Edge (Stair) Column

Catchment Area $\qquad\qquad\qquad A := 14.76 \ m^2 \ \ A_W := 7.74 \ m^2 \ \ A_E := 7.02 \ m^2$

Beam span, west $\qquad\qquad\qquad l_W := 5.8 \ m$

Beam span, east $\qquad\qquad\qquad l_E := 6.72 \ m$

East slab supporting beam reaction $\qquad R_{d.east} := A_E \cdot f_d + \left(\dfrac{l_E}{2} \cdot \omega_{edge} \right) = 80.296 \ kN$

West slab supporting beam reaction $\qquad R_{d.west} := A_W \cdot f_d + \left(\dfrac{l_W}{2} \cdot \omega_{edge} \right) = 85.051 \ kN$

Design Axial Load $\qquad\qquad\qquad N_{Ed} := \alpha_n \cdot 4 \cdot f_d \cdot A = 453.525 \ kN$

==TRIAL SECTION: UC 152x152x23==

$$h := 152.4 \ mm$$
$$t_w := 5.8 \ mm$$

$N_{b.y.3.0} := 867 \ kN \qquad\qquad N_{b.y.3.5} := 812 \ kN$
$N_{b.z.3.0} := 524 \ kN \qquad\qquad N_{b.z.3.5} := 431 \ kN$
$M_{b.Rd.3.0} := 47.3 \ kN \cdot m \qquad M_{b.Rd.3.5} := 43.9 \ kN \cdot m$
$\qquad\qquad N_{pl.Rd} := 1040 \ kN$

Interpolation (as L=3.2m): $\quad N_{b.y.Rd} := N_{b.y.3.0} - 0.2 \cdot \left(N_{b.y.3.0} - N_{b.y.3.5} \right) = 856 \ kN$

$$N_{b.z.Rd} := N_{b.z.3.0} - 0.2 \cdot \left(N_{b.z.3.0} - N_{b.z.3.5} \right) = 505.4 \ kN$$

buckling: $\quad M_{b.Rd} := M_{b.Rd.3.0} - 0.2 \cdot \left(M_{b.Rd.3.0} - M_{b.Rd.3.5} \right) = 46.62 \ kN \cdot m$

$$\therefore n := \dfrac{N_{Ed}}{N_{pl.Rd}} = 0.436 \qquad \text{\color{red}{check <0.25 (if breached, used reduced resistances)}}$$

$M_{c.y.Rd} := 58.2 \ kN{\cdot}m$

$$M_{c.z.Rd} := 18.7 \ kN \cdot m$$

$$M_{Rd} := min \left(M_{b.Rd}, M_{c.y.Rd} \right) = 46.62 \ kN \cdot m$$

I - orientation

$$M_{y.Ed} := 0 \ kN \cdot m$$

$$M_{z.Ed} := \left| \left(R_{d.east} - R_{d.west} \right) \right| \cdot \left(\frac{t_w}{2} + 100 \cdot mm \right) = 0.489 \ kN \cdot m$$

Interaction (<1): $i := \dfrac{N_{Ed}}{N_{b.z.Rd}} + \dfrac{M_{y.Ed}}{M_{Rd}} + 1.5 \cdot \dfrac{M_{z.Ed}}{M_{c.z.Rd}} = 0.937$

$$\frac{N_{Ed}}{N_{b.z.Rd}} = 0.897 \qquad \frac{M_{y.Ed}}{M_{Rd}} = 0 \qquad \frac{M_{z.Ed}}{M_{c.z.Rd}} = 0.026$$

H - orientation

$$M_{y.Ed} := \left| \left(R_{d.east} - R_{d.west} \right) \right| \cdot \left(\frac{h}{2} + 100 \cdot mm \right) = 0.838 \ kN \cdot m$$

$$M_{z.Ed} := 0 \ kN \cdot m$$

Interaction (<1): $i := \dfrac{N_{Ed}}{N_{b.z.Rd}} + \dfrac{M_{y.Ed}}{M_{Rd}} + 1.5 \cdot \dfrac{M_{z.Ed}}{M_{c.z.Rd}} = 0.915$

$$\frac{N_{Ed}}{N_{b.z.Rd}} = 0.897 \qquad \frac{M_{y.Ed}}{M_{Rd}} = 0.018 \qquad \frac{M_{z.Ed}}{M_{c.z.Rd}} = 0$$

(3) Internal Column

Catchment Area $A := 19.62 \ m^2 \qquad A_W := 15.49 \ m^2 \quad A_E := 4.13 \ m^2$

East slab supporting beam reaction $R_{d.east} := A_E \cdot f_d = 38.689 \ kN$

West slab supporting beam reaction $R_{d.west} := A_W \cdot f_d = 145.108 \ kN$

Design Axial Load $N_{Ed} := \alpha_n \cdot 4 \cdot f_d \cdot A = 602.856 \ kN$

$$h := 161.8 \ mm$$
$$t_w := 8 \ mm$$

$$N_{b.y.3.0} := 1420 \ kN \qquad N_{b.y.3.5} := 1340 \ kN$$
$$N_{b.z.3.0} := 889 \ kN \qquad N_{b.z.3.5} := 738 \ kN$$
$$M_{b.Rd.3.0} := 93.1 \ kN \cdot m \qquad M_{b.Rd.3.5} := 88.4 \ kN \cdot m$$
$$N_{pl.Rd} := 1670 \ kN$$

Interpolation (as L=3.2m): $N_{b.y.Rd} := N_{b.y.3.0} - 0.2 \cdot \left(N_{b.y.3.0} - N_{b.y.3.5} \right) = 1404 \ kN$

$$N_{b.z.Rd} := N_{b.z.3.0} - 0.2 \cdot \left(N_{b.z.3.0} - N_{b.z.3.5} \right) = 858.8 \ kN$$

buckling: $M_{b.Rd} := M_{b.Rd.3.0} - 0.2 \cdot \left(M_{b.Rd.3.0} - M_{b.Rd.3.5} \right) = 92.16 \ kN \cdot m$

$$\therefore n := \frac{N_{Ed}}{N_{pl.Rd}} = 0.361 \qquad$$ check <0.25 (if breached, used reduced resistances)

$$M_{c.y.Rd} := 75 \ kN \cdot m$$
$$M_{c.z.Rd} := 47.5 \ kN \cdot m$$

$$M_{Rd} := min \left(M_{b.Rd}, M_{c.y.Rd} \right) = 75 \ kN \cdot m$$

I - orientation

$$M_{y.Ed} := 0 \ kN \cdot m$$

$$M_{z.Ed} := \left| \left(R_{d.east} - R_{d.west} \right) \right| \cdot \left(\frac{t_w}{2} + 100 \cdot mm \right) = 11.068 \ kN \cdot m$$

Interaction (<1): $i := \dfrac{N_{Ed}}{N_{b.z.Rd}} + \dfrac{M_{y.Ed}}{M_{Rd}} + 1.5 \cdot \dfrac{M_{z.Ed}}{M_{c.z.Rd}} = 1.051$

$$\frac{N_{Ed}}{N_{b.z.Rd}} = 0.702 \qquad \frac{M_{y.Ed}}{M_{Rd}} = 0 \qquad \frac{M_{z.Ed}}{M_{c.z.Rd}} = 0.233$$

H - orientation

$$M_{y.Ed} := \left| \left(R_{d.east} - R_{d.west} \right) \right| \cdot \left(\frac{h}{2} + 100 \cdot mm \right) = 19.251 \ kN \cdot m$$

$$M_{z.Ed} := 0 \ kN \cdot m$$

Interaction (<1): $i := \dfrac{N_{Ed}}{\ } + \dfrac{M_{y.Ed}}{\ } + 1.5 \cdot \dfrac{M_{z.Ed}}{\ } = 0.959$

$$\frac{N_{Ed}}{N_{b.z.Rd}} = 0.702 \qquad \frac{M_{y.Ed}}{M_{Rd}} = 0.257 \qquad \frac{M_{z.Ed}}{M_{c.z.Rd}} = 0$$

(4) Edge (Clear) Column

Catchment Area $\qquad\qquad A := 15.48 \ m^2$

Beam span, north $\qquad\qquad l_N := 5.8 \ m$

Beam span, south $\qquad\qquad l_S := 5.8 \ m$

East slab supporting beam reaction $\qquad R_{d.east} := A \cdot f_d = 145.015 \ kN$

North wall supporting beam reaction $\qquad R_{d.north} := \left(\frac{l_N}{2} \cdot \omega_{edge} \right) = 12.544 \ kN$

South wall supporting beam reaction $\qquad R_{d.south} := \left(\frac{l_S}{2} \cdot \omega_{edge} \right) = 12.544 \ kN$

Design Axial Load $\qquad\qquad N_{Ed} := \alpha_n \cdot 4 \cdot f_d \cdot A = 475.648 \ kN$

TRIAL SECTION: UC 152x152x37

$$h := 161.8 \ mm$$
$$t_w := 8 \ mm$$

$N_{b.y.3.0} := 1420 \ kN \qquad\qquad N_{b.y.3.5} := 1340 \ kN$
$N_{b.z.3.0} := 889 \ kN \qquad\qquad N_{b.z.3.5} := 738 \ kN$
$M_{b.Rd.3.0} := 93.1 \ kN \cdot m \qquad M_{b.Rd.3.5} := 88.4 \ kN \cdot m$
$N_{pl.Rd} := 1670 \ kN$

Interpolation (as L=3.2m): $\quad N_{b.y.Rd} := N_{b.y.3.0} - 0.2 \cdot \left(N_{b.y.3.0} - N_{b.y.3.5} \right) = 1404 \ kN$

$$N_{b.z.Rd} := N_{b.z.3.0} - 0.2 \cdot \left(N_{b.z.3.0} - N_{b.z.3.5} \right) = 858.8 \ kN$$

buckling: $\quad M_{b.Rd} := M_{b.Rd.3.0} - 0.2 \cdot \left(M_{b.Rd.3.0} - M_{b.Rd.3.5} \right) = 92.16 \ kN \cdot m$

$$\therefore n := \frac{N_{Ed}}{N_{pl.Rd}} = 0.285 \qquad \text{\textcolor{red}{check <0.25 (if breached, used reduced resistances)}}$$

$$M_{c.y.Rd} := 87.5 \ kN \cdot m$$
$$M_{c.z.Rd} := 49.3 \ kN \cdot m$$

$$M_{Rd} := min\left(M_{b.Rd}, M_{c.y.Rd}\right) = 87.5 \ kN \cdot m$$

I - orientation

$$M_{y.Ed} := 0 \ kN \cdot m$$

$$M_{z.Ed} := \left|R_{d.east}\right| \cdot \left(\frac{t_w}{2} + 100 \cdot mm\right) = 15.082 \ kN \cdot m$$

Interaction (<1): $i := \dfrac{N_{Ed}}{N_{b.z.Rd}} + \dfrac{M_{y.Ed}}{M_{Rd}} + 1.5 \cdot \dfrac{M_{z.Ed}}{M_{c.z.Rd}} = 1.013$

$$\frac{N_{Ed}}{N_{b.z.Rd}} = 0.554 \qquad \frac{M_{y.Ed}}{M_{Rd}} = 0 \qquad \frac{M_{z.Ed}}{M_{c.z.Rd}} = 0.306$$

H - orientation

$$M_{y.Ed} := \left|R_{d.east}\right| \cdot \left(\frac{h}{2} + 100 \cdot mm\right) = 26.233 \ kN \cdot m$$

$$M_{z.Ed} := 0 \ kN \cdot m$$

Interaction (<1): $i := \dfrac{N_{Ed}}{N_{b.z.Rd}} + \dfrac{M_{y.Ed}}{M_{Rd}} + 1.5 \cdot \dfrac{M_{z.Ed}}{M_{c.z.Rd}} = 0.854$

$$\frac{N_{Ed}}{N_{b.z.Rd}} = 0.554 \qquad \frac{M_{y.Ed}}{M_{Rd}} = 0.3 \qquad \frac{M_{z.Ed}}{M_{c.z.Rd}} = 0$$

Appendix D

Timber-Steel Beams

Domestic residence, hence $\qquad \psi_0 := 0.7 \qquad$ UK NA to BS EN 1990, Table NA.1.1

floor-floor height, $\qquad h_{storey} := 3 \; m$

density of CLT, $\qquad \gamma_{CLT} := 4.8 \; \dfrac{kN}{m^3}$

wall panel thickness, (double panel) $\qquad t_{wall} := 256 \; mm$

Hence, approx. edge load $\qquad \omega_{edge} := 1.1 \cdot t_{wall} \cdot h_{storey} \cdot \gamma_{CLT} = 4.055 \; \dfrac{kN}{m}$

Dead Load from slab $\qquad d := 200 \; mm$

$$g_{k.slab} := \gamma_{CLT} \cdot d = 0.96 \; \dfrac{kN}{m^2}$$

Services and finishes $\qquad g_{k.services} := 1.5 \; \dfrac{kN}{m^2}$

Permanent Load $\qquad g_k := g_{k.slab} + g_{k.services} = 2.46 \; \dfrac{kN}{m^2}$

Imposed Load $\qquad q_k := 1.5 \; \dfrac{kN}{m^2} \qquad\qquad g_k + q_k = 3.96 \; \dfrac{kN}{m^2}$

$\xi := 0.925 \qquad \gamma_g := 1.35 \qquad \gamma_q := 1.5$

working UDL $\qquad f_d := \xi \cdot \gamma_g \cdot g_k + \gamma_q \cdot q_k = 5.322 \; \dfrac{kN}{m^2}$

Construction

$q_c := 0.75 \; \dfrac{kN}{m^2} \qquad$ personnel + small equipment

$g_c := g_{k.slab} = 0.96 \; \dfrac{kN}{m^2} \qquad$ slab units

$ASB249:=0$
$ASB196:=1$
$ASB185:=2$
$ASB155:=3$
$ASB153:=4$
$ASB136:=5$
$ASB124:=6$
$ASB105:=7$
$ASB100:=8$
$ASB74:=9$
$ASBhyp:=10$

W $\left(\dfrac{kg}{m}\right)$	h (mm)	b_t (mm)	b_b (mm)	t_w (mm)	t_f (mm)	r (mm)
249	342	203	313	40	40	27
196	342	183	293	20	40	27
185	320	195	305	32	29	27
155	326	179	289	16	32	27
153	310	190	300	27	24	27
136	288	190	300	25	22	24
124	296	178	288	13	26	24
105	288	176	286	11	22	24
100	276	184	294	19	16	24
73.6	272	175	285	10	14	24
50.9	240	150	240	7.5	12	8.9

I_{yy} $\left(cm^4\right)$	I_{zz} $\left(cm^4\right)$	k_y (cm)	k_z (cm)	$W_{el.y}$ $\left(cm^3\right)$	z_e (cm)	z_p (cm)	$W_{pl.y}$ $\left(cm^3\right)$	$W_{pl.z}$ $\left(cm^3\right)$	U	X	I_w $\left((0.1\,m)^6\right)$	I_T $\left(cm^4\right)$	A $\left(cm^2\right)$
52900	13200	12.9	6.4	2760	19.2	22.6	3760	1510	0.82	6.8	2	2000	318
45900	10500	13.6	6.48	2320	19.8	28.1	3060	1230	0.84	7.86	1.5	1180	249
35700	8750	12.3	6.1	1980	18	21	2660	1030	0.82	8.56	1.2	871	235
34500	7990	13.2	6.35	1830	18.9	27.3	2360	950	0.84	9.4	1.07	620	198
28400	6840	12.1	5.93	1630	17.4	20.4	2160	817	0.82	9.97	0.895	513	195
22200	6260	11.3	6	1370	16.3	19.2	1810	741	0.81	10.2	0.71	379	174
23500	6410	12.2	6.37	1360	17.3	25.7	1730	761	0.83	10.5	0.721	332	158
19200	5300	12	6.3	1150	16.8	25.3	1440	633	0.83	12.1	0.574	207	133
15500	4250	11	5.76	995	15.6	18.4	1290	511	0.81	13.2	0.451	160	128
12200	3330	11.4	5.96	776	15.7	21.3	978	403	0.83	16.7	0.338	72	93.7
6591	1721	10.1	5.16	470	14	18.8	590				0.156	26	64.8

$E:=210\ GPa \qquad G:=81\ GPa \qquad f_y:=355\ MPa$

$\gamma_{M0}:=1.0 \qquad \gamma_{M1}:=1.0$

Beam Type 1

Beam span $\qquad L := 5.34 \ m$

Beam spacing $\qquad s := 5.8 \ m$

$$beam := ASBhyp = 10$$

$$W_{beam} := \mathrm{submatrix}\,(W, beam, beam, 0, 0) = [50.9] \ \frac{kg}{m}$$
$$h_{beam} := \mathrm{submatrix}\,(h, beam, beam, 0, 0) = [0.24] \ m$$
$$b_{t.beam} := \mathrm{submatrix}\,(b_t, beam, beam, 0, 0) = [150] \ mm$$
$$b_{b.beam} := \mathrm{submatrix}\,(b_b, beam, beam, 0, 0) = [240] \ mm$$
$$t_{w.beam} := \mathrm{submatrix}\,(t_w, beam, beam, 0, 0) = [7.5] \ mm$$
$$t_{f.beam} := \mathrm{submatrix}\,(t_f, beam, beam, 0, 0) = [12] \ mm$$
$$r_{beam} := \mathrm{submatrix}\,(r, beam, beam, 0, 0) = [8.9] \ mm$$
$$I_{yy.beam} := \mathrm{submatrix}\,(I_{yy}, beam, beam, 0, 0) = [6.591 \cdot 10^{-5}] \ m^4$$
$$I_{zz.beam} := \mathrm{submatrix}\,(I_{zz}, beam, beam, 0, 0) = [1.721 \cdot 10^{-5}] \ m^4$$
$$k_{y.beam} := \mathrm{submatrix}\,(k_y, beam, beam, 0, 0) = [0.101] \ m$$

$$k_{z.beam} := \mathrm{submatrix}\,(k_z, beam, beam, 0, 0) = [0.052] \ m$$
$$W_{el.y.beam} := \mathrm{submatrix}\,(W_{el.y}, beam, beam, 0, 0) = [470] \ cm^3$$
$$z_{e.beam} := \mathrm{submatrix}\,(z_e, beam, beam, 0, 0) = [0.14] \ m$$
$$z_{p.beam} := \mathrm{submatrix}\,(z_p, beam, beam, 0, 0) = [0.188] \ m$$
$$W_{pl.y.beam} := \mathrm{submatrix}\,(W_{pl.y}, beam, beam, 0, 0) = [590] \ cm^3$$
$$W_{pl.z.beam} := \mathrm{submatrix}\,(W_{pl.z}, \boxed{beam}, beam, 0, 0) = ? \ cm^3$$
$$U_{beam} := \mathrm{submatrix}\,(U, \boxed{beam}, beam, 0, 0) = ?$$
$$X_{beam} := \mathrm{submatrix}\,(X, \boxed{beam}, beam, 0, 0) = ?$$
$$I_{w.beam} := \mathrm{submatrix}\,(I_w, beam, beam, 0, 0) = [1.56 \cdot 10^{-7}] \ m^6$$
$$I_{T.beam} := \mathrm{submatrix}\,(I_T, beam, beam, 0, 0) = [2.6 \cdot 10^{-7}] \ m^4$$
$$A_{beam} := \mathrm{submatrix}\,(A, beam, beam, 0, 0) = [64.8] \ cm^2$$

Construction Cases - Torsion effects

$$f_{d.c1} := \left(\gamma_g \cdot g_c + \gamma_q \cdot q_c\right) \cdot \frac{s}{2} + \left(\gamma_g \cdot g \cdot W_{beam}\right) = \left[7.695\right] \frac{kN}{m} \qquad \text{CLT + const : 0}$$

$$f_{d.c2} := \left(\gamma_g \cdot g_c \cdot s\right) + \left(\gamma_q \cdot q_c \cdot \frac{s}{2}\right) + \left(\gamma_g \cdot g \cdot W_{beam}\right) = \left[11.453\right] \frac{kN}{m} \quad \text{CLT + const : CLT}$$

$$f_{d.c3} := \left(\gamma_g \cdot g_c + \gamma_q \cdot q_c\right) \cdot s + g \cdot W_{beam} = \left[14.541\right] \frac{kN}{m} \qquad \text{CLT + const : CLT + const}$$

$$M_{y.Ed1} := f_{d.c1} \cdot \frac{L^2}{8} = \left[27.428\right] kN \cdot m \qquad\qquad V_{Ed.1} := f_{d.c1} \cdot \frac{L}{2} = \left[20.545\right] kN$$

$$M_{y.Ed2} := f_{d.c2} \cdot \frac{L^2}{8} = \left[40.824\right] kN \cdot m \qquad\qquad V_{Ed.2} := f_{d.c2} \cdot \frac{L}{2} = \left[30.58\right] kN$$

$$M_{y.Ed3} := f_{d.c3} \cdot \frac{L^2}{8} = \left[51.831\right] kN \cdot m \qquad\qquad V_{Ed.3} := f_{d.c3} \cdot \frac{L}{2} = \left[38.824\right] kN$$

Assume bearing zone reduced to 40mm on side 1 (allowance for tolerance of unit length and placement), nominal of 80mm on side 2.

$$e_1 := \frac{b_{b.beam}}{2} - 20 \ mm = \left[0.1\right] m \qquad\qquad e_2 := \frac{b_{b.beam}}{2} - 40 \ mm = \left[0.08\right] m$$

$$T_{p.1} := \gamma_g \cdot g_c \cdot \frac{s}{2} \cdot e_1 \cdot L = \left[2.007\right] kN \cdot m \qquad T_{p.2} := -\gamma_g \cdot g_c \cdot \frac{s}{2} \cdot e_2 \cdot L = \left[-1.606\right] kN \cdot m$$

$$T_{c.1} := \gamma_q \cdot q_c \cdot \frac{s}{2} \cdot e_1 \cdot L = \left[1.742\right] kN \cdot m \qquad T_{c.2} := -\gamma_q \cdot q_c \cdot \frac{s}{2} \cdot e_2 \cdot L = \left[-1.394\right] kN \cdot m$$

$$T_{d.1} := T_{p.1} + T_{c.1} = \left[3.749\right] kN \cdot m$$

$$T_{d.2} := T_{p.1} + T_{c.1} + T_{p.2} = \left[2.144\right] kN \cdot m$$

$$T_{d.3} := T_{p.1} + T_{c.1} + T_{p.2} + T_{c.2} = \left[0.75\right] kN \cdot m$$

$$a := \sqrt{\frac{E \cdot I_{w.beam}}{G \cdot I_{T.beam}}} = 1.247 \ m \qquad\qquad \frac{L}{a} = 4.282 \qquad\qquad x := \frac{L}{2}$$

$$\phi_1 := \frac{T_{d.1} \cdot a^2}{G \cdot I_{T.beam} \cdot L} \left(\frac{\left(x \cdot L - x^2\right)}{2 \, a^2} + \cosh\left(\frac{x}{a}\right) - \tanh\left(\frac{L}{2 \, a}\right) \sinh\left(\frac{x}{a}\right) - 1 \right) = 0.079 \; \boldsymbol{rad}$$

$$\phi_1 = 4.526 \; °$$

$$\phi''_1 := \frac{T_{d.1}}{G \cdot I_{T.beam} \cdot L} \left(-1 + \cosh\left(\frac{x}{a}\right) - \tanh\left(\frac{L}{2 \, a}\right) \sinh\left(\frac{x}{a}\right) \right) = -0.026 \; \frac{1}{\boldsymbol{m}^2}$$

$$M_{w.1.Ed} := \frac{E \cdot I_{w.beam} \cdot \phi''_1}{h_{beam} - t_{f.beam}} = -3.679 \; \boldsymbol{kN \cdot m}$$

$$\phi_2 := \frac{T_{d.2} \cdot a^2}{G \cdot I_{T.beam} \cdot L} \left(\frac{\left(x \cdot L - x^2\right)}{2 \, a^2} + \cosh\left(\frac{x}{a}\right) - \tanh\left(\frac{L}{2 \, a}\right) \sinh\left(\frac{x}{a}\right) - 1 \right) = 0.045 \; \boldsymbol{rad}$$

$$\phi_2 = 2.588 \; °$$

$$\phi''_2 := \frac{T_{d.2}}{G \cdot I_{T.beam} \cdot L} \left(-1 + \cosh\left(\frac{x}{a}\right) - \tanh\left(\frac{L}{2 \, a}\right) \sinh\left(\frac{x}{a}\right) \right) = -0.015 \; \frac{1}{\boldsymbol{m}^2}$$

$$M_{w.2.Ed} := \frac{E \cdot I_{w.beam} \cdot \phi''_2}{h_{beam} - t_{f.beam}} = -2.104 \; \boldsymbol{kN \cdot m}$$

$$\phi_3 := \frac{T_{d.3} \cdot a^2}{G \cdot I_{T.beam} \cdot L} \left(\frac{\left(x \cdot L - x^2\right)}{2 \, a^2} + \cosh\left(\frac{x}{a}\right) - \tanh\left(\frac{L}{2 \, a}\right) \sinh\left(\frac{x}{a}\right) - 1 \right) = 0.016 \; \boldsymbol{rad}$$

$$\phi_3 = 0.905 \; °$$

$$\phi''_3 := \frac{T_{d.3}}{G \cdot I_{T.beam} \cdot L} \left(-1 + \cosh\left(\frac{x}{a}\right) - \tanh\left(\frac{L}{2 \, a}\right) \sinh\left(\frac{x}{a}\right) \right) = -0.005 \; \frac{1}{\boldsymbol{m}^2}$$

$$M_{w.3.Ed} := \frac{E \cdot I_{w.beam} \cdot \phi''_3}{h_{beam} - t_{f.beam}} = -0.736 \; \boldsymbol{kN \cdot m}$$

Cross Section Resistance

Bending Resistance about major axis

$$M_{y.Rd} := \frac{W_{pl.y.beam} \cdot f_y}{\gamma_{M0}} = [209.45] \ kN \cdot m$$

$$M_{y.Ed} := \max\left(M_{y.Ed1}, M_{y.Ed2}, M_{y.Ed3}\right) = 51.831 \ kN \cdot m$$

$$M_{y.Rd} > M_{y.Ed}$$

Warping Resistance of top flange

$$W_{pl.z.tf} := \frac{t_{f.beam} \cdot b_{t.beam}^2}{4} = 67.5 \ cm^3$$

$$M_{w.Rd} := \frac{W_{pl.z.tf} \cdot f_y}{\gamma_{M0}} = 23.963 \ kN \cdot m$$

$$M_{w.Ed} := \max\left(\left|M_{w.1.Ed}\right|, \left|M_{w.2.Ed}\right|, \left|M_{w.3.Ed}\right|\right) = 3.679 \ kN \cdot m$$

$$M_{w.Rd} > M_{w.Ed}$$

Plastic Interaction Criterion

$$\left(\frac{M_{y.Ed}}{M_{y.Rd}}\right)^2 + \frac{M_{w.Ed}}{M_{w.Rd}} = [0.215] \qquad < 1 \text{ therefore OK}$$

Shear Resistance

Plastic Shear resistance (without torsion)

$$A_V := A_{beam} - \left(b_{t.beam} \cdot t_{f.beam}\right) - \left(b_{b.beam} \cdot t_{f.beam}\right) + \left(t_{w.beam} + 2 \ r_{beam}\right) t_{f.beam} = [21.036] \ cm^2$$

$$V_{pl.Rd} := \frac{\left(A_V \cdot f_y\right)}{\gamma_{M0} \cdot \sqrt{3}} = [431.152] \ kN$$

Reduced shear resistance in presence of torsion is not thought to be limiting, and is therefore not considered

Lateral Torsional Buckling

$$L_{cr} := L = 5.34 \ m$$

$$M_{cr.0} := \frac{\pi^2 \ E \cdot I_{zz.beam}}{L_{cr}^2} \left(\frac{I_{w.beam}}{I_{zz.beam}} + \frac{L_{cr}^2 \ G \cdot I_{T.beam}}{\pi^2 \ E \cdot I_{zz.beam}} \right)^{0.5} = [201.313] \ kN \cdot m$$

$$C_1 := 1.132 \qquad \text{for UDL}$$

$$M_{cr} := C_1 \cdot M_{cr.0} = [227.886] \ kN \cdot m$$

$$\lambda_{LT} := \sqrt{\frac{W_{pl.y.beam} \cdot f_y}{M_{cr}}} = 0.959$$

$$\alpha_{LT} := 0.21 \qquad \text{using buckling curve a, as ASB section}$$

$$\phi_{LT} := 0.5 \ \left(1 + \alpha_{LT} \cdot \left(\lambda_{LT} - 0.2 \right) + \lambda_{LT}^2 \right) = 1.039$$

$$\chi_{LT} := \frac{1}{\phi_{LT} + \sqrt{\phi_{LT}^2 - \lambda_{LT}^2}} = 0.694$$

$$M_{b.Rd} := \frac{\chi_{LT} \cdot W_{pl.y.beam} \cdot f_y}{\gamma_{M1}} = [145.422] \ kN \cdot m$$

$$\frac{M_{y.Ed}}{M_{b.Rd}} = [0.356] \qquad \text{...Therefore fine}$$

Interaction of LTB, minor axis bending, torsion

Case 1:

$$k_w := 0.7 - 0.2 \ \frac{\left| M_{w.1.Ed} \right|}{M_{w.Rd}} = 0.669$$

$$k_\alpha := \frac{1}{1 - \left(\dfrac{M_{y.Ed1}}{M_{cr}} \right)} = 1.137$$

$$\frac{M_{y.Ed1}}{M_{b.Rd}} + \frac{k_w \cdot k_\alpha \cdot \left| M_{w.1.Ed} \right|}{M_{w.Rd}} = 0.305$$

Case 2: $k_w := 0.7 - 0.2 \; \dfrac{\left|M_{w.2.Ed}\right|}{M_{w.Rd}} = 0.682$

$$k_\alpha := \dfrac{1}{1 - \left(\dfrac{M_{y.Ed2}}{M_{cr}}\right)} = 1.218$$

$$\dfrac{M_{y.Ed2}}{M_{b.Rd}} + \dfrac{k_w \cdot k_\alpha \cdot \left|M_{w.2.Ed}\right|}{M_{w.Rd}} = 0.354$$

Case 3: $k_w := 0.7 - 0.2 \; \dfrac{\left|M_{w.3.Ed}\right|}{M_{w.Rd}} = 0.694$

$$k_\alpha := \dfrac{1}{1 - \left(\dfrac{M_{y.Ed3}}{M_{cr}}\right)} = 1.294$$

$$\dfrac{M_{y.Ed3}}{M_{b.Rd}} + \dfrac{k_w \cdot k_\alpha \cdot \left|M_{w.3.Ed}\right|}{M_{w.Rd}} = 0.384$$

Normal Stage - Torsion effects

$$f_{d.1} := (\gamma_g \cdot g_k \cdot s) + \left(\gamma_q \cdot q_k \cdot \frac{s}{2}\right) + (\gamma_g \cdot g \cdot W_{beam}) = [26.461] \; \frac{kN}{m}$$ s.dead + live : s.dead

$$f_{d.2} := (\gamma_g \cdot g_k + \gamma_q \cdot q_k) \cdot s + g \cdot W_{beam} = [32.811] \; \frac{kN}{m}$$ s.dead + live : s.dead + live

$$M_{y.Ed1} := f_{d.1} \cdot \frac{L^2}{8} = [94.318] \; kN \cdot m \qquad V_{Ed.1} := f_{d.1} \cdot \frac{L}{2} = [70.65] \; kN$$

$$M_{y.Ed2} := f_{d.2} \cdot \frac{L^2}{8} = [116.953] \; kN \cdot m \qquad V_{Ed.2} := f_{d.2} \cdot \frac{L}{2} = [87.605] \; kN$$

Assume bearing zone reduced to 40mm on side 1 (allowance for tolerance of unit length and placement), nominal of 80mm on side 2.

$$T_{sdead.1} := \gamma_g \cdot g_k \cdot \frac{s}{2} \cdot e_1 \cdot L = [5.143] \; kN \cdot m \qquad T_{sdead.2} := -\gamma_g \cdot g_k \cdot \frac{s}{2} \cdot e_2 \cdot L = [-4.114] \; kN \cdot m$$

$$T_{imposed.1} := \gamma_q \cdot q_k \cdot \frac{s}{2} \cdot e_1 \cdot L = [3.484] \; kN \cdot m \qquad T_{imposed.2} := -\gamma_q \cdot q_k \cdot \frac{s}{2} \cdot e_2 \cdot L = [-2.787] \; kN \cdot m$$

$$T_{d.1} := T_{sdead.1} + T_{imposed.1} + T_{sdead.2} = [4.513] \; kN \cdot m$$

$$T_{d.2} := T_{sdead.1} + T_{imposed.1} + T_{sdead.2} + T_{imposed.2} = [1.725] \; kN \cdot m$$

$$\phi_1 := \frac{T_{d.1} \cdot a^2}{G \cdot I_{T.beam} \cdot L} \left(\frac{(x \cdot L - x^2)}{2 \, a^2} + \cosh\left(\frac{x}{a}\right) - \tanh\left(\frac{L}{2 \, a}\right) \sinh\left(\frac{x}{a}\right) - 1 \right) = 0.095 \; rad$$

$$\phi_1 = 5.448 \; °$$

$$\phi''_1 := \frac{T_{d.1}}{G \cdot I_{T.beam} \cdot L} \left(-1 + \cosh\left(\frac{x}{a}\right) - \tanh\left(\frac{L}{2 \, a}\right) \sinh\left(\frac{x}{a}\right) \right) = -0.031 \; \frac{1}{m^2}$$

$$M_{w.1.Ed} := \frac{E \cdot I_{w.beam} \cdot \phi''_1}{h_{beam} - t_{f.beam}} = -4.429 \; kN \cdot m$$

$$\phi_2 := \frac{T_{d.2} \cdot a^2}{G \cdot I_{T.beam} \cdot L} \left(\frac{\left(x \cdot L - x^2 \right)}{2\,a^2} + \cosh\left(\frac{x}{a}\right) - \tanh\left(\frac{L}{2\,a}\right) \sinh\left(\frac{x}{a}\right) - 1 \right) = 0.036 \ \boldsymbol{rad}$$

$$\phi_2 = 2.083 \ °$$

$$\phi''_2 := \frac{T_{d.2}}{G \cdot I_{T.beam} \cdot L} \left(-1 + \cosh\left(\frac{x}{a}\right) - \tanh\left(\frac{L}{2\,a}\right) \sinh\left(\frac{x}{a}\right) \right) = -0.012 \ \frac{1}{\boldsymbol{m^2}}$$

$$M_{w.2.Ed} := \frac{E \cdot I_{w.beam} \cdot \phi''_2}{h_{beam} - t_{f.beam}} = -1.693 \ \boldsymbol{kN \cdot m}$$

Cross Section Resistance

Bending Resistance about major axis
$$M_{y.Rd} := \frac{W_{pl.y.beam} \cdot f_y}{\gamma_{M0}} = \left[209.45 \right] \ \boldsymbol{kN \cdot m}$$

$$M_{y.Ed} := \max\left(M_{y.Ed1}, M_{y.Ed2} \right) = 116.953 \ \boldsymbol{kN \cdot m}$$

$$M_{y.Rd} > M_{y.Ed}$$

Warping Resistance of top flange
$$W_{pl.z.tf} := \frac{t_{f.beam} \cdot b_{t.beam}^{\ 2}}{4} = 67.5 \ \boldsymbol{cm^3}$$

$$M_{w.Rd} := \frac{W_{pl.z.tf} \cdot f_y}{\gamma_{M0}} = 23.963 \ \boldsymbol{kN \cdot m}$$

$$M_{w.Ed} := \max\left(\left| M_{w.1.Ed} \right|, \left| M_{w.2.Ed} \right| \right) = 4.429 \ \boldsymbol{kN \cdot m}$$

$$M_{w.Rd} > M_{w.Ed}$$

Plastic Interaction Criterion

$$\left(\frac{M_{y.Ed}}{M_{y.Rd}} \right)^2 + \frac{M_{w.Ed}}{M_{w.Rd}} = \left[0.497 \right] \qquad < 1 \text{ therefore OK}$$

Shear Resistance

Plastic Shear resistance (without torsion)

$$V_{pl.Rd} = \begin{bmatrix} 431.152 \end{bmatrix} \; kN$$

Reduced shear resistance in presence of torsion is not thought to be limiting, and is therefore not considered

Lateral Torsional Buckling

$$M_{b.Rd} = \begin{bmatrix} 145.422 \end{bmatrix} \; kN \cdot m$$

$$\frac{M_{y.Ed}}{M_{b.Rd}} = \begin{bmatrix} 0.804 \end{bmatrix} \qquad \text{...Therefore fine}$$

Interaction of LTB, minor axis bending, torsion

Case 1:
$$k_w := 0.7 - 0.2 \, \frac{\left| M_{w.1.Ed} \right|}{M_{w.Rd}} = 0.663$$

$$k_\alpha := \frac{1}{1 - \left(\dfrac{M_{y.Ed1}}{M_{cr}} \right)} = 1.706$$

$$\frac{M_{y.Ed1}}{M_{b.Rd}} + \frac{k_w \cdot k_\alpha \cdot \left| M_{w.1.Ed} \right|}{M_{w.Rd}} = 0.858$$

Case 2:
$$k_w := 0.7 - 0.2 \, \frac{\left| M_{w.2.Ed} \right|}{M_{w.Rd}} = 0.686$$

$$k_\alpha := \frac{1}{1 - \left(\dfrac{M_{y.Ed2}}{M_{cr}} \right)} = 2.054$$

$$\frac{M_{y.Ed2}}{M_{b.Rd}} + \frac{k_w \cdot k_\alpha \cdot \left| M_{w.2.Ed} \right|}{M_{w.Rd}} = 0.904$$

Deflection Check

Construction - horizontal

$$T_{p.1} := g_c \cdot \frac{s}{2} \cdot e_1 \cdot L = [1.487] \ kN \cdot m$$

$$T_{c.1} := q_c \cdot \frac{s}{2} \cdot e_1 \cdot L = [1.161] \ kN \cdot m$$

$$T_q := T_{p.1} + T_{c.1} = [2.648] \ kN \cdot m$$

$$I_{yc} := \frac{t_{f.beam} \cdot b_{t.beam}^{3}}{12} = 337.5 \ cm^4$$

$$I_{yt} := \frac{t_{f.beam} \cdot b_{b.beam}^{3}}{12} = \left(1.382 \cdot 10^3\right) \ cm^4$$

$$y_o := \frac{\left(h_{beam} - z_{e.beam} - t_{f.beam}\right) \cdot I_{yt} - \left(z_{e.beam} - \frac{t_{f.beam}}{2}\right) \cdot I_{yc}}{I_{yt} + I_{yc}} = [0.044] \ m$$

Distance to shear centre: $\quad h_{sc} := z_{e.beam} + y_o = [0.184] \ m$

$$\phi := \frac{T_q \cdot a^2}{G \cdot I_{T.beam} \cdot L} \left(\frac{\left(x \cdot L - x^2\right)}{2 \ a^2} + \cosh\left(\frac{x}{a}\right) - \tanh\left(\frac{L}{2 \ a}\right) \sinh\left(\frac{x}{a}\right) - 1 \right) = 0.056 \ rad$$

$$\phi = 3.197 \ °$$

$$\delta_{c.horiz} := h_{sc} \cdot \phi = [10.291] \ mm$$

$$\text{Limit} = \frac{L}{500} = 10.68 \ mm$$

Therefore OK

Construction vertical

$$\delta_c := \frac{5}{384} \frac{\left(\left(g_{k.slab} \cdot s\right) + \left(W_{beam} \cdot g\right)\right) \cdot L^4}{E \cdot I_{yy.beam}} = 4.641 \ mm$$

$$\text{Limit} = \frac{L}{200} = 26.7 \ mm$$

Therefore OK

Normal Stage Imposed Load deflection

$$\delta_{IL} := \frac{5}{384} \frac{\left(q_k \cdot s\right) \cdot L^4}{E \cdot I_{yy.beam}} = \left[6.655\right] \; mm$$

Limit = $\dfrac{L}{360} = 14.833 \; mm$

Therefore OK

Normal Stage Total Deflection

$$\delta_{SDL} := \frac{5}{384} \frac{\left(g_{k.services} \cdot s\right) \cdot L^4}{E \cdot I_{yy.beam}} = \left[6.655\right] \; mm$$

$$\delta := \delta_c + \delta_{IL} + \delta_{SDL} = \left[17.951\right] \; mm$$

Limit = $\dfrac{L}{200} = 26.7 \; mm$

Therefore OK

Appendix E

Timber-Steel Edge Beams

Domestic residence, hence $\quad\quad\quad \psi_0 := 0.7 \quad\quad$ UK NA to BS EN 1990, Table NA.1.1

floor-floor height, $\quad\quad\quad\quad\quad\quad h_{storey} := 3 \ m$

density of CLT, $\quad\quad\quad\quad\quad\quad \gamma_{CLT} := 4.8 \ \dfrac{kN}{m^3}$

wall panel thickness, (double panel) $\quad t_{wall} := 256 \ mm$

$\quad\quad\quad$ Hence, approx. edge load $\quad\quad \omega_{edge} := 1.1 \cdot t_{wall} \cdot h_{storey} \cdot \gamma_{CLT} = 4.055 \ \dfrac{kN}{m}$

Dead Load from slab $\quad\quad\quad\quad\quad d := 200 \ mm$

$\quad\quad\quad\quad\quad\quad\quad\quad\quad\quad g_{k.slab} := \gamma_{CLT} \cdot d = 0.96 \ \dfrac{kN}{m^2}$

Services and finishes $\quad\quad\quad\quad g_{k.services} := 1.5 \ \dfrac{kN}{m^2}$

Permanent Load $\quad\quad\quad\quad\quad g_k := g_{k.slab} + g_{k.services} = 2.46 \ \dfrac{kN}{m^2}$

Imposed Load $\quad\quad\quad\quad\quad q_k := 1.5 \ \dfrac{kN}{m^2} \quad\quad\quad f_{SLS} := g_k + q_k = 3.96 \ \dfrac{kN}{m^2}$

$\quad \xi := 0.925 \quad\quad \gamma_g := 1.35 \quad\quad \gamma_q := 1.5$

$\quad\quad\quad$ working UDL $\quad\quad\quad\quad f_d := \xi \cdot \gamma_g \cdot g_k + \gamma_q \cdot q_k = 5.322 \ \dfrac{kN}{m^2}$

Construction

$\quad\quad\quad\quad q_c := 0.75 \ \dfrac{kN}{m^2} \quad\quad$ personnel + small equipment

$\quad\quad\quad\quad g_c := g_{k.slab} = 0.96 \ \dfrac{kN}{m^2} \quad\quad$ slab units

$\quad\quad\quad\quad\quad\quad\quad\quad f_{d.c} := \xi \cdot \gamma_g \cdot g_c + \gamma_q \cdot q_c = 2.324 \ \dfrac{kN}{m^2}$

$\quad\quad\quad\quad\quad\quad\quad\quad f_{SLS.c} := g_c + q_c = 1.71 \ \dfrac{kN}{m^2}$

$RHSFB200.150.8 := 0$
$RHSFB200.150.10 := 1$
$RHSFB200.150.12 := 2$
$RHSFB250.150.8 := 3$
$RHSFB250.150.10 := 4$
$RHSFB250.150.12 := 5$
$RHSFB300.200.8 := 6$
$RHSFB300.200.10 := 7$
$RHSFB300.200.12 := 8$
$RHSFB400.200.8 := 9$
$RHSFB400.200.10 := 10$
$RHSFB400.200.12 := 11$
$RHSFB450.250.8 := 12$
$RHSFB450.250.10 := 13$
$RHSFB450.250.12 := 14$
$RHSFBhyp1 := 15$
$RHSFBhyp2 := 16$

W $\left(\frac{kg}{m}\right)$	D (mm)	B_{RHS} (mm)	B_p (mm)	t_{RHS} (mm)	t_p (mm)	I_{yy} (cm^4)	I_{zz} (cm^4)	r_y (cm)
69.7	200	150	240	8	15	5451	4055	6.8
79.3	200	150	240	10	15	6251	4461	6.6
90.8	200	150	240	12.5	15	7107	4903	6.5
76	250	150	240	8	15	9087	4484	6.8
87.1	250	150	240	10	15	10449	4975	6.7
100.6	250	150	240	12.5	15	11938	5517	6.6
94.4	300	200	290	8	15	16614	8795	8.6
108.6	300	200	290	10	15	19226	9931	8.5
126.0	300	200	290	12.5	15	22147	11228	8.4
106.9	400	200	290	8	15	32322	10308	8.7
124.3	400	200	290	10	15	37511	11772	8.6
146.1	400	200	290	12.5	15	43409	13461	8.5
125.4	450	250	340	8	15	48873	17759	10.5
146	450	250	340	10	15	56914	20482	10.5
171	450	250	340	12.5	15	66155	23677	10.4
44.4	200	100	190	5	15	3132		
55.9	220	120	210	6.3	15	5037		

$W_{el.b}$	z_e	z_p	$W_{pl.y}$	$W_{t.RHS}$		I_T	A
(cm^3)	(cm)	(cm)	(cm^3)	(cm^3)		(cm^4)	(cm^2)
763	14.4	19.4	549	398		3670	88.8
816	13.8	18.9	661	475		4436	100.9
872	13.3	17.2	783	559		5314	115.6
1002	17.4	23.7	775	506		5048	96.8
1077	16.8	21.5	926	605		6117	110.9
1162	16.2	19.7	1087	717		7353	128.1
1538	20.7	28.6	1169	840		10595	120.3
1665	20.0	25.9	1404	1020		12941	138.4
1811	19.3	23.7	1661	1220		15710	160.5
2173	26.6	33.6	1810	1140		15768	136.3
2373	25.7	30.9	2146	1380		19292	158.5
2610	24.9	28.7	2507	1660		23471	185.5
2946	29.9	38.4	2401	1630		27121	160
3229	28.8	35.2	2861	1990		33322	186
3564	27.9	32.7	3383	2410		40757	218
			301.4	172.1		1201	56.5
			458.5	282.8		2309	71.2

$G := 81 \ GPa$

$\gamma_{M1} := 1.0$

$E := 210 \ GPa$

$\gamma_{M0} := 1.0$

$f_y := 355 \ MPa$

EDGE BEAM - WALL ONLY

$$W_{beam} := 21 \; \frac{kg}{m}$$

$$I_{yy.beam} := 1150 \; cm^4$$

$$W_{pl.y.beam} := 157 \; cm^3$$

$$L := 5.8 \; m$$

$$\delta_{Ed.swt} := \frac{5 \cdot W_{beam} \cdot g \cdot L^4}{384 \cdot E \cdot I_{yy.beam}} = 1.257 \; mm$$

$$M_{Ed.swt} := \frac{\gamma_g \cdot W_{beam} \cdot g \cdot L^2}{8} = 1.169 \; kN \cdot m$$

$$\delta_{Ed.wall} := \frac{5 \; \omega_{edge} \cdot L^4}{384 \cdot E \cdot I_{yy.beam}} = 24.742 \; mm$$

$$M_{Ed.wall} := \frac{\gamma_g \cdot \omega_{edge} \cdot L^2}{8} = 23.019 \; kN \cdot m$$

$$\delta := \delta_{Ed.swt} + \delta_{Ed.wall} = 25.998 \; mm \qquad \delta_{limit} := \frac{L}{200} = 29 \; mm$$

$$M_{Ed} := M_{Ed.swt} + M_{Ed.wall} = 24.189 \; kN \cdot m \qquad M_{Rd} := \frac{W_{pl.y.beam} \cdot f_y}{\gamma_{M0}} = 55.735 \; kN \cdot m$$

BEAM TYPE 3

Beam span $\qquad L := 6.72 \ m$

Beam spacing
$$s_a := 1.15 \ m$$
$$s_b := 1.75 \ m$$
$$a := 1.984 \ m$$

$$beam := RHSFBhyp2 = 16$$

$$W_{beam} := \text{submatrix}\left(W, beam, beam, 0, 0\right) = \left[55.9\right] \frac{kg}{m}$$
$$D_{beam} := \text{submatrix}\left(D, beam, beam, 0, 0\right) = \left[0.22\right] m$$
$$B_{RHS.beam} := \text{submatrix}\left(B_{RHS}, beam, beam, 0, 0\right) = \left[120\right] mm$$
$$B_{p.beam} := \text{submatrix}\left(B_p, beam, beam, 0, 0\right) = \left[210\right] mm$$
$$t_{RHS.beam} := \text{submatrix}\left(t_{RHS}, beam, beam, 0, 0\right) = \left[6.3\right] mm$$
$$t_{p.beam} := \text{submatrix}\left(t_p, beam, beam, 0, 0\right) = \left[15\right] mm$$
$$r_{y.beam} := \text{submatrix}\left(r_y, \boxed{beam}, beam, 0, 0\right) = ? \ mm$$
$$I_{yy.beam} := \text{submatrix}\left(I_{yy}, beam, beam, 0, 0\right) = \left[5.037 \cdot 10^3\right] cm^4$$
$$I_{zz.beam} := \text{submatrix}\left(I_{zz}, \boxed{beam}, beam, 0, 0\right) = ?$$

$$W_{el.b.beam} := \text{submatrix}\left(W_{el.b}, \boxed{beam}, beam, 0, 0\right) = ? \ cm^3$$
$$z_{e.beam} := \text{submatrix}\left(z_e, \boxed{beam}, beam, 0, 0\right) = ?$$
$$z_{p.beam} := \text{submatrix}\left(z_p, \boxed{beam}, beam, 0, 0\right) = ?$$

$$W_{pl.y.beam} := \text{submatrix}\left(W_{pl.y}, beam, beam, 0, 0\right) = \left[458.5\right] cm^3$$
$$W_{t.RHS.beam} := \text{submatrix}\left(W_{t.RHS}, beam, beam, 0, 0\right) = \left[282.8\right] cm^3$$

$$I_{T.beam} := \text{submatrix}\left(I_T, beam, beam, 0, 0\right) = \left[2.309 \cdot 10^{-5}\right] m^4$$
$$A_{beam} := \text{submatrix}\left(A, beam, beam, 0, 0\right) = \left[71.2\right] cm^2$$

$$M_{Ed.slab} := f_d \cdot \left(\frac{2 \cdot s_a \cdot a^2}{4} + \frac{s_b \cdot L^2}{8} \right) = 64.617 \ kN \cdot m$$

$$V_{Ed.slab} := f_d \cdot \left(\frac{2 \cdot s_a \cdot a}{2} + \frac{s_b \cdot L}{2} \right) = 43.435 \ kN$$

$$\delta_{Ed.slab} := f_{SLS} \cdot \left(\frac{2 \cdot s_a \cdot a^2 \cdot \left(3 \ L^2 - 2 \ a^2 \right)}{96 \ E \cdot I_{yy.beam}} + \frac{5 \ s_b \cdot L^4}{384 \ E \cdot I_{yy.beam}} \right) = \left[21.901 \right] \ mm$$

$$\delta_{Ed.swt} := \frac{5 \cdot W_{beam} \cdot g \cdot L^4}{384 \cdot E \cdot I_{yy.beam}} = 1.376 \ mm$$

$$M_{Ed.swt} := \frac{\gamma_g \cdot W_{beam} \cdot g \cdot L^2}{8} = \left[4.177 \right] \ kN \cdot m$$

$$V_{Ed.swt} := \frac{\gamma_g \cdot W_{beam} \cdot g \cdot L}{2} = \left[2.487 \right] \ kN$$

$$M_{Ed.wall} := \frac{\gamma_g \cdot \omega_{edge} \cdot L^2}{8} = 30.901 \ kN \cdot m$$

$$V_{Ed.wall} := \frac{\gamma_g \cdot \omega_{edge} \cdot L}{2} = 18.394 \ kN$$

$$\delta_{Ed.wall} := \frac{5 \ \omega_{edge} \cdot L^4}{384 \cdot E \cdot I_{yy.beam}} = \left[10.179 \right] \ mm$$

$$M_{Ed.c} := f_{d.c} \cdot \left(\frac{2 \cdot s_a \cdot a^2}{4} + \frac{s_b \cdot L^2}{8} \right) = 28.215 \ kN \cdot m$$

$$V_{Ed.c} := f_{d.c} \cdot \left(\frac{2 \cdot s_a \cdot a}{2} + \frac{s_b \cdot L}{2} \right) = 18.966 \ kN$$

$$\delta_{Ed.c} := f_{SLS.c} \cdot \left(\frac{2 \cdot s_a \cdot a^2 \cdot \left(3 \ L^2 - 2 \ a^2 \right)}{96 \ E \cdot I_{yy.beam}} + \frac{5 \ s_b \cdot L^4}{384 \ E \cdot I_{yy.beam}} \right) = \left[9.457 \right] \ mm$$

$$\delta_{Ed} := \delta_{Ed.slab} + \delta_{Ed.wall} + \delta_{Ed.swt} = \left[33.457 \right] \ mm$$

$$\delta_{limit} := \frac{L}{\quad} = 33.6 \ mm$$

$$I_{T.plate} := \frac{B_{p.beam} \cdot t_{p.beam}^3}{3} \left(1 - 0.21 \frac{t_{p.beam}}{B_{p.beam}} \left(1 - \frac{t_{p.beam}^4}{12 \, B_{p.beam}^4}\right)\right) = 23.271 \; cm^4$$

$$W_{t.plate} := \frac{I_{T.plate}}{t_{p.beam}} = [15.514] \; cm^3$$

$$I_{T.tot} := I_{T.beam} = [2.309 \cdot 10^3] \; cm^4$$

$$W_{t.beam} := W_{t.RHS.beam} + W_{t.plate} = [298.314] \; cm^3$$

Assume shear centre of beam lies at centre of RHS. Hence, lever arm of slab loading is 40mm + 10mm + (RHS width/2).

$$e := 50 \; mm + \left(\frac{B_{RHS.beam}}{2}\right) = [0.11] \; m$$

$$T_{Ed} := f_d \cdot (L \cdot s_b + 2 \cdot a \cdot s_a) \cdot e = [9.556] \; (kN \cdot m)$$

$$\phi := \frac{\left(\frac{T_{Ed}}{4}\right) \cdot \frac{L}{2}}{G \cdot I_{T.tot}} = 0.004 \; rad$$

$$\phi = 0.246 \; °$$ rotation at mid-span - negligible hence negligible minor axis moment

$$T_{Rd} := \frac{W_{t.beam} \cdot f_y}{\gamma_{M0} \sqrt{3}} = [61.142] \; kN \cdot m$$

$$M_{Ed} := M_{Ed.slab} + M_{Ed.wall} + M_{Ed.swt} = [99.696] \; kN \cdot m$$

$$M_{Rd} := \frac{W_{pl.y.beam} \cdot f_y}{\gamma_{M0}} = [162.768] \; kN \cdot m$$

$$V_{Ed} := V_{Ed.slab} + V_{Ed.wall} + V_{Ed.swt} = [64.316] \; kN \qquad A_v := \frac{A_{beam} \cdot D_{beam}}{B_{RHS.beam} + D_{beam}} = [46.071] \; cm^2$$

$$V_{Rd} := \frac{A_v \cdot f_y}{\gamma_{M0} \sqrt{3}} = [944.26] \; kN$$

BEAM TYPE 2

Beam span $\qquad\qquad L := 5.34 \; m$

Beam spacing $\qquad\qquad s := 2.9 \; m$

$$beam := RHSFBhyp1 = 15$$

$$W_{beam} := \text{submatrix}\,(W, beam, beam, 0, 0) = [44.4] \; \frac{kg}{m}$$
$$D_{beam} := \text{submatrix}\,(D, beam, beam, 0, 0) = [0.2] \; m$$
$$B_{RHS.beam} := \text{submatrix}\,(B_{RHS}, beam, beam, 0, 0) = [100] \; mm$$
$$B_{p.beam} := \text{submatrix}\,(B_p, beam, beam, 0, 0) = [190] \; mm$$
$$t_{RHS.beam} := \text{submatrix}\,(t_{RHS}, beam, beam, 0, 0) = [5] \; mm$$
$$t_{p.beam} := \text{submatrix}\,(t_p, beam, beam, 0, 0) = [15] \; mm$$
$$r_{y.beam} := \text{submatrix}\,(r_y, \boxed{beam}, beam, 0, 0) = ? \; mm$$
$$I_{yy.beam} := \text{submatrix}\,(I_{yy}, beam, beam, 0, 0) = [3.132 \cdot 10^{-5}] \; m^4$$
$$I_{zz.beam} := \text{submatrix}\,(I_{zz}, \boxed{beam}, beam, 0, 0) = ?$$

$$W_{el.b.beam} := \text{submatrix}\,(W_{el.b}, \boxed{beam}, beam, 0, 0) = ? \; cm^3$$
$$z_{e.beam} := \text{submatrix}\,(z_e, \boxed{beam}, beam, 0, 0) = ?$$
$$z_{p.beam} := \text{submatrix}\,(z_p, \boxed{beam}, beam, 0, 0) = ?$$

$$W_{pl.y.beam} := \text{submatrix}\,(W_{pl.y}, beam, beam, 0, 0) = [301.4] \; cm^3$$
$$W_{t.RHS.beam} := \text{submatrix}\,(W_{t.RHS}, beam, beam, 0, 0) = [172.1] \; cm^3$$
$$U_{beam} := \text{submatrix}\,(\boxed{U}, beam, beam, 0, 0) = ?$$
$$X_{beam} := \text{submatrix}\,(\boxed{X}, beam, beam, 0, 0) = ?$$
$$I_{w.beam} := \text{submatrix}\,(\boxed{I_w}, beam, beam, 0, 0) = ? \; m^6$$
$$I_{T.beam} := \text{submatrix}\,(I_T, beam, beam, 0, 0) = [1.201 \cdot 10^{-5}] \; m^4$$
$$A_{beam} := \text{submatrix}\,(A, beam, beam, 0, 0) = [56.5] \; cm^2$$

$$M_{Ed.slab} := f_d \cdot \left(\frac{s \cdot L^2}{8}\right) = 55.012 \ kN \cdot m$$

$$V_{Ed.slab} := f_d \cdot \frac{s \cdot L}{2} = 41.208 \ kN$$

$$\delta_{Ed.slab} := f_{SLS} \cdot \frac{5 \ s \cdot L^4}{384 \ E \cdot I_{yy.beam}} = [18.487] \ mm$$

$$\delta_{Ed.swt} := \frac{5 \cdot W_{beam} \cdot g \cdot L^4}{384 \cdot E \cdot I_{yy.beam}} = 0.701 \ mm$$

$$M_{Ed.swt} := \frac{\gamma_g \cdot W_{beam} \cdot g \cdot L^2}{8} = [2.095] \ kN \cdot m$$

$$V_{Ed.swt} := \frac{\gamma_g \cdot W_{beam} \cdot g \cdot L}{2} = [1.569] \ kN$$

$$M_{Ed.wall} := \frac{\gamma_g \cdot \omega_{edge} \cdot L^2}{8} = 19.513 \ kN \cdot m$$

$$V_{Ed.wall} := \frac{\gamma_g \cdot \omega_{edge} \cdot L}{2} = 14.616 \ kN$$

$$\delta_{Ed.wall} := \frac{5 \ \omega_{edge} \cdot L^4}{384 \cdot E \cdot I_{yy.beam}} = [6.528] \ mm$$

$$M_{Ed.c} := f_{d.c} \cdot \left(\frac{s \cdot L^2}{8}\right) = 24.021 \ kN \cdot m$$

$$V_{Ed.c} := f_{d.c} \cdot \left(\frac{s \cdot L}{2}\right) = 17.993 \ kN$$

$$\delta_{Ed.c} := f_{SLS.c} \cdot \frac{5 \ s \cdot L^4}{384 \ E \cdot I_{yy.beam}} = [7.983] \ mm$$

$$\delta_{Ed} := \delta_{Ed.slab} + \delta_{Ed.wall} + \delta_{Ed.swt} = [25.715] \ mm$$

$$\delta_{limit} := \frac{L}{200} = 26.7 \ mm$$

$$I_{T.plate} := \frac{B_{p.beam} \cdot t_{p.beam}^3}{3} \left(1 - 0.21 \, \frac{t_{p.beam}}{B_{p.beam}} \left(1 - \frac{t_{p.beam}^4}{12 \, B_{p.beam}^4}\right)\right) = 21.021 \; cm^4$$

$$W_{t.plate} := \frac{I_{T.plate}}{t_{p.beam}} = [14.014] \; cm^3$$

$$I_{T.tot} := I_{T.beam} = [1.201 \cdot 10^3] \; cm^4$$

$$W_{t.beam} := W_{t.RHS.beam} + W_{t.plate} = [186.114] \; cm^3$$

Assume shear centre of beam lies at centre of RHS. Hence, lever arm of slab loading is 40mm + 10mm + (RHS width/2).

$$e := 50 \; mm + \left(\frac{B_{RHS.beam}}{2}\right) = [0.1] \; m$$

$$T_{Ed} := f_d \cdot (L \cdot s_b + 2 \cdot a \cdot s_a) \cdot e = [7.402] \; (kN \cdot m)$$

$$\phi := \frac{\left(\frac{T_{Ed}}{4}\right) \cdot \frac{L}{2}}{G \cdot I_{T.tot}} = 0.005 \; rad$$

$$\phi = 0.291 \; °$$ rotation at mid-span - negligible hence negligible minor axis moment

$$T_{Rd} := \frac{W_{t.beam} \cdot f_y}{\gamma_{M0} \, \sqrt{3}} = [38.146] \; kN \cdot m$$

$$M_{Ed} := M_{Ed.slab} + M_{Ed.wall} + M_{Ed.swt} = [76.62] \; kN \cdot m$$

$$M_{Rd} := \frac{W_{pl.y.beam} \cdot f_y}{\gamma_{M0}} = [106.997] \; kN \cdot m$$

$$V_{Ed} := V_{Ed.slab} + V_{Ed.wall} + V_{Ed.swt} = [57.394] \; kN \qquad A_v := \frac{A_{beam} \cdot D_{beam}}{B_{RHS.beam} + D_{beam}} = [37.667] \; cm^2$$

$$V_{Rd} := \frac{A_v \cdot f_y}{\gamma_{M0} \, \sqrt{3}} = [772.014] \; kN$$

Appendix F

Timber Steel Tie-Beams

Domestic residence, hence $\qquad \psi_0 := 0.7 \qquad$ UK NA to BS EN 1990, Table NA.1.1

floor-floor height,

$$h_{storey} := 3 \; m$$

density of CLT, $\qquad \gamma_{CLT} := 4.8 \; \dfrac{kN}{m^3}$

wall panel thickness, (double panel) $\qquad t_{wall} := 256 \; mm$

Hence, approx. edge load $\qquad \omega_{edge} := 1.1 \cdot t_{wall} \cdot h_{storey} \cdot \gamma_{CLT} = 4.055 \; \dfrac{kN}{m}$

Dead Load from slab $\qquad d := 200 \; mm$

$$g_{k.slab} := \gamma_{CLT} \cdot d = 0.96 \; \dfrac{kN}{m^2}$$

Services and finishes $\qquad g_{k.services} := 1.5 \; \dfrac{kN}{m^2}$

Permanent Load $\qquad g_k := g_{k.slab} + g_{k.services} = 2.46 \; \dfrac{kN}{m^2}$

Imposed Load $\qquad q_k := 1.5 \; \dfrac{kN}{m^2} \qquad\qquad f_{SLS} := g_k + q_k = 3.96 \; \dfrac{kN}{m^2}$

$\xi := 0.925 \qquad \gamma_g := 1.35 \qquad \gamma_q := 1.5$

working UDL $\qquad f_d := \xi \cdot \gamma_g \cdot g_k + \gamma_q \cdot q_k = 5.322 \; \dfrac{kN}{m^2}$

Construction

$\qquad q_c := 0.75 \; \dfrac{kN}{m^2} \qquad$ personnel + small equipment

$\qquad g_c := g_{k.slab} = 0.96 \; \dfrac{kN}{m^2} \qquad$ slab units

$$f_{d.c} := \xi \cdot \gamma_g \cdot g_c + \gamma_q \cdot q_c = 2.324 \; \dfrac{kN}{m^2}$$

$$f_{SLS.c} := g_c + q_c = 1.71 \; \dfrac{kN}{m^2}$$

Structure in question is Residential building of 9 storeys. Hence building falls into Consequence Class 2B.

$$\psi_1 := 0.5 \qquad \text{Table NA1.1 of NA to EC0}$$

$$s := 6.72 \ m$$
$$L := 5.8 \ m$$

$$T_i := 0.8 \ \left(g_k + \psi_1 \cdot q_k\right) \cdot s \cdot L = 100.09 \ kN$$

$$T_p := 0.4 \ \left(g_k + \psi_1 \cdot q_k\right) \cdot s \cdot L = 50.045 \ kN \qquad \text{...do not include cladding load}$$

$$f_y := 345 \ MPa \qquad \text{S355, 16mm<t<40mm}$$

$$A_{min.1} := \frac{T_i}{f_y} = 2.901 \ cm^2$$

$$d_{min} := \frac{L}{40} = 145 \ mm$$

$$A_{min.2} := \frac{T_p}{f_y} = 1.451 \ cm^2$$

Allocate T split from UKB102x152x17 for internal Tie-Beams.

Appendix G

Timber-Steel Columns

floor-floor height, $h := 3.2 \ m$

density of CLT, $\gamma_{CLT} := 4.8 \ \dfrac{kN}{m^3}$

wall panel thickness, (double panel) $t_{wall} := 256 \ mm$

  Hence, approx. edge load $\omega_{edge} := 1.1 \cdot t_{wall} \cdot h \cdot \gamma_{CLT} = 4.325 \ \dfrac{kN}{m}$

Dead Load from slab $d := 200 \ mm$

$$\gamma_{conc} := 24 \ \dfrac{kN}{m^3}$$

$$g_{k.slab} := \gamma_{CLT} \cdot d = 0.96 \ \dfrac{kN}{m^2}$$

Services and finishes $g_{k.services} := 1.5 \ \dfrac{kN}{m^2}$

Permanent Load $g_k := g_{k.slab} + g_{k.services} = 2.46 \ \dfrac{kN}{m^2}$

Imposed Load $q_k := 1.5 \ \dfrac{kN}{m^2}$

  $\xi := 0.925$ $\gamma_g := 1.35$ $\gamma_q := 1.5$

  working UDL $f_d := \xi \cdot \gamma_g \cdot g_k + \gamma_q \cdot q_k = 5.322 \ \dfrac{kN}{m^2}$

BASE STOREY

(1) Corner Column

Catchment Area $\qquad A := 7.74 \ m^2$

Beam span, north $\qquad l_N := 5.8 \ m$

Beam span, east $\qquad l_E := 5.3 \ m$

Slab supporting beam
reaction
$$R_{d.slab} := \left(\frac{l_N}{2}\right) \cdot f_d \cdot \left(\frac{l_E}{2}\right) + \left(\frac{l_E}{2} \cdot \omega_{edge}\right) = 52.361 \ kN$$

Wall supporting beam
reaction
$$R_{d.wall} := \left(\frac{l_N}{2} \cdot \omega_{edge}\right) = 12.544 \ kN$$

Design Axial Load $\qquad N_{Ed} := 7 \cdot f_d \cdot A = 288.342 \ kN$

<mark>TRIAL SECTION: UC 152x152x23</mark>

$$h := 152.4 \ mm$$
$$t_w := 5.8 \ mm$$

$N_{b.y.3.0} := 867 \ kN$	$N_{b.y.3.5} := 812 \ kN$
$N_{b.z.3.0} := 524 \ kN$	$N_{b.z.3.5} := 431 \ kN$
$M_{b.Rd.3.0} := 47.3 \ kN \cdot m$	$M_{b.Rd.3.5} := 43.9 \ kN \cdot m$

$$N_{pl.Rd} := 1040 \ kN$$

Interpolation (as L=3.2m): $\quad N_{b.y.Rd} := N_{b.y.3.0} - 0.2 \cdot \left(N_{b.y.3.0} - N_{b.y.3.5}\right) = 856 \ kN$

$$N_{b.z.Rd} := N_{b.z.3.0} - 0.2 \cdot \left(N_{b.z.3.0} - N_{b.z.3.5}\right) = 505.4 \ kN$$

buckling: $\quad M_{b.Rd} := M_{b.Rd.3.0} - 0.2 \cdot \left(M_{b.Rd.3.0} - M_{b.Rd.3.5}\right) = 46.62 \ kN \cdot m$

$$\therefore n := \frac{N_{Ed}}{N_{pl.Rd}} = 0.277 \qquad \text{\textcolor{red}{check <0.25 (if breached,}}$$
$$\text{\textcolor{red}{used reduced resistances)}}$$

$$M_{c.y.Rd} := 58.2 \ kN \cdot m$$
$$M_{c.z.Rd} := 18.7 \ kN \cdot m$$

$$M_{Rd} := min\left(M_{b.Rd}, M_{c.y.Rd}\right) = 46.62 \ kN \cdot m$$

I - orientation

$$M_{y.Ed} := R_{d.wall} \cdot \left(\frac{h}{2} + 100 \cdot mm\right) = 2.21 \ kN \cdot m$$

$$M_{z.Ed} := R_{d.slab} \cdot \left(\frac{t_w}{2} + 100 \cdot mm\right) = 5.388 \ kN \cdot m$$

Interaction (<1): $\quad i := \dfrac{N_{Ed}}{N_{b.z.Rd}} + \dfrac{M_{y.Ed}}{M_{Rd}} + 1.5 \cdot \dfrac{M_{z.Ed}}{M_{c.z.Rd}} = 1.05$

$$\frac{N_{Ed}}{N_{b.z.Rd}} = 0.571 \qquad \frac{M_{y.Ed}}{M_{Rd}} = 0.047 \qquad \frac{M_{z.Ed}}{M_{c.z.Rd}} = 0.288$$

H - orientation

$$M_{y.Ed} := R_{d.slab} \cdot \left(\frac{h}{2} + 100 \cdot mm\right) = 9.226 \ kN \cdot m$$

$$M_{z.Ed} := R_{d.wall} \cdot \left(\frac{t_w}{2} + 100 \cdot mm\right) = 1.291 \ kN \cdot m$$

Interaction (<1): $\quad i := \dfrac{N_{Ed}}{N_{b.z.Rd}} + \dfrac{M_{y.Ed}}{M_{Rd}} + 1.5 \cdot \dfrac{M_{z.Ed}}{M_{c.z.Rd}} = 0.872$

$$\frac{N_{Ed}}{N_{b.z.Rd}} = 0.571 \qquad \frac{M_{y.Ed}}{M_{Rd}} = 0.198 \qquad \frac{M_{z.Ed}}{M_{c.z.Rd}} = 0.069$$

(2) Edge (Stair) Column

Catchment Area $\qquad\qquad\qquad A := 14.76 \ m^2 \ A_W := 7.74 \ m^2 \ A_E := 7.02 \ m^2$

Beam span, west $\qquad\qquad\qquad l_W := 5.8 \ m$

Beam span, east $\qquad\qquad\qquad l_E := 6.72 \ m$

East slab supporting beam reaction $\qquad R_{d.east} := A_E \cdot f_d + \left(\frac{l_E}{2} \cdot \omega_{edge}\right) = 51.893 \ kN$

West slab supporting beam reaction $\qquad R_{d.west} := A_W \cdot f_d + \left(\frac{l_W}{2} \cdot \omega_{edge}\right) = 53.735 \ kN$

Design Axial Load $\qquad\qquad\qquad N_{Ed} := 7 \cdot f_d \cdot A = 549.861 \ kN$

TRIAL SECTION: UC 152x152x30

$$h := 157.6 \; mm$$
$$t_w := 6.5 \; mm$$

$N_{b.y.3.0} := 1150 \; kN$ $N_{b.y.3.5} := 1080 \; kN$

$N_{b.z.3.0} := 714 \; kN$ $N_{b.z.3.5} := 592 \; kN$

$M_{b.Rd.3.0} := 72.4 \; kN \cdot m$ $M_{b.Rd.3.5} := 67.9 \; kN \cdot m$

$$N_{pl.Rd} := 1360 \; kN$$

Interpolation (as L=3.2m): $N_{b.y.Rd} := N_{b.y.3.0} - 0.2 \cdot \left(N_{b.y.3.0} - N_{b.y.3.5} \right) = 1136 \; kN$

$$N_{b.z.Rd} := N_{b.z.3.0} - 0.2 \cdot \left(N_{b.z.3.0} - N_{b.z.3.5} \right) = 689.6 \; kN$$

buckling: $M_{b.Rd} := M_{b.Rd.3.0} - 0.2 \cdot \left(M_{b.Rd.3.0} - M_{b.Rd.3.5} \right) = 71.5 \; kN \cdot m$

$$\therefore n := \frac{N_{Ed}}{N_{pl.Rd}} = 0.404$$ check <0.25 (if breached, used reduced resistances)

$$M_{c.y.Rd} := 60.3 \; kN \cdot m$$
$$M_{c.z.Rd} := 38 \; kN \cdot m$$

$$M_{Rd} := min \left(M_{b.Rd}, M_{c.y.Rd} \right) = 60.3 \; kN \cdot m$$

<u>I - orientation</u>

$$M_{y.Ed} := 0 \; kN \cdot m$$

$$M_{z.Ed} := \left| \left(R_{d.east} - R_{d.west} \right) \right| \cdot \left(\frac{t_w}{2} + 100 \cdot mm \right) = 0.19 \; kN \cdot m$$

Interaction (<1): $i := \dfrac{N_{Ed}}{N_{b.z.Rd}} + \dfrac{M_{y.Ed}}{M_{Rd}} + 1.5 \cdot \dfrac{M_{z.Ed}}{M_{c.z.Rd}} = 0.805$

$$\frac{N_{Ed}}{N_{b.z.Rd}} = 0.797 \quad \frac{M_{y.Ed}}{M_{Rd}} = 0 \quad \frac{M_{z.Ed}}{M_{c.z.Rd}} = 0.005$$

<u>H - orientation</u>

$$M_{y.Ed} := \left| \left(R_{d.east} - R_{d.west} \right) \right| \cdot \left(\frac{h}{2} + 100 \cdot mm \right) = 0.329 \; kN \cdot m$$

$$M_{z.Ed} := 0 \; kN \cdot m$$

Interaction (<1): $\quad i := \dfrac{N_{Ed}}{N_{b.z.Rd}} + \dfrac{M_{y.Ed}}{M_{Rd}} + 1.5 \cdot \dfrac{M_{z.Ed}}{M_{c.z.Rd}} = 0.803$

$$\dfrac{N_{Ed}}{N_{b.z.Rd}} = 0.797 \qquad \dfrac{M_{y.Ed}}{M_{Rd}} = 0.005 \qquad \dfrac{M_{z.Ed}}{M_{c.z.Rd}} = 0$$

(3) Internal Column

Catchment Area $\qquad A := 19.62 \ m^2 \qquad A_W := 15.49 \ m^2 \quad A_E := 4.13 \ m^2$

East slab supporting beam reaction $\qquad R_{d.east} := A_E \cdot f_d = 21.98 \ kN$

West slab supporting beam reaction $\qquad R_{d.west} := A_W \cdot f_d = 82.437 \ kN$

Design Axial Load $\qquad N_{Ed} := 7 \cdot f_d \cdot A = 730.913 \ kN$

<mark>TRIAL SECTION: UC 152x152x44</mark>

$$h := 166 \ mm$$
$$t_w := 9.5 \ mm$$

$N_{b.y.3.0} := 1700 \ kN \qquad\qquad N_{b.y.3.5} := 1600 \ kN$
$N_{b.z.3.0} := 1070 \ kN \qquad\qquad N_{b.z.3.5} := 894 \ kN$
$M_{b.Rd.3.0} := 115 \ kN \cdot m \qquad\quad M_{b.Rd.3.5} := 110 \ kN \cdot m$
$$N_{pl.Rd} := 1990 \ kN$$

Interpolation (as L=3.2m): $\quad N_{b.y.Rd} := N_{b.y.3.0} - 0.2 \cdot (N_{b.y.3.0} - N_{b.y.3.5}) = 1680 \ kN$

$$N_{b.z.Rd} := N_{b.z.3.0} - 0.2 \cdot (N_{b.z.3.0} - N_{b.z.3.5}) = 1034.8 \ kN$$

buckling: $\quad M_{b.Rd} := M_{b.Rd.3.0} - 0.2 \cdot (M_{b.Rd.3.0} - M_{b.Rd.3.5}) = 114 \ kN \cdot m$

$\therefore n := \dfrac{N_{Ed}}{N_{pl.Rd}} = 0.367$ check <0.25 (if breached, used reduced resistances)

$$M_{c.y.Rd} := 90.3 \ kN \cdot m$$
$$M_{c.z.Rd} := 57.4 \ kN \cdot m$$

$M_{Rd} := min(M_{b.Rd}, M_{c.y.Rd}) = 90.3 \ kN \cdot m$

I - orientation

$$M_{y.Ed} := 0 \ kN \cdot m$$

$$M_{z.Ed} := \left| \left(R_{d.east} - R_{d.west} \right) \right| \cdot \left(\frac{t_w}{2} + 100 \cdot mm \right) = 6.333 \ kN \cdot m$$

Interaction (<1): $\quad i := \dfrac{N_{Ed}}{N_{b.z.Rd}} + \dfrac{M_{y.Ed}}{M_{Rd}} + 1.5 \cdot \dfrac{M_{z.Ed}}{M_{c.z.Rd}} = 0.872$

$$\frac{N_{Ed}}{N_{b.z.Rd}} = 0.706 \qquad \frac{M_{y.Ed}}{M_{Rd}} = 0 \qquad \frac{M_{z.Ed}}{M_{c.z.Rd}} = 0.11$$

H - orientation

$$M_{y.Ed} := \left| \left(R_{d.east} - R_{d.west} \right) \right| \cdot \left(\frac{h}{2} + 100 \cdot mm \right) = 11.064 \ kN \cdot m$$

$$M_{z.Ed} := 0 \ kN \cdot m$$

Interaction (<1): $\quad i := \dfrac{N_{Ed}}{N_{b.z.Rd}} + \dfrac{M_{y.Ed}}{M_{Rd}} + 1.5 \cdot \dfrac{M_{z.Ed}}{M_{c.z.Rd}} = 0.829$

$$\frac{N_{Ed}}{N_{b.z.Rd}} = 0.706 \qquad \frac{M_{y.Ed}}{M_{Rd}} = 0.123 \qquad \frac{M_{z.Ed}}{M_{c.z.Rd}} = 0$$

(4) Edge (Clear) Column

Catchment Area $\qquad\qquad\qquad A := 15.48 \ m^2$

Beam span, north $\qquad\qquad\qquad l_N := 5.8 \ m$

Beam span, south $\qquad\qquad\qquad l_S := 5.8 \ m$

East slab supporting beam reaction $\qquad R_{d.east} := A \cdot f_d = 82.383 \ kN$

North wall supporting beam reaction $\qquad R_{d.north} := \left(\frac{l_N}{2} \cdot \omega_{edge} \right) = 12.544 \ kN$

South wall supporting beam reaction $\qquad R_{d.south} := \left(\frac{l_S}{2} \cdot \omega_{edge} \right) = 12.544 \ kN$

Design Axial Load $\qquad N_{Ed} := 7 \cdot f_d \cdot A = 576.684 \; kN$

$$h := 161.8 \; mm$$
$$t_w := 8 \; mm$$

$N_{b.y.3.0} := 1420 \; kN \qquad\qquad N_{b.y.3.5} := 1340 \; kN$
$N_{b.z.3.0} := 889 \; kN \qquad\qquad N_{b.z.3.5} := 738 \; kN$
$M_{b.Rd.3.0} := 93.1 \; kN \cdot m \qquad\quad M_{b.Rd.3.5} := 88.4 \; kN \cdot m$
$$N_{pl.Rd} := 1670 \; kN$$

Interpolation (as L=3.2m): $\quad N_{b.y.Rd} := N_{b.y.3.0} - 0.2 \cdot \left(N_{b.y.3.0} - N_{b.y.3.5} \right) = 1404 \; kN$

$$N_{b.z.Rd} := N_{b.z.3.0} - 0.2 \cdot \left(N_{b.z.3.0} - N_{b.z.3.5} \right) = 858.8 \; kN$$

buckling: $\qquad M_{b.Rd} := M_{b.Rd.3.0} - 0.2 \cdot \left(M_{b.Rd.3.0} - M_{b.Rd.3.5} \right) = 92.16 \; kN \cdot m$

$$\therefore n := \frac{N_{Ed}}{N_{pl.Rd}} = 0.345 \qquad \text{\color{red}check <0.25 (if breached,}$$
$$\text{\color{red}used reduced resistances)}$$

$$M_{c.y.Rd} := 75 \; kN \cdot m$$
$$M_{c.z.Rd} := 47.5 \; kN \cdot m$$

$$M_{Rd} := min \left(M_{b.Rd}, M_{c.y.Rd} \right) = 75 \; kN \cdot m$$

<u>I - orientation</u>
$$M_{y.Ed} := 0 \; kN \cdot m$$

$$M_{z.Ed} := \left| R_{d.east} \right| \cdot \left(\frac{t_w}{2} + 100 \cdot mm \right) = 8.568 \; kN \cdot m$$

Interaction (<1): $\quad i := \dfrac{N_{Ed}}{N_{b.z.Rd}} + \dfrac{M_{y.Ed}}{M_{Rd}} + 1.5 \cdot \dfrac{M_{z.Ed}}{M_{c.z.Rd}} = 0.942$

$$\frac{N_{Ed}}{N_{b.z.Rd}} = 0.671 \qquad \frac{M_{y.Ed}}{M_{Rd}} = 0 \qquad \frac{M_{z.Ed}}{M_{c.z.Rd}} = 0.18$$

<u>H - orientation</u>

$$M_{y.Ed} := \left| R_{d.east} \right| \cdot \left(\frac{h}{2} + 100 \cdot mm \right) = 14.903 \ kN \cdot m$$

$$M_{z.Ed} := 0 \ kN \cdot m$$

Interaction (<1): $i := \dfrac{N_{Ed}}{N_{b.z.Rd}} + \dfrac{M_{y.Ed}}{M_{Rd}} + 1.5 \cdot \dfrac{M_{z.Ed}}{M_{c.z.Rd}} = 0.87$

$$\frac{N_{Ed}}{N_{b.z.Rd}} = 0.671 \qquad \frac{M_{y.Ed}}{M_{Rd}} = 0.199 \qquad \frac{M_{z.Ed}}{M_{c.z.Rd}} = 0$$

xxxxxxxxxxxxxxxxxxxxxxxxxxxxxxxxxxxxxxxxxxxxxxxxxxxxxxxxxxxxxxxxxxxxxxxxxxxxxxxxxxxx

4th Floor Column

(1) Corner Column

Catchment Area $A := 7.74 \ m^2$

Beam span, north $l_N := 5.8 \ m$

Beam span, east $l_E := 5.3 \ m$

Slab supporting beam reaction $R_{d.slab} := \left(\frac{l_N}{2} \right) \cdot f_d \cdot \left(\frac{l_E}{2} \right) + \left(\frac{l_E}{2} \cdot \omega_{edge} \right) = 52.361 \ kN$

Wall supporting beam reaction $R_{d.wall} := \left(\frac{l_N}{2} \cdot \omega_{edge} \right) = 12.544 \ kN$

Design Axial Load $N_{Ed} := 4 \cdot f_d \cdot A = 164.767 \ kN$

$$h := 152.4 \ mm$$
$$t_w := 5.8 \ mm$$

$$N_{b.y.3.0} := 867 \ kN \qquad N_{b.y.3.5} := 812 \ kN$$
$$N_{b.z.3.0} := 524 \ kN \qquad N_{b.z.3.5} := 431 \ kN$$
$$M_{b.Rd.3.0} := 47.3 \ kN \cdot m \qquad M_{b.Rd.3.5} := 43.9 \ kN \cdot m$$
$$N_{pl.Rd} := 1040 \ kN$$

Interpolation (as L=3.2m): $N_{b.y.Rd} := N_{b.y.3.0} - 0.2 \cdot \left(N_{b.y.3.0} - N_{b.y.3.5}\right) = 856 \ kN$

$$N_{b.z.Rd} := N_{b.z.3.0} - 0.2 \cdot \left(N_{b.z.3.0} - N_{b.z.3.5}\right) = 505.4 \ kN$$

buckling: $M_{b.Rd} := M_{b.Rd.3.0} - 0.2 \cdot \left(M_{b.Rd.3.0} - M_{b.Rd.3.5}\right) = 46.62 \ kN \cdot m$

$$\therefore n := \frac{N_{Ed}}{N_{pl.Rd}} = 0.158 \qquad \text{check <0.25 (if breached,}$$
used reduced resistances)

$$M_{c.y.Rd} := 58.2 \ kN \cdot m$$
$$M_{c.z.Rd} := 18.7 \ kN \cdot m$$

$$M_{Rd} := min\left(M_{b.Rd}, M_{c.y.Rd}\right) = 46.62 \ kN \cdot m$$

I - orientation

$$M_{y.Ed} := R_{d.wall} \cdot \left(\frac{h}{2} + 100 \cdot mm\right) = 2.21 \ kN \cdot m$$
$$M_{z.Ed} := R_{d.slab} \cdot \left(\frac{t_w}{2} + 100 \cdot mm\right) = 5.388 \ kN \cdot m$$

Interaction (<1): $i := \frac{N_{Ed}}{N_{b.z.Rd}} + \frac{M_{y.Ed}}{M_{Rd}} + 1.5 \cdot \frac{M_{z.Ed}}{M_{c.z.Rd}} = 0.806$

$$\frac{N_{Ed}}{N_{b.z.Rd}} = 0.326 \qquad \frac{M_{y.Ed}}{M_{Rd}} = 0.047 \qquad \frac{M_{z.Ed}}{M_{c.z.Rd}} = 0.288$$

H - orientation

$$M_{y.Ed} := R_{d.slab} \cdot \left(\frac{h}{2} + 100 \cdot mm\right) = 9.226 \ kN \cdot m$$
$$M_{z.Ed} := R_{d.wall} \cdot \left(\frac{t_w}{2} + 100 \cdot mm\right) = 1.291 \ kN \cdot m$$

Interaction (<1): $i := \dfrac{N_{Ed}}{N_{b.z.Rd}} + \dfrac{M_{y.Ed}}{M_{Rd}} + 1.5 \cdot \dfrac{M_{z.Ed}}{M_{c.z.Rd}} = 0.627$

$$\dfrac{N_{Ed}}{N_{b.z.Rd}} = 0.326 \qquad \dfrac{M_{y.Ed}}{M_{Rd}} = 0.198 \qquad \dfrac{M_{z.Ed}}{M_{c.z.Rd}} = 0.069$$

(2) Edge (Stair) Column

Catchment Area
$$A := 14.76 \ m^2 \quad A_W := 7.74 \ m^2 \quad A_E := 7.02 \ m^2$$

Beam span, west
$$l_W := 5.8 \ m$$

Beam span, east
$$l_E := 6.72 \ m$$

East slab supporting beam reaction
$$R_{d.east} := A_E \cdot f_d + \left(\dfrac{l_E}{2} \cdot \omega_{edge}\right) = 51.893 \ kN$$

West slab supporting beam reaction
$$R_{d.west} := A_W \cdot f_d + \left(\dfrac{l_W}{2} \cdot \omega_{edge}\right) = 53.735 \ kN$$

Design Axial Load
$$N_{Ed} := 4 \cdot f_d \cdot A = 314.206 \ kN$$

==TRIAL SECTION: UC 152x152x23==

$$h := 152.4 \ mm$$
$$t_w := 5.8 \ mm$$

$N_{b.y.3.0} := 867 \ kN$ $\qquad\qquad$ $N_{b.y.3.5} := 812 \ kN$
$N_{b.z.3.0} := 524 \ kN$ $\qquad\qquad$ $N_{b.z.3.5} := 431 \ kN$
$M_{b.Rd.3.0} := 47.3 \ kN \cdot m$ $\qquad\;$ $M_{b.Rd.3.5} := 43.9 \ kN \cdot m$
$\qquad\qquad$ $N_{pl.Rd} := 1040 \ kN$

Interpolation (as L=3.2m): $N_{b.y.Rd} := N_{b.y.3.0} - 0.2 \cdot \left(N_{b.y.3.0} - N_{b.y.3.5}\right) = 856 \ kN$

$$N_{b.z.Rd} := N_{b.z.3.0} - 0.2 \cdot \left(N_{b.z.3.0} - N_{b.z.3.5}\right) = 505.4 \ kN$$

buckling: $M_{b.Rd} := M_{b.Rd.3.0} - 0.2 \cdot \left(M_{b.Rd.3.0} - M_{b.Rd.3.5}\right) = 46.62 \ kN \cdot m$

$$\therefore n := \dfrac{N_{Ed}}{N_{pl.Rd}} = 0.302 \qquad \color{red}{\text{check <0.25 (if breached, used reduced resistances)}}$$

$$M_{c.y.Rd} := 58.2 \ kN \cdot m$$
$$M_{c.z.Rd} := 18.7 \ kN \cdot m$$

$$M_{Rd} := min\left(M_{b.Rd}, M_{c.y.Rd}\right) = 46.62 \; kN \cdot m$$

I - orientation

$$M_{y.Ed} := 0 \; kN \cdot m$$

$$M_{z.Ed} := \left|\left(R_{d.east} - R_{d.west}\right)\right| \cdot \left(\frac{t_w}{2} + 100 \cdot mm\right) = 0.19 \; kN \cdot m$$

Interaction (<1):
$$i := \frac{N_{Ed}}{N_{b.z.Rd}} + \frac{M_{y.Ed}}{M_{Rd}} + 1.5 \cdot \frac{M_{z.Ed}}{M_{c.z.Rd}} = 0.637$$

$$\frac{N_{Ed}}{N_{b.z.Rd}} = 0.622 \qquad \frac{M_{y.Ed}}{M_{Rd}} = 0 \qquad \frac{M_{z.Ed}}{M_{c.z.Rd}} = 0.01$$

H - orientation

$$M_{y.Ed} := \left|\left(R_{d.east} - R_{d.west}\right)\right| \cdot \left(\frac{h}{2} + 100 \cdot mm\right) = 0.325 \; kN \cdot m$$

$$M_{z.Ed} := 0 \; kN \cdot m$$

Interaction (<1):
$$i := \frac{N_{Ed}}{N_{b.z.Rd}} + \frac{M_{y.Ed}}{M_{Rd}} + 1.5 \cdot \frac{M_{z.Ed}}{M_{c.z.Rd}} = 0.629$$

$$\frac{N_{Ed}}{N_{b.z.Rd}} = 0.622 \qquad \frac{M_{y.Ed}}{M_{Rd}} = 0.007 \qquad \frac{M_{z.Ed}}{M_{c.z.Rd}} = 0$$

(3) Internal Column

Catchment Area
$$A := 19.62 \; m^2 \qquad A_W := 15.49 \; m^2 \quad A_E := 4.13 \; m^2$$

East slab supporting beam reaction
$$R_{d.east} := A_E \cdot f_d = 21.98 \; kN$$

West slab supporting beam reaction
$$R_{d.west} := A_W \cdot f_d = 82.437 \; kN$$

Design Axial Load
$$N_{Ed} := 4 \cdot f_d \cdot A = 417.665 \; kN$$

$$h := 157.6 \ mm$$
$$t_w := 6.5 \ mm$$

$$N_{b.y.3.0} := 1150 \ kN \qquad N_{b.y.3.5} := 1080 \ kN$$
$$N_{b.z.3.0} := 714 \ kN \qquad N_{b.z.3.5} := 592 \ kN$$
$$M_{b.Rd.3.0} := 72.4 \ kN \cdot m \qquad M_{b.Rd.3.5} := 67.9 \ kN \cdot m$$
$$N_{pl.Rd} := 1360 \ kN$$

Interpolation (as L=3.2m): $N_{b.y.Rd} := N_{b.y.3.0} - 0.2 \cdot \left(N_{b.y.3.0} - N_{b.y.3.5}\right) = 1136 \ kN$

$$N_{b.z.Rd} := N_{b.z.3.0} - 0.2 \cdot \left(N_{b.z.3.0} - N_{b.z.3.5}\right) = 689.6 \ kN$$

buckling: $M_{b.Rd} := M_{b.Rd.3.0} - 0.2 \cdot \left(M_{b.Rd.3.0} - M_{b.Rd.3.5}\right) = 71.5 \ kN \cdot m$

$$\therefore n := \frac{N_{Ed}}{N_{pl.Rd}} = 0.307$$ check <0.25 (if breached, used reduced resistances)

$$M_{c.y.Rd} := 70.3 \ kN \cdot m$$
$$M_{c.z.Rd} := 39.4 \ kN \cdot m$$

$$M_{Rd} := min \left(M_{b.Rd}, M_{c.y.Rd}\right) = 70.3 \ kN \cdot m$$

I - orientation

$$M_{y.Ed} := 0 \ kN \cdot m$$

$$M_{z.Ed} := \left|\left(R_{d.east} - R_{d.west}\right)\right| \cdot \left(\frac{t_w}{2} + 100 \cdot mm\right) = 6.242 \ kN \cdot m$$

Interaction (<1): $i := \dfrac{N_{Ed}}{N_{b.z.Rd}} + \dfrac{M_{y.Ed}}{M_{Rd}} + 1.5 \cdot \dfrac{M_{z.Ed}}{M_{c.z.Rd}} = 0.843$

$$\frac{N_{Ed}}{N_{b.z.Rd}} = 0.606 \qquad \frac{M_{y.Ed}}{M_{Rd}} = 0 \qquad \frac{M_{z.Ed}}{M_{c.z.Rd}} = 0.158$$

H - orientation

$$M_{y.Ed} := \left|\left(R_{d.east} - R_{d.west}\right)\right| \cdot \left(\frac{h}{2} + 100 \cdot mm\right) = 10.81 \ kN \cdot m$$

$$M_{z.Ed} := 0 \ kN \cdot m$$

Interaction (<1): $i := \dfrac{N_{Ed}}{} + \dfrac{M_{y.Ed}}{} + 1.5 \cdot \dfrac{M_{z.Ed}}{} = 0.759$

$$\frac{N_{Ed}}{N_{b.z.Rd}} = 0.606 \qquad \frac{M_{y.Ed}}{M_{Rd}} = 0.154 \qquad \frac{M_{z.Ed}}{M_{c.z.Rd}} = 0$$

(4) Edge (Clear) Column

Catchment Area	$A := 15.48 \ m^2$	
Beam span, north	$l_N := 5.8 \ m$	
Beam span, south	$l_S := 5.8 \ m$	

East slab supporting beam reaction

$$R_{d.east} := A \cdot f_d = 82.383 \ kN$$

North wall supporting beam reaction

$$R_{d.north} := \left(\frac{l_N}{2} \cdot \omega_{edge}\right) = 12.544 \ kN$$

South wall supporting beam reaction

$$R_{d.south} := \left(\frac{l_S}{2} \cdot \omega_{edge}\right) = 12.544 \ kN$$

Design Axial Load

$$N_{Ed} := 4 \cdot f_d \cdot A = 329.534 \ kN$$

TRIAL SECTION: UC 152x152x30

$$h := 157.6 \ mm$$
$$t_w := 6.5 \ mm$$

$N_{b.y.3.0} := 1150 \ kN$ $N_{b.y.3.5} := 1080 \ kN$

$N_{b.z.3.0} := 714 \ kN$ $N_{b.z.3.5} := 592 \ kN$

$M_{b.Rd.3.0} := 72.4 \ kN \cdot m$ $M_{b.Rd.3.5} := 67.9 \ kN \cdot m$

$$N_{pl.Rd} := 1360 \ kN$$

Interpolation (as L=3.2m): $N_{b.y.Rd} := N_{b.y.3.0} - 0.2 \cdot \left(N_{b.y.3.0} - N_{b.y.3.5}\right) = 1136 \ kN$

$$N_{b.z.Rd} := N_{b.z.3.0} - 0.2 \cdot \left(N_{b.z.3.0} - N_{b.z.3.5}\right) = 689.6 \ kN$$

buckling: $M_{b.Rd} := M_{b.Rd.3.0} - 0.2 \cdot \left(M_{b.Rd.3.0} - M_{b.Rd.3.5}\right) = 71.5 \ kN \cdot m$

$$\therefore n := \frac{N_{Ed}}{N_{pl.Rd}} = 0.242 \qquad \text{check <0.25 (if breached, used reduced resistances)}$$

$$M_{c.y.Rd} := 87.9 \ kN \cdot m$$
$$M_{c.z.Rd} := 39.6 \ kN \cdot m$$

$$M_{Rd} := min\left(M_{b.Rd}, M_{c.y.Rd}\right) = 71.5 \ kN \cdot m$$

I - orientation

$$M_{y.Ed} := 0 \ kN \cdot m$$

$$M_{z.Ed} := \left|R_{d.east}\right| \cdot \left(\frac{t_w}{2} + 100 \cdot mm\right) = 8.506 \ kN \cdot m$$

Interaction (<1): $\quad i := \dfrac{N_{Ed}}{N_{b.z.Rd}} + \dfrac{M_{y.Ed}}{M_{Rd}} + 1.5 \cdot \dfrac{M_{z.Ed}}{M_{c.z.Rd}} = 0.8$

$$\frac{N_{Ed}}{N_{b.z.Rd}} = 0.478 \qquad \frac{M_{y.Ed}}{M_{Rd}} = 0 \qquad \frac{M_{z.Ed}}{M_{c.z.Rd}} = 0.215$$

H - orientation

$$M_{y.Ed} := \left|R_{d.east}\right| \cdot \left(\frac{h}{2} + 100 \cdot mm\right) = 14.73 \ kN \cdot m$$

$$M_{z.Ed} := 0 \ kN \cdot m$$

Interaction (<1): $\quad i := \dfrac{N_{Ed}}{N_{b.z.Rd}} + \dfrac{M_{y.Ed}}{M_{Rd}} + 1.5 \cdot \dfrac{M_{z.Ed}}{M_{c.z.Rd}} = 0.684$

$$\frac{N_{Ed}}{N_{b.z.Rd}} = 0.478 \qquad \frac{M_{y.Ed}}{M_{Rd}} = 0.206 \qquad \frac{M_{z.Ed}}{M_{c.z.Rd}} = 0$$

Appendix H

Hypothetical Asymmetric Steel Beams

Domestic residence, hence $\quad\quad\quad \psi_0 := 0.7 \quad\quad$ UK NA to BS EN 1990, Table NA.1.1

floor-floor height, $\quad\quad\quad\quad\quad\quad h_{storey} := 3 \ m$

density of CLT, $\quad\quad\quad\quad\quad\quad \gamma_{CLT} := 4.8 \ \dfrac{kN}{m^3}$

wall panel thickness, (double panel) $\quad t_{wall} := 256 \ mm$

$\quad\quad\quad$ Hence, approx. edge load $\quad\quad \omega_{edge} := 1.1 \cdot t_{wall} \cdot h_{storey} \cdot \gamma_{CLT} = 4.055 \ \dfrac{kN}{m}$

Dead Load from slab $\quad\quad\quad\quad\quad d := 200 \ mm$

$\quad\quad\quad\quad\quad\quad\quad\quad\quad\quad g_{k.slab} := \gamma_{CLT} \cdot d = 0.96 \ \dfrac{kN}{m^2}$

Services and finishes $\quad\quad\quad\quad g_{k.services} := 1.5 \ \dfrac{kN}{m^2}$

Permanent Load $\quad\quad\quad\quad\quad g_k := g_{k.slab} + g_{k.services} = 2.46 \ \dfrac{kN}{m^2}$

Imposed Load $\quad\quad\quad\quad\quad q_k := 1.5 \ \dfrac{kN}{m^2} \quad\quad\quad g_k + q_k = 3.96 \ \dfrac{kN}{m^2}$

$\quad \xi := 0.925 \quad\quad \gamma_g := 1.35 \quad\quad \gamma_q := 1.5$

$\quad\quad\quad$ working UDL $\quad\quad\quad\quad f_d := \xi \cdot \gamma_g \cdot g_k + \gamma_q \cdot q_k = 5.322 \ \dfrac{kN}{m^2}$

Construction
$\quad\quad\quad\quad\quad\quad q_c := 0.75 \ \dfrac{kN}{m^2} \quad\quad$ personnel + small equipment
$\quad\quad\quad\quad\quad\quad g_c := g_{k.slab} = 0.96 \ \dfrac{kN}{m^2} \quad\quad$ slab units

$ASB249 := 0$
$ASB196 := 1$
$ASB185 := 2$
$ASB155 := 3$
$ASB153 := 4$
$ASB136 := 5$
$ASB124 := 6$
$ASB105 := 7$
$ASB100 := 8$
$ASB74 := 9$
$ASBhyp := 10$

W	h	b_t	b_b	t_w	t_f	r
$\left(\dfrac{kg}{m}\right)$	(mm)	(mm)	(mm)	(mm)	(mm)	(mm)
249	342	203	313	40	40	27
196	342	183	293	20	40	27
185	320	195	305	32	29	27
155	326	179	289	16	32	27
153	310	190	300	27	24	27
136	288	190	300	25	22	24
124	296	178	288	13	26	24
105	288	176	286	11	22	24
100	276	184	294	19	16	24
73.6	272	175	285	10	14	24
50.9	240	150	240	7.5	12	8.9

I_{yy}	I_{zz}	k_y	k_z	$W_{el.y}$	z_e	z_p	$W_{pl.y}$	$W_{pl.z}$	U	X	I_w	I_T	A
(cm^4)	(cm^4)	(cm)	(cm)	(cm^3)	(cm)	(cm)	(cm^3)	(cm^3)			$\left((0.1\ m)^6\right)$	(cm^4)	(cm^2)
52900	13200	12.9	6.4	2760	19.2	22.6	3760	1510	0.82	6.8	2	2000	318
45900	10500	13.6	6.48	2320	19.8	28.1	3060	1230	0.84	7.86	1.5	1180	249
35700	8750	12.3	6.1	1980	18	21	2660	1030	0.82	8.56	1.2	871	235
34500	7990	13.2	6.35	1830	18.9	27.3	2360	950	0.84	9.4	1.07	620	198
28400	6840	12.1	5.93	1630	17.4	20.4	2160	817	0.82	9.97	0.895	513	195
22200	6260	11.3	6	1370	16.3	19.2	1810	741	0.81	10.2	0.71	379	174
23500	6410	12.2	6.37	1360	17.3	25.7	1730	761	0.83	10.5	0.721	332	158
19200	5300	12	6.3	1150	16.8	25.3	1440	633	0.83	12.1	0.574	207	133
15500	4250	11	5.76	995	15.6	18.4	1290	511	0.81	13.2	0.451	160	128
12200	3330	11.4	5.96	776	15.7	21.3	978	403	0.83	16.7	0.338	72	93.7
6591	1721	10.1	5.16	470	14	18.8	590				0.156	26	64.8

$E := 210\ GPa$ $G := 81\ GPa$ $f_y := 355\ MPa$

$\gamma_{M0} := 1.0$ $\gamma_{M1} := 1.0$

$$t_f := 12 \ mm \qquad t_w := 8 \ mm \qquad\qquad r := 8.9 \ mm$$

$$B_b := 240 \ mm \qquad\qquad B_t := \frac{B_b}{1.6} = 0.15 \ m \qquad\qquad h := 240 \ mm$$

$$A_{hyp} := \left(h - 2 \ t_f\right) \cdot t_w + t_f \cdot \left(B_b + B_t\right) + r^2 \cdot (4 - \pi) = 64.76 \ cm^2$$

$$W_{hyp} := 7860 \ \frac{kg}{m^3} \cdot A_{hyp} = 50.901 \ \frac{kg}{m}$$

$$\frac{73.6 \ kg}{93.7 \ cm^2} = \left(7.855 \cdot 10^3\right) \frac{kg}{m^2}$$

$$170 \ mm \cdot 15 \ mm \cdot 7860 \ \frac{kg}{m^3} = 20.043 \ \frac{kg}{m}$$

$$A_{tf} := t_f \cdot B_t = 18 \ cm^2 \qquad A_{bf} := t_f \cdot B_b = 28.8 \ cm^2 \qquad A_w := \left(h - 2 \ t_f\right) \cdot t_w = 17.28 \ cm^2$$

$$h_{tf} := h - \left(\frac{t_f}{2}\right) = 234 \ mm \qquad h_{bf} := \frac{t_f}{2} = 6 \ mm \qquad h_w := \frac{h}{2} = 120 \ mm$$

$$y := \frac{\left(A_{tf} \cdot h_{tf} + A_{bf} \cdot h_{bf} + A_w \cdot h_w\right)}{A_{hyp}} = 99.728 \ mm$$

$$I_{tf} := \frac{B_t \cdot t_f^{\ 3}}{12} + \left(A_{tf} \cdot h_{tf}^{\ 2}\right) = \left(9.858 \cdot 10^3\right) \ cm^4$$

$$I_{bf} := \frac{B_b \cdot t_f^{\ 3}}{12} + \left(A_{bf} \cdot h_{bf}^{\ 2}\right) = 13.824 \ cm^4$$

$$I_{web} := \frac{t_w \cdot \left(h - 2 \ t_f\right)^3}{12} + A_w \cdot h_w^{\ 2} = \left(3.16 \cdot 10^3\right) \ cm^4$$

$$I_{yy.hyp} := \left(I_{tf} + I_{bf} + I_{web}\right) - A_{hyp} \cdot y^2 = 6591.377 \ cm^4$$

$$I_{tf} := \frac{B_t^{\ 3} \cdot t_f}{12} = 337.5 \ cm^4$$

$$I_{bf} := \frac{B_b^{\ 3} \cdot t_f}{12} = \left(1.382 \cdot 10^3\right) \ cm^4$$

$$I_{web} := \frac{t_w^{\ 3} \cdot \left(h - 2 \ t_f\right)}{12} = 0.922 \ cm^4$$

$$I_{zz.hyp} := I_{tf} + I_{bf} + I_{web} = 1720.822 \ cm^4$$

$$k_y := \sqrt{\frac{I_{yy.hyp}}{A_{hyp}}} = 10.089 \ cm \qquad\qquad k_z := \sqrt{\frac{I_{zz.hyp}}{A_{hyp}}} = 5.155 \ cm$$

$$z_e := h - y = 14.027 \ cm$$

$$z_p := \frac{\left(\left(B_b - B_t\right) \cdot t_f\right)}{2 \ t_w} + t_f + \left(\frac{h - 2 \ t_f}{2}\right) = 18.75 \ cm$$

$$W_e := \frac{I_{yy.hyp}}{z_e} = 469.901 \ cm^3$$

$$c_{upper} := \frac{2 \cdot \left(B_t \cdot t_f \cdot \left(\frac{t_f}{2}\right) + t_w \cdot \left(z_p - t_f\right) \cdot \left(t_f + \frac{z_p - t_f}{2}\right)\right)}{A_{hyp}} = 4.659 \ cm$$

$$c_{lower} := 2 \cdot \frac{\left(B_b \cdot t_f \cdot \left(h - \frac{t_f}{2}\right) + t_w \cdot \left(h - t_f - z_p\right) \cdot \left(z_p + \left(\frac{h - t_f - z_p}{2}\right)\right)\right)}{A_{hyp}} = 22.892 \ cm$$

$$W_{pl} := \left(\left(z_p - c_{upper}\right) + \left(c_{lower} - z_p\right)\right) \cdot \frac{A_{hyp}}{2} = 590.382 \ cm^3$$

$$e_{s.bf} := \frac{\left(h - t_f\right) \cdot \left(\frac{t_f \cdot B_t^{\ 3}}{12}\right)}{\left(\left(\frac{t_f \cdot B_t^{\ 3}}{12}\right) + \left(\frac{t_f \cdot B_b^{\ 3}}{12}\right)\right)} = 44.741 \ mm$$

$$I_T := \frac{\left(\left(B_t + B_b\right) \cdot t_f^{\ 3} + \left(h - 2 \ t_f\right) \cdot t_w^{\ 3}\right)}{3} = 26.15 \ cm^4$$

$$I_W := \frac{t_f \cdot h^2}{12} \cdot \frac{B_b^{\ 3} \cdot B_t^{\ 3}}{B_b^{\ 3} + B_t^{\ 3}} = 0.156 \ \left(0.1 \ m\right)^6$$

$RHSFB200.150.8 := 0$
$RHSFB200.150.10 := 1$
$RHSFB200.150.12 := 2$
$RHSFB250.150.8 := 3$
$RHSFB250.150.10 := 4$
$RHSFB250.150.12 := 5$
$RHSFB300.200.8 := 6$
$RHSFB300.200.10 := 7$
$RHSFB300.200.12 := 8$
$RHSFB400.200.8 := 9$
$RHSFB400.200.10 := 10$
$RHSFB400.200.12 := 11$
$RHSFB450.250.8 := 12$
$RHSFB450.250.10 := 13$
$RHSFB450.250.12 := 14$

W $\left(\dfrac{kg}{m}\right)$	D (mm)	B_{RHS} (mm)	B_p (mm)	t_{RHS} (mm)	t_p (mm)	I_{yy} (cm^4)	I_{zz} (cm^4)	r_y (cm)
69.7	200	150	240	8	15	5451	4055	6.8
79.3	200	150	240	10	15	6251	4461	6.6
90.8	200	150	240	12.5	15	7107	4903	6.5
76	250	150	240	8	15	9087	4484	6.8
87.1	250	150	240	10	15	10449	4975	6.7
100.6	250	150	240	12.5	15	11938	5517	6.6
94.4	300	200	290	8	15	16614	8795	8.6
108.6	300	200	290	10	15	19226	9931	8.5
126.0	300	200	290	12.5	15	22147	11228	8.4
106.9	400	200	290	8	15	32322	10308	8.7
124.3	400	200	290	10	15	37511	11772	8.6
146.1	400	200	290	12.5	15	43409	13461	8.5
125.4	450	250	340	8	15	48873	17759	10.5
146	450	250	340	10	15	56914	20482	10.5
171	450	250	340	12.5	15	66155	23677	10.4

$W_{el.b}$	z_e	z_p	$W_{pl.y}$	$W_{t.RHS}$		I_T	A
(cm^3)	(cm)	(cm)	(cm^3)	(cm^3)		(cm^4)	(cm^2)
763	14.4	19.4	549	398		3670	88.8
816	13.8	18.9	661	475		4436	100.9
872	13.3	17.2	783	559		5314	115.6
1002	17.4	23.7	775	506		5048	96.8
1077	16.8	21.5	926	605		6117	110.9
1162	16.2	19.7	1087	717		7353	128.1
1538	20.7	28.6	1169	840		10595	120.3
1665	20.0	25.9	1404	1020		12941	138.4
1811	19.3	23.7	1661	1220		15710	160.5
2173	26.6	33.6	1810	1140		15768	136.3
2373	25.7	30.9	2146	1380		19292	158.5
2610	24.9	28.7	2507	1660		23471	185.5
2946	29.9	38.4	2401	1630		27121	160
3229	28.8	35.2	2861	1990		33322	186
3564	27.9	32.7	3383	2410		40757	218

$G := 81\ GPa$
$\gamma_{M1} := 1.0$

$E := 210\ GPa$
$\gamma_{M0} := 1.0$
$f_y := 355\ MPa$

BASE SECTION: RHS200x100x5

$$D := 220 \ mm \qquad B := 120 \ mm \qquad t := 6.3 \ mm \qquad r_o := 1 \ t = 6.3 \ mm$$
$$r_i := t = 6.3 \ mm$$

$$A_{RHS} := \left(2 \ B + 2 \ D - 8 \ r_o\right) \cdot t = 39.665 \ cm^2$$

$$w := B - 2 \ r_o = 0.107 \ m \qquad h := D - 2 \ r_o$$

$$I_1 := \frac{\left(B - 2 \ r_o\right) D^3}{12} = \left(9.53 \cdot 10^3\right) \ cm^4 \qquad I_2 := \frac{2 \cdot r_o \cdot \left(h - 2 \ r_o\right)^3}{12} = 776.169 \ cm^4$$

$$I_3 := \left(\frac{\pi \cdot r_o^4}{4}\right) \cdot \left(1 - \left(\frac{64}{9 \cdot \pi^2}\right)\right) + \left(\pi \cdot r_o^2\right) \cdot \left(\frac{h}{2} - r_o \cdot \left(1 - \frac{4}{3 \cdot \pi}\right)\right)^2 = 124.909 \ cm^4$$

$$I_4 := \frac{\left(B - 2 \ t - 2 \ r_i\right) \cdot \left(D - 2 \ t\right)^3}{12} = \left(7.048 \cdot 10^3\right) \ cm^4$$

$$I_5 := \frac{2 \ r_i \cdot \left(D - 2 \ t - 2 \ r_i\right)^3}{12} = 776.169 \ cm^4$$

$$I_6 := \left(\frac{\pi \cdot r_i^4}{4}\right) \cdot \left(1 - \frac{64}{9 \ \pi^2}\right) + \pi \cdot r_i^2 \cdot \left(\left(\frac{h - 2 \ t}{2}\right) - r_i \cdot \left(1 - \frac{4}{3 \ \pi}\right)\right)^2 = 109.681 \ cm^4$$

$$I_y := I_1 + I_2 + I_3 - \left(I_4 + I_5\right) = \left(2.607 \cdot 10^3\right) \ cm^4$$

$$I_{yy.RHS} := I_y = 2607.072 \ cm^4$$

$$t_p := 15 \ mm$$
$$B_p := B + 90 \ mm = 210 \ mm$$

$$A_{hyp} := A_{RHS} + t_p \cdot B_p = 71.165 \ cm^2$$

$$W_{hyp} := 7860 \ \frac{kg}{m^3} \cdot A_{hyp} = 55.936 \ \frac{kg}{m}$$

$$A_p := t_p \cdot B_p = 31.5 \ cm^2$$

$$h_{RHS} := \frac{D}{2} + t_p = 125 \ mm \qquad h_p := \frac{t_p}{2} = 7.5 \ mm$$

$$y := \frac{\left(A_{RHS} \cdot h_{RHS} + A_p \cdot h_p\right)}{A_{hyp}} = 72.99 \ mm$$

$$I_{RHS} := I_{yy.RHS} + \left(A_{RHS} \cdot h_{RHS}^2\right) = \left(8.805 \cdot 10^3\right) \ cm^4$$

$$I_p := \frac{B_p \cdot t_p^{\ 3}}{12} + \left(A_p \cdot h_p^{\ 2}\right) = 23.625 \ cm^4$$

$$I_{yy.hyp} := \left(I_{RHS} + I_p\right) - A_{hyp} \cdot y^2 = 5036.943 \ cm^4$$

$$A_h := (B - t) \cdot (D - t) - \left(\frac{r_i + r_o}{2}\right)^2 \cdot (4 - \pi) = 242.636 \ cm^2$$

$$h := 2 \cdot \left((B - t) + (D - t)\right) - 2 \cdot \left(\frac{r_i + r_o}{2}\right) \cdot (4 - \pi) = 64.398 \ cm$$

$$I_{T.RHS} := \frac{4 \cdot A_h^{\ 2} \cdot t}{h} + \frac{t^3 \cdot h}{3} = \left(2.309 \cdot 10^3\right) \ cm^4$$

$$W_{t.RHS} := \frac{I_{T.RHS}}{\left(t + \dfrac{2 \cdot A_h}{h}\right)} = 282.791 \ cm^3$$

$$z_1 := 2 \cdot r_o \cdot (B - 2 \ r_o) \cdot \left(\frac{D}{2} - \frac{r_o}{2}\right) = 144.594 \ cm^3 \quad z_2 := 2 \cdot \frac{\left(B \cdot \left(\dfrac{D}{2} - r_o\right) \cdot (D - 2 \ r_o)\right)}{4} = \left(1.29 \cdot 10^3\right) \ cm^3$$

$$z_3 := 2 \cdot \left(\frac{\pi \cdot r_o^{\ 2}}{2}\right) \cdot \left(\frac{D}{2} - r_o + \frac{4 \cdot r_o}{3 \ \pi}\right) = 13.264 \ cm^3$$

$$z_4 := 2 \cdot \left(r_i \cdot \left(B - 2 \cdot (t + r_i)\right) \cdot \left(\frac{D - 2 \ t - r_i}{2}\right)\right) = 120.105 \ cm^3$$

$$z_5 := 2 \cdot \left((B - 2 \ t) \cdot \left(\frac{D}{2} - t - r_i\right) \cdot \left(\frac{D - 2 \ t - 2 \ r_i}{4}\right)\right) = \left(1.019 \cdot 10^3\right) \ cm^3$$

$$z_6 := 2 \cdot \left(\frac{\pi \cdot r_i^{\ 2}}{2}\right) \cdot \left(\frac{D}{2} - t - r_i + \frac{4 \cdot r_i}{3 \cdot \pi}\right) = 12.478 \ cm^3$$

$$W_{pl.y.RHS} := 0.97 \cdot \left(z_1 + z_2 + z_3 - \left(z_4 + z_5 + z_6\right)\right) = 287.934 \ cm^3$$

$$A_{RHS} = 39.665 \ cm^2 \qquad\qquad A_p = 31.5 \ cm^2$$

$$t_p = 1.5 \ cm \qquad B_p = 21 \ cm$$

$$y_{PNA} := \left\| \begin{array}{l} \text{if } A_p > A_{RHS} \\ \quad \left\| \left(\left(\dfrac{A_p - A_{RHS}}{2 \cdot B_p} \right) + D \right) \right. \\ \text{else if } \left(\dfrac{A_{RHS} - A_p}{2} \right) > (t \cdot B) \\ \quad \left\| \left\| \left(D - t - \left(\dfrac{A_{RHS} - A_p - (t \cdot B)}{4 \ t} \right) \right) \right. \right. \\ \text{else} \\ \quad \left\| \left(D - \left(\dfrac{A_{RHS} - A_p}{2 \ B} \right) \right) \right. \end{array} \right.$$

$$y_{PNA} = 216.598 \ mm$$

$$c_u := \left\| \begin{array}{l} \text{if } A_p > A_{RHS} \\ \quad \left\| \left(D + t_p - \dfrac{A_{RHS} \cdot \left(\dfrac{D}{2} + t_p \right) + (y_{PNA} - D) \cdot B_p \cdot \left(\dfrac{y_{PNA} - D}{2} + (D + t_p - y_{PNA}) \right)}{A_{RHS} + (y_{PNA} - D) \cdot B_p} \right) \right. \\ \text{else if } \left(\dfrac{A_{RHS} - A_p}{2} \right) < (t \cdot B) \\ \quad \left\| \left\| \left(D + t_p - \dfrac{\left(A_{RHS} \cdot \left(\dfrac{D}{2} + t_p \right) \right) - (D - y_{PNA}) \cdot B \cdot \left(\dfrac{D - y_{PNA}}{2} + t_p \right)}{A_{RHS} - (D - y_{PNA}) \cdot B} \right) \right. \right. \\ \text{else} \\ \quad \left\| \left(D + t_p - \dfrac{B \cdot t \cdot \left(D - \left(\dfrac{t}{2} \right) + t_p \right) + \left(2 \cdot t \cdot (y_{PNA} - t) \cdot \left(D - \left(\dfrac{y_{PNA} - t}{2} \right) + t_p \right) \right)}{A_{RHS} - (B \cdot t) - 2 \cdot (D - t - y_{PNA}) \cdot t} \right) \right. \end{array} \right.$$

$$c_u = 97.575 \ mm$$

$$c_l := \left\| \begin{array}{l} \text{if } A_p > A_{RHS} \\ \quad \left\| \left(D + t_p - \left(\dfrac{D + t_p - y_{PNA}}{2} \right) \right) \right. \\ \text{else if } \left(\dfrac{A_{RHS} - A_p}{2} \right) < (t \cdot B) \\ \quad \left\| \left(\dfrac{\left(A_p \cdot \left(D + \dfrac{t_p}{2} \right) \right) + (D - y_{PNA}) \cdot B \cdot \left(D - \left(\dfrac{D - y_{PNA}}{2} \right) \right)}{A_p + (D - y_{PNA}) \cdot B} \right) \right. \\ \text{else} \\ \quad \left\| \left(\dfrac{A_p \cdot \left(D + \dfrac{t_p}{2} \right) + \left(B \cdot t \cdot \left(D - \dfrac{t}{2} \right) \right) + \left(2 \cdot t \cdot (D - t - y_{PNA}) \cdot \left(D - t - \left(\dfrac{D - t - y_{PNA}}{2} \right) \right) \right)}{A_p + (B \cdot t) + 2 \cdot (D - t - y_{PNA}) \cdot t} \right) \right. \end{array} \right.$$

$$c_l = 226.444 \ mm$$

$$W_{pl.hyp} := \left(\dfrac{A_{RHS} + A_p}{2} \right) \cdot \left(\left| y_{PNA} - c_u \right| + \left| y_{PNA} - c_l \right| \right) = 458.5 \ cm^3$$

$B = 120 \ mm$ $\qquad$ $D = 220 \ mm$ $\qquad$ $t = 6.3 \ mm$ $\qquad$ $t_p = 15 \ mm$

$\qquad$ $A_{hyp} = 71.165 \ cm^2$ $\quad$ $W_{hyp} = 55.936 \ \dfrac{kg}{m}$ $\qquad$ $B_p = 210 \ mm$

$I_{yy.hyp} = 5037 \ cm^4$

$\qquad$ $W_{t.RHS} = 282.8 \ cm^3$

$I_{T.RHS} = 2309 \ cm^4$

Appendix I

Environmental Data and Calculation

	Timber	Timber (hyp)	Steel Comp	RC Fame	CLT only
CLT	203.5	203.5	-	-	300
Steel	54.3	43.9	43.2		TONNES
Concrete	-	-	890	1213	
Reinforcement			28	2.3	

	CLT	CLT - Designed Beams	Composite	RC
Superstructure Mass	257.8	247.4	966.7	1215.5

Timber Design

Beams *Steel*

Type	Designation	Weight/m	Length(m)	No per floor	no. floors	Total Mass
1	200ASB74	73.6	5.34	4	8	12576.77
2	RHSFB200x150x8	69.7	5.34	4	8	11910.34
3.edge	RHSFB200x150x8	69.7	6.72	2	8	7494.144
4	200ASB74	73.6	1.984	2	8	2336.358
EDGE	RHS180x100x5	21	5.8	6	8	5846.4
TIE	UKT102x152x17	16.4	5.8	4	8	3043.84
					TOTAL	43207.85

Beams *Steel (hypothetical)*

Type	Designation	Weight/m	Length(m)	No per floor	no. floors	Total Mass
1	ASBhyp	50.9	5.34	4	8	8697.792
2	RHSFBhyp1	44.4	5.34	4	8	7587.072
3.edge	RHSFBhyp2	55.9	6.72	2	8	6010.368
4	ASBhyp	50.9	1.984	2	8	1615.77
EDGE	RHS180x100x5	21	5.8	6	8	5846.4
TIE	UKT102x152x17	16.4	5.8	4	8	3043.84
					TOTAL	32801.24

Columns *Steel*

Type	Designation	Weight/m (kg)	Length	No per floor	no. floors	Total Mass
1. Base	UC152x152x23	23	3.2	4	3	883.2
1.upper	UC152x152x23	23	3.2	4	5	1472
2. base	UC152x152x30	30	3.2	4	3	1152
2. upper	UC152x152x23	23	3.2	4	5	1472
3. base	UC152x152x44	44	3.2	2	3	844.8
3. upper	UC152x152x30	30	3.2	4	5	1920
4. base	UC152x152x37	37	3.2	4	3	1420.8
4.upper	UC152x152x30	30	3.2	4	5	1920
					TOTAL	11084.8

Slab *CLT* 480 kg/m^3

Designation	Depth mm	Area per floor n	Volume m^3	no. floors	Total Mass
	200	265	53	8	203520

Steel Design

Beams Steel

Type	Designation	Weight/m	Length	No per floor	no. floors	Total Mass
1	UB356x171x51	51	5.34	4	8	8714.88
2	UB254x146x37	37	5.34	4	8	5297.28
3	UB305x165x54	54	6.72	2	8	5806.08
4	UB254x146x31	31	1.984	2	8	984.064
EDGE	RHS180x100x5	21	5.8	6	8	5846.4
TIE	UKT102x152x17	16.4	5.8	4	8	3043.84
					TOTAL	29692.54

Columns *Steel*

Type	Designation	Weight/m	Length	No per floor	no. floors	Total Mass
1. Base	UC152x152x30	30	3.2	4	3	1152
1.upper	UC152x152x30	30	3.2	4	5	1920
2. base	UC152x152x37	37	3.2	4	3	1420.8
2. upper	UC152x152x23	23	3.2	4	5	1472
3. base	UC203x203x46	46	3.2	2	3	883.2
3. upper	UC152x152x37	37	3.2	4	5	2368
4. base	UC152x152x51	51	3.2	4	3	1958.4
4.upper	UC152x152x37	37	3.2	4	5	2368
					TOTAL	13542.4

Slab *Concrete* 2400 kg/m^3

Designation	Depth mm	Area per floor m	Volume m^3	no. floors	Total Mass
	175	265	46.375	8	890400
Reinforcement	13.4	265		8	28408
mesh (A142)	2.2	265		8	4664

kg/m^2

RC Frame

Beams *Concrete*

Type	Designation
NONE	

Columns *Concrete*

Type	Designation	Weight/m	Length	No per floor	no. floors	Total Mass
internal	375x375	337.5	2.6	4	8	28080
edge	375x225	202.5	2.6	6	8	25272
corner	275x275	181.5	2.6	4	8	15100.8

Slab *Concrete* 2400 kg/m^3

Designation	Depth mm	Area per floor m^2	Volume m^3	no. floors	Total Mass
	225	265	59.625	8	1144800
		Reinforcement			2289.6

CLT Design – Option 1

The University Of Sheffield.

Results

Embodied Energy

Total embodied energy of foundations is	0 MJ
Total embodied energy of ground floor slab is	0 MJ
Embodied energy of steel columns is	238328 MJ
Total embodied energy of columns is	238328 MJ
Embodied energy of steel beams is	928972 MJ
Total embodied energy of beams is	928972 MJ
Embodied energy of cross-laminated timber is	2442240 MJ
Total embodied energy of upper floor systems is	2442240 MJ
Total embodied energy of roof system is	0 MJ

Total embodied energy is	3609540 MJ
Embodied energy per m^2 is	1703 MJ/m^2
Total embodied energy if structure DfD* is	1804770 MJ
Embodied energy if stucture DfD per m^2 is	851 MJ/m^2

Total embodied energy saving if DfD is	1804770 MJ

Embodied Carbon

Total embodied carbon of foundations is	0 kg CO_2e
Total embodied carbon of ground floor slab is	0 kg CO_2e
Embodied carbon of steel columns is	16960 kg CO_2e
Total embodied carbon of columns is	16960 kg CO_2e
Embodied carbon of steel beams is	66108 kg CO_2e
Total embodied carbon of beams is	66108 kg CO_2e
Embodied carbon of cross-laminated timber is	85478 kg CO_2e
Total embodied carbon of upper floor systems is	85478 kg CO_2e
Total embodied carbon of roof system is	0 kg CO_2e

Total embodied carbon is	168547 kg CO_2e
Embodied carbon per m^2 is	80 kg CO_2e/m^2
Total embodied carbon if structure DfD* is	84273 kg CO_2e
Embodied carbon if structure DfD per m^2 is	40 kg CO_2e/m^2

Total embodied carbon saving if DfD is	84273 kg CO_2e

CLT Design – Option 2, hypo

Results

Embodied Energy

Total embodied energy of foundations is	0 MJ
Total embodied energy of ground floor slab is	0 MJ
Embodied energy of steel columns is	238306 MJ
Total embodied energy of columns is	238306 MJ
Embodied energy of steel beams is	705222 MJ
Total embodied energy of beams is	705222 MJ
Embodied energy of cross-laminated timber is	2442240 MJ
Total embodied energy of upper floor systems is	2442240 MJ
Total embodied energy of roof system is	0 MJ

Total embodied energy is	3385768 MJ
Embodied energy per m^2 is	1597 MJ/m^2
Total embodied energy if structure DfD* is	1692884 MJ
Embodied energy if stucture DfD per m^2 is	799 MJ/m^2

Total embodied energy saving if DfD is	1692884 MJ

Embodied Carbon

Total embodied carbon of foundations is	0 kg CO_2e
Total embodied carbon of ground floor slab is	0 kg CO_2e
Embodied carbon of steel columns is	16959 kg CO_2e
Total embodied carbon of columns is	16959 kg CO_2e
Embodied carbon of steel beams is	50186 kg CO_2e
Total embodied carbon of beams is	50186 kg CO_2e
Embodied carbon of cross-laminated timber is	85478 kg CO_2e
Total embodied carbon of upper floor systems is	85478 kg CO_2e
Total embodied carbon of roof system is	0 kg CO_2e

Total embodied carbon is	152622 kg CO_2e
Embodied carbon per m^2 is	72 kg CO_2e/m^2
Total embodied carbon if structure DfD* is	76311 kg CO_2e
Embodied carbon if structure DfD per m^2 is	36 kg CO_2e/m^2

Total embodied carbon saving if DfD is	76311 kg CO_2e

Logou

CLT Building – Composite Design

The
University
Of
Sheffield.

Results

Embodied Energy

Total embodied energy of foundations is	0 MJ
Total embodied energy of ground floor slab is	0 MJ
Embodied energy of steel columns is	291153 MJ
Total embodied energy of columns is	291153 MJ
Embodied energy of steel beams is	638378 MJ
Total embodied energy of beams is	638378 MJ
Embodied energy of concrete in composite floor is	810264 MJ
Embodied energy of steel deck in composite floor is	642021 MJ
Total embodied energy of upper floor systems is	1533438 MJ
Total embodied energy of roof system is	0 MJ

Total embodied energy is	2462969 MJ
Embodied energy per m^2 is	1162 MJ/m^2
Total embodied energy if structure DfD* is	2317393 MJ
Embodied energy if stucture DfD per m^2 is	1093 MJ/m^2

Total embodied energy saving if DfD is	145577 MJ

Embodied Carbon

Total embodied carbon of foundations is	0 kg CO_2e
Total embodied carbon of ground floor slab is	0 kg CO_2e
Embodied carbon of steel columns is	20719 kg CO_2e
Total embodied carbon of columns is	20719 kg CO_2e
Embodied carbon of steel beams is	45429 kg CO_2e
Total embodied carbon of beams is	45429 kg CO_2e
Embodied carbon of concrete in composite floor is	124656 kg CO_2e
Embodied carbon of steel deck in composite floor is	43748 kg CO_2e
Total embodied carbon of upper floor systems is	174934 kg CO_2e
Total embodied carbon of roof system is	0 kg CO_2e

Total embodied carbon is	241082 kg CO_2e
Embodied carbon per m^2 is	114 kg CO_2e/m^2
Total embodied carbon if structure DfD* is	230722 kg CO_2e
Embodied carbon if structure DfD per m^2 is	109 kg CO_2e/m^2

Total embodied carbon saving if DfD is	10360 kg CO_2e

Logou

CLT Building – Concrete Design

The University Of Sheffield.

Results

Embodied Energy

Total embodied energy of foundations is	0 MJ
Total embodied energy of ground floor slab is	0 MJ
Embodied energy of concrete in columns is	62291 MJ
Total embodied energy of columns is	62291 MJ
Total embodied energy of beams is	0 MJ
Embodied energy of concrete in in-situ concrete is	1041768 MJ
Embodied energy of reinforcement in in-situ concrete is	39829 MJ
Total embodied energy of upper floor systems is	1081597 MJ
Total embodied energy of roof system is	0 MJ

Total embodied energy is	1143888 MJ
Embodied energy per m^2 is	540 MJ/m^2
Total embodied energy if structure DfD* is	1143888 MJ
Embodied energy if stucture DfD per m^2 is	540 MJ/m^2

Total embodied energy saving if DfD is	0 MJ

Embodied Carbon

Total embodied carbon of foundations is	0 kg CO_2e
Total embodied carbon of ground floor slab is	0 kg CO_2e
Embodied carbon of concrete in columns is	9583 kg CO_2e
Total embodied carbon of columns is	9583 kg CO_2e
Total embodied carbon of beams is	0 kg CO_2e
Embodied carbon of concrete in in-situ concrete is	160272 kg CO_2e
Embodied carbon of reinforcement in in-situ concrete is	3205 kg CO_2e
Total embodied carbon of upper floor systems is	163477 kg CO_2e
Total embodied carbon of roof system is	0 kg CO_2e

Total embodied carbon is	173060 kg CO_2e
Embodied carbon per m^2 is	82 kg CO_2e/m^2
Total embodied carbon if structure DfD* is	173060 kg CO_2e
Embodied carbon if structure DfD per m^2 is	82 kg CO_2e/m^2

Total embodied carbon saving if DfD is	0 kg CO_2e

Using ICE data

		Mass	EC Factor	EC Total	EE Factor	EE Total	Notes		kgCO2	MJ
		kg	kg CO2e/kg		MJ/kg				EC/m^2	EE/m^2
CLT Design	CLT	203500	0.167	33984.5	7.89	1605615	Using glue laminated timber factor		16.0	757.4
	Steel	54300	1.53	83079	21.5	1167450	(UK typical recycled cont)		39.2	550.7
	Total			117063.5		2773065			55.2	1308.0
CLT Design Hypo	CLT	203500	0.167	33984.5	7.89	1605615	Using glue laminated timber factor		16.0	757.4
	Steel	43900	1.53	67167	21.5	943850	(UK typical recycled cont)		31.7	445.2
	Total			101151.5		2549465			47.7	1202.6	Area (m^2)
Steel Com Design	Steel	43200	1.53	66096	21.5	928800	(UK typical recycled cont)		31.2	438.1	2120
	Concrete	890000	0.113	100570	0.78	694200	25/30 Mpa conc strength		47.4	327.5
	Mesh	4700	1.4	6580	17.4	81780	Using rebar factor		3.1	38.6
	Steel Deck	28400	1.54	43736	22.6	641840	UK typ recycled, galvanised deck		20.6	302.8
	Total			216982		2346620			102.4	1106.9
Concrete Design	Concrete	1213000	0.113	137069	0.78	946140	25/30 Mpa conc strength		64.7	446.3
	Reinforceme	2300	1.4	3220	17.4	40020	UK typical recycled cont		1.5	18.9
	Total			140289		986160			66.2	465.2

Summary Table				After Sakura				EC Tonnes			EE GJ	
	EC	EE	EC	EE				EC	EC		EE	EC
CLT	117063.5	2773065	58531.75	1386533				117	59		2773	1387
CLT - Designed Bea	101151.5	2549465	50575.75	1274733				101	51		2549	1275
Composite	241082	2462969	230722	2317393				241	231		2463	2317
RC	173060	1143888	173060	1143888				173	173		1144	1144

Embodied Carbon (Tonnes CO2e)

Embodied Energy (GJ)
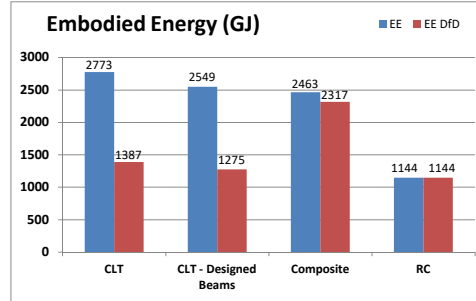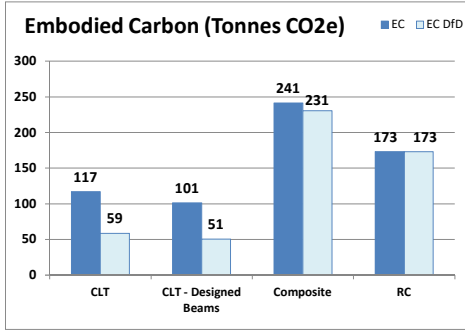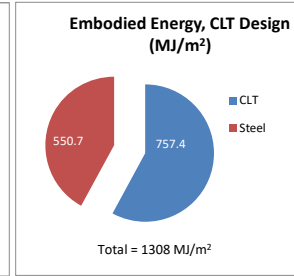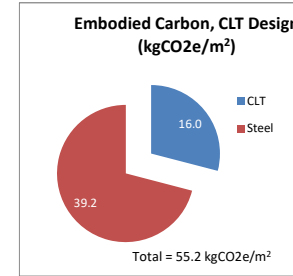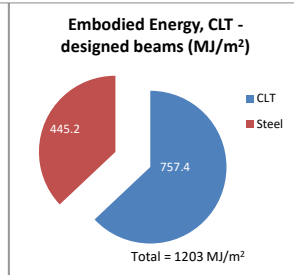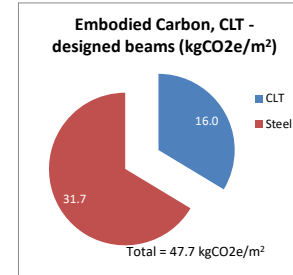
hypo	EC cf. steel	0.219206	
	EC cf.conc	0.292244	EE cf. conc	1.114386
standard	EC cf. steel	0.25369	
	EC cf.conc	0.338217	EE cf. conc	1.212123

Superstructure Mass (Tonnes)

Embodied Carbon, CLT - designed beams (kgCO2e/m²) — Total = 47.7 kgCO2e/m²

Embodied Energy, CLT - designed beams (MJ/m²) — Total = 1203 MJ/m²

Embodied Carbon, CLT Design (kgCO2e/m²) — Total = 55.2 kgCO2e/m²

Embodied Energy, CLT Design (MJ/m²) — Total = 1308 MJ/m²

Embodied Carbon, Steel Composite Design (kgCO2e/m²) — Total = 102.4 kgCO2e/m²

Embodied Energy, Steel Composite Design (MJ/m²) — Total = 1106 MJ/m²

Embodied Carbon, Concrete Design (kgCO2e/m²) — Total = 66.2 kgCO2e/m²

Embodied Energy, Concrete Design (MJ/m²) — Total = 465 MJ/m²